

TRANSLATIONAL CARDIOLOGY

FOR

ISCHEMIC HEART DISEASE

TRANSLATIONELE CARDIOLOGIE

voor ischemische hartziekte

(met een samenvatting in het Nederlands)

Proefschrift

ter verkrijging van de graad van doctor aan de Universiteit Utrecht op gezag van de rector magnificus, prof. dr. G.J. van der Zwaan, ingevolge het besluit van het college voor promoties
in het openbaar te verdedigen
op donderdag 30 maart 2017 des middags te 4:15

door

Janine Christine Deddens

geboren op 28 juni 1987

te Rotterdam

Promotor: Prof. dr. P.A.F.M. Doevendans

Co-promotoren: Dr. J.P.G. Sluiter
Dr. L.W. van Laake

Table of contents

Chapter 1	General introduction	5
Chapter 2	Circulating microRNAs as novel biomarkers for the early diagnosis of acute coronary syndrome	17
Chapter 3	Circulating extracellular vesicles contain miRNAs and are released as early biomarkers for cardiac injury	43
Chapter 4	Circulating microRNAs as diagnostic biomarkers for myocardial ischemia in stable outpatients: not fulfilling their promise	69
Chapter 5	Feasibility of echo-guided intramyocardial injections in mice for cardiac progenitor cell delivery in chronic cardiac remodeling	87
Chapter 6	Targeting chronic cardiac remodeling with cardiac progenitor cells in a murine model of ischemia/reperfusion injury	103
Chapter 7	Rapid immune activation after human stem cell injection in Balb/C and NOD-SCID mice	133
Chapter 8	Modeling the human scarred heart <i>in vitro</i> : toward new tissue engineered models	149
Chapter 9	Anti-fibrotic effects of cardiac progenitor cells in a 3D-model of human cardiac fibrosis	199
Chapter 10	General discussion	225
Appendix	Summary	241

1

General introduction

Ischemic heart disease

Coronary artery disease

As the human embryo develops, coronary arteries arise, that will provide nutrients and oxygen to the heart for the entire lifespan [1]. Unfortunately, risk factors such as age, gender, hypertension, diabetes, dyslipidemia and smoking interfere with the homeostasis of the coronary arteries and contribute to atherosclerotic changes and microvascular dysfunction [2, 3]. To date, coronary artery disease (CAD) is the most prevalent disease in the western world and is accountable for the death of 7.4 million people each year worldwide [4, 5]. Moreover, a large part of the health care costs and use of resources are attributed to CAD.

CAD can be grouped in roughly three clinical manifestations, which are a continuum and worsening of the same disease [6]. CAD includes patients with 1) stable angina pectoris, 2) unstable angina pectoris and 3) acute myocardial infarction (MI). Stable angina pectoris is characterized by reversible myocardial ischemia and transient chest pain. The treatment of stable angina pectoris aims at reducing risk factors (e.g. smoking, dyslipidemia) and symptoms by lifestyle interventions and pharmacological therapy and, if applicable, restoring proper blood flow through the coronaries by revascularization strategies [7]. Early treatment of CAD might reduce deterioration to the most dreaded manifestations of CAD: unstable angina pectoris and MI [8–10]. Both unstable angina pectoris and MI are part of the acute coronary syndrome (ACS), a clinical diagnosis used to identify patients in need for early revascularization. Unstable angina pectoris is defined as myocardial ischemia in the absence of cardiomyocytes necrosis. In contrast to stable angina pectoris, the complaints and ischemia occur at rest and might precede irreversible injury. MI, mainly caused by atherosclerotic plaque rupture followed by thrombus formation, results in cardiomyocyte apoptosis and necrosis due to prolonged periods of ischemia [8, 10, 11]. Based on ECG features, MI can be categorized in ST-segment elevation MI (STEMI) and non-ST segment elevation MI (NSTEMI) of which a STEMI is mostly due to a complete vessel occlusion [6].

Detection of coronary artery disease – Stable angina pectoris and ACS

Identification of CAD in an early stage is crucial to reduce CAD-related mortality and morbidity and to lower healthcare costs. Currently, the diagnosis of significant CAD for patients with SA relies on non-invasive imaging techniques to assess coronary anatomy (e.g. computed tomography (CT)) and myocardial blood flow (e.g. stress imaging). It has been demonstrated that the calcium score, as measured by coronary-CT [12], is associated with the severity of CAD and is a powerful tool to classify cardiovascular risk [13–15]. Likewise, patients with a stress-induced reversible perfusion deficit > 10% of the total LV myocardium as assessed by imaging techniques represent a high risk population and early coronary arteriography is recommended [16, 17]. Unfortunately, no biomarkers for SA are available and as a consequence, the diagnostic work-up is expensive and referral to the out-patient clinic is necessary.

The clinical diagnosis of ACS at the emergency department (ED) is based on 1) clinical symptoms (e.g. chest pain, vasovagal response), 2) changes on the electrocardiogram, consisting of ST-segment elevation or depression or new pathological Q- waves; and 3) rise and fall of circulating biomarkers, preferably troponin [9]. As different subtypes of ACS exist (unstable angina pectoris, NSTEMI and STEMI), the diagnostic strategy is not identical for each. For patients with a STEMI, diagnosis and immediate treatment do not rely on the rise and fall of biomarkers since the occurring ECG changes are pathognomonic for MI [8]. However, the diagnosis of NSTEMI and unstable angina pectoris is less straightforward and requires additional information provided by circulating biomarkers or explorative angiography [10]. For NSTEMI and unstable angina pectoris, decision-making can be challenging, which especially applies to patients presenting early after the onset of symptoms, when circulating biomarkers may not be detectable yet.

Upon MI, the heart releases different enzymes, growth factors and cytokines, which can serve as markers of cardiac injury. Cardiac troponin (cTn) and creatine kinase MB (CK-MB) are the most commonly used biomarkers for MI [9, 18]. Due to the relative late rise of these biomarkers, 10 to 15% of patients presenting with a MI have a negative blood test upon arrival in the

hospital [19, 20]. However, with the development of high and-ultra sensitivity cTnI (hs-cTnI) assays, the diagnostic potential of cTnI is improved [18, 21, 22]. As expected, the introduction of hs-TnI resulted in an increased proportion of MI and decreased proportion of unstable angina pectoris in ACS patients [10], based on adjusted definitions.

Delayed confirmation of MI results in increased morbidity and mortality. On the contrary, delay in the non-MI confirmation prolongs the time spent in the hospital and increases healthcare costs [22]. To guide early identification of patients with a low risk for MI, to accelerate immediate treatment in the emergency department for patients with a high risk of cardiac death, and to minimize healthcare costs there is an ongoing need for novel early biomarkers for CAD [23].

Increasing evidence suggests that circulating microRNAs (miRNA) can be potential biomarker candidates due to their highly specific elevation in blood upon stress, including MI [19, 24, 25]. MiRNAs are short (~22 nucleotides) non-coding RNAs [26] that negatively regulate gene expression at a post-transcriptional level [27, 28]. Moreover, miRNAs are released in the extracellular environment and can be detected in bodily fluids, including peripheral blood.[29] Altered expression of specific circulating miRNAs has been observed in various cardiovascular diseases, such as stable angina, AMI and heart failure [19, 23, 29–32]. In the search for new biomarkers, the pathophysiology of the involved processes in CAD may point the way to future standards.

Chronic heart failure

Patients surviving the initial ischemic event often develop chronic heart failure (CHF). New data shows that even one in four patients is diagnosed with heart failure within four years of a first heart attack [33]. CHF is a major public health issue and has an overall prevalence of 1-3% in the adult western population, which even increases up to 10% for patients > 75 years [34]. Despite advances in therapy, the burden of disease is high and the 5-year mortality rate is still 60%. CHF is a multifactorial disease and, independent of etiology, associated with cardiac

remodeling. In response to stress, injury or disease, cardiac remodeling is primarily initiated to meet the requirements of nutrient and oxygen supply [35]. However, cardiac remodeling eventually influences normal systolic and/or diastolic function. Systolic heart failure, or heart failure with reduced ejection fraction (HFrEF), characterizes at least half of the patients with heart failure and involves progressive adverse cardiac remodeling [36].

Negative cardiac remodeling

A key player in cardiac remodeling is the cardiac fibroblast (CF), which produces and maintains the extracellular matrix (ECM). Upon cardiac injury, naïve CF are activated by a broad network of molecules, but primarily through the TGF- β /Smad signaling pathway [37, 38]. The activated fibroblasts are characterized by cellular expression of alpha-smooth muscle actin (α -SMA) microfilaments and an increased matrix production [39, 40]. The initial activation of fibroblasts upon e.g. acute myocardial damage is necessary to maintain the integrity of the heart and to prevent myocardial rupture. However, in later stages, when fibroblasts fail to undergo apoptosis and remain constitutively active, ongoing matrix deposition results in perpetuation of pro-fibrotic signaling. This is demonstrated by a higher proportion of activated fibroblasts in human failing hearts compared to control hearts [41]. Additionally, pathological signaling from co-morbidities such as diabetes, hypertension, and inflammation aggravates cardiac remodeling [42, 43] by activation of for instance the renin-angiotensin-aldosterone (RAAS) and sympathetic system. Treatment of CHF focuses on the prevention of heart failure progression to improve survival and quality of life. To achieve this, pharmacological treatment to inhibit the neurohumoral pathways is recommended for all-cause chronic systolic heart failure [36].

Several novel therapies that might interfere with adverse cardiac remodeling have been proposed [44, 45]. Recently, promising results of a clinical trial with the angiotensin receptor-neprilysin inhibitor (LCZ696) [46] showed a decrease in hospitalization, cardiovascular death and all-cause mortality compared to current standard therapy with an ACE-inhibitor. Also, administration of cardiac stem cells to patients with CHF seems to be beneficial [47].

Additionally, it has been demonstrated that heart failure patients receiving mechanical support with a Left Ventricular Assist Device (LVAD) can display reverse remodeling, reduced fibrosis and an improved cardiac function [48]. These studies suggest a therapeutic window for novel treatment strategies to halt disease progression and induce disease regression. Although these potential therapies are promising for patients with CHF, their mechanism of action is largely unknown and hampered by a lack of mechanistic insights in matrix remodeling and the role of associated CF. Hence, the need for a better understanding of matrix remodeling and the search for novel anti-fibrotic targets necessitate proper *in vivo* and *in vitro* models.

Regenerative therapy

Classically, it was thought that the heart is a post-mitotic organ with terminally differentiated cardiomyocytes [49]. Later, this paradigm was challenged by the discovery of mitotic cells in the human adult myocardium in the beginning of this century [50, 51]. In addition, this was elegantly substantiated by the observation of ¹⁴C integration in heart muscle cells, an unexpected opportunity provided by the nuclear bomb tests during the Cold War [52]. The maximum reported cardiomyocyte renewal of 1% per year, however, is not sufficient for the enormous cell loss caused by MI or other myocardial disease [53, 54].

Cell based therapies have been implied as a novel approach for cardiac protection and myocardial repair. Ever since the first clinical application of stem cells for acute ischemic heart disease more than a decade ago [55, 56], various studies demonstrated tentatively promising results regarding quality of life and cardiac parameters [47, 57, 58]. Different cell sources were investigated of which bone marrow mononuclear cells (BMMNC), mesenchymal stem cells (MSC) and cardiac progenitor cells (CPC) are the most investigated [59]. Of these, the CPC is of great interest due to its capacity to differentiate towards the different cardiac lineages [60, 61].

Targets of cell therapy include the different manifestations of CAD, including refractory angina pectoris, MI and CHF [57, 62]. In these processes, transplanted cells may prevent cardiomyocyte death, attenuate inflammation, enhance angiogenesis, decrease matrix formation

or form new contractile tissue. The general thinking that grafted cells would directly contribute to cardiac repair by electromechanical integration is still under debate. The low graft retention and low number of newly formed cardiomyocytes upon cell transplantation points toward an alternative, paracrine mechanism where the effect of therapy is attributable to activation of endogenous repair mechanisms by paracrine mediators [63].

Since the clinical results of cell therapy are a long way from the observed potency in *in vitro* and preclinical studies [57, 64–66], it is important to define the biological targets and to govern the choice of stem cell type and delivery accordingly [66].

Thesis outline

Ischemic heart disease is a great burden for society in terms of public health and healthcare costs. To improve quality of life in patients suffering from CAD, advancements in early detection and targeted treatment of chronic manifestations are mandatory. Considering the heterogeneity of CAD and the quest for translational research, efforts should be made to design and employ appropriate (pre)clinical studies. Therefore, the overall aim of this thesis is to improve the diagnosis and treatment of ischemic heart disease by advancing translational research.

PART ONE- Early detection of (acute) coronary artery disease

The first part of this thesis focuses on novel biomarkers for the diagnosis of the different manifestations of CAD. First, an overview of circulating miRNAs as potential biomarker for ACS is given in [chapter 2](#). For clinical translation of miRNAs as biomarkers it is important to understand their temporal and spatial characteristics. Therefore, we studied the temporal release, potential source and transportation via extracellular vesicles of circulating miRNAs in different animal models of I/R injury in [chapter 3](#). Next, in [chapter 4](#) we address the question whether circulating miRNAs could be used to identify patients with significant myocardial ischemia in a patient population with transient chest pain complaints referred to the out-patient clinic.

PART TWO- Translational small animal models for regenerative therapy

Next to investigating novel possibilities to limit myocardial injury, attention for novel treatment modalities for CHF is evenly important, as one in four patients with a MI develops heart failure in the first four years [33]. The second part of this thesis describes murine models used to gain insight in the basic science of cardiac cell therapy. As the beneficial effect of cardiac stem cell therapy remains controversial, we aim to contribute to translational success by developing novel translatable models. We touch upon several factors potentially contributing to translational failure of cardiac cell therapy, e.g. injury model and timing of therapy. In [chapter 5](#),

we provide a standardized method to create a chronic murine model of I/R injury. Moreover, we aim to examine the feasibility of a minimally invasive echo-based local delivery strategy at several time-points after induction of I/R injury. Subsequently, we use this chronic murine model to examine the effect of minimally invasive application of CPC in cardiac remodeling, which is described in [chapter 6](#). In [chapter 7](#), we contemplate on the use of human stem cells in murine models. We evaluate cell engraftment in immune competent and immune incompetent mice and examine the immune response upon cell transplantation.

PART THREE- Cardiac tissue engineering

In line with the high need for novel treatment modalities for CHF, the third part of this thesis describes the potential of tissue engineering for disease modeling and drug testing. [Chapter 8](#) describes the current understanding of cardiac fibrosis and discusses approaches that are using hydrogel-based tissue engineered heart constructs to contemplate key challenges for modeling tissue engineered cardiac fibrosis. In [chapter 9](#), a novel *in vitro* model of cardiac fibrosis, to gain insight in the pathophysiology of adverse cardiac remodeling, is described. As a proof-of-principle, we use this cardiac fibrosis model to investigate the potential anti-fibrotic effects of CPC.

PART FOUR- Summary and discussion

[Chapter 10](#) provides a summary and critical appraisal of the previous chapters and current literature.

References

1. Reese DE. Development of the Coronary Vessel System. *Circ Res* 2002;91:761–768.
2. Ross R. Atherosclerosis--an inflammatory disease. *N Engl J Med* 1999;340:115–26.
3. Pries AR, Reglin B. Coronary microcirculatory pathophysiology: can we afford it to remain a black box? *Eur Heart J* 2016;ehv760.
4. Mozaffarian D, Benjamin EJ, Go AS, et al. Heart Disease and Stroke Statistics-2015 Update: A Report From the American Heart Association. *Circulation* 2014;131:e29--322.
5. Anon. WHO | Cardiovascular diseases (CVDs).
6. Montalescot G, Sechtem U, Achenbach S, et al. 2013 ESC guidelines on the management of stable coronary artery disease: the Task Force on the management of stable coronary artery disease of the European Society of Cardiology. *Eur Heart J* 2013;34:2949–3003.
7. Henderson RA, O'Flynn N. Management of stable angina: summary of NICE guidance. *Heart* 2012;98:500–7.
8. Steg PG, James SK, Atar D, et al. ESC Guidelines for the management of acute myocardial infarction in patients presenting with ST-segment elevation. *Eur Heart J* 2012;33:2569–619.
9. Thygesen K, Alpert JS, Jaffe AS, et al. Third universal definition of myocardial infarction. *Eur Heart J* 2012;33:2551–67.
10. Roffi M, Patrono C, Collet J-P, et al. 2015 ESC Guidelines for the management of acute coronary syndromes in patients presenting without persistent ST-segment elevation. *Eur Heart J* 2015;37:ehv320.
11. Oerlemans MIFJ, Koudstaal S, Chamuleau SA, de Kleijn DP, Doevendans PA, Sluijter JPG. Targeting cell death in the reperfused heart: pharmacological approaches for cardioprotection. *Int J Cardiol* 2013;165:410–22.
12. Agatston AS, Janowitz WR, Hildner FJ, Zusmer NR, Viamonte M, Detrano R. Quantification of coronary artery calcium using ultrafast computed tomography. *J Am Coll Cardiol* 1990;15:827–32.
13. Yeboah J, McClelland RL, Polonsky TS, et al. Comparison of novel risk markers for improvement in cardiovascular risk assessment in intermediate-risk individuals. *JAMA* 2012;308:788–95.
14. Silverman MG, Blaha MJ, Krumholz HM, et al. Impact of coronary artery calcium on coronary heart disease events in individuals at the extremes of traditional risk factor burden: the Multi-Ethnic Study of Atherosclerosis. *Eur Heart J* 2014;35:2232–41.
15. Budoff MJ, Shaw LJ, Liu ST, et al. Long-term prognosis associated with coronary calcification: observations from a registry of 25,253 patients. *J Am Coll Cardiol* 2007;49:1860–70.
16. Hachamovitch R, Rozanski A, Shaw LJ, et al. Impact of ischaemia and scar on the therapeutic benefit derived from myocardial revascularization vs. medical therapy among patients undergoing stress-rest myocardial perfusion scintigraphy. *Eur Heart J* 2011;32:1012–24.
17. Lin FY, Dunning AM, Narula J, et al. Impact of an automated multimodality point-of-order decision support tool on rates of appropriate testing and clinical decision making for individuals with suspected coronary artery disease: a prospective multicenter study. *J Am Coll Cardiol* 2013;62:308–16.
18. Keller T, Zeller T, Peetz D, et al. Sensitive troponin I assay in early diagnosis of acute myocardial infarction. *N Engl J Med* 2009;361:868–77.
19. Oerlemans MIFJ, Mosterd A, Dekker MS, et al. Early assessment of acute coronary syndromes in the emergency department: the potential diagnostic value of circulating microRNAs. *EMBO Mol Med* 2012;4:1176–85.
20. Meder B, Keller A, Vogel B, et al. MicroRNA signatures in total peripheral blood as novel biomarkers for acute myocardial infarction. *Basic Res Cardiol* 2011;106:13–23.
21. Reichlin T, Hochholzer W, Bassetti S, et al. Early diagnosis of myocardial infarction with sensitive cardiac troponin assays. *N Engl J Med* 2009;361:858–67.
22. Shah AS V, Anand A, Sandoval Y, et al. High-sensitivity cardiac troponin I at presentation in patients with suspected acute coronary syndrome: a cohort study. *Lancet (London,*

- England) 2015;386:2481–8.
23. Deddens JC, Colijn JM, Oerlemans MIFJ, et al. Circulating MicroRNAs as Novel Biomarkers for the Early Diagnosis of Acute Coronary Syndrome. *J Cardiovasc Transl Res* 2013;6:884–898.
 24. Rhees B, Wingrove JA. Developing Peripheral Blood Gene Expression-Based Diagnostic Tests for Coronary Artery Disease: a Review. *J Cardiovasc Transl Res* 2015;8:372–80.
 25. Friede KA, Ginsburg GS, Voora D. Gene Expression Signatures and the Spectrum of Coronary Artery Disease. *J Cardiovasc Transl Res* 2015;8:339–52.
 26. Lagos-Quintana M, Rauhut R, Lendeckel W, Tuschl T. Identification of novel genes coding for small expressed RNAs. *Science* 2001;294:853–8.
 27. Sluijter JPG, van Mil A, van Vliet P, et al. MicroRNA-1 and -499 regulate differentiation and proliferation in human-derived cardiomyocyte progenitor cells. *Arterioscler Thromb Vasc Biol* 2010;30:859–68.
 28. Lin CJ-F, Gong H-Y, Tseng H-C, Wang W-L, Wu J-L. miR-122 targets an anti-apoptotic gene, Bcl-w, in human hepatocellular carcinoma cell lines. *Biochem Biophys Res Commun* 2008;375:315–20.
 29. Mitchell PS, Parkin RK, Kroh EM, et al. Circulating microRNAs as stable blood-based markers for cancer detection. *Proc Natl Acad Sci U S A* 2008;105:10513–8.
 30. van Rooij E, Sutherland LB, Thatcher JE, et al. Dysregulation of microRNAs after myocardial infarction reveals a role of miR-29 in cardiac fibrosis. *Proc Natl Acad Sci U S A* 2008;105:13027–32.
 31. Bostjancic E, Zidar N, Stajer D, Glavac D. MicroRNAs miR-1, miR-133a, miR-133b and miR-208 are dysregulated in human myocardial infarction. *Cardiology* 2010;115:163–9.
 32. Wang G-K, Zhu J-Q, Zhang J-T, et al. Circulating microRNA: a novel potential biomarker for early diagnosis of acute myocardial infarction in humans. *Eur Heart J* 2010;31:659–66.
 33. JMIH Gho, AF Schmidt, S Koudstaal, M Pujades-Rodriguez, S Denaxas, CP Gale, AW Hoes, JG Cleland, H Hemingway FA. Heart failure following myocardial infarction: a cohort study of incidence and prognostic factors in 24 745 patients using linked electronic records. *Eur J Hear Fail Abstr Suppl* 2016;18:442.
 34. Bui AL, Horwich TB, Fonarow GC. Epidemiology and risk profile of heart failure. *Nat Rev Cardiol* 2011;8:30–41.
 35. Li A-H, Liu PP, Villarreal FJ, Garcia RA. Dynamic changes in myocardial matrix and relevance to disease: translational perspectives. *Circ Res* 2014;114:916–27.
 36. McMurray JJ V, Adamopoulos S, Anker SD, et al. ESC guidelines for the diagnosis and treatment of acute and chronic heart failure 2012: The Task Force for the Diagnosis and Treatment of Acute and Chronic Heart Failure 2012 of the European Society of Cardiology. Developed in collaboration with the Heart. *Eur J Heart Fail* 2012;14:803–69.
 37. Dobaczewski M, Chen W, Frangogiannis NG. Transforming growth factor (TGF)- β signaling in cardiac remodeling. *J Mol Cell Cardiol* 2011;51:600–6.
 38. Goumans M-J, Liu Z, ten Dijke P. TGF-beta signaling in vascular biology and dysfunction. *Cell Res* 2009;19:116–27.
 39. Tomasek JJ, Gabbiani G, Hinz B, Chaponnier C, Brown RA. Myofibroblasts and mechano-regulation of connective tissue remodelling. *Nat Rev Mol Cell Biol* 2002;3:349–63.
 40. Hinz B, Phan SH, Thannickal VJ, et al. Recent developments in myofibroblast biology: paradigms for connective tissue remodeling. *Am J Pathol* 2012;180:1340–1355.
 41. Li J, Philip JL, Xu X, Theccanat T, Abdur Razzaque M, Akhter SA. β -Arrestins regulate human cardiac fibroblast transformation and collagen synthesis in adverse ventricular remodeling. *J Mol Cell Cardiol* 2014;76:73–83.
 42. Sedgwick B, Riches K, Bageghni SA, O'Regan DJ, Porter KE, Turner NA. Investigating inherent functional differences between human cardiac fibroblasts cultured from nondiabetic and Type 2 diabetic donors. *Cardiovasc Pathol* 23:204–10.
 43. Kawano H, Do YS, Kawano Y, et al. Angiotensin II has multiple profibrotic effects in human cardiac fibroblasts. *Circulation* 2000;101:1130–7.
 44. Leask A. Potential therapeutic targets for cardiac fibrosis: TGFbeta, angiotensin, endothelin, CCN2, and PDGF, partners in fibroblast activation. *Circ Res* 2010;106:1675–80.

45. Leask A. Getting to the Heart of the Matter: New Insights Into Cardiac Fibrosis. *Circ Res* 2015;116:1269–1276.
46. McMurray JJV, Packer M, Desai AS, et al. Angiotensin–Neprilysin Inhibition versus Enalapril in Heart Failure. *N Engl J Med* 2014;371:140830040023009.
47. Makkar RR, Smith RR, Cheng K, et al. Intracoronary cardiosphere-derived cells for heart regeneration after myocardial infarction (CADUCEUS): a prospective, randomised phase 1 trial. *Lancet (London, England)* 2012;379:895–904.
48. Birks EJ, George RS. Molecular changes occurring during reverse remodelling following left ventricular assist device support. *J Cardiovasc Transl Res* 2010;3:635–42.
49. Tam SK, Gu W, Mahdavi V, Nadal-Ginard B. Cardiac myocyte terminal differentiation. Potential for cardiac regeneration. *Ann N Y Acad Sci* 1995;752:72–9.
50. Quaini F, Urbanek K, Beltrami AP, et al. Chimerism of the transplanted heart. *N Engl J Med* 2002;346:5–15.
51. Beltrami AP, Urbanek K, Kajstura J, et al. Evidence that human cardiac myocytes divide after myocardial infarction. *N Engl J Med* 2001;344:1750–7.
52. Bergmann O, Bhardwaj RD, Bernard S, et al. Evidence for cardiomyocyte renewal in humans. *Science* 2009;324:98–102.
53. Robey TE, Saiget MK, Reinecke H, Murry CE. Systems approaches to preventing transplanted cell death in cardiac repair. *J Mol Cell Cardiol* 2008;45:567–81.
54. Segers VFM, Lee RT. Stem-cell therapy for cardiac disease. *Nature* 2008;451:937–42.
55. Menasché P, Hagege AA, Scorsin M, et al. Myoblast transplantation for heart failure. *Lancet (London, England)* 2001;357:279–80.
56. Strauer BE, Brehm M, Zeus T, et al. Repair of infarcted myocardium by autologous intracoronary mononuclear bone marrow cell transplantation in humans. *Circulation* 2002;106:1913–8.
57. Abdel-Latif A, Bolli R, Tleyjeh IM, et al. Adult bone marrow-derived cells for cardiac repair: a systematic review and meta-analysis. *Arch Intern Med* 2007;167:989–97.
58. Schächinger V, Erbs S, Elsässer A, et al. Intracoronary bone marrow-derived progenitor cells in acute myocardial infarction. *N Engl J Med* 2006;355:1210–21.
59. Madonna R, Van Laake LW, Davidson SM, et al. Position Paper of the European Society of Cardiology Working Group Cellular Biology of the Heart: cell-based therapies for myocardial repair and regeneration in ischemic heart disease and heart failure. *Eur Heart J* 2016.
60. Oh H, Bradfute SB, Gallardo TD, et al. Cardiac progenitor cells from adult myocardium: homing, differentiation, and fusion after infarction. *Proc Natl Acad Sci U S A* 2003;100:12313–8.
61. Smits AM, van Vliet P, Metz CH, et al. Human cardiomyocyte progenitor cells differentiate into functional mature cardiomyocytes: an in vitro model for studying human cardiac physiology and pathophysiology. *Nat Protoc* 2009;4:232–243.
62. Mann I, Rodrigo SF, van Ramshorst J, et al. Repeated Intramyocardial Bone Marrow Cell Injection in Previously Responding Patients With Refractory Angina Again Improves Myocardial Perfusion, Anginal Complaints, and Quality of Life. *Circ Cardiovasc Interv* 2015;8.
63. Gneocchi M, Zhang Z, Ni A, Dzau VJ. Paracrine mechanisms in adult stem cell signaling and therapy. *Circ Res* 2008;103:1204–19.
64. Zwetsloot PP, Végh AM, Jansen Of Lorkeers SJ, et al. Cardiac Stem Cell Treatment in Myocardial Infarction: A Systematic Review and Meta-Analysis of Preclinical Studies. *Circ Res* 2016.
65. Jansen Of Lorkeers SJ, Eding JEC, Vesterinen HM, et al. Similar effect of autologous and allogeneic cell therapy for ischemic heart disease: systematic review and meta-analysis of large animal studies. *Circ Res* 2015;116:80–6.
66. Goumans M-J, Maring JA, Smits AM. A straightforward guide to the basic science behind cardiovascular cell-based therapies. *Heart* 2014;100:1153–7.

Circulating microRNAs as novel biomarkers for the early diagnosis of acute coronary syndrome

J.C. Deddens

J.M. Colijn

M.I.F.J. Oerlemans

G. Pasterkamp

S.A. Chamuleau

P.A. Doevendans

J.P.G. Sluijter

Journal of Cardiovascular Translational Research 2013;6(6):884-98.

Abstract

Small non-coding microRNAs (miRNAs) are important physiological regulators of post-transcriptional gene expression. miRNAs not only reside in the cytoplasm, but are also stably present in several extracellular compartments, including the circulation. For that reason, miRNAs are proposed as diagnostic biomarkers for various diseases. Early diagnosis of non-ST elevated myocardial infarction is obligatory for optimal treatment outcome, and due to the ongoing need for additional identifiers, miRNAs are of special interest as biomarkers for acute coronary syndrome (ACS). This review highlights the nature and cellular release mechanisms of circulating miRNAs and therefore their potential role in the diagnosis of myocardial infarction. We will give an update of clinical studies addressing the role of circulating miRNA expression after myocardial infarction and explore the diagnostic value of this potential biomarker.

Introduction

Cardiovascular disease is still one of the leading causes of death in the Western world [1]. Acute coronary syndrome (ACS), a clinical diagnosis used to identify patients in need for cardiac revascularization, includes ST-elevated myocardial infarction (STEMI), non-ST-elevated myocardial infarction (NSTEMI), and unstable angina pectoris (UA). Here, myocardial infarction (MI) is defined as myocardial cell death due to prolonged periods of ischemia characterized by an imbalance between myocardial oxygen supply and demand [2, 3], which is mediated by necrotic and apoptotic cell death [2, 4, 5]. The main mechanisms of MI include coronary artery occlusion caused by atherosclerotic plaque rupture followed by thrombus formation and acute occlusion of a coronary artery by emboli or spasm.

The clinical diagnosis of ACS in the hospital is based on: 1) clinical symptoms, like chest pain and a vasovagal response, 2) changes on the electrocardiogram, consisting of ST-segment elevation or depression or new pathological Q-waves, and 3) circulating biomarkers level changes, preferably troponin as described in the guidelines of the European Society of Cardiology and the American College of Cardiology [2]. At the emergency department these parameters are used to classify patients with ACS. As explained above, different causes can lead to ACS, thereby including 3 subtypes; ST-elevated MI (STEMI), non-ST elevated MI (NSTEMI) and unstable angina pectoris (UA). In the clinical setting, circulating biomarkers are very important to confirm the diagnosis of ACS, since patients with NSTEMI or UA cannot be diagnosed based on clinical symptoms and ECG only. After final diagnosis of ACS, including STEMI, NSTEMI, and UA, clinical treatment for the different subgroups is similar.

Up to date, the most commonly used biomarker for MI is cardiac troponin (cTn) [2]. Troponin I and T subunits are part of the contractile myofibrils of cardiomyocytes and are released into the circulation after cardiomyocyte necrosis. The disadvantage of cTn is its time-restrain, since it is only detectable 3 to 6 hours after clinical symptoms of cardiac ischemia have started [6–8], in contrast to e.g. chemical cardiac injury where cTnT can already be detected 15 minutes after injury [9]. Therefore, 10 to 15% of patients with MI presenting to the emergency department do not yet have a positive cTn test [10, 11]. Since early diagnosis of MI maximizes the effects of cardiac revascularization therapy, there is an ongoing search for early diagnostic biomarkers.

Newly developed high-sensitive cardiac troponin T (hs-cTnT) assays have led to an improved diagnosis of MI as early as 3 hours after the onset of symptoms [12, 13]. Nevertheless, guidelines still advise measuring troponin at presentation to the hospital and 3-6 hours later [2] in order to see temporal

changes in cTn concentrations, suggestive for MI. The main disadvantage of hs-cTnT assays is that in a substantial part of the population, especially elderly, continuously elevated levels of cTn are measured due to heart failure or chronic kidney disease [14, 15], resulting in false positive hs-cTnT assays [14].

An alternative to cTn is creatine kinase MB (CK-MB). Similar to cTn, CK-MB is released into the circulation upon cardiomyocyte necrosis and is related to infarct size and inversely to long-term survival [16]. The disadvantage of CK-MB as a biomarker of MI is its lower tissue specificity compared to cTn [17] and its delayed elevation (7 hours) after the onset of symptoms [18]. Besides cTn and CK-MB, there are more candidate biomarkers for MI investigated that are released in the circulation upon cardiac damage, such as Heart-type fatty acid binding protein (H-FABP) [19, 20], C-reactive protein (CRP) [21], B-type natriuretic peptide (BNP) [22], C-terminal portion of proavopressin (copeptin) [23], and ischemia modified albumin (IMA) [24]. However, none of these biomarkers are elevated as early as hs-cTnT or are as specific as hs-cTnT [12, 25].

Despite the fact that hs-cTnT reveals an excellent diagnostic potential for the diagnosis of MI, having a large area under the curve (AUC) in receiver operator characteristics (ROC) analysis, there is still a need for new biomarkers that are able to reduce time between the onset of MI and the actual therapeutic interventions to further prevent cardiac ischemia and subsequent cell death. An ideal biomarker has seven different properties, including 1) high sensitivity and specificity for the disease of interest, 2) high reproducibility, 3) high stability inside and outside the human body, 4) measurable in linear proportion to myocardial damage 5) directly measurable after disease onset, 6) a long biological half-life, and 7) advantages above the existing biomarkers. Moreover, preferably it should be measured relatively inexpensive [25–27]. In the continuous search for new biomarkers, posttranscriptional processing have recently received an increased interest via the release and presence of small regulatory RNAs, called microRNAs (miRNAs), into several body fluids [28–31]. Emerging evidence indicate that miRNAs are involved in various diseases and appeared to be circulating in the blood [30, 32], providing opportunities for new biomarker discoveries. Here, we review the advantages and disadvantages of circulating miRNAs as biomarkers for the diagnosis of myocardial infarction and briefly discuss the potential origin of identified miRNAs and their expression in cardiovascular disease.

MicroRNAs

MicroRNAs (miRNAs) are ~22 nucleotides long non-coding RNAs that regulate gene expression at post-transcriptional level [33]. miRNAs are transcribed in the nucleus as precursor molecules, called primary miRNAs (pri-miRNA), and subsequently processed by RNase III enzyme, Drosha and DCGR8, into a precursor miRNA (pre-miRNAs). This molecule is transported by exportin-5 into the cytoplasm, where they are further processed by Dicer, another RNase III enzyme, into the mature single stranded miRNA. Mature miRNAs regulate post-transcriptional gene expression by their uptake into the RNA-induced silencing complex (RISC) and subsequently binding to the 3', and sometimes the 5', untranslated region (UTR) of mRNA through imperfect basepairing [34], thereby repressing its translation via deadenylation or promotion of mRNA degradation [35, 36]. More detailed information on the biogenesis and function of miRNAs is described in reviews written by Bartel *et al.* [37], Ghildiyal *et al.* [38], Winter *et al.* [39], and Guo *et al.* [40]. Translational repression by miRNAs is thought to regulate various cellular processes in the human body including cell differentiation [41], proliferation [41, 42] and apoptosis [43]. Since mRNA targets, regulated by miRNAs, are still largely unknown, possible target sites can be predicted genome-wide by evaluation of complementary nucleotide sequences.

Deregulation of miRNAs is associated with abnormal expression and translation of mRNAs and consequently with development of various pathological conditions. The first discovered miRNAs that were found to be involved in human disease were miRNA-15 and 16, that were both down-regulated due to a deletion of a small region on the coding 13q14 gene, thereby causing lymphatic leukemia [44]. Emerging evidence has indicated that miRNAs also play a role in various other diseases such as progressive liver disease [45], neurodegenerative disease [28], and cardiovascular diseases [46]. Specific up- and down-regulation of miRNAs give cardiovascular disease-specific miRNA expression signatures for e.g. atherosclerosis [47, 48], angiogenesis [49], heart failure [50] and coronary artery disease (CAD) [51]. These differences in expression patterns are found through genome-wide miRNA profiling techniques, mainly via miRNA microarray analysis or deep sequencing techniques. Other traditional techniques that can be used for detection of these small RNA molecules are Northern blotting, the 'golden standard', and quantitative real-time PCR [52, 53].

Circulating miRNAs

Originally miRNAs appeared to be located in the cytoplasm, but later studies revealed the presence of miRNAs in extracellular fluid, e.g. blood [30] and urine [54]. At first, the function of circulating miRNAs was unclear, but later it was proposed that these extracellular circulating miRNAs are transported to different cells and are able to regulate posttranscriptional gene expression in recipient cells [55, 56]. Moreover, despite the presence of ribonucleases, miRNAs appeared to be stable in the extracellular fluids. Interestingly, it was observed that circulating miRNAs could resist multiple freezing and thawing cycles, high and low pH, and boiling [32], which makes them extremely suitable for biomarker research from large existing biobanks, and raised the question on how miRNAs are kept from degradation outside the protective cellular environment. There has been an increasing focus on the biological role of circulating miRNAs and their different transports methods in fluids [57]. Up to now there are three established modes of miRNA transport and stabilization outside the cell (see Figure 1):

1) Protein-miRNA complexes - The majority of circulating miRNAs are stabilized by binding proteins [58]. The protein and miRNA form a protein-miRNA complex that protects the miRNA from RNAses in the plasma. Argonaute2 proteins [58] and Nucleophomin [59] are identified binding proteins found to pack and protect miRNAs in plasma and cell culture medium, respectively, but there may be other proteins that carry miRNAs which remain to be discovered.

2) High-density lipoproteins - High-density lipoproteins (HDL) bind and transport endogenous miRNA to recipient cells [60]. The trigger for miRNA export out of the cell is not known, although it is postulated that the ceramide pathway plays a role in inhibiting the export of miRNA to HDL. Ceramide is a sphingolipid which is regulated by sphingomyelinases, and inhibition of neutral sphingomyelase 2 (nSMase 2) in macrophages results in increased miRNA export via HDL [60]. In addition, it is demonstrated that HDL-bound miRNA delivery to cells *in vitro* is mediated by scavenger receptor class B type I (SR-BI) [60, 61]. Recent studies suggest that miRNA-92a, -126, and -223 are miRNAs most abundantly bound to HDL [61] and might be taken up by endothelial cells [60]. Moreover, HDL isolated from patients with stable CAD alters the miRNA expression pattern of smooth muscle cells and peripheral blood mononuclear cells *in vitro* [61].

3) *Encapsulation in vesicles* – Microvesicles, formed by outward budding of the cell membrane [62], contain miRNAs, which are protected from RNase dependent degradation outside the cell [63]. Some of the miRNAs found in microvesicles are hardly located in the cytoplasm [62], suggesting active transport of miRNAs into microvesicles. Since it is demonstrated that microvesicles incorporate into target cells and regulate gene expression [62], it is thought that intercellular communication is, among other communication mechanisms, mediated by these microvesicles. Another type of membranous microvesicles are apoptotic bodies. These apoptotic bodies can also contain miRNAs and release them to neighboring cells [55]. Interestingly, there are only a few miRNAs enriched in apoptotic bodies compared to the abundant level of other miRNAs in the cell, e.g. miRNA-21 and -126. This would suggest, along with miRNA enrichment in microvesicles, that there is an active form of transport of certain miRNAs to other cells [55, 56, 62, 64].

An additional mode of miRNA transport is by exosomes, which are smaller nano-sized vesicles that can also export miRNAs to other cell types [56, 65]. Exosomes are released from the cell when a multivesicular body fuses with the plasma membrane [66, 67] (see Figure 1). It was observed that ceramide triggers the formation and release of exosomes [68], which is in contrast to the repression of miRNA export to HDL. Another stimulus that can trigger the extracellular amount of miRNA transported by exosomes, in a dose dependent manner, is an increased intracellular Ca^{2+} concentration [69, 70], mimicked by calcium ionophore A23 [71].

Additionally, there is possibly also a passive release of free miRNAs into the circulation after e.g. cardiomyocyte necrosis. However, which of these modes of transport plays a role under physiological conditions and in states of disease remains to be elucidated. Each mechanism alone or together could play a role in the elevation or decrease of the amount of circulating miRNAs upon stress responses.

Circulating miRNAs in cardiovascular disease

As stated before, several recent studies have shown that miRNAs play a physiological role in cardiovascular homeostasis and in the pathogenesis of cardiovascular diseases (CVD). For comprehensive overviews of the biological role of miRNAs we would like to refer to excellent reviews on target recognition [72], regulatory functions [72–76], and clinical implications [73, 75] in the cardiovascular field. Many miRNAs are known to be up- or down-regulated as a cause or consequence of these pathologic

processes, moreover, upon these stress signals also the extracellular presence of miRNAs is altered and even detectable in body fluids. By using differences in miRNA expression levels, new cardiovascular biomarkers can be discovered and used for diagnostic, prognostic or therapeutic purposes [77, 78]. Several interesting new biomarker candidates have promising potential, including miRNA 423-5p, which is expressed in cardiomyocytes and increased in blood samples from patients having heart failure [50], and miRNA-145, -155, -92a, -17 and -126 which are significantly altered in patients with CAD, compared to healthy controls [79]. Here, we will focus on miRNAs that are identified and could be used for the diagnosis of ACS and thereby monitor myocardial damage.

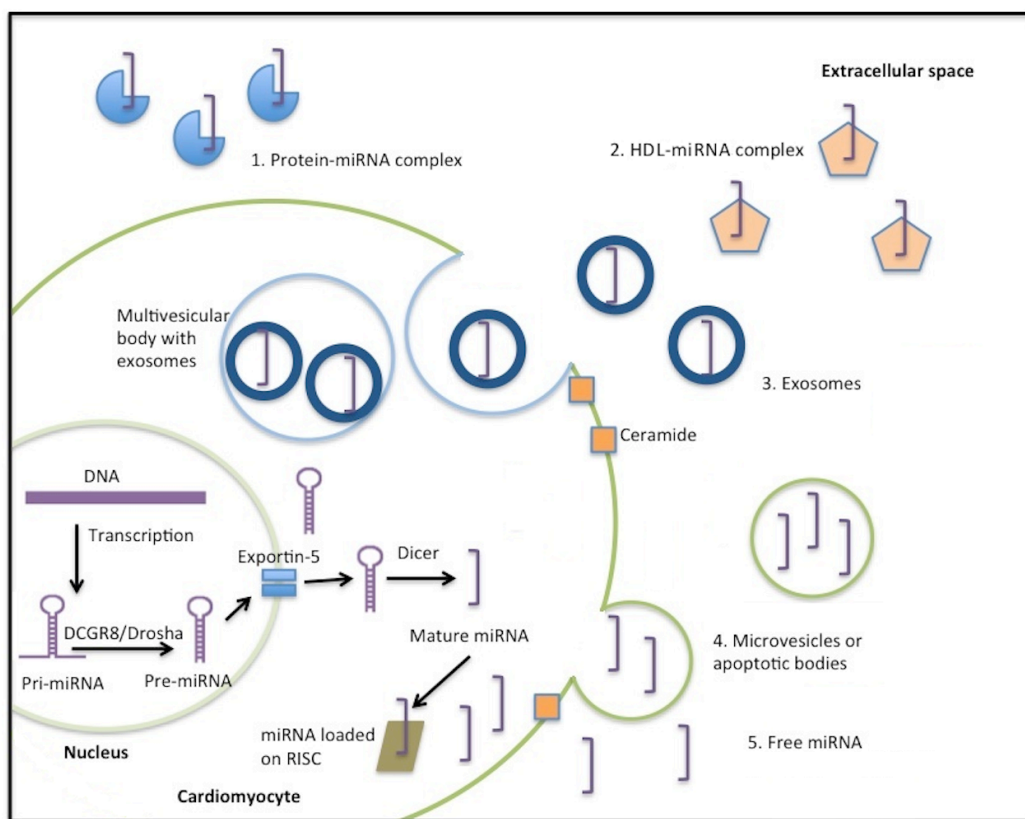


Figure 1. miRNA production, processing, and different modes of transport. Pri-miRNA is transcribed from DNA, processed by DCGR8 and Drosha to pre-miRNA and subsequently transported out of the nucleus by Exportin-5. Dicer processes the pre-miRNA into a single stranded mature miRNA which can be loaded into the RISC complex and thereby will silence mRNA translation. It is thought that normal miRNA function is cytosolic, but precursor and mature miRNAs can also be transported outside the cell via (1) Protein-miRNA complexes, (2) HDL-miRNA complexes, (3) Exosomes which are released when a multivesicular body fuses with the cell membrane, (4) Microvesicles or apoptotic bodies, and (5) Free miRNAs by natural spill or necrosis

Cardiac miRNA expression after MI

Expression pattern studies of myocardial tissue reveal that several miRNAs are up- or down-regulated upon MI [49, 80]. Studies in this field are predominantly performed in murine models, showing deregulation of multiple miRNAs in the border zone of the infarcted area. Of these, miRNA-1, -29b, -126, and -499-5p are down-regulated one week after MI. Interestingly, these miRNAs were all recovered towards baseline expression levels 14 days after MI [81]. In contrast, another study revealed that miRNA-1 and -206 are increasingly elevated in the infarcted ventricle over a period of weeks after MI [82]. A study in mice showed that levels of miRNA-1, -133a, -208a, and -499 were reduced in the infarcted tissue 24 hours (h) after MI compared to healthy sham-operated mice hearts [71]. The reduction of miRNAs in the border zone of the infarction might suggest a release of miRNAs out of the cells upon MI, but could also reflect the remaining viable myocardial tissue.

In confirmation of the results, already shown in mice and rats, studies are performed on miRNA expression after MI in human patient heart samples. It was found that miRNA-1 and -133a/b were down-regulated in infarcted tissue and miRNA-1 was up-regulated in the remote tissue of the heart. In addition, miRNA-150, -186, -208, -210, and -451 levels were increased in infarcted heart tissue and border zone samples, compared to healthy hearts [83–85]. Furthermore, an up-regulation of miRNA-21, -214, and -233 and down-regulation of miRNA-29b and -149 in the border zone of human infarcted myocardium was shown [86].

The shift in miRNA expression is caused by (1) miRNA release from the cells, (2) changes in miRNA production, and (3) posttranscriptional processing. Furthermore, it is demonstrated that MI can induce a specific expression pattern of miRNAs that are directly related and expressed by the myocardium or specifically induced by other cell types upon myocardial damage. These miRNAs can be potential therapeutic targets to reduce myocardial damage [73] and to influence adverse remodeling, but also used as biomarkers in a clinical setting as circulating miRNAs for the diagnosis of MI.

Circulating miRNAs after MI

Up to date, ~20 clinical studies have been performed to investigate whether circulating miRNAs can serve as potential new biomarkers for myocardial infarction (see summary in Table 1). The major goal of these studies was to assess whether miRNAs are suited for diagnosis of MI. Besides the diagnostic value of miRNAs, biological characteristics of the studied miRNAs are sometimes addressed as well. Both spatial

changes [87, 88] and temporal changes are determined, which are of importance for the evaluation of potential new biomarkers and demonstrate the direct causal link to the disease. The different miRNAs studied, which are expressed in several tissues or cell types that are involved upon myocardial damage [89], can be divided into four groups:

1. Myocardium and muscle expressed miRNAs

Probably the most useful biomarker for myocardial damage will be coming from the heart itself and since some muscle specific miRNAs are known, including miRNA-1, -133a/b, -208, and -499 [90–92], these are the most abundantly studied.

miRNA-1

miRNA-1 is expressed both in the myocardium as in skeletal muscles, but most abundantly expressed in cardiomyocytes. The miRNA-1 family consists of miRNA-1-1 and miRNA-1-2 which have the same sequence but are located on different chromosomes (Chr), Chr 20 and 18, respectively [93]. miRNA-1 is well known to play a role in cardiogenesis [94], muscle differentiation [90,94], and cardiac conduction [90, 95, 96]. It is demonstrated that miRNA-1 inhibits both *KCNJ2*, which codes for a K⁺ channel sub-unit Kir2.1, and *GJA1*, coding for connexin 43 gap junction channels [95]. In addition, a relation between cardiac conduction, widening of the QRS-complex, and the expression of miRNA-1 is shown [97].

All studies that measured miRNA-1 expression in the circulation have shown that miRNA-1 is increased in the circulation after STEMI [71, 78, 88, 97–105], NSTEMI [11, 88, 101, 104, 106], and UA [11, 104]. The level of up-regulation differs between study groups. It is reported that miRNA-1 expression levels increased 100-fold to 300-fold within 12 h after the onset of symptoms [98, 100]. In contrast, another study demonstrated only a mild increase of three times, which did not reach significance [99]. Since it is demonstrated that these cardiac miRNAs are correlated with the glomerular filtration rate (GFR) [100], fast renal elimination of miRNA-1 might explain the discrepancy in levels between these studies. In addition, for the muscle-related miRNAs, skeletal muscle turnover can very well influence the baseline values of the circulating miRNAs. An increase in miRNA-1 expression in the circulation after the onset of MI can already be measured within 3 to 4 h after the onset of symptoms [71, 102], even before the peak time and potential detection of cTnT [71, 78] and normalizes to baseline only after three days [98]. Interestingly, another study could not detect an elevation of miRNA-1 already after 15 h [71]. Additionally,

miRNA-1 is correlated with GFR [100], CK-MB [98], and hs-TnT [104], but not with risk-factors such as age, gender, blood pressure, and diabetes mellitus [11]. Overall, the ROC analysis showed AUC values between 0.78 [71] and 0.98 [100], which ranges for a biomarker from reasonable to excellent.

miRNA-133a/b

miRNA-133a and miRNA-133b differ from each other by a single nucleotide [93, 107]. Although these two miRNAs are located on different chromosomes, they are both expressed in smooth muscle cells, skeletal muscle cells, and cardiomyocytes [90]. miRNA-133 is a key regulator of vascular smooth muscle cell proliferation, influencing the progression of atherosclerosis and playing a role in vascular remodeling [77, 90, 96, 108]. Furthermore, miRNA-133 is associated with enhanced myoblast proliferation [90] in skeletal muscles and with cardiogenesis [96] and modulation of cardiac hypertrophy [77] in pathophysiological conditions.

Circulating miRNA-133b expression has been rarely investigated but limited studies that included miRNA-133b [78, 104] found an increased expression after MI for all subgroups of ACS. Circulating miRNA-133a is up-regulated after MI and correlates with the concentration of cTn, suggesting that the release of miRNA-133a is associated with the extent of myocardial damage [87]. This was confirmed by the study of De Rosa *et al.*, in which they explored the trans-coronary gradient of miRNA-133a in the aorta and in the coronary sinus, observing a positive gradient and thereby indicating that miRNA-133a is released from cardiomyocytes in the coronary circulation [87]. Like miRNA-1, miRNA-133 is significantly increased in UA patients as well, although lower as compared to patients presenting with a (N)STEMI [71, 104], possibly explained by less myocardial damage in UA patients. miRNA-133a and miRNA-133b reached their peak levels even before cTnI, which peaked at 3 h [71, 78, 109]. The increased serum presence in time of miRNA-133b remains debatable, since it varies from 33 h [71] up to 90 days [105]. According to Wang *et al.* miRNA-133a is superior to hs-cTnT since it is demonstrated that the concentration of miRNA-133a in suspected patients is not subject to chronic kidney disease [109], and thereby very promising since the weakness of the currently used biomarker cTn, especially the cTnT isoform [110], is the late elevation after MI combined with the low specificity in older patients with chronic kidney disease.

miRNA-208a/b

miRNA-208a is a cardiomyocyte specific miRNA and therefore has gained high interest in diagnosing acute MI [111]. The miRNA-208 family consists of three members; miRNA208a, miRNA-208b and miRNA-499. miRNA-208a and miRNA-208b are both located on Chr 14 and have identical nucleotide sequences of the seed region, the main target recognition site, but have a difference of three nucleotides in the remaining sequence. miRNA-208a is transcribed from an intron in the *Myh6* gene (also known as α -MHC) and is expressed in the heart and miRNA-208b from an intron in the *Myh7* gene (also known as β -MHC) in both heart and skeletal muscle, where they control myosin characteristics and myofibril specifications [87]. Functionally, miRNA-208 plays a role in cardiac fibrosis and cardiomyocyte hypertrophy during stress and hypothyroidism [111]. Moreover, miRNA-208a plays a role in cardiac conduction by regulating, among other proteins, gap junction protein connexin 40 [112].

The findings on miRNA-208a are diverse and several groups were not able to conclusively detect circulating miRNA-208a [11, 78, 100, 106, 113]. It is therefore suggested that miRNA-208a is not a good biomarker, however, we were able to find a significant increase in miRNA-208a levels in NSTEMI patients [11] and not in patients with UA or non-ACS patients. Wang *et al.* found detectable miRNA-208a in 90.9% of patients with MI and not in healthy people or with coronary heart disease without MI [103]. Consistent with these results higher levels of circulating miRNA-208a in (N)STEMI patients compared to patients with UA are shown [104]. In contrast to the disappointing results mentioned before [71, 78], these results demonstrated the discriminative power of miRNA-208a for MI. The ROC analysis showed an AUC of 0.965 which is very close to the AUC of cTn (0.987) [103]. In addition, it has been demonstrated that within 4 h after the onset of symptoms 100% of the MI patients have elevated levels of miRNA-208a, while only 85% of these patients have a cTnT elevation [103]. Subgroup analysis revealed a better specificity and sensitivity for miRNA-208a in patients presenting with chest pain and an initially negative cTn, suggesting an important role for miRNA208a as an early diagnostic biomarker for ACS [103]. A possible explanation for variation in detection of miRNA-208 between different study groups is the variety in the time of sampling (8.5-48 h) after onset of symptoms. It is thought that miRNA-208a is rapidly cleared from circulation and therefore is not detectable at later time points, e.g. 48h.

miRNA-208b is also up-regulated after MI [113], ranging from 1600-fold to [99] 5×10^5 -fold [114] and remained up to 3 days [100]. A difference was also found between STEMI vs. NSTEMI patients with an 8-fold increase of miRNA-208b levels in STEMI patients [114]. In addition, there is a good correlation with

cTn 24 h post-MI [100], suggesting a correlation with myocardial damage. ROC analysis demonstrated an AUC varying from 0.89 [101] to 1[100], suggesting good to excellent accuracy and specificity to diagnose MI.

miRNA-499

As stated before, miRNA-499 is a family member of miRNA-208 and is located in an intron of the *Myh7b* gene and almost exclusively produced in the heart [113], although maybe limited in slow contracting skeletal muscles [92]. miRNA-499 is co-expressed with MYH7B β [41] and regulates the myosin gene and mitochondrial dynamics [41, 115]. Also, miRNA-499 was demonstrated to be involved in cell proliferation and cardiomyocyte differentiation [41] and is therefore proposed as a target for regenerative therapy [116].

Similar as the other muscle-specific miRNAs, miRNA-499 levels were found to be increased between 100-fold [99] and 3000-fold [114] after MI. miRNA-499-5p circulating levels increase in the circulation within a few hours [11] and having a peak time between 6 and 12 h [113] after MI, which is slower compared to cTnI [78]. A positive transcoronary gradient was also demonstrated for miRNA-499, which suggests its release from myocardial cells during MI [87], further supported by the correlation of miRNA-499-5p with cTnT [106], hs-TnT[87, 114], and CK-MB [113].

The ROC of miRNA-499 showed AUC values between 0.822 [103] and 0.97 [114], suggesting that miRNA-499 would be a good diagnostic biomarker. In a subgroup of samples, obtained from patients with initially low levels of cTn, the AUC of miRNA-499-5p was superior to both cTnT and hs-cTnT [11], suggesting that miRNA-499-5p could improve fast diagnosis of MI, although we do not know yet how fast this is detectable post-MI.

Based on these results, miRNA-1, -208, and -499 seem to be good biomarkers for early detection of MI. It is demonstrated that miRNA-1 and -133a, which are co-transcribed and correlated after MI [100], are not up-regulated in other heart diseases [103] and after non-myocardial ischemia such as hindlimb ischemia. However, healthy people might show low levels in their blood of all three miRNAs due to normal muscle turnover [103] and it is demonstrated that in situations of skeletal muscle damage an up-regulation of all three miRNAs could be observed [103, 117], which might give false positive outcomes. miRNA-1, -208, and -499 demonstrate a better diagnostic value compared to miRNA-133 [99, 100], as

shown by the AUC of the ROC analysis curve. For early diagnosis of ACS, a single miRNA as biomarker might not be as powerful as the combination of several miRNAs in a biomarker panel. It is postulated that [118] a multi-marker approach is cost attractive, might increase diagnostic power and provide more insight in the process of myocardial damage after MI. In addition to these muscle-specific miRNAs, e.g. vascular wall- and leukocyte associated miRNAs might add more profound information of underlying mechanisms and an earlier detection of myocardial stress.

2. Vascular wall expressed miRNAs

Since vascular changes and stress signals are also following MI, miRNAs associated with the vasculature might be of interest to add to the cardiac specific miRNAs, e.g. miRNA-126 [119], miRNA-92a [49], and miRNA-145 [120].

miRNA-126

miRNA-126 is located on Chr 9 and is highly expressed in endothelial cells where it is found to modulate both vasculogenesis and angiogenesis [121, 122]. Moreover, miR-126 regulates the turnover of vascular smooth muscle cells and plays a role in the protection against atherosclerotic lesion development in ApoE knockout mice [55, 123].

Circulating levels of miRNA-126 are down regulated post-MI, as compared to healthy subjects [102], and these levels correlate with the time trend seen in cTnI expression [102]. Down-regulation is already seen 4 h after the onset of symptoms and reaches its lowest point after 24 h, after which miRNA-126 normalizes and reaches a second low point again after one week. This suggests that it is also involved in later phases post-MI, like inflammation or angiogenesis that usually follow MI.

Interestingly, a 5-fold increase in the expression of miRNA-126 is found in blood sample taken from the aortic bulb [87]. In their trans-coronary experiments, they observed a further decrease in levels of circulating miRNA-126 within the coronary system as compared to the aortic bulb, and this decrease was related to the amount of cardiac damage. This would suggest a form of 'consumption' of miRNA-126 in the coronary arteries after MI [87] and possibly in the arterial- and venous system as well, which is possibly explained by an increased uptake of miRNA-126 in blood vessels after MI thereby referring to an active signaling cascade.

Table 1. Overview of clinical studies describing the role of circulating miRNAs as diagnostic biomarkers for ACS.

Ref	Major findings	ROC (AUC)	Patients	Controls	h after onset symptoms
[113]	miRNA-499 in AMI patients ↑, correlated with CK-MB in AMI	-	14; 9 AMI, 5UA	10; Healthy	< 48h
[97]	miRNA-1 ↑, correlated with widening of QRS-complex	0.77	93; AMI, age 58.2 (+/- 10.2) years, 67 M	66; Healthy, age 55.1 (+/- 9.6 years, 39 M)	On admission
[98]	miRNA-1 ↑, 20x within 24h, correlated with CK-MB	-	31; STEMI, age 57 (+/- 10.1) years, 18 M	20; Healthy, age and sex matched	<9h
[99]	miRNA-208b ↑, 1600x, correlated with troponin T and CPK. miRNA-499 ↑, 100x, correlated with troponin T and CPK. miRNA-133a ↑ miRNA-223 ↓	0.94 0.92	32; AMI (STEMI)	36; Atypical chest pain	<12h
[78]	miRNA-1 ↑, 48x miRNA-133a/b ↑, 5426x/312x miRNA-499-5p ↑, 299x miRNA-122 ↓ miRNA-375 ↓ miRNA-208a only detectable in 3 out of 9 patients	-	25 STEMI (I) and 8; STEMI (II) with troponin comparison	17; Healthy	I: <9h II: <3h
[87]	miRNA-133a ↑ 11x in aorta, correlated with hs-cTn T miRNA-208a ↑ 5x in aorta miRNA-499a ↑ 20x in aorta, correlated with hs-cTn T miRNA-92a ↑ 5x in aorta miRNA-126 ↑ 2x in aorta	-	19; ACS with hsTnT > 100pg/ml.	7; Stable CAD, normal hsTnT	-
[114]	miRNA-208b ↑, correlated with cTnT and CK, STEMI<NSTEMI miRNA-499 ↑, correlated with cTnT and CK, STEMI<NSTEMI	0.69 0.97 0.97	113; NSTEMI and 397; STEMI	87; Healthy	-
[100]	miRNA-1 ↑ 300x, correlates with GFR and are detectable in urine miRNA-133a ↑ 70x, correlates with GFR and are detectable in urine miRNA-208b ↑ 3000x, correlates with EF and troponin on day 1 miRNA-499-5p ↑ 250x	0.98 1.00 0.86 0.99 (Onset <12hr)	25; STEMI(20 M, age 64.75 +/- 2.70 years old)	11; Healthy (7 M, age 65.09 +/- 3.51 years old)	<24h.
[88]	miRNA-1 ↑ and correlated with LVEF miRNA-208b ↑ and correlated with LVEF miRNA-499-5p ↑ and correlated with LVEF	0.82 0.79 0.95	424; Suspected ACS pain (STEMI, NSTEMI)	-; Suspected ACS-> non-MI	<24h (for 71%)
[71]	miRNA-1 ↑ correlates with cTnT. miRNA-133a ↑ correlates with cTnT. miRNA-208a only detectable in 5.6% of patients	0.78 0.93	29; ACS(23 M, age 69.7 +/- 2.4 years old)	42; Non-ACS (24 M, 69.2 +/- 2.2 years old)	<24h
[101]	miRNA-1 ↑ 3x miRNA-133a ↑ 5x miRNA-208b ↑ 50x miRNA-499 ↑ 10x no difference in miRNA level between STEMI and NSTEMI	0.83	67; AMI, (44 STEMI, 23 NSTEMI)(age 63.84 +/- 11.17) years, 52 M)	32; Healthy (age 61.75 (+/- 9.58) years, 22 M)	<12h
[102]	miRNA-1 ↑ 15x exhibited same trend as cTnI miRNA-126 ↓ exhibited same trend as cTnI	0.92 0.86	17; AMI, transmural (age 53 +/- 12.5) years, 13 M)	25; Healthy (age 51 (+/- 12.3) years, 18 M)	< 4h
[132]	miRNA-30a ↑ after 8h, 10x miRNA-195 ↑ after 8h, 10x miRNA-let-7b ↓ Samples <4h no significant difference vs. controls.	0.93 0.89 0.85	18; AMI, transmural (age 55 +/- 11.4) years, 13 M)	30; Healthy (age 50 +/- 12.3 years, 17 M)	<4h
[10]	121 miRNAs significantly different AMI vs. non-AMI (37% up-regulated, 63% down-regulated) miRNA-21 not up-regulated compared to control group miRNA-145, -30c correlate up to 0.71 with cTnT	0.77 0.91 0.94 Combined 20: 0.99	20; STEMI(age 59.3 (+/- 14) years, 16 M)	20; Routine CAG (age 63.3 +/- (14.8 years), 14 M), healthy	<3h
[11]	miRNA-1 ↑ 10x, miRNA-208a ↑ 2x miRNA-499 ↑ 20x miRNA-21 ↑ 12x miRNA-146a ↑ 19x Elevation of studied miRNAs for total group and initially hs- cTnT-negative subgroup miRNA-1, -499, -21 AUC ↑ on top of clinical model and hs-TnT	Single miRNA< hs-TnT miRNA+hsTnT> hsTnT <i>trop neg. subgroup:</i> single miRNA> hs-TnT combined miRNA>single miRNA	106; NSTEMI and Unstable angina(age 68.7 (+/-12.6) years, 70 M)	226; Chest pain, no ACS (age 60.2 (+/- 14.3) years, 120 M)	<4h
[106]	miRNA-1 ↑ NSTEMI vs control miRNA-21 ↑ NSTEMI vs control vs. CHF miRNA-133a ↑ NSTEMI vs control miRNA-423-5p ↑ NSTEMI vs control miRNA-499-5p ↑ NSTEMI vs control vs. CHF, correlates with cTnT and discriminative power is comparable miRNA-208a excluded due to low detection levels	AMI vs acute CHF: 0.86 hs-TnT: 0.70	92; NSTEMI (age 82.6 (+/-6.9) years, 39M)	81; Acute heart failure & healthy age matched controls	<6h
[109]	miRNA-133 ↑ in plasma 4x, correlated with cTnI miRNA-328 ↑ in plasma 11x, correlated with cTnI	<i>Whole blood/plasma</i> 0.70/0.89 0.81/0.87	51; AMI	28; Healthy	<24h
[103]	miRNA-1 ↑ AMI vs. CVD and healthy miRNA-133a ↑ AMI vs. CVD and healthy miRNA-499 ↑ AMI vs. CVD and healthy miRNA-208a ↑ AMI vs. CVD and healthy, only in samples from AMI miRNA-16, -451: no difference	0.97 0.82 0.85 0.87	33; AMI	66; Chest pain (CVD n=33), Healthy n=30	<6h
[104]	miRNA-1 ↑ (N)STEMI vs UA (overlap), associated with hs-TnT miRNA-133a ↑ (N)STEMI vs. UA (overlap), associated with hs-TnT miRNA-208b ↑ (N)STEMI vs. UA (overlap), associated with hs-TnT	-	444; ACS (age 55-73 years) 336 M	-	On admission
[105]	Correlation between miRNA-92a and LV-EDV.	-	12; MI(age 61 +/- 2 years, 5 M)	12; Healthy (age 58 +/- 3 years, 9 M)	On admission

miRNA92a and miRNA-145

Circulating miRNA-92a is located on Chr 13 and controls angiogenesis as described in mouse models [49]. Like miRNA-126, circulating miRNA-92a seems to be up-regulated two-fold after MI in the aortic bulb blood sample, compared to people with stable coronary artery disease. A similar decrease in gradient of this miRNA was seen in the trans-coronary experiment, although it did not reach statistical significance [87].

Circulating miRNA-145 plays a role in the differentiation of vascular smooth muscle cells and represses their proliferation [120]. After MI, an increase in miRNA-145 levels is observed, which might be related to plaque rupture and vessel injury [10], which is correlated with cTnT (0.71).

Although differently expressed, both miRNA -92a and miRNA-126 would not serve as good biomarkers since a decrease in abundance is more difficult to detect as an increase in a general patient population. In addition, the AUC of miRNA-126 is not as good as studies have shown for cTn. In order to determine the clinical diagnostic value for miRNA-145 as a biomarker, more research is necessary.

3. Leukocyte and platelet expressed miRNAs

miRNAs associated with circulating leukocytes, such as miRNA-146 and -155, can be valuable for the diagnosis of MI since e.g. peripheral blood monocytes are involved in plaque stability, plaque rupture, and have a role in early inflammation after MI [124], and therefore may be monitors of early stress and for myocardial damage [51].

To our knowledge several miRNAs are associated with platelets and are functional released upon MI, thereby taken up by endothelial cells and affect their cellular behavior [125], these include miRNA-21, -22, -24, -34, -126, -185, -191, -197, -223, -320b, and -423-5p.

miRNA-146, miRNA-155 and miRNA-223

miRNA-155 is located on Chr 21 and present in activated macrophages [126]. Additionally, miRNA-155 is expressed in several other cell types [127], playing a role in the Ig class switch of B-lymphocytes [128], or is involved in cell death, by improving cell survival and modulating protease activity [129, 130]. miRNA-233 is located on Chr X [93, 107] and is involved in several processes, e.g. progenitor cell proliferation, granulocyte function [131], and attenuation of inflammation [132]. Furthermore, a micro-

array on myocardial tissue after ischemia reperfusion injury revealed that miRNA-223 is up-regulated after 1 and 3 days and correlates with the inflammatory response. Besides its expression in leukocytes, miRNA-223 is also highly enriched in platelets [132]. In the study of De Rosa *et al.* miRNA-155 and -223 levels were modestly, not statistically significant, elevated after MI [85]. Corsten *et al.* found a statistically significant decrease of miRNA-223 in AMI patients [99]. Both studies did not find an association of miRNA-223 with cTn [87, 99], also miRNA-155 was not associated with circulating cTn [87].

miRNA-146 is located on Chr 5 and involved in the inflammatory response of leukocytes, its expression can be induced by LPS and it regulates Toll Like Receptor (TLR) and cytokine signaling [133]. We have observed that circulating miRNA-146a levels were increased 11.7-fold 3.2 h after MI [11] and apparently more elevated in NSTEMI patients compared to UA. In a subgroup of 152 patients, who presented in the hospital within 3 h after the start of complains, the miRNA-146a concentration was already elevated [11]. In addition, in the hs-cTnT-negative subgroup of 194 patients, miRNA-146a was significantly elevated, suggesting that miRNA-146a is an earlier biomarker than hs-cTnT for myocardial damage, however, when three miRNAs, miRNA-1, -21, and -499, are taken together to diagnose MI, miRNA146a does not add any additional diagnostic value for hs-cTnT negative patients [11].

Up to now, although miRNAs associated with leukocytes are increased upon MI their predictive value seems to add little to muscle cell related miRNAs for the diagnosis of MI.

miRNA-21

miRNA-21 is located on Chr 17 and plays a role in the regulation of cardiac hypertrophy, where miRNA-21 is down-regulated compared to healthy hearts [134], moreover, it plays a role in the formation of cardiac fibrosis by influencing the ERK-MAP kinase signaling pathway [135].

Circulating miRNA-21 was elevated 18.9-fold after MI and also detectable in the hs-cTnT negative subgroup, moreover, miRNA-21 was elevated even within 3 h after the onset of symptoms [11]. At day 2 post-MI, the levels of miRNA-21 decreased but surprisingly increased again at day 5. At day 90 the concentration had returned to baselines [105]. The individual ROC of miRNA-21 had an AUC of 0.76 and is thereby lower than cTn or hs-cTnT. However, combined with miRNA-499 and -1, miRNA-21 adds diagnostic value (AUC 0.89) compared to hs-cTnT (0.86) [11]. Therefore, miRNA-21 does have an advantage at early time points after MI when cTn is not detectable yet.

4. Other miRNAs

Besides the most abundantly studied miRNAs described above, relatively new miRNAs are discovered due to high throughput micro-array screening, e.g. miRNA-122, -145, -375, -663b, and -1291 [10, 78, 113]. After MI, miRNA-122 and -375 are down-regulated and reach their minimum at approximately 1-2 days after onset of symptoms [78]. Furthermore, a selection of miRNAs (both up- and down-regulated) can be combined for a higher discriminative and diagnostic power, but still need validation in large patient cohorts to elucidate their role as diagnostic biomarkers.

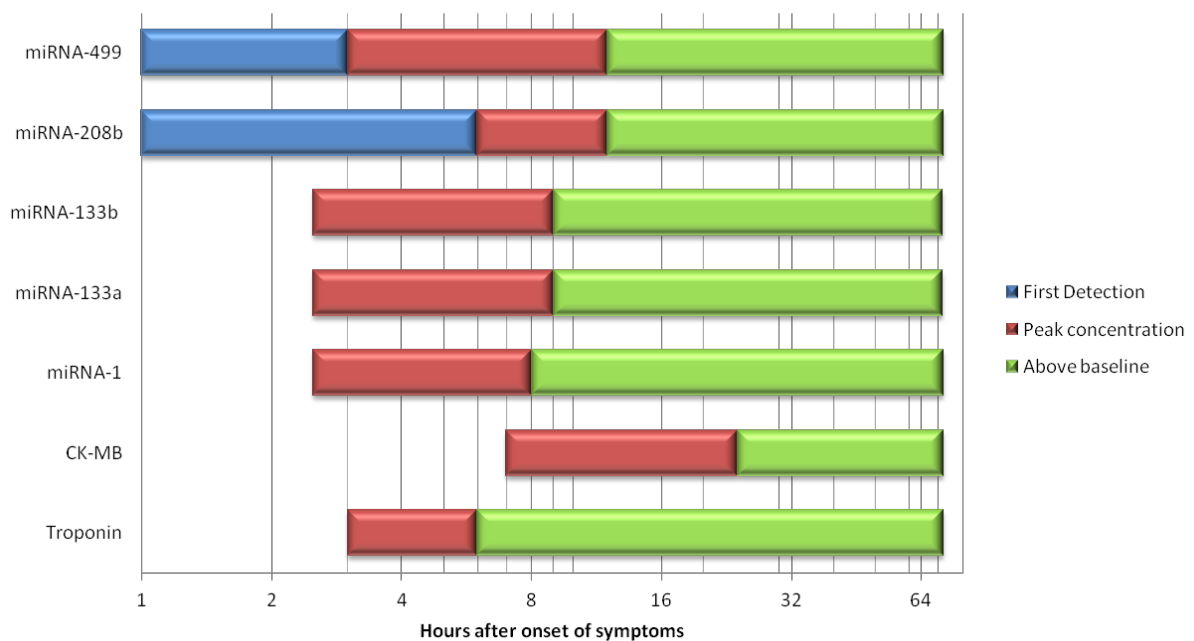


Figure 2. Detection of miRNAs after MI. The moment of first detection (blue), peak range (red), and concentration above baseline level (green) in hours after MI [11, 71, 78, 102, 113, 114], compared to cTn and CK-MB [18, 137].

Discussion

miRNAs play an important role in almost all cellular processes and are involved in the initiation and progression of different cardiovascular diseases where they are deregulated in both tissue as well as extracellular fluids. Although miRNAs are well known for their complex working mechanism, targeting multiple genes in different types of tissue, the specific expression patterns of circulating miRNAs in CVD, their stability and early release from e.g. cardiomyocytes into the circulation make them extremely suitable as biomarkers for ACS. The release of cardiac tissue specific miRNAs have a possible functional advantage compared to non-cardiac tissue specific miRNAs, however, both can be used as biomarkers of ACS when proved specific.

Compared to cTn, the biochemical golden standard for diagnosis of ACS, miRNAs are detectable in the circulation at an earlier timepoint after MI. cTn is part of the myofibrillar apparatus, being large protein complexes, whereas the majority of miRNAs are also protein bound, but relatively smaller and are released in a controlled way, which can explain the time difference in release after MI (Figure 2). miRNAs can be released more quickly, which benefits early MI diagnosis and revascularization therapy.

Although miRNAs as early biomarkers for ACS appear to be very promising, the translation of these markers from bench to bedside is delayed by some limitation, e.g. the currently used study populations and the time needed for RNA detection. From these, the major drawback for using miRNAs as biomarkers for clinical diagnosis of ACS is their laborious isolation and detection procedures. Compared to the detection of cTn, which is an ELISA based method, circulating miRNAs are detected based on PCR techniques which is very time consuming, and for that reason, cTn is still the best biomarker in clinical practice. In order to decrease the time of uncertainty until the diagnosis, there is an urgent need for further technical development of miRNA detection in non-classical RNA detection approaches.

Another limitation is that most of the clinical studies included small numbers of patients, usually using healthy controls as references and displayed a large variation in the time of blood sampling after MI and in isolation and detection methods to analyze miRNAs. The use of a healthy control group is debatable since a biomarker for MI should discriminate between patients presenting to daily clinical practice, e.g. at the emergency department with chest pain caused by ACS or non-ACS. It is demonstrated that in the majority of the clinical studies, the discriminative power of a single miRNA is still lower compared to cTn, possibly caused by the type of study group, study group size, and unstandardized methods.

Fortunately, three studies did investigate miRNAs of patients with chest pain suspicious for MI presenting at the emergency department [11, 99, 103]. In a cumulative comparison of multiple miRNAs an increased specificity and sensitivity for the diagnosis of MI is shown [11, 136]. Even in combination with hs-cTnT and a clinical model, including patient history and cardiovascular risk factors, miRNAs add discriminative power, which support the notion that circulating miRNAs can be used as independent early diagnostic markers for ACS [86], with an advantage compared to hs-cTnT for the patients presenting with chest pain suspicious for ACS with an initial negative troponin [11]. The combined assessment of multiple circulating miRNAs together with cTn could be used to increase specificity and sensitivity and accelerate MI diagnosis. A deliberately chosen selection of miRNAs, e.g. muscle, vascular wall-, and leukocyte associated miRNAs, can increase diagnostic power. A panel like this should contain miRNAs, both up- and down-regulated, that embodies the full mechanism of myocardial damage and subsequent inflammatory and reparative process, thereby optimizing diagnostic power of miRNAs for early diagnosis of ACS.

In conclusion, circulating miRNAs as biomarkers for ACS holds great potential. Up to date, ~20 studies are performed which show an early up-regulation of muscle specific miRNAs after MI, related to the extent of myocardial damage with clear discriminating and diagnostic power. Currently investigated miRNAs for early diagnosis of MI should be validated in larger patient cohorts and the additional value of new biomarker candidates from micro-array discoveries need to be elucidated.

Acknowledgements

We acknowledge the support from “Stichting Swaeneborgh” and the Netherlands CardioVascular Research Initiative: the Dutch Heart Foundation, Dutch Federation of University Medical Centers, the Netherlands Organization for Health Research and Development and the Royal Netherlands Academy of Sciences.

References

1. Go AS, Mozaffarian D, Roger VL, et al. Heart disease and stroke statistics--2013 update: a report from the American Heart Association. *Circulation* 2013;127:e6–e245.
2. Thygesen K, Alpert JS, Jaffe AS, et al. Third universal definition of myocardial infarction. *Eur Heart J* 2012;33:2551–67.
3. Anderson JL, Adams CD, Antman EM, et al. 2012 ACCF/AHA Focused Update Incorporated Into the ACCF/AHA 2007 Guidelines for the Management of Patients With Unstable Angina/Non-ST-Elevation Myocardial Infarction: A Report of the American College of Cardiology Foundation/American Heart Association Task Force on Practice Guidelines. *J Am Coll Cardiol* 2013;61:e179–347.
4. Oerlemans MIFJ, Liu J, Arslan F, et al. Inhibition of RIP1-dependent necrosis prevents adverse cardiac remodeling after myocardial ischemia-reperfusion in vivo. *Basic Res Cardiol* 2012;107:270.
5. Oerlemans MIFJ, Koudstaal S, Chamuleau SA, de Kleijn DP, Doevendans PA, Sluijter JPG. Targeting cell death in the reperfused heart: pharmacological approaches for cardioprotection. *Int J Cardiol* 2013;165:410–22.
6. Bodor GS, Porter S, Landt Y, Ladenson JH. Development of monoclonal antibodies for an assay of cardiac troponin-I and preliminary results in suspected cases of myocardial infarction. *Clin Chem* 1992;38:2203–2214.
7. Cummins B, Auckland ML, Cummins P. Cardiac-specific troponin-I radioimmunoassay in the diagnosis of acute myocardial infarction. *Am Heart J* 1987;113:1333–1344.
8. Hamm CW, Goldmann BU, Heeschen C, Kreyman G, Berger J, Meinertz T. Emergency room triage of patients with acute chest pain by means of rapid testing for cardiac troponin T or troponin I. *N Engl J Med* 1997;337:1648–1653.
9. Liebetrau C, Mollmann H, Nef H, et al. Release kinetics of cardiac biomarkers in patients undergoing transcatheter ablation of septal hypertrophy. *Clin Chem* 2012;58:1049–1054.
10. Meder B, Keller A, Vogel B, et al. MicroRNA signatures in total peripheral blood as novel biomarkers for acute myocardial infarction. *Basic Res Cardiol* 2011;106:13–23.
11. Oerlemans MI, Mosterd A, Dekker MS, et al. Early assessment of acute coronary syndromes in the emergency department: the potential diagnostic value of circulating microRNAs. *EMBO Mol Med* 2012;4:1176–1185.
12. Keller T, Zeller T, Peetz D, et al. Sensitive troponin I assay in early diagnosis of acute myocardial infarction. *N Engl J Med* 2009;361:868–77.
13. Reiter M, Twerenbold R, Reichlin T, et al. Early diagnosis of acute myocardial infarction in the elderly using more sensitive cardiac troponin assays. *Eur Heart J* 2011;32:1379–1389.
14. de Lemos JA, Drazner MH, Omland T, et al. Association of troponin T detected with a highly sensitive assay and cardiac structure and mortality risk in the general population. *JAMA* 2010;304:2503–2512.
15. Eggers KM, Lind L, Ahlstrom H, et al. Prevalence and pathophysiological mechanisms of elevated cardiac troponin I levels in a population-based sample of elderly subjects. *Eur Heart J* 2008;29:2252–2258.
16. Grande P, Hansen BF, Christiansen C, Naestoft J. Acute myocardial infarct size estimated by serum CK-MB determinations: clinical accuracy and prognostic relevance utilizing a practical modification of the isoenzyme approach. *Am Heart J* 1981;101:582–586.
17. Alpert JS, Thygesen K, Antman E, Bassand JP. Myocardial infarction redefined--a consensus document of The Joint European Society of Cardiology/American College of Cardiology Committee for the redefinition of myocardial infarction. *J Am Coll Cardiol* 2000;36:959–969.
18. de Winter RJ, Koster RW, Sturk A, Sanders GT. Value of myoglobin, troponin T, and CK-MB mass in ruling out an acute myocardial infarction in the emergency room. *Circulation* 1995;92:3401–3407.
19. Ishii J, Wang JH, Naruse H, et al. Serum concentrations of myoglobin vs human heart-type cytoplasmic fatty acid-binding protein in early detection of acute myocardial infarction. *Clin Chem* 1997;43:1372–1378.
20. Freund Y, Chenevier-Gobeaux C, Leumani F, et al. Heart-type fatty acid binding protein and the diagnosis of acute coronary syndrome in the ED. *Am J Emerg Med* 2012;30:1378–1384.
21. James SK, Oldgren J, Lindback J, Johnston N, Siegbahn A, Wallentin L. An acute inflammatory reaction induced by myocardial damage is superimposed on a chronic inflammation in unstable coronary artery disease. *Am Heart J* 2005;149:619–626.
22. Morita E, Yasue H, Yoshimura M, et al. Increased plasma levels of brain natriuretic peptide in patients with acute myocardial infarction. *Circulation* 1993;88:82–91.
23. Afzali D, Erren M, Pavenstadt HJ, et al. Impact of copeptin on diagnosis, risk stratification, and intermediate-term prognosis of acute coronary syndromes. *Clin Res Cardiol* 2013.

24. Peacock F, Morris DL, Anwaruddin S, et al. Meta-analysis of ischemia-modified albumin to rule out acute coronary syndromes in the emergency department. *Am Heart J* 2006;152:253–262.
25. Lindahl B. Acute coronary syndrome - the present and future role of biomarkers. *Clin Chem Lab Med* 2013;1–8.
26. Tijssen AJ, Pinto YM, Creemers EE. Circulating microRNAs as diagnostic biomarkers for cardiovascular diseases. *Am J Physiol Heart Circ Physiol* 2012;303:H1085-95.
27. Li C, Pei F, Zhu X, Duan DD, Zeng C. Circulating microRNAs as novel and sensitive biomarkers of acute myocardial Infarction. *Clin Biochem* 2012;45:727–732.
28. Cogswell JP, Ward J, Taylor IA, et al. Identification of miRNA changes in Alzheimer's disease brain and CSF yields putative biomarkers and insights into disease pathways. *J Alzheimers Dis* 2008;14:27–41.
29. Park NJ, Zhou H, Elashoff D, et al. Salivary microRNA: discovery, characterization, and clinical utility for oral cancer detection. *Clin Cancer Res* 2009;15:5473–5477.
30. Mitchell PS, Parkin RK, Kroh EM, et al. Circulating microRNAs as stable blood-based markers for cancer detection. *Proc Natl Acad Sci U S A* 2008;105:10513–8.
31. Zubakov D, Boersma AW, Choi Y, van Kuijk PF, Wiemer EA, Kayser M. MicroRNA markers for forensic body fluid identification obtained from microarray screening and quantitative RT-PCR confirmation. *Int J Legal Med* 2010;124:217–226.
32. Chen X, Ba Y, Ma L, et al. Characterization of microRNAs in serum: a novel class of biomarkers for diagnosis of cancer and other diseases. *Cell Res* 2008;18:997–1006.
33. Lagos-Quintana M, Rauhut R, Lendeckel W, Tuschl T. Identification of novel genes coding for small expressed RNAs. *Science* 2001;294:853–8.
34. Lytle JR, Yario TA, Steitz JA. Target mRNAs are repressed as efficiently by microRNA-binding sites in the 5' UTR as in the 3' UTR. *Proc Natl Acad Sci U S A* 2007;104:9667–9672.
35. Pillai RS, Bhattacharyya SN, Artus CG, et al. Inhibition of translational initiation by Let-7 MicroRNA in human cells. *Science* 2005;309:1573–1576.
36. Wu L, Fan J, Belasco JG. MicroRNAs direct rapid deadenylation of mRNA. *Proc Natl Acad Sci U S A* 2006;103:4034–4039.
37. Bartel DP. MicroRNAs: genomics, biogenesis, mechanism, and function. *Cell* 2004;116:281–297.
38. Ghildiyal M, Zamore PD. Small silencing RNAs: an expanding universe. *Nat Rev* 2009;10:94–108.
39. Winter J, Jung S, Keller S, Gregory RI, Diederichs S. Many roads to maturity: microRNA biogenesis pathways and their regulation. *Nat Cell Biol* 2009;11:228–234.
40. Guo H, Ingolia NT, Weissman JS, Bartel DP. Mammalian microRNAs predominantly act to decrease target mRNA levels. *Nature* 2010;466:835–840.
41. Sluijter JPG, van Mil A, van Vliet P, et al. MicroRNA-1 and -499 regulate differentiation and proliferation in human-derived cardiomyocyte progenitor cells. *Arterioscler Thromb Vasc Biol* 2010;30:859–68.
42. Kota J, Chivukula RR, O'Donnell KA, et al. Therapeutic microRNA delivery suppresses tumorigenesis in a murine liver cancer model. *Cell* 2009;137:1005–1017.
43. Lin CJ-F, Gong H-Y, Tseng H-C, Wang W-L, Wu J-L. miR-122 targets an anti-apoptotic gene, Bcl-w, in human hepatocellular carcinoma cell lines. *Biochem Biophys Res Commun* 2008;375:315–20.
44. Calin GA, Dumitru CD, Shimizu M, et al. Frequent deletions and down-regulation of micro- RNA genes miR15 and miR16 at 13q14 in chronic lymphocytic leukemia. *Proc Natl Acad Sci U S A* 2002;99:15524–15529.
45. Murakami Y, Toyoda H, Tanaka M, et al. The progression of liver fibrosis is related with overexpression of the miR-199 and 200 families. *PLoS One* 2011;6:e16081.
46. Chen JF, Murchison EP, Tang R, et al. Targeted deletion of Dicer in the heart leads to dilated cardiomyopathy and heart failure. *Proc Natl Acad Sci U S A* 2008;105:2111–2116.
47. Madrigal-Matute J, Rotllan N, Aranda JF, Fernandez-Hernando C. MicroRNAs and atherosclerosis. *Curr Atheroscler Rep* 2013;15:322–013–0322-z.
48. Rayner KJ, Suarez Y, Davalos A, et al. MiR-33 contributes to the regulation of cholesterol homeostasis. *Science* 2010;328:1570–1573.
49. Bonauer A, Carmona G, Iwasaki M, et al. MicroRNA-92a controls angiogenesis and functional recovery of ischemic tissues in mice. *Science* 2009;324:1710–1713.
50. Tijssen AJ, Creemers EE, Moerland PD, et al. MiR423-5p as a circulating biomarker for heart failure. *Circ Res* 2010;106:1035–1039.
51. Hoekstra M, van der Lans CAC, Halvorsen B, et al. The peripheral blood mononuclear cell microRNA signature of coronary artery disease. *Biochem Biophys Res Commun* 2010;394:792–7.
52. Lu J, Getz G, Miska EA, et al. MicroRNA expression profiles classify human cancers. *Nature* 2005;435:834–838.

53. Liu CG, Calin GA, Meloon B, et al. An oligonucleotide microchip for genome-wide microRNA profiling in human and mouse tissues. *Proc Natl Acad Sci U S A* 2004;101:9740–9744.
54. Hanke M, Hoefig K, Merz H, et al. A robust methodology to study urine microRNA as tumor marker: microRNA-126 and microRNA-182 are related to urinary bladder cancer. *Urol Oncol* 2010;28:655–661.
55. Zernecke A, Bidzhekov K, Noels H, et al. Delivery of microRNA-126 by apoptotic bodies induces CXCL12-dependent vascular protection. *Sci Signal* 2009;2:ra81.
56. Valadi H, Ekström K, Bossios A, Sjöstrand M, Lee JJ, Lötvall JO. Exosome-mediated transfer of mRNAs and microRNAs is a novel mechanism of genetic exchange between cells. *Nat Cell Biol* 2007;9:654–9.
57. Xu L, Yang BF, Ai J. MicroRNA transport: A new way in cell communication. *J Cell Physiol* 2013;228:1713–1719.
58. Arroyo JD, Chevillet JR, Kroh EM, et al. Argonaute2 complexes carry a population of circulating microRNAs independent of vesicles in human plasma. *Proc Natl Acad Sci U S A* 2011;108:5003–8.
59. Wang K, Zhang S, Weber J, Baxter D, Galas DJ. Export of microRNAs and microRNA-protective protein by mammalian cells. *Nucleic Acids Res* 2010;38:7248–59.
60. Vickers KC, Palmisano BT, Shoucri BM, Shamburek RD, Remaley AT. Mi1. Vickers KC, Palmisano BT, Shoucri BM, Shamburek RD, Remaley AT. MicroRNAs are transported in plasma and delivered to recipient cells by high-density lipoproteins. *Nat Cell Biol* 2011;13:423–33. croRNAs are transported in plasma and delivered to recipie. *Nat Cell Biol* 2011;13:423–33.
61. Wagner J, Riwanto M, Besler C, et al. Characterization of Levels and Cellular Transfer of Circulating Lipoprotein-Bound MicroRNAs. *Arterioscler Thromb Vasc Biol* 2013;33:1392–1400.
62. Collino F, Deregibus MC, Bruno S, et al. Microvesicles derived from adult human bone marrow and tissue specific mesenchymal stem cells shuttle selected pattern of miRNAs. *PLoS One* 2010;5:e11803.
63. El-Hefnawy T, Raja S, Kelly L, et al. Characterization of amplifiable, circulating RNA in plasma and its potential as a tool for cancer diagnostics. *Clin Chem* 2004;50:564–573.
64. Guduric-Fuchs J, O'Connor A, Camp B, O'Neill CL, Medina RJ, Simpson DA. Selective extracellular vesicle-mediated export of an overlapping set of microRNAs from multiple cell types. *BMC Genomics* 2012;13:357.
65. Stoorvogel W. Functional transfer of microRNA by exosomes. *Blood* 2012;119:646–648.
66. Keller S, Sanderson MP, Stoeck A, Altevogt P. Exosomes: from biogenesis and secretion to biological function. *Immunol Lett* 2006;107:102–8.
67. Théry C. Exosomes: secreted vesicles and intercellular communications. *F1000 Biol Rep* 2011;3:15.
68. Kosaka N, Iguchi H, Yoshioka Y, Takeshita F, Matsuki Y, Ochiya T. Secretory mechanisms and intercellular transfer of microRNAs in living cells. *J Biol Chem* 2010;285:17442–17452.
69. Savina A, Furlan M, Vidal M, Colombo MI. Exosome release is regulated by a calcium-dependent mechanism in K562 cells. *J Biol Chem* 2003;278:20083–20090.
70. Savina A, Fader CM, Damiani MT, Colombo MI. Rab11 promotes docking and fusion of multivesicular bodies in a calcium-dependent manner. *Traffic* 2005;6:131–143.
71. Kuwabara Y, Ono K, Horie T, et al. Increased microRNA-1 and microRNA-133a levels in serum of patients with cardiovascular disease indicate myocardial damage. *Circ Cardiovasc Genet* 2011;4:446–54.
72. Bartel DP. MicroRNAs: target recognition and regulatory functions. *Cell* 2009;136:215–233.
73. Weber C. MicroRNAs: from basic mechanisms to clinical application in cardiovascular medicine. *Arterioscler Thromb Vasc Biol* 2013;33:168–169.
74. Mendell JT, Olson EN. MicroRNAs in stress signaling and human disease. *Cell* 2012;148:1172–1187.
75. Fiedler J, Thum T. MicroRNAs in myocardial infarction. *Arterioscler Thromb Vasc Biol* 2013;33:201–205.
76. He L, Hannon GJ. MicroRNAs: small RNAs with a big role in gene regulation. *Nat Rev* 2004;5:522–531.
77. Care A, Catalucci D, Felicetti F, et al. MicroRNA-133 controls cardiac hypertrophy. *Nat Med* 2007;13:613–618.
78. D'Alessandra Y, Devanna P, Limana F, et al. Circulating microRNAs are new and sensitive biomarkers of myocardial infarction. *Eur Heart J* 2010;31:2765–73.
79. Fichtlscherer S, Rosa S De, Fox H, et al. Circulating microRNAs in patients with coronary artery disease. *Circ Res* 2010;107:677–684.
80. Fiedler J, Jazbutyte V, Kirchmaier BC, et al. MicroRNA-24 regulates vascularity after myocardial infarction. *Circulation* 2011;124:720–730.
81. Shi B, Guo Y, Wang J, Gao W. Altered expression of microRNAs in the myocardium of rats with acute myocardial infarction. *BMC Cardiovasc Disord* 2010;10:11.
82. Shan ZX, Lin QX, Fu YH, et al. Upregulated expression of miR-1/miR-206 in a rat model of myocardial

- infarction. *Biochem Biophys Res Commun* 2009;381:597–601.
83. Bostjancic E, Zidar N, Glavac D. MicroRNA microarray expression profiling in human myocardial infarction. *Dis Markers* 2009;27:255–268.
 84. Bostjancic E, Zidar N, Stajner D, Glavac D. MicroRNAs miR-1, miR-133a, miR-133b and miR-208 are dysregulated in human myocardial infarction. *Cardiology* 2010;115:163–9.
 85. Bostjancic E, Zidar N, Stajner D, Glavac D. MicroRNA miR-1 is up-regulated in remote myocardium in patients with myocardial infarction. *Folia Biol (Praha)* 2010;56:27–31.
 86. van Rooij E, Sutherland LB, Thatcher JE, et al. Dysregulation of microRNAs after myocardial infarction reveals a role of miR-29 in cardiac fibrosis. *Proc Natl Acad Sci U S A* 2008;105:13027–32.
 87. De Rosa S, Fichtlscherer S, Lehmann R, Assmus B, Dimmeler S, Zeiher AM. Transcoronary concentration gradients of circulating microRNAs. *Circulation* 2011;124:1936–44.
 88. Gidlof O, Smith JG, Miyazu K, et al. Circulating cardio-enriched microRNAs are associated with long-term prognosis following myocardial infarction. *BMC Cardiovasc Disord* 2013;13:12.
 89. Sluijter J. MicroRNAs in Cardiovascular Regenerative Medicine: Directing Tissue Repair and Cellular Differentiation. *ISRN Vasc Med* 2013;2013.
 90. Chen JF, Mandel EM, Thomson JM, et al. The role of microRNA-1 and microRNA-133 in skeletal muscle proliferation and differentiation. *Nat Genet* 2006;38:228–233.
 91. Kloosterman WP, Steiner FA, Berezikov E, et al. Cloning and expression of new microRNAs from zebrafish. *Nucleic Acids Res* 2006;34:2558–2569.
 92. van Rooij E, Quiat D, Johnson BA, et al. A family of microRNAs encoded by myosin genes governs myosin expression and muscle performance. *Dev Cell* 2009;17:662–673.
 93. of Manchester F of LS. *miRBase*. 2012;2013.
 94. Zhao Y, Samal E, Srivastava D. Serum response factor regulates a muscle-specific microRNA that targets Hand2 during cardiogenesis. *Nature* 2005;436:214–220.
 95. Yang B, Lin H, Xiao J, et al. The muscle-specific microRNA miR-1 regulates cardiac arrhythmogenic potential by targeting GJA1 and KCNJ2. *Nat Med* 2007;13:486–491.
 96. Catalucci D, Latronico M V, Condorelli G. MicroRNAs control gene expression: importance for cardiac development and pathophysiology. *Ann N Y Acad Sci* 2008;1123:20–29.
 97. Ai J, Zhang R, Li Y, et al. Circulating microRNA-1 as a potential novel biomarker for acute myocardial infarction. *Biochem Biophys Res Commun* 2010;391:73–77.
 98. Cheng Y, Tan N, Yang J, et al. A translational study of circulating cell-free microRNA-1 in acute myocardial infarction. *Clin Sci (Lond)* 2010;119:87–95.
 99. Corsten MF, Dennert R, Jochems S, et al. Circulating MicroRNA-208b and MicroRNA-499 reflect myocardial damage in cardiovascular disease. *Circ Cardiovasc Genet* 2010;3:499–506.
 100. Gidlof O, Andersson P, van der Pals J, Gotberg M, Erlinge D. Cardiospecific microRNA plasma levels correlate with troponin and cardiac function in patients with ST elevation myocardial infarction, are selectively dependent on renal elimination, and can be detected in urine samples. *Cardiology* 2011;118:217–226.
 101. Li YQ, Zhang MF, Wen HY, et al. Comparing the diagnostic values of circulating microRNAs and cardiac troponin T in patients with acute myocardial infarction. *Clinics (Sao Paulo)* 2013;68:75–80.
 102. Long G, Wang F, Duan Q, et al. Human circulating microRNA-1 and microRNA-126 as potential novel indicators for acute myocardial infarction. *Int J Biol Sci* 2012;8:811–818.
 103. Wang G-K, Zhu J-Q, Zhang J-T, et al. Circulating microRNA: a novel potential biomarker for early diagnosis of acute myocardial infarction in humans. *Eur Heart J* 2010;31:659–66.
 104. Widera C, Gupta SK, Lorenzen JM, et al. Diagnostic and prognostic impact of six circulating microRNAs in acute coronary syndrome. *J Mol Cell Cardiol* 2011;51:872–5.
 105. Zile MR, Mehurg SM, Arroyo JE, Stroud RE, DeSantis SM, Spinale FG. Relationship between the temporal profile of plasma microRNA and left ventricular remodeling in patients after myocardial infarction. *Circ Cardiovasc Genet* 2011;4:614–9.
 106. Olivieri F, Antonicelli R, Lorenzi M, et al. Diagnostic potential of circulating miR-499-5p in elderly patients with acute non ST-elevation myocardial infarction. *Int J Cardiol* 2012.
 107. Griffiths-Jones S, Grocock RJ, van Dongen S, Bateman A, Enright AJ. *miRBase*: microRNA sequences, targets and gene nomenclature. *Nucleic Acids Res* 2006;34:D140–4.
 108. Torella D, Iaconetti C, Catalucci D, et al. MicroRNA-133 controls vascular smooth muscle cell phenotypic switch in vitro and vascular remodeling in vivo. *Circ Res* 2011;109:880–893.
 109. Wang R, Li N, Zhang Y, Ran Y, Pu J. Circulating microRNAs are promising novel biomarkers of acute myocardial infarction. *Intern Med* 2011;50:1789–1795.
 110. Thygesen K, Mair J, Katus H, et al. Recommendations for the use of cardiac troponin measurement in acute cardiac care. *Eur Heart J* 2010;31:2197–2204.

111. van Rooij E, Sutherland LB, Qi X, Richardson JA, Hill J, Olson EN. Control of stress-dependent cardiac growth and gene expression by a microRNA. *Science* 2007;316:575–9.
112. Callis TE, Pandya K, Seok HY, et al. MicroRNA-208a is a regulator of cardiac hypertrophy and conduction in mice. *J Clin Invest* 2009;119:2772–2786.
113. Adachi T, Nakanishi M, Otsuka Y, et al. Plasma microRNA 499 as a biomarker of acute myocardial infarction. *Clin Chem* 2010;56:1183–5.
114. Devaux Y, Vausort M, Goretti E, et al. Use of circulating microRNAs to diagnose acute myocardial infarction. *Clin Chem* 2012;58:559–67.
115. Wang JX, Jiao JQ, Li Q, et al. miR-499 regulates mitochondrial dynamics by targeting calcineurin and dynamin-related protein-1. *Nat Med* 2011;17:71–78.
116. Hosoda T, Zheng H, Cabral-da-Silva M, et al. Human cardiac stem cell differentiation is regulated by a mircrine mechanism. *Circulation* 2011;123:1287–1296.
117. Cacchiarelli D, Legnini I, Martone J, et al. miRNAs as serum biomarkers for Duchenne muscular dystrophy. *EMBO Mol Med* 2011;3:258–265.
118. Salic K, Windt LJ De. MicroRNAs as biomarkers for myocardial infarction. *Curr Atheroscler Rep* 2012;14:193–200.
119. Wang S, Aurora AB, Johnson BA, et al. The endothelial-specific microRNA miR-126 governs vascular integrity and angiogenesis. *Dev Cell* 2008;15:261–271.
120. Cordes KR, Sheehy NT, White MP, et al. miR-145 and miR-143 regulate smooth muscle cell fate and plasticity. *Nature* 2009;460:705–710.
121. Fish JE, Santoro MM, Morton SU, et al. miR-126 regulates angiogenic signaling and vascular integrity. *Dev Cell* 2008;15:272–284.
122. Kuhnert F, Mancuso MR, Hampton J, et al. Attribution of vascular phenotypes of the murine *Egfl7* locus to the microRNA miR-126. *Development* 2008;135:3989–3993.
123. Zhou J, Li JY, Nguyen P, et al. Regulation of Vascular Smooth Muscle Cell Turnover by Endothelial Cell-secreted MicroRNA-126: Role of Shear Stress. *Circ Res* 2013.
124. Konstandin MH, Aksoy H, Wabnitz GH, et al. Beta2-integrin activation on T cell subsets is an independent prognostic factor in unstable angina pectoris. *Basic Res Cardiol* 2009;104:341–351.
125. Gidlöf O, van der Brug M, Ohman J, et al. Platelets activated during myocardial infarction release functional miRNA, which can be taken up by endothelial cells and regulate ICAM1 expression. *Blood* 2013;121:3908–3917.
126. O'Connell RM, Taganov KD, Boldin MP, Cheng G, Baltimore D. MicroRNA-155 is induced during the macrophage inflammatory response. *Proc Natl Acad Sci U S A* 2007;104:1604–1609.
127. Gironella M, Seux M, Xie MJ, et al. Tumor protein 53-induced nuclear protein 1 expression is repressed by miR-155, and its restoration inhibits pancreatic tumor development. *Proc Natl Acad Sci U S A* 2007;104:16170–16175.
128. Vigorito E, Perks KL, Abreu-Goodger C, et al. microRNA-155 regulates the generation of immunoglobulin class-switched plasma cells. *Immunity* 2007;27:847–859.
129. Liu J, van Mil A, Vrijksen K, et al. MicroRNA-155 prevents necrotic cell death in human cardiomyocyte progenitor cells via targeting RIP1. *J Cell Mol Med* 2011;15:1474–1482.
130. Liu J, van Mil A, Aguor EN, et al. MiR-155 inhibits cell migration of human cardiomyocyte progenitor cells (hCMPCs) via targeting of MMP-16. *J Cell Mol Med* 2012;16:2379–2386.
131. Johnnidis JB, Harris MH, Wheeler RT, et al. Regulation of progenitor cell proliferation and granulocyte function by microRNA-223. *Nature* 2008;451:1125–1129.
132. Oerlemans M, van Mil A, Liu J, et al. Inhibition of miR-223 reduces inflammation but not adverse cardiac remodelling after myocardial ischemia-reperfusion in vivo. *Discov Biol Med* 2012;1:3–10.
133. Taganov KD, Boldin MP, Chang KJ, Baltimore D. NF-kappaB-dependent induction of microRNA miR-146, an inhibitor targeted to signaling proteins of innate immune responses. *Proc Natl Acad Sci U S A* 2006;103:12481–12486.
134. Tatsuguchi M, Seok HY, Callis TE, et al. Expression of microRNAs is dynamically regulated during cardiomyocyte hypertrophy. *J Mol Cell Cardiol* 2007;42:1137–1141.
135. Thum T, Gross C, Fiedler J, et al. MicroRNA-21 contributes to myocardial disease by stimulating MAP kinase signalling in fibroblasts. *Nature* 2008;456:980–4.
136. Li C, Fang Z, Jiang T, et al. Serum microRNAs profile from genom-wide serves as a fingerprint for diagnosis of acute myocardial infarction and angina pectoris. *BMC Med Genomics* 2013;6:16.
137. Gupta S, Singh KN, Bapat V, Mishra V, Agarwal DK, Gupta P. Diagnosis of acute myocardial infarction: CK-MB versus cTn-T in Indian patients. *Indian J Clin Biochem* 2008;23:89–91.

Circulating extracellular vesicles contain miRNAs and are released as early biomarkers for cardiac injury

J.C. Deddens

K.R. Vrijssen

J.M. Colijn

M.I. Oerlemans

C.H.G. Metx

E.J. van der Vlist

E.N.M. Nolte-'t Hoen

K den Ouden

S.J. Jansen of Lorkeers

T.I.G. van der Spoel

S. Koudstaal

G.J. Arkesteijn

M. H.M. Wauben

L.W. van Laake

P.A. Doevendans

S.A.J. Chamuleau

J.P.G. Sluijter

Abstract

Plasma circulating microRNAs have been implicated as novel early biomarkers for myocardial infarction (MI) due to their high specificity for cardiac injury. For swift clinical translation of this potential biomarker it is important to understand their temporal and spatial characteristics upon MI. Therefore, we studied the temporal release, potential source and transportation of circulating miRNAs in different models of ischemia reperfusion (I/R) injury. We demonstrated that extracellular vesicles are released from the ischemic myocardium upon I/R injury. Moreover, we provided evidence that cardiac and muscle specific miRNAs are transported by extracellular vesicles and are rapidly detectable in plasma. Since these vesicles are enriched for the released miRNAs and their detection precedes traditional damage markers, they hold great potential as specific early biomarkers for MI.

Keywords: circulating microRNA; biomarkers; myocardial infarction; extracellular vesicles; exosomes

Introduction

Upon myocardial infarction (MI), the heart releases different enzymes, growth factors and cytokines, which can serve as markers of cardiac injury. Cardiac troponin (cTn) and creatine kinase MB (CK-MB) are the most commonly used biomarkers for MI [1, 2]. Although high-sensitive cTn assays can detect cTn 2-3 hours after onset of complaints, guidelines still advise to do serial measurements after 6-9 hours for correct diagnosis of MI [1]. Due to the relative late rise of these biomarkers, 10 to 15% of patients presenting with a MI have a negative blood test upon arrival in the hospital [3, 4]. Delayed confirmation of MI results in increased morbidity and mortality. On the contrary, delayed ruling out of MI prolongs the time spent in the hospital and increases healthcare costs [5]. To guide immediate treatment in the emergency department and to minimize healthcare costs there is an ongoing need for novel early biomarkers for MI [6].

Increasing evidence suggests that circulating microRNAs (miRNA) can be potential biomarker candidates due to their highly specific elevation in blood upon stresses, including MI [3, 7, 8]. MiRNAs are short (~22 nucleotides) non-coding RNAs [9] that regulate gene expression at a post-transcriptional level [10, 11]. Besides their regulatory intracellular function, they can be released into the extracellular environment where they can contribute to intercellular signalling mechanisms. Circulating miRNAs are closely associated with proteins, lipids and extracellular vesicles (EV) [12–15].

In a large cohort of patients with suspected acute coronary syndrome (ACS) [3], we found that several miRNAs (miRNA-1, -21, 146a, -208, and -499) are increased in plasma upon injury and have a good diagnostic value to predict MI. However, important detailed information regarding the temporal release profile and potential source and transportation of these miRNAs in the circulation is largely lacking.

EV are the most investigated entities of extracellular miRNA transport and include vesicles derived from the plasma membrane and exosomes, which originate from the endosomal pathway [16]. Exosomes are small lipid bilayer vesicles (30-100 nm) with a density of

approximately 1.10-1.17 g/ml [17, 18]. They are enriched with membrane proteins (e.g. CD9 and Flotillin-1 [19]) and contain (specific) cellular cargo [17, 20].

Interestingly, high numbers of microparticles and EV are associated with the presence of cardiovascular disease (CVD) [21]. It is demonstrated that the release of EV correlates with the severity of cardiac injury [22]. In addition, plasma EV packed protein and miRNAs showed potential benefit as biomarkers in the diagnosis of CVD [23, 24]. The combination of both the amount and content of EV in CVD consequently holds great potential for EV as biomarker of MI [21].

Since EV represent major transport vehicles for circulating miRNAs, we assessed the temporal release of extracellular vesicles by the injured myocardium. Moreover, we investigated the potential of EV-linked miRNAs as early biomarkers for MI.

Methods

Animal experiments were approved by the Animal Ethical Experimentation Committee of Utrecht University and carried out in accordance with the Guide for Care and Use of Laboratory Animals.

Mouse model

Myocardial ischemia reperfusion

To assess EV release after myocardial infarction *in vivo*, male C57BL/6 mice (aged 10-12 weeks) were anesthetized intraperitoneally with fentanyl 0.05 mg/kg, midazolam 5 mg/kg, and medetomidine 0.5 mg/kg. Myocardial infarction was induced by ligation of the left anterior descending coronary artery (LAD) as previously described [25]. After 30 minutes of occlusion, the ligature was removed to allow reperfusion of the myocardium for another two hours (see Figure 1a) [26]. For control experiments, plasma was obtained from healthy or sham-operated mice. The sham operations included all of the procedures used for I/R, including length of operation procedure, except the occlusion and successive reperfusion of the LAD. Blood was collected via cardiac puncture of the left ventricle and twice centrifuged at 2,000 x g for 20 minutes to isolate the plasma fraction.

Operations were performed in three different experiments. The total number of mice included in the study is n= 8 (healthy), n= 7 (sham) and n= 9 (I/R). As the amount of obtained plasma per mice was low and the amount needed for analysis high, pooling of samples was performed for FACS and Westernblot analyses.

To assess the extent of cardiac injury, individual plasma levels of total lactate dehydrogenase (LDH) were determined by LDH based toxicology assay kit (Sigma; TOX7), according to manufactures protocol.

Langendorff

C57BL/6 mice were injected with heparin 100 IU/kg via the tail vein to prepare for Langendorff retrograde perfusion (n= 4) [27]. In short, mice were anesthetized as described above and hearts were quickly excised and placed in ice-cold tyrode buffer solution (NaCl 124 mM; KCl 4,7 mM; MgCl₂ 1,0 mM; NaHCO₃ 24 mM; CaCl₂ 1,3 mM; Glucose 11,0; Pyruvic Acid 5,0 mM, pH= 7,4). Explanted mouse hearts were cannulated through the aortic opening and connected to the Langendorff perfusion system to allow for 2-3 hours of retrograde perfusion. The perfusion buffer was kept at 37 °C and was gassed with carbogen (85% O₂ + 15% CO₂) at a constant pressure of 73 mmHg. For induction of myocardial ischemia, the LAD was ligated. During perfusion, the heart flow-through was collected for isolation of EV.

Porcine model of myocardial infarction

Female Dutch Landrace pigs (approx. 70 kg, n= 6) were anesthetized in the supine position and intubated with an endotracheal tube. The animals were mechanically ventilated by positive-pressure ventilation with a mixture of oxygen and air (FiO₂ 0.5). General anesthesia and analgesia was maintained with midazolam (0,5 mg/kg/h; Roche), sufentanyl bromid (2 µg/kg/h; Janssen-Cilag) and pancuronium bromid (0.1 mg/kg/h; Organon) as previously described [28]. During the entire procedure, the electrocardiogram, arterial pressure and capnogram were continuously monitored. After administration of heparin, MI was created by percutaneous balloon inflation of the LAD below the second bifurcation [29]. Ischemia lasted for 90 minutes upon which deflation of the angioplasty balloon caused restoration of the blood flow and reperfusion of the tissue. During the procedure, blood samples (citrate) were drawn from the arteria femoralis at several time points; 1) pre-ischemia, 2) 60 minutes after occlusion, 3) 90 minutes after occlusion, 4) one hour after reperfusion, 5) two hours after reperfusion (see Figure 3a).

Citrate blood was centrifuged twice at 2,000 x g for 20 minutes to isolate plasma, which was stored at -80°C and used for further analysis. Troponin I levels were analyzed using a clinical chemistry analyzer (AU5811) with a cut-off value of 40 ng/L.

Extracellular microvesicles

Isolation of extracellular microvesicles

To isolate EV, which sediment at $\geq 10,000 \times g$, mouse plasma samples were diluted with PBS (1:1) and centrifuged for 30 minutes at 2,000 x g, followed by one hour at 100,000 x g (Beckmann Coulter LE-80K Optima, SW60). Pellets with EV were resuspended in PBS and stored for flow cytometric analysis. EV, including exosomes, from mouse and pig plasma and Langendorff perfused hearts were isolated by differential centrifugation, as described before [30, 31]. In short, diluted plasma or flow-through was successively centrifuged at 2,000 x g, 10,000 x g and 100,000 x g. The resulting 100,000 x g pellet was resuspended in PBS and centrifuged again at 100,000 x g. The washed EV pellet was resuspended in a small volume of PBS and the EV protein concentration was determined with the BCA protein assay kit (ThermoScientific). EV were stored at 4 °C until used for electron microscopy and Western blot analysis.

Isolation of pig plasma derived EV (n= 4), to be used for miRNA analysis, was performed by Exoquick isolation, according to the manufacturers protocol (System Biosciences). In short, plasma was centrifuged for 30 minutes at 10,000 x g to remove larger vesicles, and 250 µl of the supernatant was added to 63 µl Exoquick. The final pellet was resuspended in diethylpyrocarbonate (DEPC) water and stored in Trizol at -80 °C.

Electron microscopy

Isolated EV were resuspended in phosphate buffer containing 1% glutaraldehyde (Polyscience; 00216) and subsequently loaded onto formvar/carbon-coated electron

microscopy grids. Contrast of the samples was enhanced with uranyl acetate (SPI; 02624-AB). Images were captured using a transmission electron microscope JEOL 1200EX [32, 33].

PKH-67 labelling and flow cytometric analysis

Mouse plasma derived EV were stained with PKH-67 (Sigma; PKH67GL) to allow for particle detection by flow cytometric analysis [34]. Briefly, EV or an equivalent volume of PBS (control) were dissolved in Diluent C and stained with 7.5 μ M PKH-67. After 3 minutes, PKH-67 labeling was abrogated using 50 μ l of vesicle-depleted fetal bovine serum (FBS, centrifuged O/N at 150,000 x g). To separate PKH-67 labelled EV from unincorporated PKH-67 label, the mixtures were subjected to sucrose density gradient centrifugation, as previously described [30]. Briefly, EV were resuspended in 2.5 M sucrose and layered with decreasing molarities of sucrose before centrifugation for 15 hr at 200,000 x g. After centrifugation, twelve fractions of consecutive densities were collected and diluted ten times in double filtered PBS. As the lower three fractions possibly contain unbound PKH-26, these fractions were excluded from further analysis. EV were analysed by high resolution flow cytometry (hFC) using fluorescence threshold triggering as previously described [34, 35]. By means of the low plasma volume of mice, the samples for flow cytometry contained plasma of 2-4 mice in order to obtain measurable numbers of EV.

SDS-PAGE and Western blots

Isolated and sucrose gradient purified EV were resuspended in 4x laemmli buffer and subjected to SDS-PAGE using pre-casted gels (Novex; NP0335BOX). To compare different experimental conditions (healthy control, sham, I/R injury), samples were corrected for initial plasma volume and loaded in separate lanes. Proteins were transferred to methanol activated PVDF membranes (Millipore; IPVH00010) to assess the expression of microvesicle enriched proteins. Membranes were blocked in 5% milk (BioRad; 170-6404) dissolved in PBS-T20 (0.1%) and incubated with appropriate antibodies, diluted in 5% milk-PBS-T20; flotillin-1 (0.4 μ g/ml;

Santa-Cruz Biotechnology; SC25506), CD9 (0.5 µg/ml, Santa-Cruz Biotechnology; SC53679), CD63 (1.0 µg/ml, BD; 556019). The proteins were detected with chemiluminescent peroxidase substrate using a Chemi Doc™ XRS+ system (Bio-Rad) and Image Lab™ software.

Assessment of circulating miRNAs

RNA-isolation and Real Time-PCR (RT-PCR)

RNA from total pig plasma (n= 6) and plasma derived EV (n= 4) was extracted using the miRNeasy kit for plasma (Qiagen) and Trizol LS, respectively. Both protocols were performed according to the manufactures descriptions. To correct for isolation variability and to enable comparative analysis of total plasma and plasma EV, *C. Elegans* miRNA-39 (Quanta Biosciences) was added to the lysis buffer equalized to the starting amount of plasma. RNA quantity and quality were measured with the Nanodrop (NanoDrop Products) and the 2100 Small RNA Assay Bioanalyzer (Agilent). cDNA was synthesized with qScript™ microRNA cDNA Synthesis Kit (Quanta BioSciences), following the manufacturer's protocol. Quantitative RT-PCR (qRT-PCR) was performed in 12,5 µl duplicate reactions with PerfeCTa SYBR Green SuperMix (BioSciences), the PerfeCTa Universal PCR Primer (Quanta Biosciences), and primers specific for miRNA-1, miRNA-21, miRNA-133b, miRNA-146a miRNA-208b, miRNA-499a.

The cycle number that exceeds the fluorescence threshold is the threshold cycle (Ct value). Ct values that exceeded 40 cycles were treated as Ct 42. At missing time points the average of the other pigs in that specific group was used as the cycle number for that time point. Ct values were normalized by using the average Ct value of the spike-in miRNA.

Statistical analysis

Statistical analyses were carried out using GraphPad Prism 6.0 software (La Jolla, USA). Differences in miRNA-levels were analyzed using a one-way or two-way ANOVA test with a Dunnett's test for multiple testing correction. P-values < 0.05 were considered statistically significant. Error bars indicated Standard Error of the Mean (SEM), unless otherwise defined.

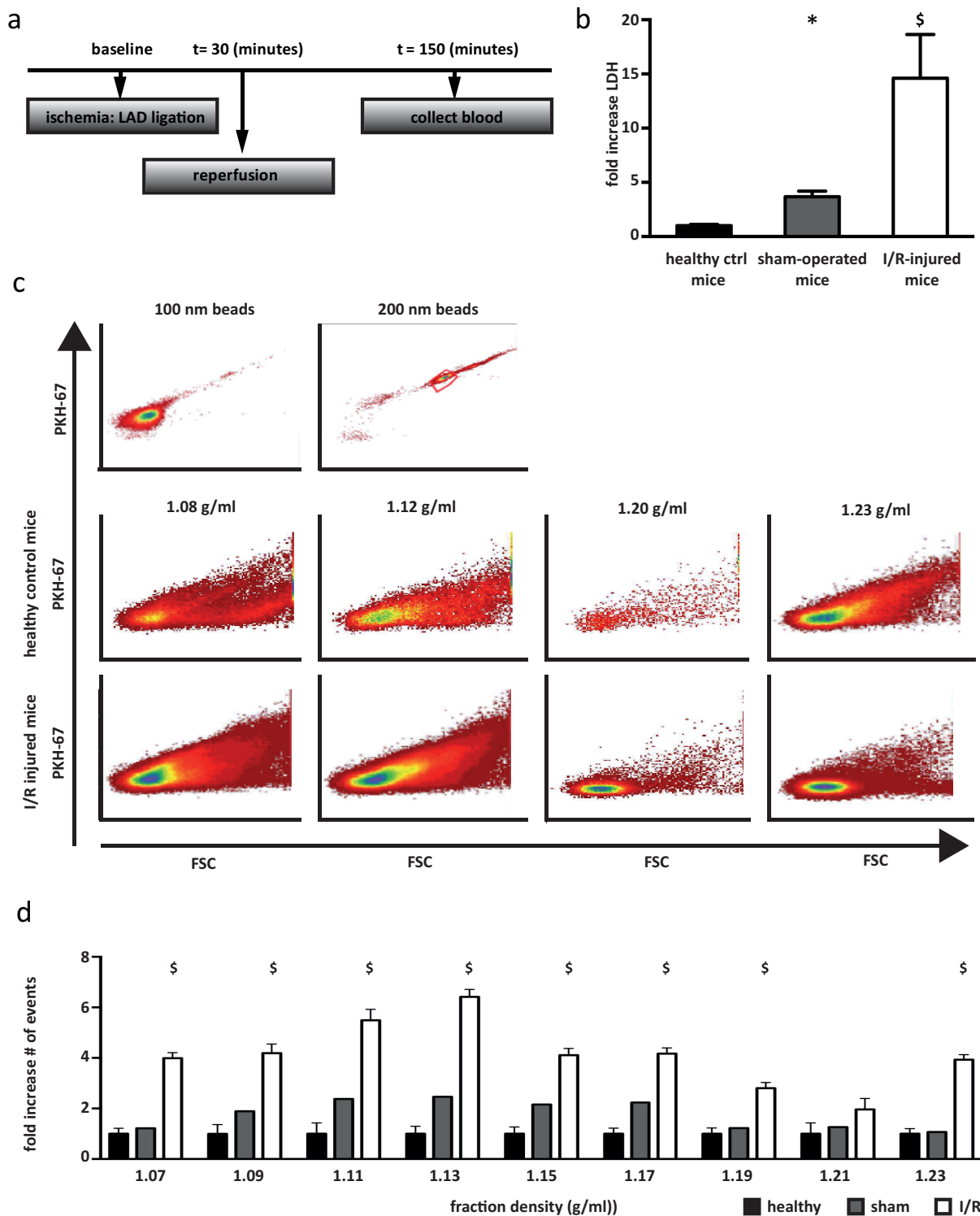


Figure 1. Release of extracellular microvesicles after cardiac ischemia/reperfusion injury in mice. **A)** Overview of I/R injury model in C57BL/6 mice. **B)** Lactate dehydrogenase (LDH) levels in plasma of healthy control mice (n= 5, reference value), sham-operated (n= 7) and I/R-injured (n= 7) mice at t = 150 minutes. **C)** Representative images of high-resolution flow cytometric analysis of isolated PKH67-labeled extracellular microvesicles (EV) from healthy control mice (middle panels) and I/R injured mice (bottom panels) in different sucrose gradient fractions. Density scatterplots show reduced wide-angle forward scatter (FSC) plotted against PKH67 fluorescence. **D)** Relative time-based quantification of EV from mouse plasma after I/R injury (n= 3) and sham-operation (n= 1) demonstrated a significant increase in vesicle density upon I/R injury, compared to healthy control mice (n= 3, reference value) at t= 150 minutes. Bars represent mean fold differences, compared to healthy control: * p< 0.05 and § p< 0.01.

Results

Ischemia reperfusion injury in mice leads to the release of extracellular microvesicles into the circulation

To examine the release of extracellular microvesicles upon extensive cardiac injury, we studied plasma from C57BL/6 mice after 30 minutes of ischemia followed by two hours of reperfusion (Figure 1a). To demonstrate the extent of ischemia/reperfusion (I/R) injury, the level of LDH was measured and showed a 15.5 ± 3.0 fold increase compared to sham operated and control animals (Figure 1a). As expected, LDH was also slightly elevated in sham operated animals (3.9 ± 0.4 fold) compared to healthy controls.

At the same time, EV from plasma of these C57BL/6 mice were isolated and analyzed by hFC [35]. Based on fluorescent labelling with PKH67, individual vesicles were measured by relative time-based quantification. The number of isolated EV from plasma after I/R was increased in all density fractions (Figure 1c, d) with EV in the fractions with density ranges from 1.11 - 1.13 g/ml showing the highest increase (5.5 ± 0.4 and 6.4 ± 0.3 fold, respectively; Figure 1d) in vesicle number ($p < 0.01$). The effect of thoracic surgery is shown by an increase in vesicle number after sham operation, however, to a lesser extent compared to I/R injury (Figure 1d).

The ischemic myocardium contributes to the release of extracellular microvesicles after cardiac injury.

To shed light on the vesicle distribution after injury, we analyzed sucrose gradient purified EV by Western blotting and electron microscopy (EM). We observed the presence of the EV-enriched proteins flotillin-1, CD9 and CD63 in these vesicles (Figure 2a, Online Resource 1a and 1b for CD9 and CD63, respectively). Flotillin-1 (and CD9) were mainly present in the EV fraction of the sucrose gradient with a density of 1.08 - 1.18 g/ml. The amount of flotillin-1, as a measure of EV number, was $5.3 (\pm 2.5)$ fold increased after I/R compared to healthy controls (Figure 2b). In addition, isolated vesicles were approximately 100 nm in size and had a lipid bilayer (Figure 2c).

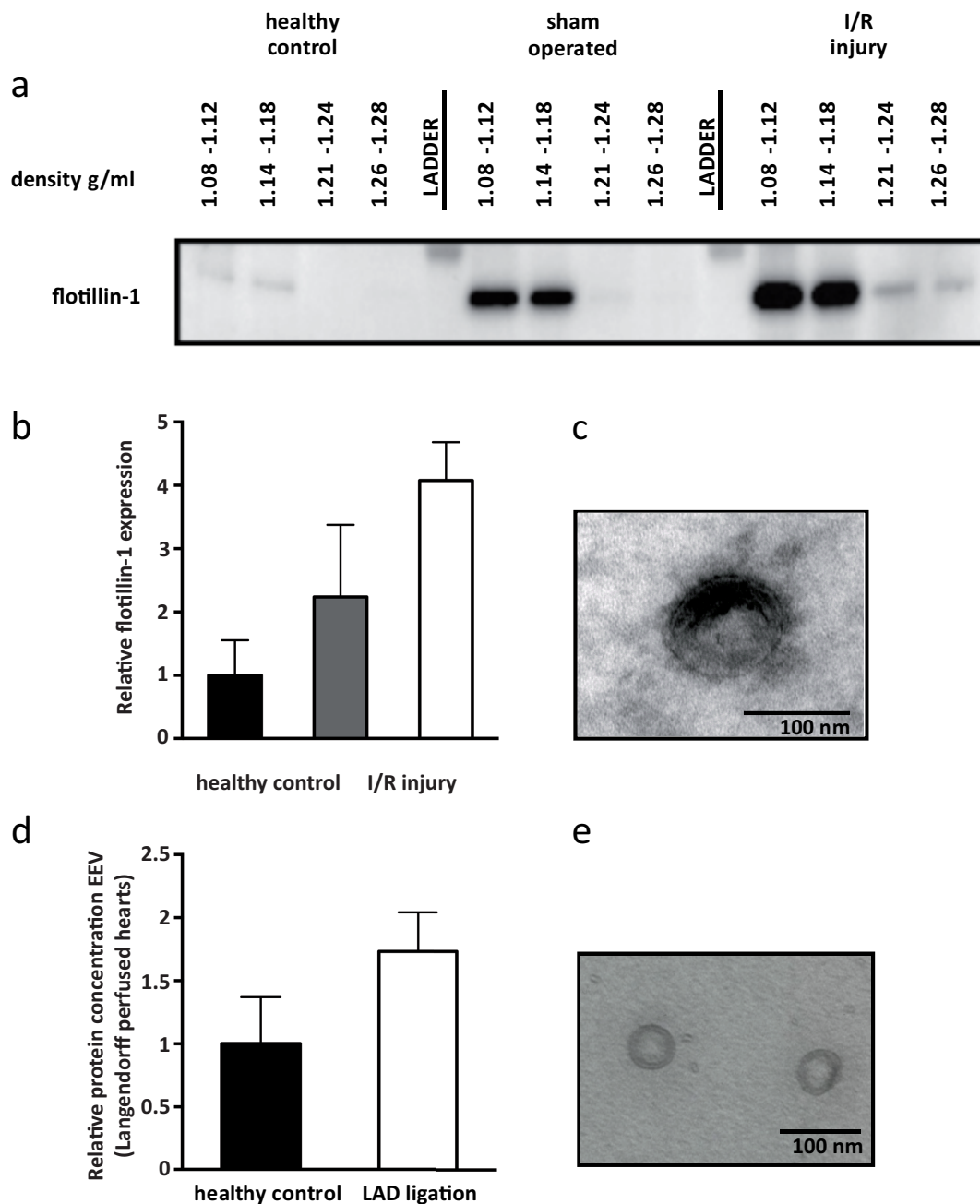


Figure 2. Characterization of mouse plasma derived extracellular microvesicles. A) Westernblot of flotillin-1 on isolated and sucrose gradient purified EV in healthy control, sham-operated and I/R injury mice (t= 150 minutes), n= 3, **(B)** showed that flotillin-1 in EV with a floating density of 1.08 - 1.12 g/ml was relatively increased. Sample loading was corrected for initial plasma volume and the level of healthy control mice was set to 1. **(C)** Electron microscopy image of isolated plasma EV. **(D)** Protein quantification of cardiac derived (Langendorff perfused heart) EV with and without LAD ligation induced cardiac ischemia (n= 2 vs. n= 2). **(E)** Electron microscopy image of isolated Langendorff perfused heart derived EV.

Next, we aimed at identifying whether the myocardium could be a source of vesicle release upon I/R injury. We harvested EV from healthy and LAD ligation induced ischemic hearts upon Langendorff perfusion and by that excluded circulating cells as a source of EV. Upon ischemia, by ligation of the LAD *ex vivo*, the EV protein concentration was increased after 120 minutes (Figure 2d), suggestive of increased vesicle release. Lipid bilayer vesicles were observed in the Langendorff flow through and although these appeared smaller in size than plasma EV (50 nm) (Figure 2e), they also contained flotillin-1 (Online Resource 1c). These results indicate that the myocardium itself is also able to release EV, including exosomes, which can potentially serve as endogenous carriers for novel biomarkers that are released upon myocardial stress.

Although the release of vesicles could be determined in individual mice for each condition (i.e. control, sham or I/R injury), their yield was too small to perform miRNA expression analysis. To compensate for the low yield of mouse plasma and to enable temporal analysis, next experiments were performed in a porcine model of myocardial reperfusion injury.

Plasma derived extracellular vesicles from a porcine model of ischemia reperfusion transport miRNAs released upon cardiac injury

To examine the role of EV as transporters of circulating miRNAs, blood samples were collected at different time points after I/R injury in a porcine model (Figure 3a, n= 6). Successful induction of MI was confirmed by the levels of cTnI in the plasma, which were significantly increased at t= 2.5 hours, $p < 0.001$ (Figure 3b). Likewise, levels of well-known circulating miRNAs after I/R injury were analyzed and were significantly upregulated at t= 2.5 hours (Figure 3c). The levels of muscle specific extracellular miRNAs (miRNA-1, -133b, -208b, and -499) in plasma (n= 6) were increased up to 750 fold ($p < 0.0001$), thereby demonstrating that miRNA-499 is the most abundantly present miRNA in plasma upon MI. Additionally, the individual levels of miRNA-1, 133b, 208b and -499 significantly correlated to the levels of cTnI ($R^2 = 0.66, 0.61, 0.72$ and 0.71 , respectively). In contrast to our clinical observations [3], the increase of the inflammatory related miRNA-21 and miRNA-146 was not statistically significant.

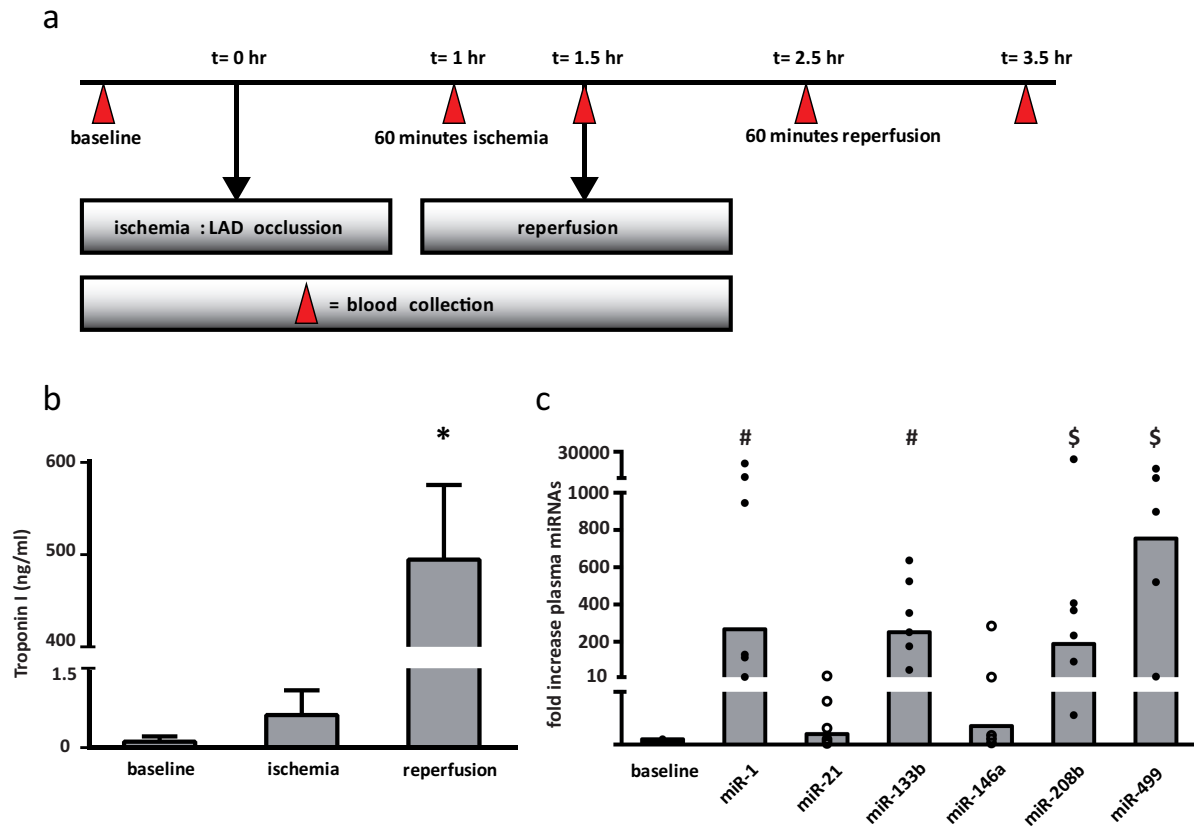


Figure 3. Circulating miRNAs as biomarkers for ischemia/reperfusion injury in a porcine model. A) Overview of a porcine model of I/R injury by 90 minutes percutaneous occlusion of the LAD, n= 6. **B)** Troponin I levels (ng/ml) of plasma at baseline, ischemia (t=1.5 hr) and reperfusion (t= 2.5 hr) demonstrated successful induction of MI. **C)** Muscle-specific miRNAs are released in the circulation at t= 2.5 hr. Dots represent fold difference of individual samples, compared to baseline. \$ p< 0.01, # p< 0.001.

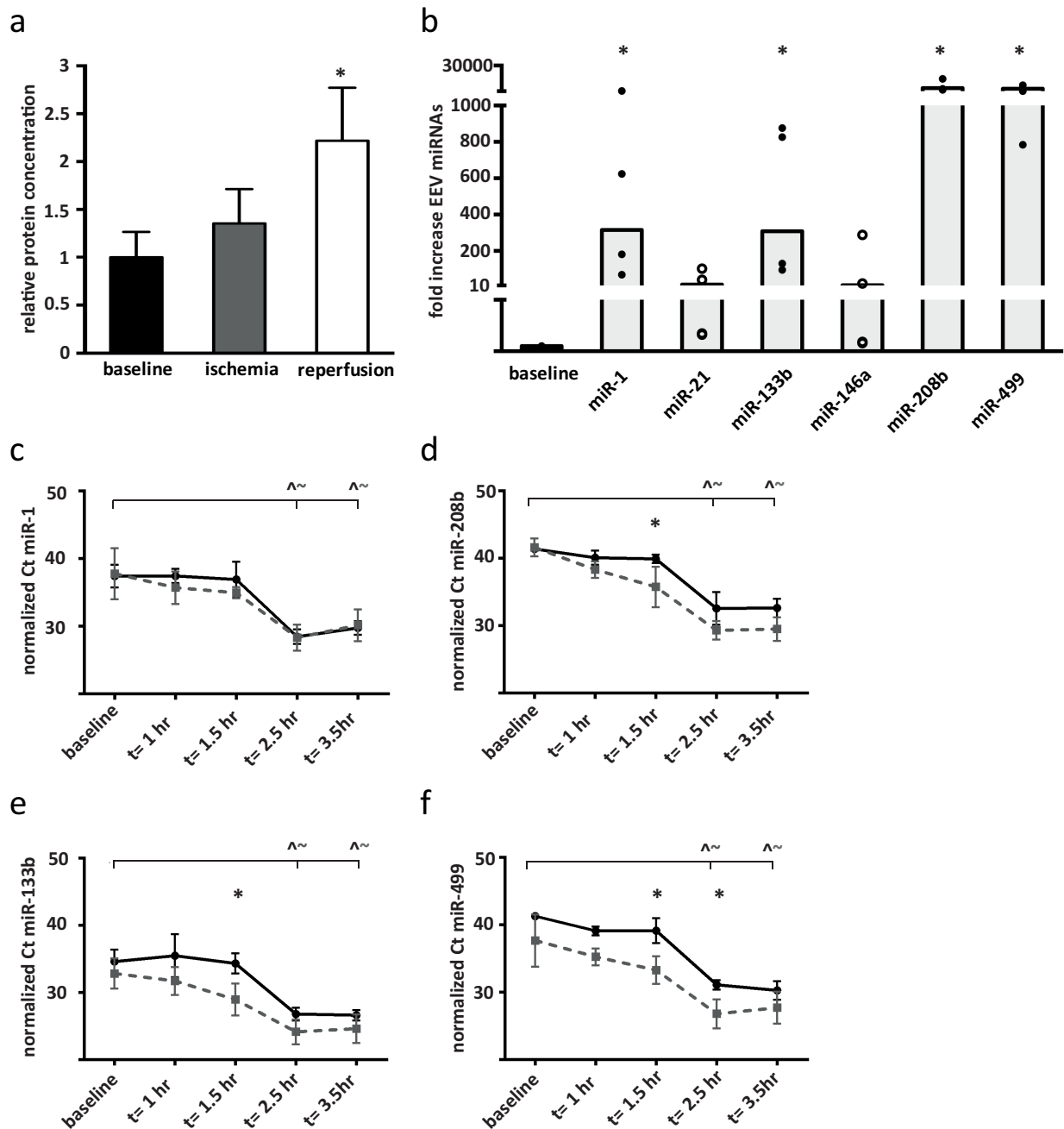


Figure 4. Porcine plasma derived extracellular microvesicles transport miRNAs after cardiac injury. A) Release of EV (100,000 x g pellet) was increased shortly after induction of MI (t= 1.5 hr). **B)** Expression levels of miRNAs in the isolated EV fraction upon I/R injury (t= 2.5 hr). Dots represent fold difference of individual samples, compared to baseline, n= 4. **C-F)** Time-dependent analysis of miRNA expression in total plasma (solid black lines) and EV fraction (dotted grey lines). Data showed an early enrichment of miRNAs in plasma derived EV at t= 1.5 hr (miRNA-133b, -208b, and -499) and t= 2.5 hr (miRNA-133b and miRNA-499). Error bars indicate standard deviation, * p< 0.05, \$ p< 0.01. For **C-F)** a significant difference (p<0.05) with baseline is marked with ^ for plasma and ~ for EV. Additionally, * marks a significant difference between plasma and plasma-EV at the given timepoint.

As in the previous described murine model, protein levels in the EV fraction increased up to 2.2 fold (± 0.6 , $p < 0.05$) 60 minutes after reperfusion ($t = 2.5$ hr). Moreover, even after 60 minutes of ischemia the amount of EV derived protein appeared to be increased (1.4 ± 0.4 fold; Figure 4a).

Since both miRNAs and EV are released in plasma upon cardiac injury, we sought to identify if EV can transport these circulating miRNAs (miRNA-1, -21, -133b, -146, -208b, and -499).

For that reason, the EV fraction was isolated from plasma after I/R injury and the miRNA content was analyzed (Figure 4b). The plasma vesicles were isolated by Exoquick precipitation after an initial centrifugation step at 10,000 x g and were termed EV, similar to the vesicles isolated with ultracentrifugation. Parallel to the increase in miRNAs in total plasma after I/R injury, a significant ($p < 0.01$) upregulation of the muscle-specific miRNAs in EV was observed 60 minutes after reperfusion ($t = 2.5$ hr). Levels of miRNA-208b and miRNA-499 were upregulated with the highest amplitude, where miRNA-21 and miRNA-146a showed no significant difference compared to baseline.

To gain insight in the temporal characteristics of miRNA release after I/R injury, a time dependent analysis was performed for both total circulating miRNAs and miRNAs in the EV fraction (Figure 4c-f, Online Resource 2a-b). Results showed that for both fractions miRNA levels are significantly different at 2.5 hr and 3.5 hr after induction of cardiac injury ($p < 0.01$, compared to baseline). Interestingly, all miRNA curves stabilized after 2.5 hr and miRNA-1 levels already decreased at $t = 3.5$ hr. This in contrast to the levels of cTnI, which kept increasing between $t = 2.5$ hr and $t = 3.5$ hr ($p = 0.03$; Online Resource 2c). Finally, results indicated that the miRNA expression levels in plasma derived EV are higher than total levels in plasma, especially after I/R injury. miRNA expression levels of EV were significant higher than plasma levels at $t = 1.5$ hr (miRNA-208b, -133b, -499) and $t = 2.5$ hr (miRNA-499) suggestive for (selective) enrichment of miRNAs in plasma EV.

Discussion

In CVD an increase in the amount of EV is observed and their content is changed dependent on the severity of disease [21]. Here, we demonstrated that EV are released upon cardiac I/R injury with a substantial contribution of the ischemic myocardium. In addition, serial plasma collection in a porcine model of MI demonstrated a significant increase in both EV and circulating miRNAs upon injury. Cardiac and muscle specific miRNAs rapidly increased in plasma 2.5 hours after the onset of ischemia while the amount of EV was already increased after 1 hour. Interestingly, plasma derived EV were selectively enriched for miRNA-133b, -208b and -499, but not for miRNA-1.

Although the release of microparticles by endothelial cells and activated platelets upon MI has been studied before [22, 36, 37], the role of the myocardium in vesicle release is less known. EV release is most commonly analyzed by measuring the protein concentration and expression of exosomal markers of the EV fraction. However, these parameters do not necessarily reflect the number of vesicles [38, 39]. Methods described for individual vesicle quantification are based on nanoparticle tracking analysis [40], tunable resistive pulse sensing [41] or hFC [34, 35]. Using hFC, we quantified EV and provided a detailed analysis of vesicles release upon cardiac injury. Our results confirm the previously described findings of increased EV release upon injury [22] and even augment the data with evidence for myocardial contribution to this process.

To get a clear impression of the characteristics of the EV fraction upon MI, we purified EV by ultracentrifugation and density gradient centrifugation. Based on the observed floating density and membrane markers of plasma EV, it can be suggested that upon cardiac injury, exosomes-like vesicles are released [17–19]. Unfortunately, the currently available knowledge and isolation methods are not sufficient to make a clear distinction between the different vesicle sources [42]. However, these findings provide insight in the pathophysiological background and origin of released vesicles, which is crucial for the development of biology-based markers of disease. In addition, profiling the content of EV upon cardiac injury might reveal even more

sensitive and specific biomarkers since vesicles can be purified and selective vesicle isolation is possible.

As we described previously [6], EV have an important role in the transport of circulating miRNAs. Several reports show the potential use of miRNAs in the diagnosis and prognosis of cardiac injury [3, 7, 8, 43–47]. Yet, the temporal release profile of miRNAs upon cardiac injury is largely unexplored. Clinical data shows that muscle-specific miRNAs are elevated within 3 hours and return back to normal in 3 to 5 days after the onset of MI [6, 48, 49]. Interestingly, in small animal models the initial increase can already be observed after 1 hour [46, 50]. However, sham operated animals show comparable patterns of which miRNA-499 is only significantly increased. Gidlof *et al* [51] described the dynamics of miRNA-1, -133a, -208b, and -499 in a large animal model of I/R injury with a rapid increase in miRNA levels after the occlusion period of 40 minutes. Although in line with our data, they observed a faster miRNA release and elimination after MI, which can be explained by the difference in occlusion time, extent of cardiac injury and body weight of the animals.

In contrast with our previous findings in humans [3], no difference in miRNA-21 [52] or miRNA-146a [53] was observed in this study. These miRNAs are differently regulated after MI [52] and are considered to be associated with the inflammatory response [54, 55]. Opposed to patients presenting with a MI, animals used for experiments do not yet suffer from cardiovascular disease prior to the onset of MI and therefore lack any comorbidities. It appears reasonable to speculate that the model we used is not sufficient regarding the levels of the inflammation related miRNA-21 and miRNA-146a and their differential expression is delayed compared to described clinical studies. Parallel to the early rise in cardiac muscle enriched miRNAs upon MI, recent evidence suggest that miRNAs can be selectively enriched in EV [24, 56]. Importantly, Jansen *et al* [24] demonstrated that miRNA-126 and miRNA-199a were predictive for cardiovascular events only when measured in EV. Additionally, specific transport to the extracellular environment via EV have been shown for miRNA-133 [57]. In accordance with these findings, we have identified that miRNA-133b, -208b and -499 are enriched in plasma

derived EV. Interestingly, no additional rise in EV bound miRNA-1 was observed, which is suggestive for selective loading of EV.

The strengths of the present study include that we incorporated several advanced methods to characterize the release of extracellular vesicles. With hFC we were able to analyze individual vesicles based on membrane staining. Additionally, the experiments with the Langendorff set up enabled us to study the contribution of the ischemic myocardium in vesicle release upon I/R injury. Moreover, we used a large animal model with high clinical relevance to provide novel insights in the temporal and spatial characteristics of circulating miRNAs. By doing so we could adequately compare the expression levels of miRNAs in total plasma and the EV fraction.

Nevertheless, this study has several limitations. The sham-operated animals were included only once in the hFC analysis (n= 1). Although the effect of I/R injury on the release of EV was more pronounced, the thoracic surgery on itself resulted in a low degree of tissue injury, which reinforces the importance of a sham-control group [58]. For this reason, we complemented the data by Westernblot-based EV quantification and showed that the majority of EV release is caused by the I/R injury and not the sham-procedure. Furthermore, the performed vesicle characterization in the murine I/R model could not be extended with analysis of EV packed miRNAs. Therefore we complemented the data in a large animal model, which translates better to the clinic. One should realize the effect heparin has on PCR-based miRNA detection in blood samples and that standardization between samples is therefore essential. However, here we did not observe an effect in time on different miRNAs that were used for normalization [59, 60]. Additionally, only a selected number of miRNAs, based on previously performed studies and their association with MI, were analyzed. Since these selected miRNAs do not fully cover all differentially expressed miRNAs upon MI, conclusions concerning differential packaging of EV are limited. Finally, EV for miRNA analysis were isolated using Exoquick precipitation solution. Although this method is faster than gradient purification, it possibly resulted in co-isolation of RNA of non-EV origin [61]. Identification of miRNAs in EV isolated with different purification methods would therefore be of interest. Furthermore, exploration of miRNAs in other specific

plasma fractions, e.g. lipids and proteins, would be of interest to better understand their temporal spatial distribution and their biological context.

In conclusion, we found that the number of EV is increased in different models of I/R injury, faster than cTnI, and are at least partly derived from the ischemic myocardium. We provided evidence that cardiac and muscle specific miRNAs are transported by EV and are rapidly detectable in plasma, which suggest that their release is stress-induced. Since EV are selectively enriched for released miRNAs, they hold great potential as specific early biomarkers for MI.

Acknowledgments

The technical assistance of Verena Schrier is greatly acknowledged.

Compliance with Ethical Standards

Funding

We acknowledge the support from Innovation and the Netherlands CardioVascular Research Initiative (CVON): The Dutch Heart Foundation, Dutch Federation of University Medical Centers, the Netherlands Organization for Health Research and Development and the Royal Netherlands Academy of Science. Additionally, the ZonMW Translational Adult Stem Cell grant 1161002016, the Wijnand M. Pon Stichting and the Interuniversity Cardiology Institute the Netherlands. This research forms part of the Project P1.04 SMARTCARE of the BioMedical Materials institute, co-funded by the Dutch Ministry of Economic Affairs, Agriculture and Innovation.

Conflict of interest

Janine C. Deddens declares that she has no conflict of interest. Krijn R. Vrijsen declares that he has no conflict of interest. Johanna M. Colijn declares that she has no conflict of interest. Martinus I. Oerlemans declares that he has no conflict of interest. Corina H.G. Metz declares that she has no conflict of interest. Els J. van der Vlist declares that she has no conflict of interest.

Esther N.M. Nolte-'t Hoen declares that she has no conflict of interest. Krista den Ouden declares that she has no conflict of interest. Sanne J. Jansen Of Lorkeers declares that she has no conflict of interest. Tycho I.G. van der Spoel declares that he has no conflict of interest. Stefan Koudstaal declares that he has no conflict of interest. Ger J. Arkesteijn declares that he has no conflict of interest. Marca H.M. Wauben declares that she has no conflict of interest. Linda W. van Laake declares that she has no conflict of interest. Pieter A. Doevendans declares that he has no conflict of interest. Steven A.J. Chamuleau declares that he has no conflict of interest. Joost P.G. Sluijter declares that he has no conflict of interest.

Ethical approval

All applicable international, national, and/or institutional guidelines for the care and use of animals were followed. This article does not contain any studies with human participants performed by any of the authors.

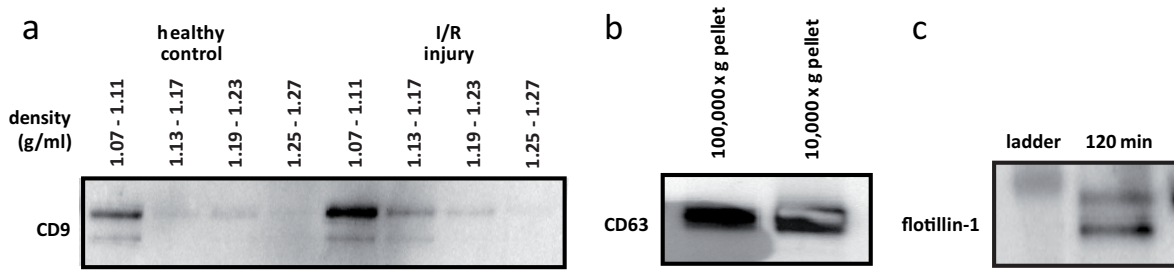
References

1. Thygesen K, Alpert JS, Jaffe AS, et al. Third universal definition of myocardial infarction. *Eur Heart J* 2012;33:2551–67.
2. Keller T, Zeller T, Peetz D, et al. Sensitive troponin I assay in early diagnosis of acute myocardial infarction. *N Engl J Med* 2009;361:868–77.
3. Oerlemans MIFJ, Mosterd A, Dekker MS, et al. Early assessment of acute coronary syndromes in the emergency department: the potential diagnostic value of circulating microRNAs. *EMBO Mol Med* 2012;4:1176–85.
4. Meder B, Keller A, Vogel B, et al. MicroRNA signatures in total peripheral blood as novel biomarkers for acute myocardial infarction. *Basic Res Cardiol* 2011;106:13–23.
5. Shah AS V, Anand A, Sandoval Y, et al. High-sensitivity cardiac troponin I at presentation in patients with suspected acute coronary syndrome: a cohort study. *Lancet (London, England)* 2015;386:2481–8.
6. Deddens JC, Colijn JM, Oerlemans MIFJ, et al. Circulating MicroRNAs as Novel Biomarkers for the Early Diagnosis of Acute Coronary Syndrome. *J Cardiovasc Transl Res* 2013;6:884–898.
7. Rhees B, Wingrove JA. Developing Peripheral Blood Gene Expression-Based Diagnostic Tests for Coronary Artery Disease: a Review. *J Cardiovasc Transl Res* 2015;8:372–80.
8. Friede KA, Ginsburg GS, Voora D. Gene Expression Signatures and the Spectrum of Coronary Artery Disease. *J Cardiovasc Transl Res* 2015;8:339–52.
9. Lagos-Quintana M, Rauhut R, Lendeckel W, Tuschl T. Identification of novel genes coding for small expressed RNAs. *Science* 2001;294:853–8.
10. Sluijter JPG, van Mil A, van Vliet P, et al. MicroRNA-1 and -499 regulate differentiation and proliferation in human-derived cardiomyocyte progenitor cells. *Arterioscler Thromb Vasc Biol* 2010;30:859–68.
11. Lin CJ-F, Gong H-Y, Tseng H-C, Wang W-L, Wu J-L. miR-122 targets an anti-apoptotic gene, Bcl-w, in human hepatocellular carcinoma cell lines. *Biochem Biophys Res Commun* 2008;375:315–20.
12. Arroyo JD, Chevillet JR, Kroh EM, et al. Argonaute2 complexes carry a population of circulating microRNAs independent of vesicles in human plasma. *Proc Natl AcadSci USA* 2011;108:5003–8.
13. Vickers KC, Palmisano BT, Shoucri BM, Shamburek RD, Remaley AT. Mi1. Vickers KC, Palmisano BT, Shoucri BM, Shamburek RD, Remaley AT. MicroRNAs are transported in plasma and delivered to recipient cells by high-density lipoproteins. *Nat Cell Biol* 2011;13:423–33. croRNAs are transported in plasma and delivered to recipie. *Nat Cell Biol* 2011;13:423–33.
14. Valadi H, Ekström K, Bossios A, Sjöstrand M, Lee JJ, Lötvalld JO. Exosome-mediated transfer of mRNAs and microRNAs is a novel mechanism of genetic exchange between cells. *Nat Cell Biol* 2007;9:654–9.
15. Collino F, Deregibus MC, Bruno S, et al. Microvesicles derived from adult human bone marrow and tissue specific mesenchymal stem cells shuttle selected pattern of miRNAs. *PLoS One* 2010;5:e11803.
16. Sluijter JPG, Verhage V, Deddens JC, van den Akker F, Doevendans PA. Microvesicles and exosomes for intracardiac communication. *Cardiovasc Res* 2014;102:302–11.
17. Théry C, Zitvogel L, Amigorena S. Exosomes: composition, biogenesis and function. *Nat Rev Immunol* 2002;2:569–79.
18. Théry C. Exosomes: secreted vesicles and intercellular communications. *F1000 Biol Rep* 2011;3:15.
19. de Gassart A, Geminard C, Fevrier B, Raposo G, Vidal M. Lipid raft-associated protein sorting in exosomes. *Blood* 2003;102:4336–44.
20. Février B, Raposo G. Exosomes: endosomal-derived vesicles shipping extracellular messages. *Curr Opin Cell Biol* 2004;16:415–21.
21. Bank IE, Timmers L, Gijsberts CM, et al. The diagnostic and prognostic potential of plasma extracellular vesicles for cardiovascular disease. *Expert Rev Mol Diagn* 2015;15:1577–88.

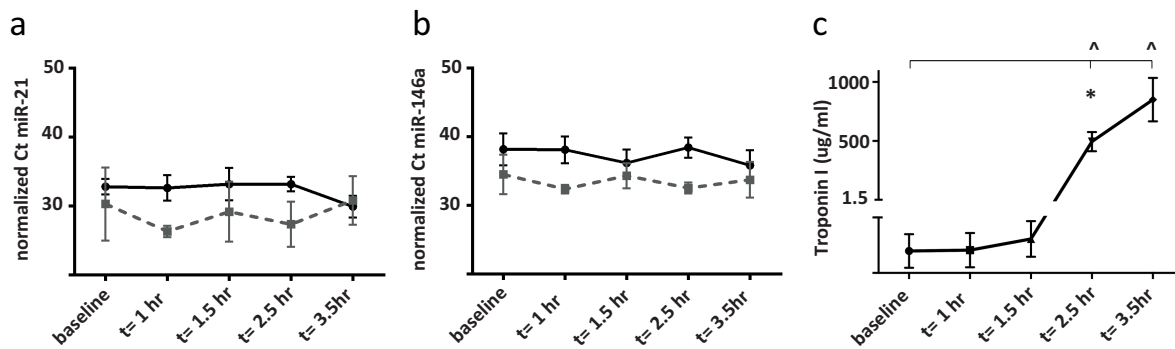
22. Jung C, Sörensson P, Saleh N, Arheden H, Rydén L, Pernow J. Circulating endothelial and platelet derived microparticles reflect the size of myocardium at risk in patients with ST-elevation myocardial infarction. *Atherosclerosis* 2012;221:226–31.
23. de Hoog VC, Timmers L, Schoneveld AH, et al. Serum extracellular vesicle protein levels are associated with acute coronary syndrome. *Eur Hear journal Acute Cardiovasc care* 2013;2:53–60.
24. Jansen F, Yang X, Proebsting S, et al. MicroRNA expression in circulating microvesicles predicts cardiovascular events in patients with coronary artery disease. *J Am Heart Assoc* 2014;3:e001249.
25. van Laake LW, Passier R, Monshouwer-Kloots J, et al. Monitoring of cell therapy and assessment of cardiac function using magnetic resonance imaging in a mouse model of myocardial infarction. *Nat Protoc* 2007;2:2551–67.
26. Oerlemans MIFJ, Liu J, Arslan F, et al. Inhibition of RIP1-dependent necrosis prevents adverse cardiac remodeling after myocardial ischemia-reperfusion in vivo. *Basic Res Cardiol* 2012;107:270.
27. van Rijen HVM, Eckardt D, Degen J, et al. Slow conduction and enhanced anisotropy increase the propensity for ventricular tachyarrhythmias in adult mice with induced deletion of connexin43. *Circulation* 2004;109:1048–55.
28. van der Spoel TIG, Vrijksen KR, Koudstaal S, et al. Transendocardial cell injection is not superior to intracoronary infusion in a porcine model of ischaemic cardiomyopathy: a study on delivery efficiency. *J Cell Mol Med* 2012;16:2768–76.
29. Timmers L, Henriques JPS, de Kleijn DP V, et al. Exenatide reduces infarct size and improves cardiac function in a porcine model of ischemia and reperfusion injury. *J Am Coll Cardiol* 2009;53:501–10.
30. Théry C, Amigorena S, Raposo G, Clayton A. Isolation and characterization of exosomes from cell culture supernatants and biological fluids. *Curr Protoc Cell Biol* 2006;Chapter 3:Unit 3.22.
31. Greening DW, Xu R, Ji H, Tauro BJ, Simpson RJ. A protocol for exosome isolation and characterization: evaluation of ultracentrifugation, density-gradient separation, and immunoaffinity capture methods. *Methods Mol Biol* 2015;1295:179–209.
32. Vrijksen KR, Sluijter JPG, Schuchardt MWL, et al. Cardiomyocyte progenitor cell-derived exosomes stimulate migration of endothelial cells. *J Cell Mol Med* 2010;14:1064–70.
33. Slot JW, Geuze HJ. Cryosectioning and immunolabeling. *Nat Protoc* 2007;2:2480–91.
34. van der Vlist EJ, Nolte-’t Hoen ENM, Stoorvogel W, Arkesteijn GJA, Wauben MHM. Fluorescent labeling of nano-sized vesicles released by cells and subsequent quantitative and qualitative analysis by high-resolution flow cytometry. *Nat Protoc* 2012;7:1311–26.
35. Nolte-’t Hoen ENM, van der Vlist EJ, Aalberts M, et al. Quantitative and qualitative flow cytometric analysis of nanosized cell-derived membrane vesicles. *Nanomedicine* 2012;8:712–20.
36. Mallat Z, Benamer H, Hugel B, et al. Elevated levels of shed membrane microparticles with procoagulant potential in the peripheral circulating blood of patients with acute coronary syndromes. *Circulation* 2000;101:841–3.
37. Bernal-Mizrachi L, Jy W, Jimenez JJ, et al. High levels of circulating endothelial microparticles in patients with acute coronary syndromes. *Am Heart J* 2003;145:962–70.
38. Ostrowski M, Carmo NB, Krumeich S, et al. Rab27a and Rab27b control different steps of the exosome secretion pathway. *Nat Cell Biol* 2010;12:19–30–13.
39. Hedlund M, Nagaeva O, Kargl D, Baranov V, Mincheva-Nilsson L. Thermal- and oxidative stress causes enhanced release of NKG2D ligand-bearing immunosuppressive exosomes in leukemia/lymphoma T and B cells. *PLoS One* 2011;6:e16899.
40. Dragovic RA, Gardiner C, Brooks AS, et al. Sizing and phenotyping of cellular vesicles using Nanoparticle Tracking Analysis. *Nanomedicine* 2011;7:780–8.
41. de Vrij J, Maas SLN, van Nispen M, et al. Quantification of nanosized extracellular membrane vesicles with scanning ion occlusion sensing. *Nanomedicine (Lond)* 2013;8:1443–58.
42. Lötvall J, Hill AF, Hochberg F, et al. Minimal experimental requirements for definition of

- extracellular vesicles and their functions: a position statement from the International Society for Extracellular Vesicles. *J Extracell vesicles* 2014;3:26913.
43. Adachi T, Nakanishi M, Otsuka Y, et al. Plasma microRNA 499 as a biomarker of acute myocardial infarction. *Clin Chem* 2010;56:1183–5.
 44. Wang G-K, Zhu J-Q, Zhang J-T, et al. Circulating microRNA: a novel potential biomarker for early diagnosis of acute myocardial infarction in humans. *Eur Heart J* 2010;31:659–66.
 45. Corsten MF, Dennert R, Jochems S, et al. Circulating MicroRNA-208b and MicroRNA-499 reflect myocardial damage in cardiovascular disease. *Circ Cardiovasc Genet* 2010;3:499–506.
 46. D'Alessandra Y, Devanna P, Limana F, et al. Circulating microRNAs are new and sensitive biomarkers of myocardial infarction. *Eur Heart J* 2010;31:2765–73.
 47. Daniels SE, Beineke P, Rhees B, et al. Biological and analytical stability of a peripheral blood gene expression score for obstructive coronary artery disease in the PREDICT and COMPASS studies. *J Cardiovasc Transl Res* 2014;7:615–22.
 48. D'Alessandra Y, Carena MC, Spazzafumo L, et al. Diagnostic potential of plasmatic MicroRNA signatures in stable and unstable angina. *PLoS One* 2013;8:e80345.
 49. G. Long. Human Circulating MicroRNA-1 and MicroRNA-126 as Potential Novel Indicators for Acute Myocardial Infarction.
 50. Cheng Y, Tan N, Yang J, et al. A translational study of circulating cell-free microRNA-1 in acute myocardial infarction. *Clin Sci (Lond)* 2010;119:87–95.
 51. Gidlöf O, Andersson P, van der Pals J, Göteborg M, Erlinge D. Cardiospecific microRNA plasma levels correlate with troponin and cardiac function in patients with ST elevation myocardial infarction, are selectively dependent on renal elimination, and can be detected in urine samples. *Cardiology* 2011;118:217–26.
 52. Dong S, Cheng Y, Yang J, et al. MicroRNA expression signature and the role of microRNA-21 in the early phase of acute myocardial infarction. *J Biol Chem* 2009;284:29514–25.
 53. Horie T, Ono K, Nishi H, et al. Acute doxorubicin cardiotoxicity is associated with miR-146a-induced inhibition of the neuregulin-ErbB pathway. *Cardiovasc Res* 2010;87:656–64.
 54. Lu TX, Munitz A, Rothenberg ME. MicroRNA-21 is up-regulated in allergic airway inflammation and regulates IL-12p35 expression. *J Immunol* 2009;182:4994–5002.
 55. Lukiw WJ, Zhao Y, Cui JG. An NF-kappaB-sensitive micro RNA-146a-mediated inflammatory circuit in Alzheimer disease and in stressed human brain cells. *J Biol Chem* 2008;283:31315–22.
 56. Wang K, Zhang S, Weber J, Baxter D, Galas DJ. Export of microRNAs and microRNA-protective protein by mammalian cells. *Nucleic Acids Res* 2010;38:7248–59.
 57. Kuwabara Y, Ono K, Horie T, et al. Increased microRNA-1 and microRNA-133a levels in serum of patients with cardiovascular disease indicate myocardial damage. *Circ Cardiovasc Genet* 2011;4:446–54.
 58. Johnson PD, Besselsen DG. Practical aspects of experimental design in animal research. *ILAR J* 2002;43:202–6.
 59. Boeckel J-N, Thomé CE, Leistner D, Zeiher AM, Fichtlscherer S, Dimmeler S. Heparin selectively affects the quantification of microRNAs in human blood samples. *Clin Chem* 2013;59:1125–7.
 60. Kaudewitz D, Lee R, Willeit P, et al. Impact of intravenous heparin on quantification of circulating microRNAs in patients with coronary artery disease. *Thromb Haemost* 2013;110:609–15.
 61. Van Deun J, Mestdagh P, Sormunen R, et al. The impact of disparate isolation methods for extracellular vesicles on downstream RNA profiling. *J Extracell vesicles* 2014;3.

Supplementary



Supplementary Figure 1. Characterization of mouse plasma derived EV. A) CD9 and CD63 **(B)** are expressed in different sucrose gradient fractions (1.07-1.11 g/ml). **C)** EV isolated from Langendorff perfusate stain positive for flotillin-1.



Supplementary Figure 2. Temporal miRNA analysis. A-B) Expression levels of miRNA-21, miRNA-146a and Troponin I **(C)** at different timepoints upon I/R injury. Error bars indicate standard deviation, in **C** a significant difference ($p < 0.05$) with baseline is marked with \wedge . * marks a significant difference between $t = 2.5$ hr and $t = 3.5$ hr.

4

Circulating microRNAs as diagnostic biomarkers for myocardial ischemia in stable outpatients: not fulfilling their promise

*J.C. Deddens

*I. E.M. Bank

G. Pasterkamp

D.P.V. de Kleijn

G.W. Dalmeijer

H.M. den Ruijter

L.A. Boven

J.M.H. de Klerk

D. Tempel

M. Rossato

C.P.J. Bekker

P.A. Doevendans

A. Mosterd

J.P.G. Sluijter

L. Timmers

*These authors contributed equally to this work

Submitted

Abstract

Rationale: Many patients have (symptoms suggestive of) angina pectoris, yet the diagnostic workup for myocardial ischemia is expensive and inefficient. The availability of a reliable blood-based biomarker may provide a good alternative for conventional ischemia testing (i.e. exercise ECG and non-invasive imaging techniques). Altered expression of specific circulating microRNAs (miRNAs) has previously been observed in patients with stable angina.

Objective: To assess whether circulating miRNAs can be used as diagnostic blood-based biomarkers for myocardial ischemia in stable outpatients.

Methods and Results: A two-phase biomarker study was conducted within a cohort of prospectively recruited patients undergoing Rubidium-82 PET/CT myocardial perfusion imaging (MPI) in the outpatient diagnostic workup for suspected myocardial ischemia (n=863, median [25th to 75th percentile] age 69 [62 to 75] years). Myocardial ischemia was confirmed in 20.5% of the patients. In the discovery phase, profiling of circulating miRNAs was performed in 12 patients with myocardial ischemia and 8 matched controls. Eleven miRNAs were selected for the validation phase, in which their diagnostic accuracy was assessed in a case-cohort study (n=346). In the validation study, none of the 11 miRNAs were significantly associated with the presence of myocardial ischemia. Also, their discriminatory accuracy was poor. The highest area under the receiver operating characteristics curve (AUC) [95% confidence interval] was 0.58 [0.52-0.64] for miR-21.

Conclusions: In this two-phase biomarker study, no circulating miRNAs could be identified that yield the potential to be used as diagnostic blood-based biomarkers for myocardial ischemia in stable outpatients.

Keywords: stable angina, myocardial ischemia, diagnostic blood test, microRNA, biomarker

Introduction

Coronary artery disease (CAD) remains an important cause of morbidity and mortality worldwide, and is mainly attributable to atherosclerosis [1]. Atherosclerotic narrowing of one or more of the major coronary arteries leads to a blood demand/supply mismatch (i.e. ischemia) in the downstream myocardium upon exercise, emotion or other stress, and is traditionally referred to as stable coronary artery disease (SCAD) [2]. An episode of reversible myocardial ischemia is typically accompanied by angina pectoris: transient chest pain, chest discomfort or dyspnea. Symptoms of angina pectoris are reported to be highly prevalent: around 4-7% of people aged 45-56 years and 10-14% of people aged 65-84 years have angina [3]. Nonetheless, many people with myocardial ischemia only experience atypical complaints (especially diabetics, elderly and women), and even severe myocardial ischemia may be completely clinically silent [2].

Early recognition and treatment of myocardial ischemia reduces the incidence of adverse atherothrombotic events, thereby preventing irreversible cardiac injury and improving prognosis [2]. Unfortunately, the identification of patients with myocardial ischemia poses a considerable clinical and health economical challenge, since the current diagnostic workup is inefficient and expensive. Whereas high sensitivity troponin plays

a pivotal role in the identification of patients with myocardial infarction (MI), no blood biochemical markers exist to identify patients with exercise- or stress-induced myocardial ischemia. As a consequence, exercise ECG and non-invasive imaging techniques as coronary computed tomography angiography (CCTA), cardiac magnetic resonance imaging (MRI) and nuclear myocardial perfusion imaging (MPI) are frequently performed. Invasive coronary angiography is often needed to confirm (or to rule out) the presence of obstructive CAD. The availability of a reliable blood -based biomarker to detect myocardial ischemia may provide a good substitute for current conventional ischemia detection techniques and may help to improve patient management and reduce healthcare costs.

MicroRNAs (miRNAs) are non-coding RNAs of ~22 nucleotides that negatively regulate gene expression at a post-transcriptional level [4, 5]. Over the past decade, miRNAs have been recognized to be regulators of a variety of pathophysiological processes involved in atherosclerosis (e.g. inflammatory and lipid homeostasis pathways and hypoxia) [6]. Previous studies investigating the diagnostic potential of circulating miRNAs in patients with stable angina have shown promising results regarding miR-1, miR-21, miR-126, miR-132 and miR-485 [7–10]. However, translation of these results towards clinical application is hampered by the limited number of patients that were studied, and by the use of (relatively) healthy controls.

Therefore, the aim of our study was to assess whether circulating miRNAs can be used as diagnostic blood-based biomarkers for myocardial ischemia, in a large, real-world cohort of patients with suspected myocardial ischemia.

Methods

Study population

The MYOMARKER (MYOcardial ischemia detection by circulating bioMARKERS) study is a prospective single-center observational cohort study involving consecutive patients (>18 years) who underwent Rubidium-82 positron emission tomography-computed tomography (PET/CT) in the outpatient diagnostic workup for suspected myocardial ischemia, as referred by their cardiologist. Venous blood was obtained ahead of myocardial perfusion imaging (MPI). After centrifugation (10min, 2100xg) the plasma component was frozen and stored at -80°C until sample analysis. Patients were enrolled at the Meander Medical Center (Amersfoort, the Netherlands), from August 2014 onwards. At the time of the current study, a total of 873 patients had been enrolled. Patients with incomplete MPI results (n=4) or unavailable of EDTA plasma for miRNA quantification (n=6) were excluded, leaving n=863 patients for the current biomarker study. The study was approved by the regional medical ethics committee and written informed consent was obtained from all participants.

Definition of myocardial ischemia

Rubidium-82 PET/CT scans were acquired using a hybrid PET/CT scanner (Biograph mCT Flow 64-slice scanner, Siemens Healthcare, Knoxville, Tennessee). In short, images were acquired in rest and after pharmacological stress with regadenoson. Myocardial ischemia was defined as the presence of reversible, stress-induced perfusion defects with a summed difference score (SDS) of at least 4, as visually (semi-quantitatively) assessed by two observers. The observers were blinded to the results of miRNA quantification. *Detailed methods in Supplement.*

Study design

The present study was conducted in two phases: (1) a discovery phase, in which miRNA profiling was performed in 12 patients with and 8 patients without myocardial ischemia (matched for age, sex, risk factors and medication use), and (2) a validation phase, in which the

diagnostic potential of the selected miRNAs was evaluated using a case-cohort design for the efficiency of biomarker evaluation. Starting with the n=863 eligible patients in the MYOMARKER cohort, the subcohort was randomly selected with a sampling fraction of $\alpha=0.25$ (n=216), and all remaining incident cases in the entire cohort were identified (n=130). The validation study thus involved n=346 patients. (Figure 1)

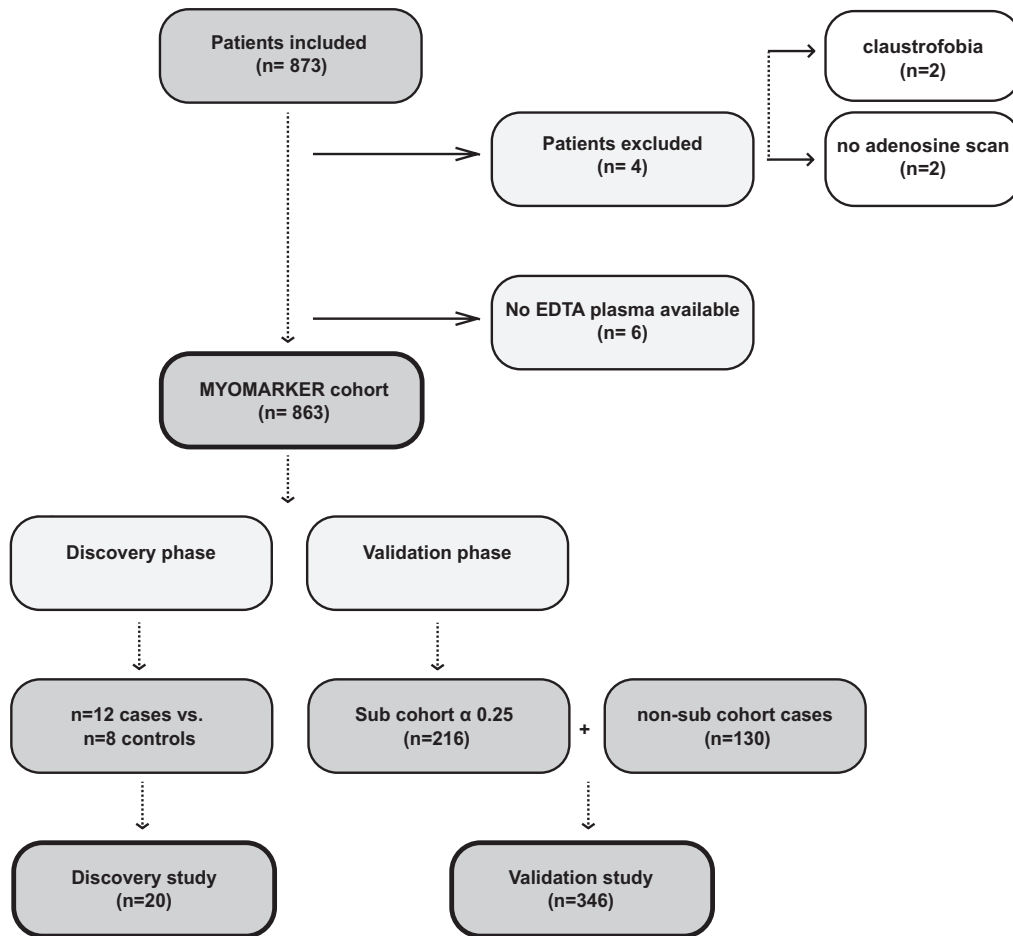


Figure 1. Flowchart

Isolation and detection of circulating microRNAs

Total RNA was extracted from plasma using the miRCURY™ RNA isolation kit – biofluids (Exiqon). Briefly, frozen EDTA plasma samples were thawed on ice and centrifuged at 3000x g for 5 min at 4°C before use. Aliquots of 250µL plasma were lysed with 60ul Lysis solution and column-based purification of RNA was performed. RNA was eluted from the column with 50ul

RNase free H₂O and supplemented with RNase inhibitor. For normalization, plasma samples were supplemented with ath-miR-159a (6pg/ul) and SNORD44/SNORD48 synthetic oligonucleotides (2.5pg/ul) before RNA extraction. Isolation accuracy was verified by analyzing the spike-in RNA levels using individual miRNA-specific primers and Multiscribe RT enzyme (Lifetechnologies) followed by real time PCR (Taqman).

For miRNA profiling, the Taqman OpenArray Human MicroRNA Panel Set v3.0 (Applied Biosystems, n=758 miRNAs) was used according to the manufacturer's recommendations. Megaplex reverse transcription and pre-amplification was performed using 2.5ul of isolated serum RNA using Taqman Open Array Human MicroRNA Megaplex™ primers, Multiscribe™ reverse transcriptase and Megaplex PreAmp primers (Applied Biosystems) in two separate pools (A+B). Taqman OpenArray Real-Time PCR master mix (Applied Biosystems) was added to the pre-amplified cDNA, and the AccuFill system was used to load the array plates. Real time amplification was performed in the Quantstudio™ 12K Flex (Applied Biosystem).

This protocol was also used in the validation phase, but the selected miRNAs (n=11) were included in Taqman Custom 56K OpenArray plates (Applied Biosystems). Ath-miRNA-159a, RNU44 and miRNA-23a-3p and miRNA-451a were included as controls in the custom plate. The ratio of miRNA-23a and miRNA-451a levels was considered a measure of hemolysis: samples with a ratio >7 were defined hemolytic.

Statistical analysis

miRNA expression data were analyzed using the Thermo Fisher Cloud Analysis software. In the profiling phase miRNA expression levels were normalized to SNORD44, and in the validation phase miRNA expression was normalized to ath-miR-159a. These normalizers were similarly expressed between the respective patients with and without myocardial ischemia (*Supplemental Figure 1*). Default threshold scores for amplification efficacy (AMP score >1.24) and calculated Crt value confidence (CQCONF> 0.8) were applied to all data. Assays that did not pass these

criteria where considered not detectable and were, in order to prevent missing data, assigned the defined maximum Crt value (Crt 32).

In the profiling phase, miRNA levels (dCrt) of patients with myocardial ischemia (SDS ≥ 4 , n=12) and the subset of patients with more extensive myocardial ischemia (SDS ≥ 7 , n=6) were compared to miRNA levels of patients without any evidence of myocardial ischemia (SDS=0, n=8) using a *t* test with Welch correction or Mann-Whitney U test as appropriate. Fold differences and area under the receiver operating characteristic (ROC) curve (AUC) were computed for differentially expressed miRNAs (p values < 0.15). Selection of miRNAs for the validation phase was on the basis of both effect size (fold difference > 1.5) and effect strength (AUC > 0.70).

In the validation phase, the Cox proportional hazards model with Prentice weighting and robust standard errors was used to allow for the oversampling of patients with myocardial ischemia in the case-cohort design.[11] Incidence rate ratios (IRR) and corresponding 95% confidence intervals (CI) were calculated for the individual miRNAs (per 1 dCrt increase in miRNA expression) for the outcome of myocardial ischemia. The time-to-event was forced to be 1 in all patients, as myocardial perfusion imaging was performed at the day of inclusion. The discriminative value of the individual miRNAs and the 11 miRNAs combined was assessed by constructing ROC curves and determining the AUC. Pre-specified subgroup analyses were performed to assess whether the miRNA levels further differed according to sex, and according to the extent of myocardial ischemia.

Statistical analysis were performed using RStudio [12] and R software[13] for statistical computing version 3.1.2. with the “Survival” package. A p value of < 0.05 was considered statistically significant and all p values were 2-sided.

Table 1. Baseline characteristics of the MYOMARKER cohort

	No Ischemia (SDS <4)	Ischemia (SDS >4)	p-value
n	671	177	
Age, years (median [IQR])*	68.0 [61.5, 75.0]	71.0 [64.0, 76.0]	0.017
Gender, % males	56.6	72.9	<0.001
BMI (median [IQR])*	26.9 [24.2, 30.2]	26.4 [24.1, 29.4]	0.516
<i>Risk factors</i>			
Diabetes(%)	20.1	28.2	0.026
Hypertension(%)	64.9	67.2	0.619
Hypercholesterolemia(%)	57.9	65.7	0.074
Smoking (%)			0.134
Current	17.3	18.4	
Former (>30days)	53.3	59.8	
Never	29.4	21.8	
Family history of CAD(%)	29.5	32.9	0.429
<i>Patient history</i>			
History of MI (%)	22.0	46.0	<0.001
History of PCI(%)	30.9	50.3	<0.001
History of CABG(%)	9.3	27.7	<0.001
GFR calculated (median [IQR])*	75.7 [60.3, 97.9]	75.0 [58.9, 93.8]	0.403
GFR < 60(%)	26.8	34.1	0.081
<i>Medication</i>			
Aspirin(%)	53.1	69.5	<0.001
Other Antiplatelet agents(%)	13.6	22.2	0.007
Anticoagulantia(%)	20.1	26.0	0.107
Beta-blocker(%)	51.1	67.8	<0.001
ACE-inhibitor(%)	32.3	46.0	0.001
Statin(%)	61.6	70.6	0.033
Other lipid lowering agent(%)	8.8	11.3	0.391
Long acting nitrate(%)	13.8	16.9	0.343

BMI, body mass index; CAD, coronary artery disease; MI, myocardial infarction; PCI, percutaneous coronary intervention; CABG, coronary artery bypass grafting; GFR, glomerular filtration rate; LVEF, left ventricular ejection fraction; SBP, systolic blood pressure; DBP, diastolic blood pressure.

Results

Prevalence of myocardial ischemia

In the MYOMARKER cohort, myocardial ischemia was documented in 20.5% of patients (n=177), and excluded in 77.8% of patients (n=671). In the remaining 1.7% of patients (n=15) the presence of myocardial remained unknown, for uninterpretable MPI due to (scaling) artifacts (n=2), discrepancy between visual scores and calculated SDS scores (n=3), or attenuation artifacts (n= 10). Baseline characteristics are depicted in *Table 1*. Compared to non-ischemic patients, patients with myocardial ischemia were more likely to be male, and more likely to have diabetes, a history of myocardial infarction myocardial infarction (MI), percutaneous coronary intervention (PCI) or coronary artery bypass grafting (CABG). They were also more likely to use aspirin, beta-blockers and angiotensin-converting-enzyme (ACE) inhibitors.

Discovery phase - miRNA profiling

Overall, the number of differentially expressed miRNAs was low (n= 15). The comparison of miRNA levels in patients with myocardial ischemia (SDS ≥ 4) versus no ischemia (SDS=0) resulted in five differentially expressed miRNAs (fold difference > 1.5 and p value < 0.15), of which 2 were upregulated. Comparing no ischemia to more extensive myocardial ischemia (SDS ≥ 7) resulted in 12 differentially expressed miRNAs, of which 10 were upregulated. Seven of the in total 15 differentially expressed miRNAs (overlap of n=2) had an AUC ≥ 0.70 and were thus selected for the validation phase of this study: miR-1-3p, miR-29a-5p, miR-211-5p, miR-301b-3p, miR-342-3p, miR-590-3p and miR-628-5p. Although miR-21-5p, miR-126-3p, miR-132-3p, and -485-3p were not differentially expressed, we them for validation based on their potential role as biomarkers for stable angina or CAD in previous studies [9, 10, 14]. The final miRNA panel for the validation cohort is depicted in *Figure 2*.

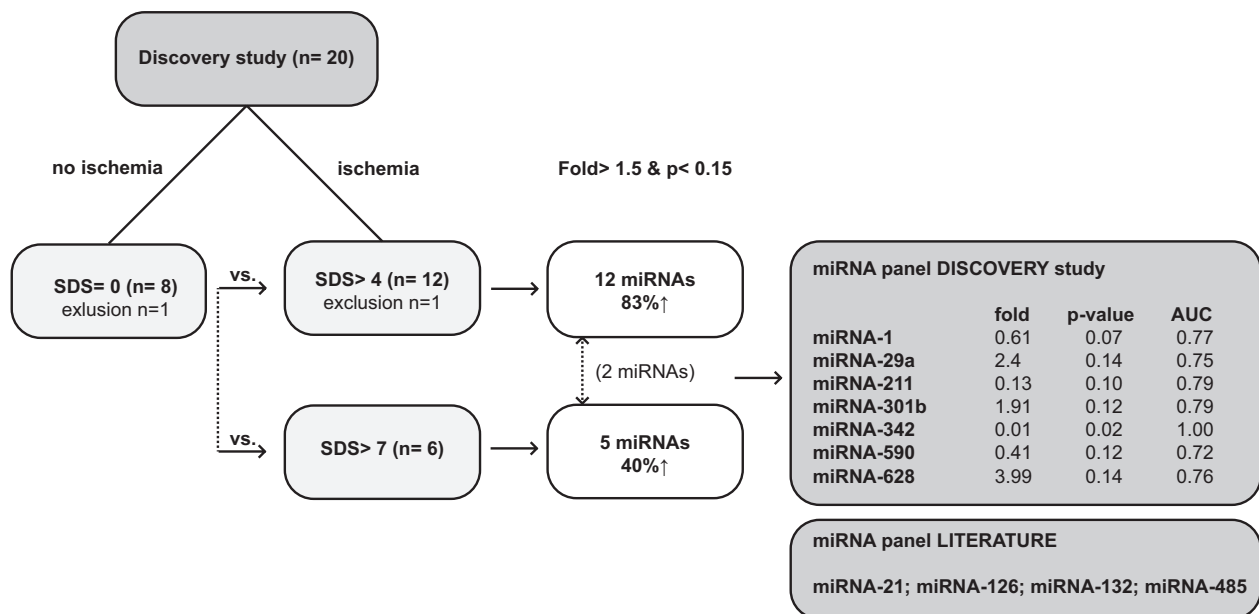


Figure 2. Discovery study – miRNA profiling.

Validation phase – biomarker validation

The case-cohort study concerned n=346 patients, n=177 (51.2%) of whom had myocardial ischemia. No ischemia (SDS<4) was present in 167 (48.3%) patients. Two patients (0.6%) were excluded from the analyses because of uninterpretable MPI results. Three samples (0.9%) had to be discarded, as none of the target or spike-in miRNAs could be detected, probably due to technical errors. Ten samples (2.9%) had a hemolysis score (ratio of miR-23a/miR-451 levels) above 7, indicating significant hemolysis.

Diagnostic potential of circulating miRNA levels for myocardial ischemia

None of the eleven selected miRNAs had circulating levels that were significantly associated with myocardial ischemia (Table 2). A trend (p value 0.053) was observed for higher miR-21 expression with myocardial ischemia (IRR 0.79, 95% CI 0.62-1.00) per 1 dCrt increase of miRNA-21 expression. All 11 miRNAs had poor discriminatory accuracy for the diagnosis of myocardial ischemia (Table 2). The highest AUC [95% confidence interval] was observed for miR-21 with an AUC of 0.58 [0.52-0.64]. None of the circulating miRNAs had an AUC >0.60. The

combination of all 11 miRNAs had an AUC of 0.63 [0.58-0.70]. These patterns were generally replicated within the subsets of females and males, and miRNA levels were not related to the extent of myocardial ischemia. In addition, none of the circulating miRNAs significantly associated with age, gender, concomitant cardiovascular risk factors (diabetes, hypertension, dyslipidemia, smoking, prior CAD), or standard medications (aspirin, beta blockers, ACE-inhibitors, statins). (*Data not shown*)

Table 2. Circulating miRNA levels and their diagnostic performance in patients with and without myocardial ischemia

<i>Biomarker</i>	<i>IRR (95% CI)</i>	<i>p value</i>	<i>AUC (95% CI)</i>	<i>% Crt32</i>
miR-1	1.02 (0.93-1.11)	0.695	0.51 (0.45-0.57)	1.5%
miR-21	0.79 (0.62-1.00)	0.053	0.58 (0.52-0.64)	0.0%
miR-29	0.99 (0.93-1.07)	0.864	0.52 (0.46-0.58)	25.5%
miR-126	0.97 (0.91-1.04)	0.415	0.52 (0.46-0.58)	2.9%
miR-132	1.01 (0.89-1.15)	0.870	0.52 (0.46-0.59)	0.9%
miR-211	1.09 (0.96-1.23)	0.190	0.52 (0.46-0.58)	3.2%
miR-301	0.98 (0.85-1.14)	0.801	0.51 (0.45-0.58)	0.6%
miR-342	0.99 (0.83-1.20)	0.950	0.52 (0.45-0.58)	0.0%
miR-485	1.01 (0.88-1.15)	0.932	0.51 (0.44-0.57)	0.0%
miR-590	1.00 (0.92-1.10)	0.966	0.51 (0.45-0.57)	0.3%
miR-628	0.91 (0.85-1.09)	0.528	0.54 (0.48-0.60)	1.2%

All incidence rate ratios (IRR) represent an increase of 1 dCrt in miRNA level in patients with ischemia versus without ischemia, Time-to-event is set at 1 for all patients. Abbreviations:

CI, confidence interval; AUC, Area under the receiver-operating-characteristic curve.

Discussion

In this two-phase biomarker study within the MYOMARKER cohort – a large, prospective single-center observational cohort study of outpatients with suspected myocardial ischemia undergoing Rubidium-82 PET/CT MPI – we were not able to identify circulating miRNAs that have potential to be used as diagnostic biomarker for myocardial ischemia. In the discovery phase, 11 miRNAs were selected for validation on the basis of miRNA profiling and literature. Upon validation however, the discriminatory accuracy of the selected miRNAs turned out to be poor, the highest AUC being 0.58 [95%CI 0.52-0.64] for miR-21.

Our findings contradict prior small case-control studies, in which various circulating miRNAs were reported to be differentially expressed in patients with stable angina and angiographically documented CAD versus matched (healthy) controls [9, 10, 15]. The preceding studies were small (n=53 patients at most) and divergent miRNA expression patterns were observed. Whereas Fichtlscherer *et al.* and Weber *et al.* primarily observed downregulation of miRNAs in diseased individuals, D'Alessandra *et al.* principally observed upregulation of miRNAs in association with disease. Noteworthy, Weber *et al.* could not replicate their findings when healthy controls were substituted for control patients who had ≥ 2 risk factors for CAD [15]. This may indicate that circulating miRNAs are not specific markers for myocardial ischemia, but instead reflect pathophysiological alterations that are already present in patients with increased cardiovascular risk, or with subclinical or non-obstructive atherosclerosis [6]. In this light, it is important to appreciate that the MYOMARKER cohort consists of real-world outpatients with a substantial cardiovascular risk factor burden and/or prior CAD, irrespective of the presence of myocardial ischemia.

Furthermore, when comparing results of our study with previous studies, the differences in the primary outcome measure should be considered, i.e. the presence of stress-induced myocardial ischemia (functional measure) versus the presence of angiographically documented CAD (anatomical measure). The absence of myocardial ischemia does not exclude the presence of non-obstructive CAD. Conversely, in patients with non-obstructive CAD, microvascular

dysfunction and coronary vasospasms may lead to myocardial ischemia. Documentation of myocardial ischemia is considered mandatory to justify revascularization in patients with stable CAD [2]. A biomarker that detects myocardial ischemia might therefore be of greater diagnostic and prognostic relevance than a biomarker that detects atherosclerosis.

Strengths and limitations

Strengths of the present study include its two-phase design - discovery and validation, aiming for clinical translation - and the by far largest number of real-world patients in which the diagnostic value of circulating miRNAs for myocardial ischemia were evaluated. Rubidium-82 PET/CT has high diagnostic accuracy and is superior to the more widely used single-photon emission tomography (SPECT) [16]. In addition, hemodynamic significance of CAD cannot be simply equated with anatomical assessment by CCTA or coronary angiography [17].

A number of limitations are acknowledged. Firstly, acute changes in miRNA expression attributable to the pharmacologically induced myocardial hypoxemia are not captured, as blood withdrawal took place before MPI. It is important to realize that this is in line with timing of biomarker testing in clinical practice; blood withdrawal will generally not take place during or shortly after an episode of stress-induced anginal complaints. Secondly, the array used for miRNA profiling allows the simultaneous analysis of only 758 miRNAs, whereas approximately >1800 different miRNAs are currently known. Thirdly, in consideration of the large number of patients and the various miRNAs of interest in the validation phase, we made use of a high-throughput customized qPCR platform, with preceding megaplex reverse transcription and pre-amplification, instead of single qPCR for the detection of the miRNAs.

Conclusions

In this two-phase biomarker study of stable outpatients undergoing Rubidium-82 PET/CT in the diagnostic work-up for suspected myocardial ischemia, no circulating miRNAs could be identified that yield the potential to be used as sensitive blood-based biomarkers for the

detection of myocardial ischemia. This stands in contrast to previously reported differential expression of several miRNAs in small case-control studies with relatively healthy controls. Circulating miRNAs may not be specific markers for myocardial ischemia, but instead reflect pathophysiological alterations present in patients with cardiovascular risk factors or subclinical atherosclerosis. The negative results of our study underscore the importance of validating results of small biomarker studies in clinically relevant patient populations to examine the true clinical impact.

Acknowledgments

The authors gratefully acknowledge the assistance of Merel Schurink and Elske Mak in the conduct of the MYOMARKER study and the technical assistance of Esther van Eeuwijk in miRNA quantification.

Sources of Funding

We acknowledge the support from Innovation and the Netherlands CardioVascular Research Initiative (CVON) HUSTCARE 2011/12: The Dutch Heart Foundation, Dutch Federation of University Medical Centers, the Netherlands Organization for Health Research and Development and the Royal Netherlands Academy of Science. We also acknowledge support from Stichting Bijstand Meander Medisch Centrum and Stichting wetenschappelijk onderzoek hart- en vaatziekten Amersfoort.

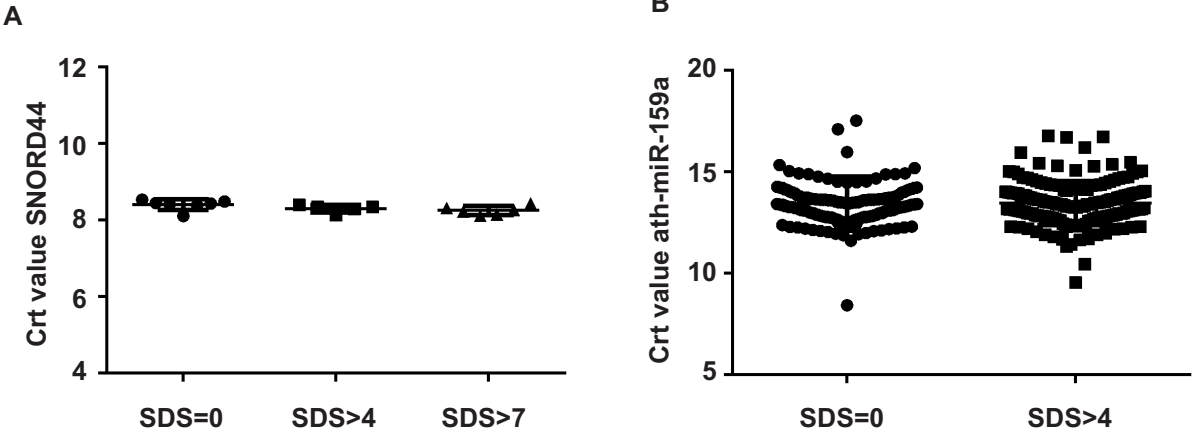
Disclosures

None

References

1. Writing Group Members, Mozaffarian D, Benjamin EJ, et al. Heart Disease and Stroke Statistics-2016 Update: A Report From the American Heart Association. *Circulation* 2016;133:e38-60.
2. Montalescot G, Sechtem U, Achenbach S, et al. 2013 ESC guidelines on the management of stable coronary artery disease: the Task Force on the management of stable coronary artery disease of the European Society of Cardiology. *Eur Heart J* 2013;34:2949–3003.
3. National Institutes of Health, National Institutes of Health. *Morbidity & Mortality: 2012 Chart Book on Cardiovascular, Lung, and Blood Diseases*. Natl Insitutes Heal 2012:116.
4. Lagos-Quintana M, Rauhut R, Lendeckel W, Tuschl T. Identification of novel genes coding for small expressed RNAs. *Science* 2001;294:853–8.
5. Sluijter JPG, van Mil A, van Vliet P, et al. MicroRNA-1 and -499 regulate differentiation and proliferation in human-derived cardiomyocyte progenitor cells. *Arterioscler Thromb Vasc Biol* 2010;30:859–68.
6. Feinberg MW, Moore KJ. MicroRNA Regulation of Atherosclerosis. *Circ Res* 2016;118:703–20.
7. Creemers EE, Tijssen AJ, Pinto YM. Circulating microRNAs: novel biomarkers and extracellular communicators in cardiovascular disease? *Circ Res* 2012;110:483–95.
8. Economou EK, Oikonomou E, Siasos G, et al. The role of microRNAs in coronary artery disease: From pathophysiology to diagnosis and treatment. *Atherosclerosis* 2015;241:624–33.
9. D'Alessandra Y, Carena MC, Spazzafumo L, et al. Diagnostic potential of plasmatic MicroRNA signatures in stable and unstable angina. *PLoS One* 2013;8:e80345.
10. Fichtlscherer S, De Rosa S, Fox H, et al. Circulating microRNAs in patients with coronary artery disease. *Circ Res* 2010;107:677–84.
11. Barlow WE, Ichikawa L, Rosner D, Izumi S. Analysis of case-cohort designs. *J Clin Epidemiol* 1999;52:1165–72.
12. Allaire J. RStudio: Integrated development environment for R. 2012.
13. R Core Team. R: A Language and Environment for Statistical Computing. In: Vienna, Austria, 2014.
14. Ren J, Zhang J, Xu N, et al. Signature of circulating microRNAs as potential biomarkers in vulnerable coronary artery disease. *PLoS One* 2013;8:e80738.
15. Weber M, Baker MB, Patel RS, Quyyumi AA, Bao G, Searles CD. MicroRNA Expression Profile in CAD Patients and the Impact of ACEI/ARB. *Cardiol Res Pract* 2011;2011:532915.
16. Mc Ardle BA, Dowsley TF, DeKemp RA, Wells GA, Beanlands RS. Does rubidium-82 PET have superior accuracy to SPECT perfusion imaging for the diagnosis of obstructive coronary disease?: A systematic review and meta-analysis. *J Am Coll Cardiol* 2012;60:1828–37.
17. Meijboom WB, Van Mieghem CAG, van Pelt N, et al. Comprehensive assessment of coronary artery stenoses: computed tomography coronary angiography versus conventional coronary angiography and correlation with fractional flow reserve in patients with stable angina. *J Am Coll Cardiol* 2008;52:636–43.

Supplementary



Supplementary Figure 1. A) Crt values of SNORD44 expression in the discovery study. SNORD44 was equally expressed across the different groups. **B)** Crt values of ath-miR-159a in replication study showed an equal expression between patients with SDS<4 and SDS>4.

5

Feasibility of echo-guided intramyocardial injections in mice for cardiac progenitor cell delivery in chronic cardiac remodeling

J.C. Deddens

D.A.M. Feyen

P.A.F.M. Doevendans

L.W. van Laake

J.P.G. Sluijter

In preparation

Abstract

In pre-clinical and clinical research, cardiac stem cell therapy is applied by either systemic or local delivery strategies. In murine models, the most common delivery strategy is intramyocardial injection after sternotomy or thoracotomy. However, the invasive nature of these procedures is arguably only convenient in experimental acute myocardial infarction (MI) and hampers stem cell studies in chronic cardiac remodeling. Since appropriate murine models are indispensable for mechanistic studies prior to clinical translation, we examined the feasibility of a minimally invasive echo-based local delivery strategy. We compared echo-guided intramyocardial injections (echo-IMI) of cardiac progenitor cells (CPC) with an open-thoracic intramyocardial injection (open-IMI) approach by measuring cell retention *in vivo*. Moreover, we examined the injection of CPC at several time-points after induction of chronic cardiac remodeling. We demonstrated that echo-IMI is an efficient and technical feasible method for stem cell delivery in a murine model of chronic cardiac remodeling. The minimal invasiveness of echo-guided injections and the numerous options regarding timing and location of therapy offer great potential to improve preclinical small animal research.

Introduction

Improvements in the acute treatment of myocardial infarction (MI) through pharmacological and interventional revascularization procedures have led to a higher initial disease survival [1]. Unfortunately, the possible subsequent development of chronic heart failure (CHF) results in a delayed morbidity and mortality and to date, current treatments are insufficient to improve cardiac function [2]. Cardiac cell therapy has emerged from the field of regenerative medicine as an innovative and hopeful approach for patients with CHF and is examined for its therapeutic potential in several large animal models and clinical trials [3]. Although the initial results were promising, the true effect of cardiac cell therapy especially for patients with CHF remains controversial and is hampered by a lack of knowledge on its mechanism of action [4]. To manage successful (pre)clinical translation, it is essential to study the basic mechanisms behind cell therapy in small animal models during this chronic remodeling phase [5]. Yet, only a limited number of studies [6–9] tested stem cell therapy in small animal models of CHF and therefore fall short on discovering the true potency of therapy.

The advantages of small animal models in preclinical research include their manageability and the opportunity to test therapies on a small scale. Moreover, to answer complex mechanistic questions, a large number of transgenic and knockout strains are available [10]. However, at later time-points after invasive MI surgery it remains difficult to apply local therapeutics due to the lack of accessibility to the heart and the difficulty to use injection catheters in the small vascular anatomy of mice. Echocardiography (echo)-guided intramyocardial injection (echo-IMI) can bypass these hurdles and by that can facilitate advances in small animal research. Although echo-IMI are already applied in several studies [9, 11], a direct comparison of stem cell injection in different phases after ischemia/ reperfusion (I/R) injury has not been performed. Therefore, our primary objective was to examine the feasibility of a minimally invasive echo-based local delivery strategy. We tested the injection of cardiac-derived progenitor cells (CPC) at several time-points after induction of chronic cardiac remodeling and specifically focused on cell retention.

Material and methods

CPC isolation, expansion and transduction

Human fetal tissue was obtained by individual permission using standard informed consent procedures and prior approval of the ethics committee of the University Medical Center Utrecht, the Netherlands. This procedure is in accordance with the principles outlined in the Declaration of Helsinki for the use of human tissue or subjects. As described previously [12, 13], CPC were isolated and subsequently transduced with a lenti-viral construct (pLV-CMV-luc-GFP) to facilitate their identification *in vivo*. Cells were cultured in SP++ (M199, EGM2, FBS, P/S, NEAA) until 80% confluency and used for *in vivo* transplantation at passage 12.

Animals

All experiments were carried out in accordance with the Guide for the Care and Use of Laboratory Animals, with prior approval by the Animal Ethical Experimentation Committee, Utrecht University, the Netherlands.

Surgical procedures

Male NOD-SCID mice (Harlan Laboratories), aged 10-12 weeks, were subjected to left coronary artery (LAD) ligation as previously described [14], followed by reperfusion. In short, mice were anesthetized with Fentanyl 0.05 mg/kg, Midazolam 5 mg/kg and Domitor 0.5 mg/kg through an intraperitoneal injection. Mice were intubated and ventilated with a mixture of oxygen and air (1:2) with a rate of 250 ventilations/min. The left hemithorax was opened between the 3th and 4th rib and the heart was inspected and freed from excessive connective tissue and fat.

For induction of I/R injury (n= 32), the LAD was ligated 2-3 mm below the left atrial appendage with a 8-0 Ethilon suture (Ethicon) around a soft tube (BD insyte-WA). After 60 minutes, reperfusion was initiated by releasing the ligature and removal of the tube. Reflow was confirmed by reversed discoloration of the heart.

For open-thorax intramyocardial injection (open-IMI), the needle tip (29 Gy) was bended with the needle opening downwards, to allow for a parallel injection position. 0.5 million CPC were injected in the anterior wall at the borders of the LAD in 2 x 5 μ l (n= 3).

After either open-IMI or induction of I/R injury, the chest was closed in layers and a mixture of Antisedan 2.5 mg/kg and Anexate 0.5 mg/kg, injected subcutaneously, antagonized anesthesia.

3D motor echocardiography

Echo was performed at baseline and prior to echo-IMI. For echo acquisition, a high-resolution ultrasound system (Vevo 2100, VisualSonics) with a 18-38 MHz transducer (MS 400, visual sonics) was used. Mice were anesthetized with 1.5%-2% isoflurane and heart rate and temperature were monitored continuously and were maintained stable at 500-550 bpm and $37 \pm 1^\circ\text{C}$, respectively. In addition, an electrocardiogram (ECG) was used to identify appropriate end-diastolic and end-systolic triggers. For reconstructed three-dimensional (3D) echo images, the transducer was positioned in the short-axis view (SAX). The left ventricle was scanned by consecutive images (0.064 mm intervals) of the short axis using a 3D-motor (VisualSonics). 3D images were reconstructed based on the drawing of approximately 10-12 volumes of interest within the left ventricular volume. The left ventricular end-diastolic volume (LVEDV) and left ventricular end-systolic volume (LVESV) were used to calculate left ventricular ejection fraction (LVEF).

Echo-guided intramyocardial injection

Healthy mice (n= 8) or mice at 7, 14, 21 or 28 days (n= 5, n= 7, n= 5, n= 6, respectively) after induction of I/R injury were injected with CPC. Mice were anesthetized with 1.5%-2% isoflurane and positioned in an adjusted parasternal long axis view (PSLAX) for intramyocardial injection. For direct visualization of the injection, Evans Blue (n= 1) was used to demonstrate the localization of the needle flush out. CPC were injected in the anterior wall via a transthoracic

approach with echo guidance. A 29 Gy needle was used and 0.5 million cells were injected in two times 5 μ l.

Bioluminescent imaging (BLI)

To determine the amount of engrafted CPC, emitted photons by CPC-luc were detected two and seven days after injection by the photon imager from Biospace Laboratory and analyzed by Photovision software as previously described [13]. In short, mice were injected intraperitoneally with Luciferase (Promega E1605) and emitted photons by CPC-luc were detected. Injections were considered successful based on location (mid-thorax) and a threshold of BLI signal at day 2 (> 20.000 ph/s/cm²/sr), as established with previously performed titrations. The absolute BLI values in the individual mice were used as primary outcome parameters and were denoted as BLI Signal Units (BSU; ph/s/cm²/sr).

Histological analysis

7 days after intramyocardial injection with CPC, mice were terminated by exsanguination under general anesthesia and their hearts were excised. The hearts were dehydrated and fixed in a 15% sucrose 0.4% PFA solution after which they were embedded in O.C.T. compound (Tissue Tek) and stored at -80 °C. Serial transverse cryosections of 7 μ m were cut, base to apex, and immunological staining was performed to trace CPC. Cryosections were incubated for 1 hour at room temperature with primary antibodies against: human Lamin A/C antibody (1:100, VP-L550, Vector) and Troponin-I (1:50, sc-15368, Santa Cruz). Subsequently, sections were incubated o/n at 4°C using the appropriate Alexa 488 and Alexa 555 antibody (Invitrogen). Nuclei were stained with Hoechst (33342).

Statistical analysis

Statistical analyses were carried out using GraphPad Prism 6.0 software (GraphPad Software). Data is presented as mean \pm SEM and were compared using the two-tailed Student's

T-test. For analyses at different time-points, the one-way ANOVA was performed with the Dunnett test as post-hoc analysis to correct for multiple testing. $p < 0.05$ was considered statically significant.

Results

Intramyocardial injection of CPC with echo guidance is comparable to an open-thorax approach

To determine the feasibility of echo-IMI of CPC (Figure 1a-c), we compared cell retention of echo-IMI to open-IMI in healthy mice. First, we performed an injection with Evans Blue in a closed-thorax model, which resulted in a defined dyed area in the anterior wall of the myocardium and thereby demonstrated the feasibility of this echo-guided injection approach (Figure 1d). Next, we injected CPC intramyocardially with either an open-thorax or closed-thorax approach (n= 3 vs. n= 8, respectively). Of the 8 mice injected under echo-guidance, 1 mouse died of a major bleeding in the thorax due to a too low placement of the needle. No events or arrhythmias were observed during or after the other procedures.

BLI showed a detectable signal in the targeted region in all injected mice (Figure 1e). No significant differences in cell retention at day 2 (Figure 1f) or day 7 (Figure 1g) were found between the open-IMI or echo-IMI approach. Yet, the variability in BLI signal at day 2 appeared larger in mice after open-IMI ($5.9 \times 10^5 \pm 4.0 \times 10^5$ (open-IMI) vs. $3.1 \times 10^5 \pm 1.0 \times 10^5$ (echo-IMI)).

Intramyocardial injection of CPC is successful in I/R injury-induced chronic cardiac remodeling

To determine retention of transplanted CPC in the distinct phases during chronic cardiac remodeling, I/R injury was induced and CPC were injected at several time-points after this. Starting at 7 days after induction of I/R injury, the LVEDV (from $56.0 \pm 1.8 \mu\text{l}$ to $86.7 \pm 8.9 \mu\text{l}$; Figure 2b) and LVESV (from $20.5 \pm 0.9 \mu\text{l}$ to $59.9 \pm 10.8 \mu\text{l}$; Figure 2c) increased significantly, with the largest increase at 28 days. Cardiac performance was affected by these changes, represented by a decreased LVEF (from $63.2 \pm 1.2 \mu\text{l}$ to $37.1 \pm 6.5 \mu\text{l}$; Figure 2d). These changes confirmed successful induction of myocardial injury and subsequent adverse cardiac remodeling.

Injected CPC were traced *in vivo* by BLI at day 2 (Figure 2e) and 7 (Figure 2f) post echo-guided injection. Analyses demonstrated that CPC injection at 7, 14, 21 or 28 days after

induction of I/R injury displayed similar cell retentions. Notably, cell retention at day 7 appeared higher in healthy mice compared to mice with I/R injury ($1.4 \times 10^4 \pm 3.1 \times 10^3$ vs. $0.9 \times 10^4 \pm 0.8 \times 10^3$).

To confirm the histological presence of CPC in injected mice hearts, CPC were traced with an anti-human lamin A/C antibody. CPC injected under echo-guidance were mainly located in the anterior- and septal wall of the LV (Figure 3a-c). CPC were located either intramyocardially (Figure 3d-e) or at the epicardial border (Figure 3f) and displayed an intact nuclear pattern. Remarkably, these injection sites were partly troponin-I negative (Figure 3), demonstrating the presence of other tissue than myocardium.

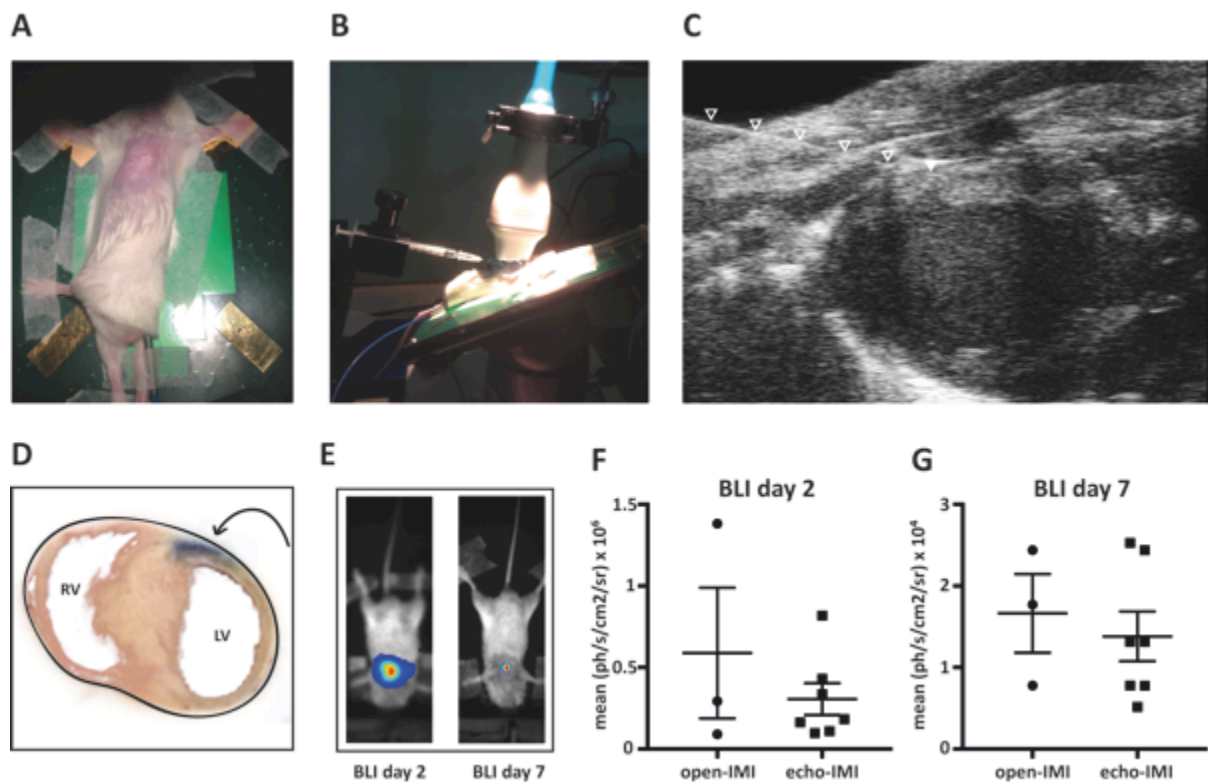


Figure 1. Feasibility of echo-guided intramyocardial injection of CPC. **(A)** Mice are positioned for an adjusted parasternal long axis view, and are **(B)** injected in the anterior wall of the myocardium using a 29 Gy needle. **(C)** Representative B-mode echo image of the actual injection. The needle and needle tip are marked with white arrowheads. **(D)** Location of the injection side as demonstrated by Evans blue injection. **(E-F)** BLI analyses 2 and 7 days after intramyocardial injection of CPC demonstrated that BLI signal was comparable for open-thorax and echo-guided intramyocardial injection (open-IMI and echo-IMI respectively). **(G)** Representative BLI images of day 2 and 7 after CPC injection. RV= right ventricle, LV= left ventricle.

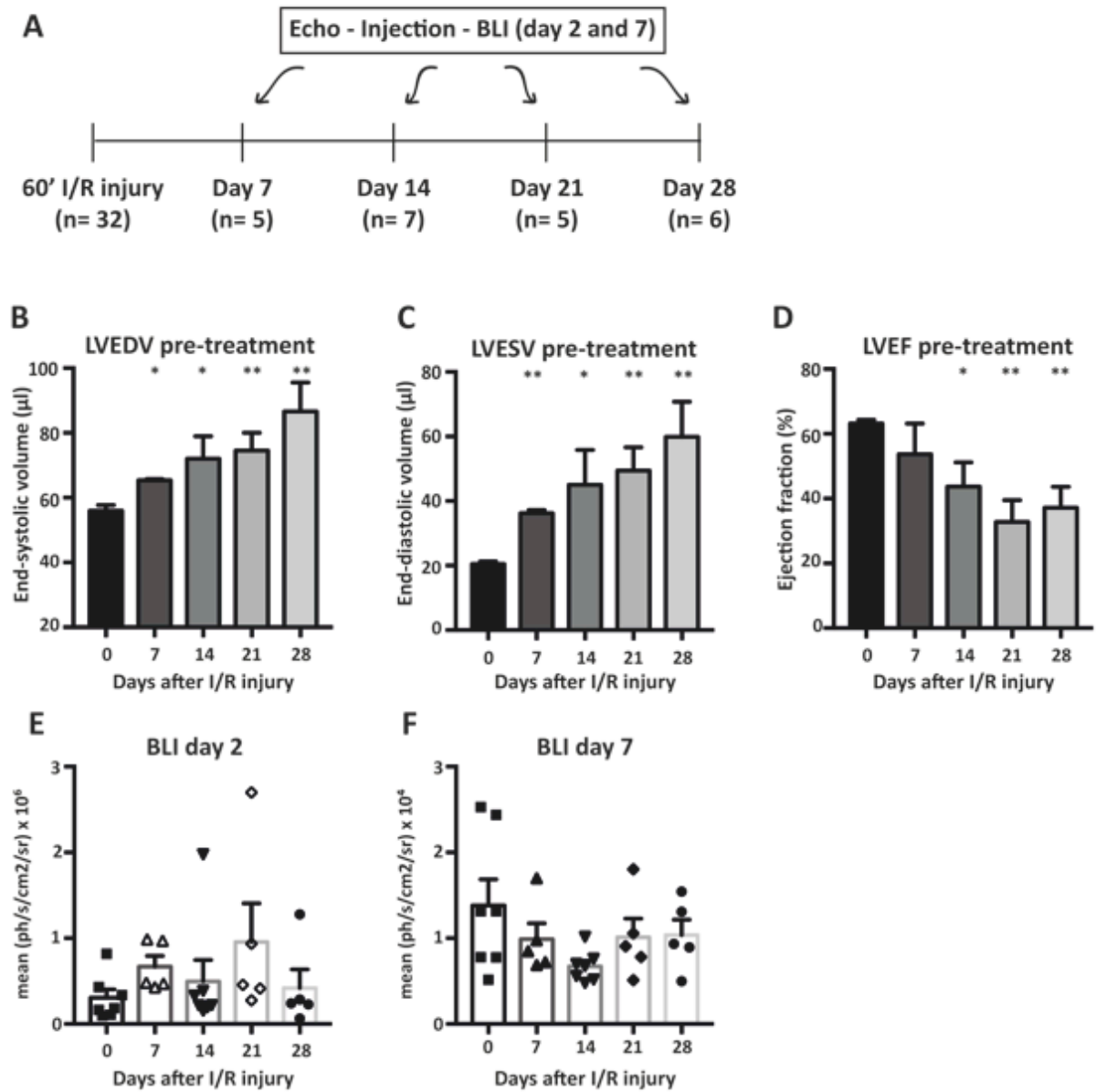


Figure 2. Cell retention upon CPC injection at different time-points after I/R injury. **A)** Schematic overview of study set-up. **(B-D)** I/R injury resulted in a significant increase in cardiac volumes and a decreased LVEF at all time-points after injury induction. **(E-F)** Cell retention was independent of the time-point of injection (day 7, 14, 21 or 28) as shown by *in vivo* BLI imaging at day 2 (**E**) and day 7 (**F**). * $p < 0.05$ and ** $p < 0.01$.

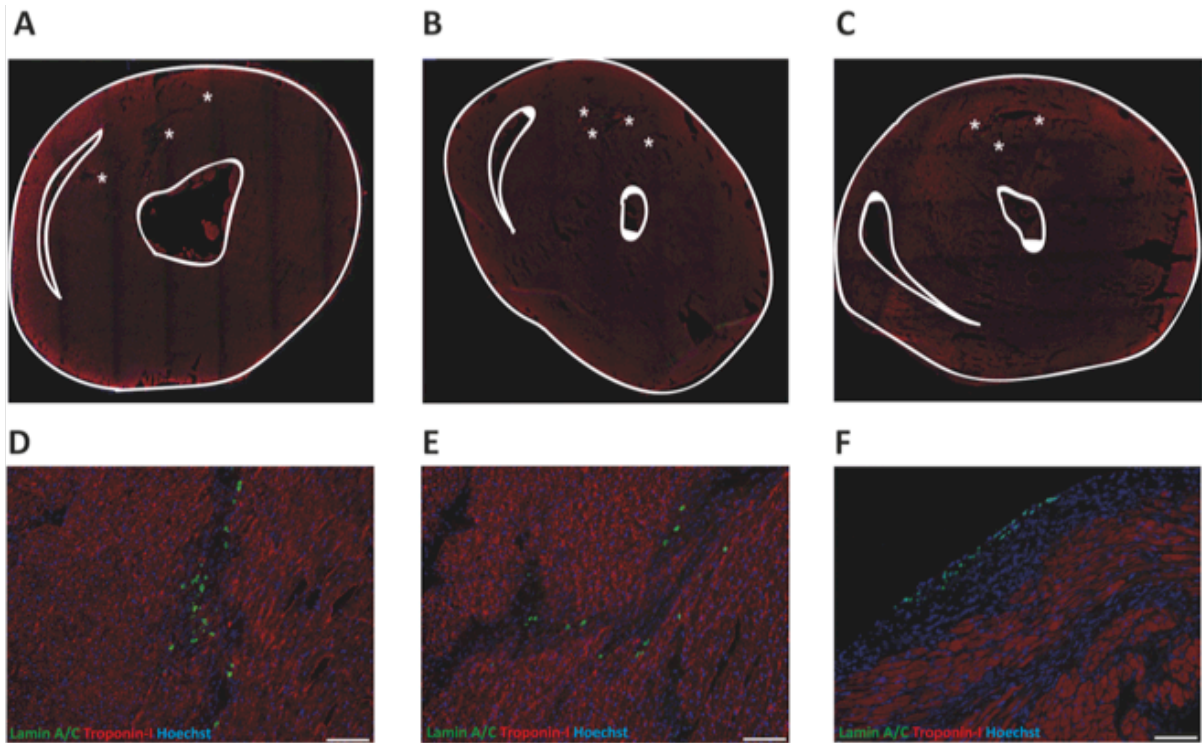


Figure 3. CPC are retained intramyocardially after echo-guided injection.

A-C) Representative images of CPC injected hearts demonstrating the anterior and septal location of traced CPC. White asterisks mark CPC clusters. At 7 days after injection, CPC were present in the myocardium (**D-E**) or epicardial layer (**F**) as visualized by immunofluorescent staining for human lamin A/C (green), troponin I (red) and nuclei (blue). White bar= 100 μ m.

Discussion

Well-defined local delivery strategies of therapeutics are indispensable to facilitate advances in small animal research. In order to achieve appropriate murine models for clinical translation it is important to consider feasibility and applicability of the proposed methods. As presented here, echo-IMI of CPC is feasible and comparable to an open-IMI approach. Additionally, results demonstrated that echo-guided injections are reproducible and safe. Upon I/R injury, adverse cardiac remodeling was initiated with a time-dependent decrease in left ventricular function. In the distinct phases of cardiac remodeling, echo-IMI resulted in comparable cell retention *in vivo*. Subsequent immuno-histochemical CPC tracing revealed the intramyocardial presence of CPC and confirmed the anterior and septal position of the injections.

In pre-clinical and clinical research, cardiac stem cell therapy is applied by either systemic or local delivery strategies. Because of their higher delivery rates, local delivery techniques such as intracoronary infusion or intramyocardial injection are the preferred methods [15]. Although coronary delivery strategies have been described in murine models [16], the most common local delivery strategy remains intramyocardial injection after sternotomy or thoracotomy. The invasive nature of the injury procedure is arguably only convenient in experimental acute myocardial infarction and hampers the development of stem cell studies in chronic cardiac remodeling. Our results demonstrated the feasibility of echo-IMI CPC injections and showed that intramyocardial injections have a higher reproducibility compared to invasive injections in the acute setting. The obtained images during echo-IMI are sufficient for a correct placement of the injection and, in contrast to injections under direct vision, allow for a better reproducibility by means of the clear landmarks and steady position of the heart. These results broadened the findings of Prendiville *et al.* and Latham *et al.* [9, 11], who demonstrated the feasibility of echo-guided intramyocardial delivery. The successes of echo-IMI provide new perspectives regarding the variety of models, which now can be used for therapeutic testing.

Next to the route of delivery, the condition of the donor heart is relevant for cell retention. Myocardial injury results in subsequent inflammation and fibrosis, which creates a hostile

environment [17]. Consequently, grafted cells are prone to a quick wash-out and cell death [13]. Although the cell retention at day 7 appeared slightly higher in healthy hearts, we did not observe a clear difference in initial cell retention between healthy and I/R injured hearts. Moreover, the fast decline in cell retention between day 2 and 7 was obvious and similar in all conditions. The substantial cell loss immediately upon injection [18] is presumably more important for low cell retention rates than the hostile environment. Since a direct relation between initial cell retention and cardiac function remains controversial [13, 19, 20], further investigation is required regarding the most beneficial timing of therapy. Similarly, exploration of cell-carriers to improve cell survival and retention would be of interest [21].

In addition to the hostile environment, the practical aspect of needle injections in a thinned myocardial wall needs to be considered. In our experiments, we did not encounter failure of echo-IMI in the I/R injured hearts. A possible explanation might be that the wall thinning upon I/R injury is less severe, compared to a model of permanent LAD ligation [22], and that the location of injection at the mid-papillary level targets the healthy or borderzone region. Furthermore, the echo-guidance enables the operator to adjust the injection position based on the observed wall function and thickness. In addition, injections could also be performed in the short-axis frame to target different, more viable regions of the heart [11].

Although this study was performed to investigate stem cell delivery during cardiac remodeling, the results can be extrapolated to the local application of a variety of drugs (e.g. FSTL-1 [23], neuregulin [24]) and injectable materials (e.g. hydrogels [25, 26]) in chronic cardiac remodeling. In addition, the safety and reproducibility of the echo-guided injections enable repetitive injections at pre-defined time-points. Interestingly, Laakman *et al.* demonstrated the feasibility of echo-guided pericardial injection in mice and showed the possibility of selective viral mediated gene transfection [27].

The strengths of the current study include our direct comparison of CPC retention between echo-IMI and open-IMI. Moreover, the I/R injury model enabled us to study CPC injection at several clinically important time-points. Nevertheless, this study has several limitations. First,

the available injection sites are constricted by the passage through the intercostal spaces, which limit precise needle manipulation in fixed imaging frames. To overcome this problem, echo planes can be adjusted during the procedure to allow for a different needle angle or position. Secondly, the immuno-histological observation that CPC are traced in partly troponin-I negative areas might suggest cardiac damage upon injection. However, these loose troponin-I negative areas could also be ascribed to the production of extracellular matrix by the grafted cells [28]. To determine the impact of echo-IMI, functional follow-up is required. Additionally, prudence is called for in experiments with multiple injections or when a larger needle is needed.

In short, we demonstrate that echo-IMI is an efficient and technically feasible method for stem cell delivery in a murine model of chronic cardiac remodeling. The minimal invasiveness of echo-guided injections and the numerous options regarding timing and location of therapy offer great potential to improve pre-clinical small animal research.

Acknowledgements

We acknowledge the support from Innovation and the Netherlands CardioVascular Research Initiative (CVON): The Dutch Heart Foundation, Dutch Federation of University Medical Centers, the Netherlands Organization for Health Research and Development and the Royal Netherlands Academy of Science. Additionally, the ZonMW Translational Adult Stem Cell grant 1161002016.

Disclosure

The authors declare they have no conflict of interest.

References

1. Mozaffarian D, Benjamin EJ, Go AS, et al. Heart Disease and Stroke Statistics-2016 Update: A Report From the American Heart Association. *Circulation* 2015;133:e38–e360.
2. McMurray JJ V, Adamopoulos S, Anker SD, et al. ESC guidelines for the diagnosis and treatment of acute and chronic heart failure 2012: The Task Force for the Diagnosis and Treatment of Acute and Chronic Heart Failure 2012 of the European Society of Cardiology. Developed in collaboration with the Heart. *Eur J Heart Fail* 2012;14:803–69.
3. Tongers J, Losordo DW, Landmesser U. Stem and progenitor cell-based therapy in ischaemic heart disease: promise, uncertainties, and challenges. *Eur Heart J* 2011;32:1197–206.
4. Goumans M-J, Maring JA, Smits AM. A straightforward guide to the basic science behind cardiovascular cell-based therapies. *Heart* 2014;100:1153–7.
5. Madonna R, Van Laake LW, Davidson SM, et al. Position Paper of the European Society of Cardiology Working Group Cellular Biology of the Heart: cell-based therapies for myocardial repair and regeneration in ischemic heart disease and heart failure. *Eur Heart J* 2016.
6. Tang X-L, Rokosh G, Sanganalmath SK, et al. Intracoronary administration of cardiac progenitor cells alleviates left ventricular dysfunction in rats with a 30-day-old infarction. *Circulation* 2010;121:293–305.
7. Rota M, Padin-Iruegas ME, Misao Y, et al. Local activation or implantation of cardiac progenitor cells rescues scarred infarcted myocardium improving cardiac function. *Circ Res* 2008;103:107–16.
8. Tseliou E, Reich H, de Couto G, et al. Cardiospheres reverse adverse remodeling in chronic rat myocardial infarction: roles of soluble endoglin and Tgf- β signaling. *Basic Res Cardiol* 2014;109:443.
9. Latham N, Ye B, Jackson R, et al. Human blood and cardiac stem cells synergize to enhance cardiac repair when cotransplanted into ischemic myocardium. *Circulation* 2013;128:S105-12.
10. Patten RD, Hall-Porter MR. Small animal models of heart failure: development of novel therapies, past and present. *Circ Heart Fail* 2009;2:138–44.
11. Prendiville TW, Ma Q, Lin Z, Zhou P, He A, Pu WT. Ultrasound-guided transthoracic intramyocardial injection in mice. *J Vis Exp* 2014:e51566.
12. Smits AM, van Vliet P, Metz CH, et al. Human cardiomyocyte progenitor cells differentiate into functional mature cardiomyocytes: an in vitro model for studying human cardiac physiology and pathophysiology. *Nat Protoc* 2009;4:232–243.
13. Feyen D, Gaetani R, Liu J, et al. Increasing short-term cardiomyocyte progenitor cell (CMPC) survival by necrostatin-1 did not further preserve cardiac function. *Cardiovasc Res* 2013;99:83–91.
14. van Laake LW, Passier R, Monshouwer-Kloots J, et al. Monitoring of cell therapy and assessment of cardiac function using magnetic resonance imaging in a mouse model of myocardial infarction. *Nat Protoc* 2007;2:2551–67.
15. van der Spoel TIG, Lee JC-T, Vrijsen K, et al. Non-surgical stem cell delivery strategies and in vivo cell tracking to injured myocardium. *Int J Cardiovasc Imaging* 2011;27:367–83.
16. Ladage D, Ishikawa K, Tilemann L, Müller-Ehmsen J, Kawase Y. Percutaneous methods of vector delivery in preclinical models. *Gene Ther* 2012;19:637–41.
17. Christia P, Bujak M, Gonzalez-Quesada C, et al. Systematic characterization of myocardial inflammation, repair, and remodeling in a mouse model of reperfused myocardial infarction. *J Histochem Cytochem* 2013;61:555–570.
18. van den Akker F, Feyen DAM, van den Hoogen P, et al. Intramyocardial stem cell injection: go(ne) with the flow. *Eur Heart J* 2016.
19. Golpanian S, Schulman IH, Ebert RF, et al. Concise Review: Review and Perspective of Cell Dosage and Routes of Administration From Preclinical and Clinical Studies of Stem Cell Therapy for Heart Disease. *Stem Cells Transl Med* 2016;5:186–91.
20. Liu J, Narsinh KH, Lan F, et al. Early stem cell engraftment predicts late cardiac functional recovery: preclinical insights from molecular imaging. *Circ Cardiovasc Imaging* 2012;5:481–

90.

21. Feyen DAM, Gaetani R, Doevendans PA, Sluijter JPG. Stem cell-based therapy: Improving myocardial cell delivery. *Adv Drug Deliv Rev* 2016.
22. Klocke R, Tian W, Kuhlmann MT, Nikol S. Surgical animal models of heart failure related to coronary heart disease. *Cardiovasc Res* 2007;74:29–38.
23. Wei K, Serpooshan V, Hurtado C, et al. Epicardial FSTL1 reconstitution regenerates the adult mammalian heart. *Nature* 2015;525:479–85.
24. Galindo CL, Kasasbeh E, Murphy A, et al. Anti-remodeling and anti-fibrotic effects of the neuregulin-1 β glial growth factor 2 in a large animal model of heart failure. *J Am Heart Assoc* 2014;3:e000773.
25. Seif-Naraghi SB, Singelyn JM, Salvatore MA, et al. Safety and efficacy of an injectable extracellular matrix hydrogel for treating myocardial infarction. *Sci Transl Med* 2013;5:173ra25.
26. Appel EA, Tibbitt MW, Webber MJ, Mattix BA, Veisoh O, Langer R. Self-assembled hydrogels utilizing polymer-nanoparticle interactions. *Nat Commun* 2015;6:6295.
27. Laakmann S, Fortmüller L, Piccini I, et al. Minimally invasive closed-chest ultrasound-guided substance delivery into the pericardial space in mice. *Naunyn Schmiedebergs Arch Pharmacol* 2013;386:227–38.
28. van Laake LW, van Donselaar EG, Monshouwer-Kloots J, et al. Extracellular matrix formation after transplantation of human embryonic stem cell-derived cardiomyocytes. *Cell Mol Life Sci* 2010;67:277–90.

6

Targeting chronic cardiac remodeling with cardiac progenitor cells in a murine model of ischemia/reperfusion injury

J.C. Deddens

D.A.M. Feyen

P.P.M. Zwetsloot

M.A.D. Brans

S. Siddiqi

L.W. van Laake

P.A.F.M. Doevendans

J.P.G. Sluijter

Submitted

Abstract

Background: Translational failure for cardiovascular disease is a substantial problem involving both high research costs and an ongoing lack of novel treatment modalities. Despite the progress already made, cell therapy for chronic heart failure in the clinical setting is still hampered by poor translation.

We used a murine model of chronic ischemia/reperfusion injury to examine the effect of minimally invasive application of cardiac progenitor cells (CPC) in cardiac remodeling and to improve clinical translation.

Methods: 28 days after the induction of I/R injury, mice were randomized to receive either CPC (0.5 million) or vehicle by echo-guided intra-myocardial injection. To determine retention, CPC were localized *in vivo* by bioluminescence imaging (BLI) two days after injection. Cardiac function was assessed by 3D echocardiography and speckle tracking analysis to quantify left ventricular geometry and regional myocardial deformation.

Results: BLI demonstrated successful injection of CPC (18/23), which were mainly located along the needle track in the anterior/septal wall. Although CPC treatment did not result in overall restoration of cardiac function, a relative preservation of the left ventricular end-diastolic volume was observed at 4 weeks follow-up compared to vehicle control ($+5.3 \pm 2.1 \mu\text{l}$ vs. $+10.8 \pm 1.5 \mu\text{l}$). This difference was reflected in an increased strain rate (+16%) in CPC treated mice.

Conclusions: CPC transplantation can be adequately studied in chronic cardiac remodeling using this study set-up and by that provide a translatable murine model facilitating advances in research for new therapeutic approaches to ultimately improve therapy for chronic heart failure.

Keywords: murine; chronic ischemic heart failure; remodeling; I/R injury; CPC; translational research

Introduction

Translational failure of novel therapies for cardiovascular disease (CVD) is a substantial problem involving both high research costs and an ongoing lack of novel treatment modalities reaching the bedside [1]. Although the overall mortality for CVD declined in the past decade, no improvement in survival after the diagnosis of heart failure is observed [2]. With a 5-year mortality rate of 50%, the high need for new treatment modalities is accentuated.

Cell based therapies have been implied as a novel approach for cardiac salvage and myocardial regeneration. Ever since the first clinical application of stem cells for acute ischemic heart disease more than a decade ago [3, 4], various studies demonstrated tentatively promising results regarding quality of life and cardiac parameters [5–7]. Despite the progress already made in a short period of time, application of cell therapy for chronic heart failure in a clinical setting is still hampered by poor translation [8]. Recent meta-analysis data shows that cell therapy in small animal models results in an improvement in ejection fraction (EF) of 11%, which is lowered to 5% when applied in large animal models and even further decreased to 3% in clinical studies [5, 9, 10].

The problem of clinical translation of stem cell therapy is complex and reasons for potential translational failure are diverse, including applied cell source, injury model and timing of therapy [11, 12]. One particular reason for the difficulty to translate functional outcomes from small to large animal models (and eventually to the clinic) is that cell therapy in small animal models is predominantly investigated in an acute myocardial injury setting [13]. Only a limited number of studies [14–17] tested stem cell therapy in small animals during chronic cardiac remodeling before switching to pre-clinical large animal research. To allow for correct (pre-)clinical translation, it is of great importance to study the basic mechanisms behind cell therapy in small animal models during this chronic remodeling phase.

In this regard, small animal models are extremely valuable in pre-clinical therapeutic research as they are easily accessible, relatively cheap and easy to manipulate genetically. However, it remains difficult to apply local therapeutics in murine chronic heart failure models

due to the lack of accessibility to the heart after invasive MI surgery and the difficulty to use injection catheters in the small vascular anatomy of mice. Therefore, in this current study we provide an integrated model of chronic cardiac remodeling in mice, where we make use of a minimally invasive echocardiography-based local delivery strategy [18, 19]. As a proof of concept, we evaluate the use of human cardiac progenitor cells (CPC), an exciting class resident heart progenitor [20, 21], in our developed murine chronic ischemia/reperfusion (I/R) model.

Material and Methods

(An expanded methods section is available in the supplementary)

Meta-regression analysis

We used the dataset of our meta-analysis [9] on placebo-controlled CPC studies in MI in small animals and complemented the data with a variable for CPC therapy timing. The primary outcome left ventricular ejection fraction (LVEF) was used for this analysis. We defined the acute setting as CPC administration within 7 days after infarct, the sub-acute setting as between 7 and 28 days and a chronic MI model as CPC treatment after MI induction at 28 days or more. We used univariable meta-regression to test for a potential difference. Since this was a hypothesis-testing endeavor, we also included groups with less than 5 comparisons for our analyses of therapy timing.

CPC isolation, expansion and transduction

Human fetal tissue was obtained by individual permission using standard informed consent procedures and prior approval of the ethics committee of the University Medical Center Utrecht, the Netherlands. This procedure is in accordance with the principles outlined in the Declaration of Helsinki for the use of human tissue or subjects. CPC were isolated by using Sca-1+ conjugated magnetic beads as described previously [22]. To facilitate identification *in vivo*, CPC were transduced with a lenti-viral construct, containing pLV-CMV-luc-GFP as described previously [23]. Cells were cultured in SP++ (M199, EGM2, FBS, P/S, NEAA) until 80% confluency and used for *in vivo* transplantation at passage 12-14.

Animals

All experiments were carried out in accordance with the Guide for the Care and Use of Laboratory Animals, with prior approval by the Animal Ethical Experimentation Committee, Utrecht University, the Netherlands.

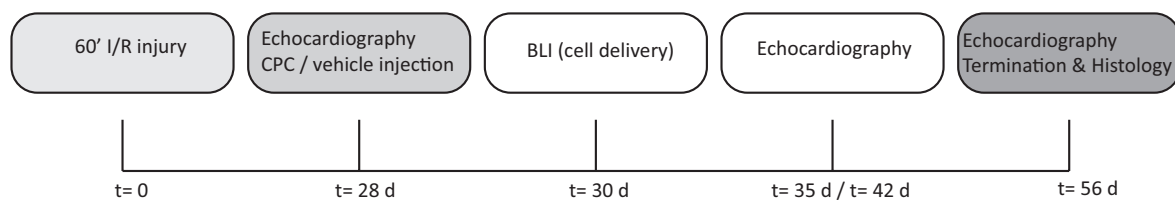
Ischemia Reperfusion model

Male NOD-SCID mice (Harlan Laboratories), aged 10-12 weeks, underwent left coronary artery (LAD) ligation as previously described [24, 25], followed by reperfusion after 60 minutes by releasing the ligature and removal of tubing. Reflow was confirmed by reversed discoloration of the heart.

Cell transplantation model

Twenty-eight days after induction of myocardial injury, animals were injected with either CPC, or vehicle (PBS) (Fig 1). To determine the extent of injury, mice underwent echocardiography (echo) followed by randomization in the different groups. Mice were positioned in an adjusted parasternal long axis view (PSLAX) for intramyocardial injection. CPC or vehicle were injected in the anterior wall via a transthoracic approach with echo guidance. A 27 Gy needle was used and 0.5 million cells were injected in two times 5 μ l.

A



B

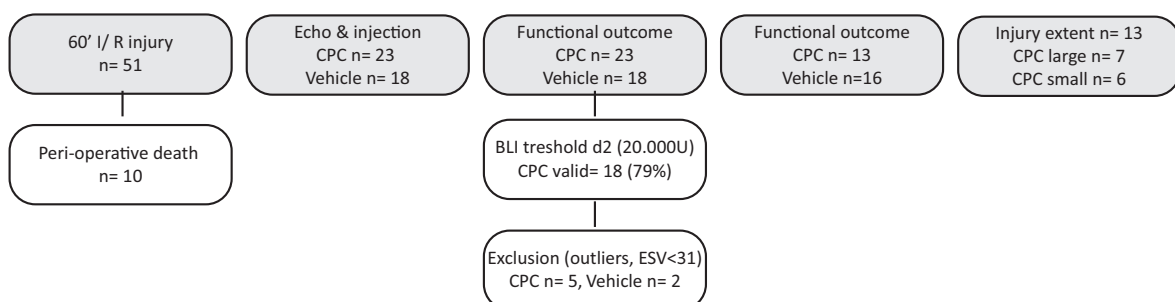


Figure 1. Study protocol. A) Timeline diagram of procedures and **(B)** flowchart of mouse experiment.

Bioluminescent imaging (BLI)

To determine the amount of engrafted CPC, emitted photons by CPC-luc were detected two days after injection by the photon imager from Biospace Laboratory and analyzed by Photovision software as previously described [23]. Injections were considered successful based on a threshold of BLI signal 2 days after injection ($> 20.000 \text{ ph/s/cm}^2/\text{sr}$), established with previously performed titrations [23]. After primary outcome analyses, animals with a low retention ($< 20.000 \text{ ph/s/cm}^2/\text{sr}$) were used for additional analyses.

3D motor echocardiography

Echo was performed at baseline, 28 days after I/R injury and at 7,14 and 28 days after treatment using a high resolution ultrasound system (Vevo 2100, VisualSonics) with a 18-38 MHz transducer (MS 400, VisualSonics). Echo acquisition and all analyses were performed by a blinded investigator. Left ventricular end-diastolic volume (LVEDV) and left ventricular end-systolic volume (LVESV) were used to calculate LVEF.

Post measurement speckle tracking based analyses were performed to determine myocardial deformation parameters (VevoStrain, VisualSonics). Echo images acquired from the PSLAX were used to measure peak velocity (cm/s), strain (%) and strain rate (SR)(1/s) in the longitudinal and radial axis. For global measurements the average of all 6 myocardial segments (basal-anterior (BA), mid-anterior (MA), apical-anterior (AA), apical-posterior (AP), mid-posterior (MP) and basal-posterior (BP)) was taken. The infarct area was defined as the average of MA, AA and AP.

Histological analysis

At day 28 after intramyocardial injection with either CPC or vehicle, mice were terminated by exsanguination under general anesthesia and their hearts were excised. The hearts were dehydrated and fixed in a 15% sucrose 0.4% PFA solution after which they were embedded in O.C.T. compound (Tissue Tek) and stored at $-80 \text{ }^\circ\text{C}$. Serial transverse cryosections of $7 \text{ }\mu\text{m}$ were

cut, base to apex, for histological and immunohistological stainings. Imaging and analysis were performed by a blinded investigator.

Statistical analysis

Statistical analyses were carried out using GraphPad Prism 6.0 software (GraphPad Software, La Jolla, USA). Data is presented as mean \pm SEM and were compared using the two-tailed Student's T-test. For analyses in time, the two-tailed paired Student's T-test was performed. $p < 0.05$ was considered statically significant.

Results

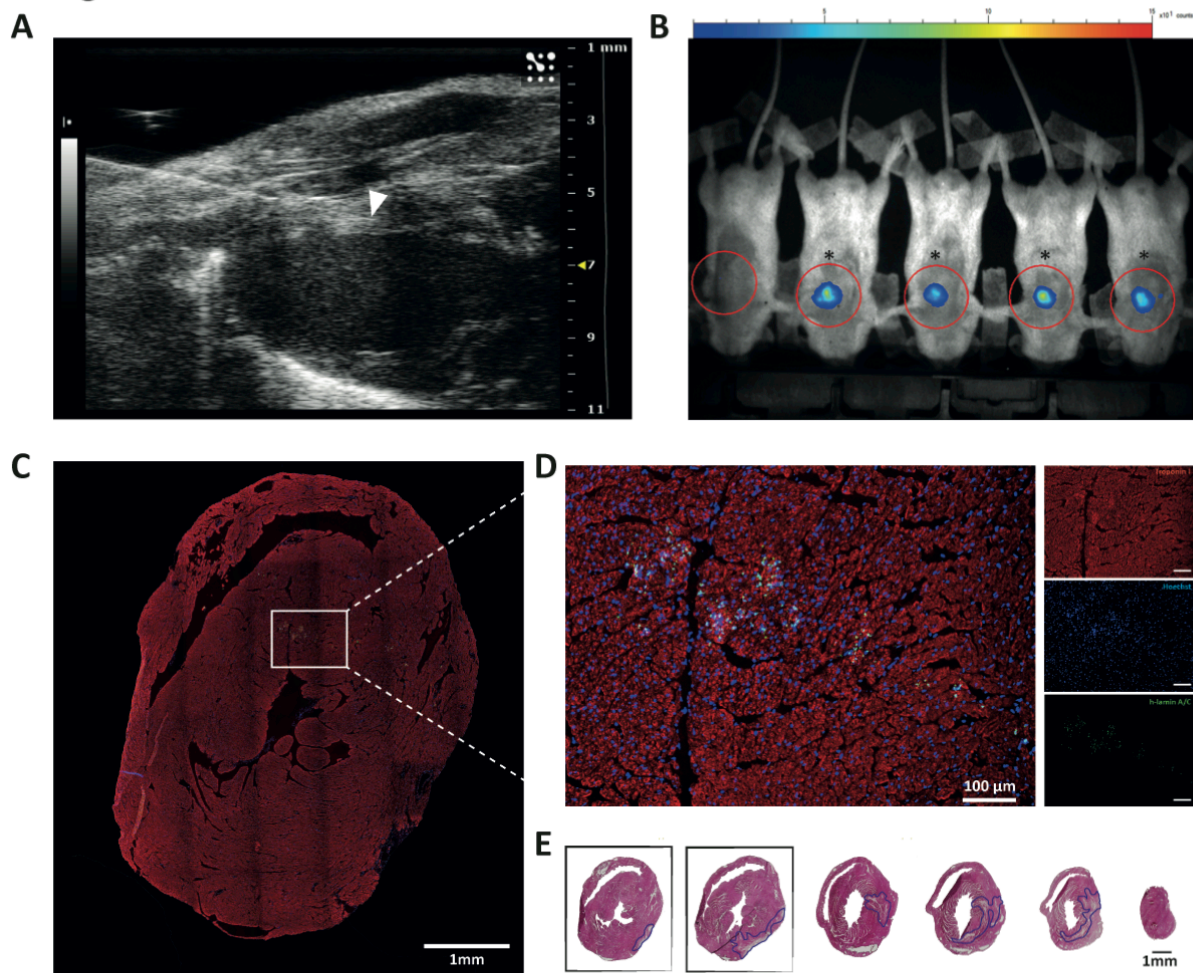
Meta-regression

To systematically explore the effect of CPC in chronic cardiac remodeling, we performed meta-regression for the timing of therapy in our dataset of placebo-controlled small animal CPC studies for MI. The dataset contained 95 comparisons, of which 5 comparisons were in the sub-acute phase (1-4 weeks) and only 2 administered their therapy in a chronic MI setting (> 4 weeks after MI induction). Meta-regression showed a large spread in effect on LVEF for the timing of therapy (S1Fig, $p = 0.258$). The low number of studies and large spread in effect endorsed our *in vivo* study.

Cardiac engraftment and localization of CPC after echo guided intra-myocardial injection

To determine retention of transplanted CPC in the chronic remodeling heart, cells were localized *in vivo* by BLI two days after echo-guided injection (Fig 2a). Furthermore, cells were traced *ex vivo* with an anti-human lamin A/C antibody to confirm their presence and human origin. BLI showed a detectable signal in the targeted region in all CPC injected mice. Seventy-eight percent (18/23) of the injections were considered successful based on our previously determined threshold of BLI signal 2 days after injection (> 20,000 ph/s/cm²/sr [23], Fig 2b). CPC remained in the tissue up to 28 days after injection and were mainly located along the needle track in the anterior and septal wall (Fig 2c-e). Transplanted CPC demonstrated an intact nuclear pattern and did not show clear tissue integration.

Figure 2. Echo-guided intramyocardial injection resulted in successful delivery of CPC. A) Representative B-mode image of intra-myocardial injection (29 Gy needle) at 4 weeks after the onset of I/R injury. The needle tip (marked by white arrowhead) is located in the anterior wall of the left ventricle. **B)** BLI images 2 days after intramyocardial injection with CPC demonstrated that 18/23 injections were successful (marked with *). **C-D)** CPC retained in the tissue up to 28 days after injection, as visualized by immunofluorescent staining for human lamin A/C (green), troponin I (red) and nuclei (blue). CPC were predominantly located along the needle track in the anterior and septal wall, **(E)** at the level of the papillary muscles (squares mark HE slides at the level of traced CPC).



I/R model in NOD-SCID mice

Pre-treatment echo measurements were analyzed and animals without significant cardiac damage, defined as an LVESV < 31 μ l (= mean baseline value + 2x standard deviation) were excluded (n=4). Additionally, 3 animals were defined as outliers using the ROUT method (Q=1%; [26]) and were excluded. Representative echocardiographic images (three-dimensional reconstructions) of LVEDV and LVESV after I/R injury can be found in S2 Fig.

The geometry of the left ventricle was significantly altered upon MI, confirming successful induction of adverse cardiac remodeling. After 4 weeks, LVEDV ($66.3 \pm 1.5 \mu$ l to $78.5 \pm 1.3 \mu$ l) and LVESV ($26.5 \pm 0.7 \mu$ l to $41.2 \pm 1.6 \mu$ l) were significantly increased ($p < 0.001$). Cardiac performance was affected by these changes, represented in a decrease in LVEF ($60.1\% \pm 0.8$ to $48.0\% \pm 1.3$, $p < 0.0001$). No differences in cardiac geometry or function were observed between both experimental groups before treatment (LVEDV $p = 0.78$, LVESV $p = 0.69$, LVEF $p = 0.95$; Fig 3a-c).

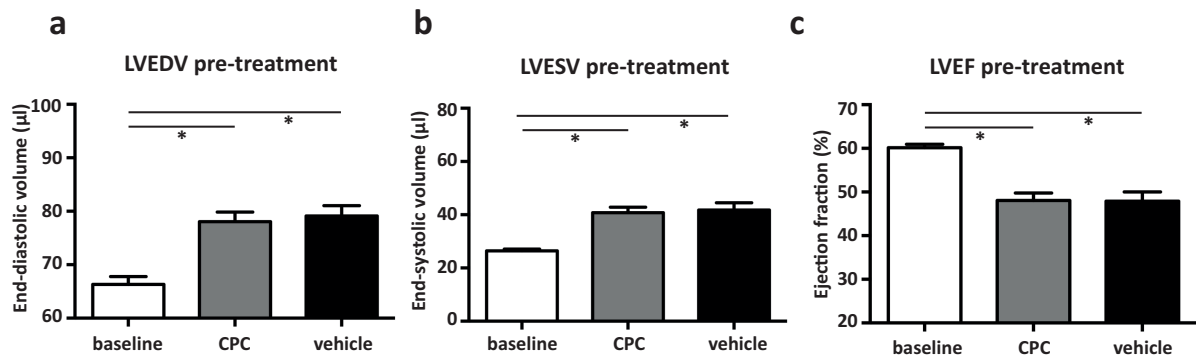


Figure 3. Functional measurements by echocardiography of day 28 (pre-treatment). Upon I/R injury the LVEDV (A) and LVESV (B) are increased, and the LVEF (C) is decreased with no differences between CPC treated or vehicle treated mice. CPC group: n= 19, Vehicle group; n= 16. * p< 0.001.

Adverse cardiac remodeling is attenuated by CPC treatment

Treatment with CPC 28 days after I/R injury resulted in preservation of the LVEDV at 4 weeks follow-up (day 56 of experiment) compared to vehicle control ($+5.3 \pm 2.1 \mu\text{l}$ vs. $+10.8 \pm 1.5 \mu\text{l}$, $p= 0.036$; Fig 4a). This difference was even more pronounced in mice with more left ventricular remodeling ($+4.4 \pm 2.6 \mu\text{l}$ vs. $+12.3 \pm 2.5 \mu\text{l}$, $p= 0.045$) compared to mice with a smaller injury ($+6.3 \pm 3.7 \mu\text{l}$ vs. $+9.3 \pm 1.7 \mu\text{l}$, $p= 0.43$) (S3 Fig). To define this difference in extent of injury, we used the median LVEDV prior to cell treatment as cut-off point. Although not significant, the differential effect of CPC treatment was already observed 14 days after treatment ($+4.7 \pm 2.5 \mu\text{l}$ vs. $+8.2 \pm 2.2 \mu\text{l}$, $p= 0.3$). Interestingly, this attenuation was not observed in the CPC group with low retention signals based on BLI two days after injection compared to vehicle control ($+12.4 \pm 5.0 \mu\text{l}$ vs. $+10.8 \pm 1.5 \mu\text{l}$, $p= 0.69$; S3 Fig). In contrast to the observed differences in LVEDV, LVESV was uniformly increased in both CPC and vehicle treated mice ($+6.4 \pm 1.8 \mu\text{l}$ vs. $+4.6 \pm 1.7 \mu\text{l}$, $p= 0.48$) and appeared to remain stable in time after therapy (Fig 4b). As a consequence, LVEF seemed slightly decreased in CPC treated mice ($-3.9 \pm 2.7\%$) compared to a minor increase ($+1.26 \pm 1.8\%$) in vehicle control ($p= 0.16$; Fig 4c).

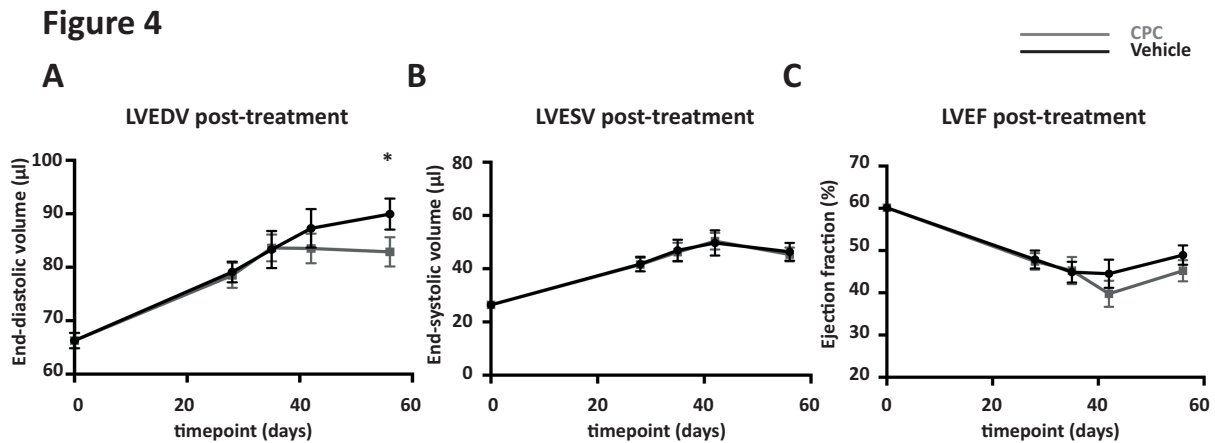


Figure 4. Functional outcome measurements by echocardiography at 1 month follow-up demonstrated preservation of the end-diastolic volume. A) LVEDV in the CPC group differed from the control group at experimental day 56 (post-treatment). No significant difference between the groups was observed for **(B)** LVESV and **(C)** LVEF. Black lines indicate vehicle treated mice (n = 16) and grey lines indicate mice treated with CPC (n= 13). * p< 0.05.

Matrix composition 28 days after CPC treatment

Since CPC solely affected the LVEDV we sought to identify local effects of CPC on the infarcted tissue and extracellular matrix. The infarct size, defined as the percentage of non-viable left ventricle, was slightly lower in the CPC group ($8.0 \pm 2.5\%$ vs. $10.6 \pm 1.8\%$, p= ns). Accordingly, mice treated with CPC seemed to have a lower collagen density compared to vehicle-treated mice (4.6 ± 0.46 vs. 5.0 ± 0.54 , mean grey value per mm² infarct area, p=ns, Fig 5a and b). Further analysis of the composition of the extracellular matrix showed that although both groups had similar amounts of matrix producing cells (vimentin⁺ cells) in the infarcted area, the ratio of collagen type I/III appeared higher in mice treated with CPC (Fig 5a and d). All effects in matrix composition favored the CPC group, not reaching statistical significance (Fig 5e).

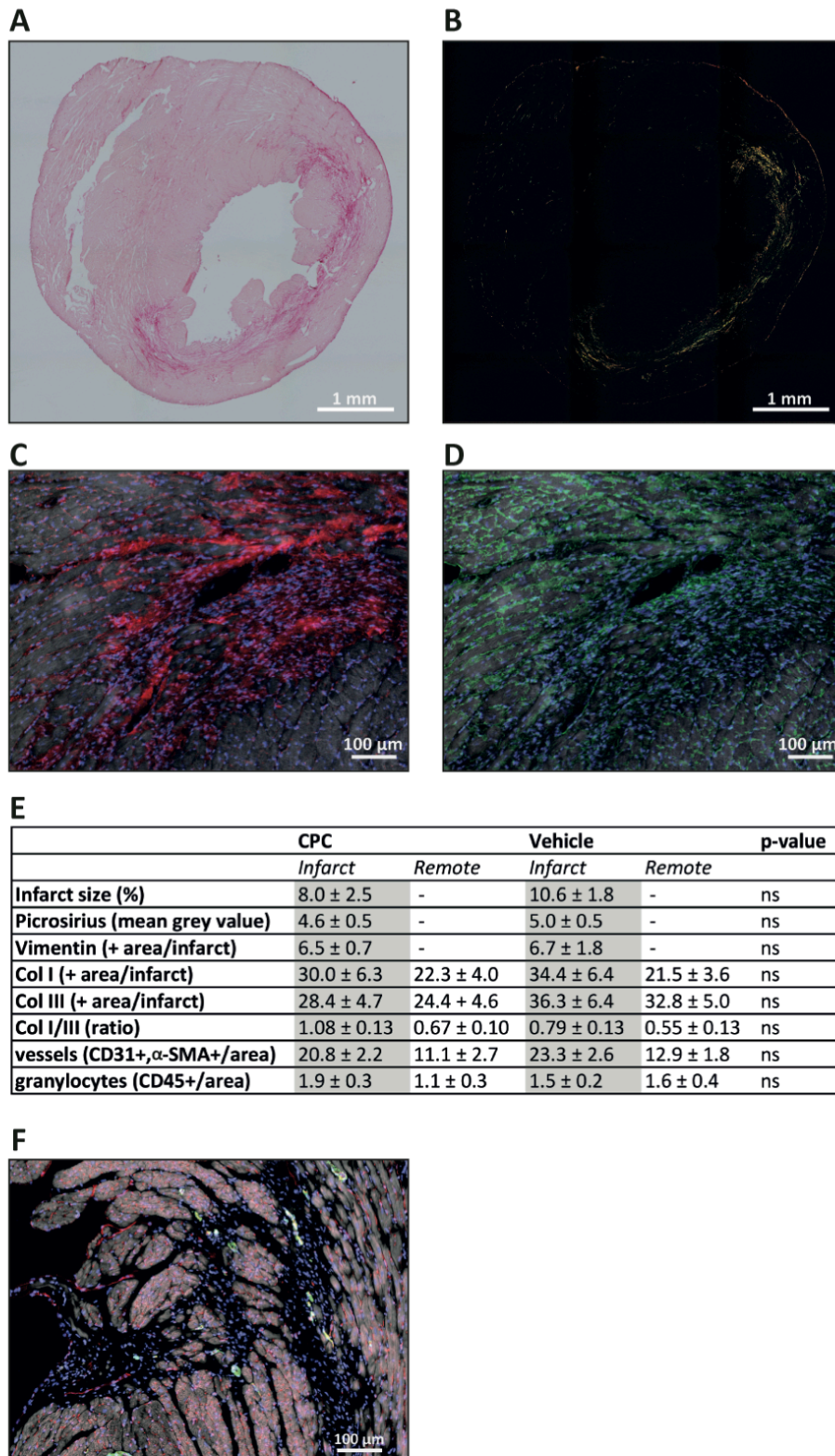


Figure 5. Histological analysis of matrix composition in the injured myocardium. Representative images of cryosections used for quantification of the collagen density of the infarcted area in brightfield (A) and polarized light (B). The collagen composition was assessed by immunofluorescent imaging of (C) collagen type I (red) and (D) collagen type III (green). (E) Quantification of stainings. (F) Immunofluorescent staining showed an increase of CD31⁺ (red) and α-SMA⁺ (green) vessels in the infarcted area compared to the remote area. No difference was observed between CPC or vehicle treated mice. Nuclei were stained with Hoechst (blue) and the myocardial structure is shown in grey.

To determine if CPC increased the vascularization of the infarct area, like we demonstrated before in an acute injury model [21], a staining for CD31 and alpha smooth muscle actin (α -SMA) positive vessels was performed (Fig 5f). The staining demonstrated a higher vascular density in the infarcted area compared to the remote area (22.1 ± 1.7 vs. 12.1 ± 1.6 , vessels/ mm^2 , $p < 0.001$). Treatment with CPC did not result in an increased vascularization (20.8 ± 2.2 vessels/ mm^2) in the infarct area compared to vehicle treatment (23.3 ± 2.6 vessels/ mm^2). In addition, no difference in CD45⁺ cells (granulocytes) was observed between the groups in the infarcted area.

Speckle tracking analysis is sensitive for early changes in matrix composition

As our histological data demonstrated, no significant difference could be observed for the analyzed individual parameters between CPC or vehicle treated mice. In order to clarify the observed attenuation of the LVEDV, we used speckle tracking analysis for more detailed visualization of the regional wall motion dimensions of the myocardium (Fig 6a-e). Upon I/R injury an expected decline in velocity, strain and SR was observed (Table 1). Global radial deformation changes were more pronounced than longitudinal deformation changes (S1 Table), with the latter being more affected in the infarcted region. Although no differences between the groups were found in conventional cardiac parameters (LVEDV and LVESV) prior to treatment, small differences were observed between the CPC group and vehicle group for radial velocity and SR, with a better performance for the vehicle group. Radial velocity was 0.7 ± 0.06 cm/s in the CPC group and 0.9 ± 0.06 cm/s in the vehicle group ($p = 0.02$). SR was 6.1 ± 0.4 %/s in the CPC group vs. 8.0 ± 0.6 %/s in the vehicle group ($p = 0.01$; Table 1).

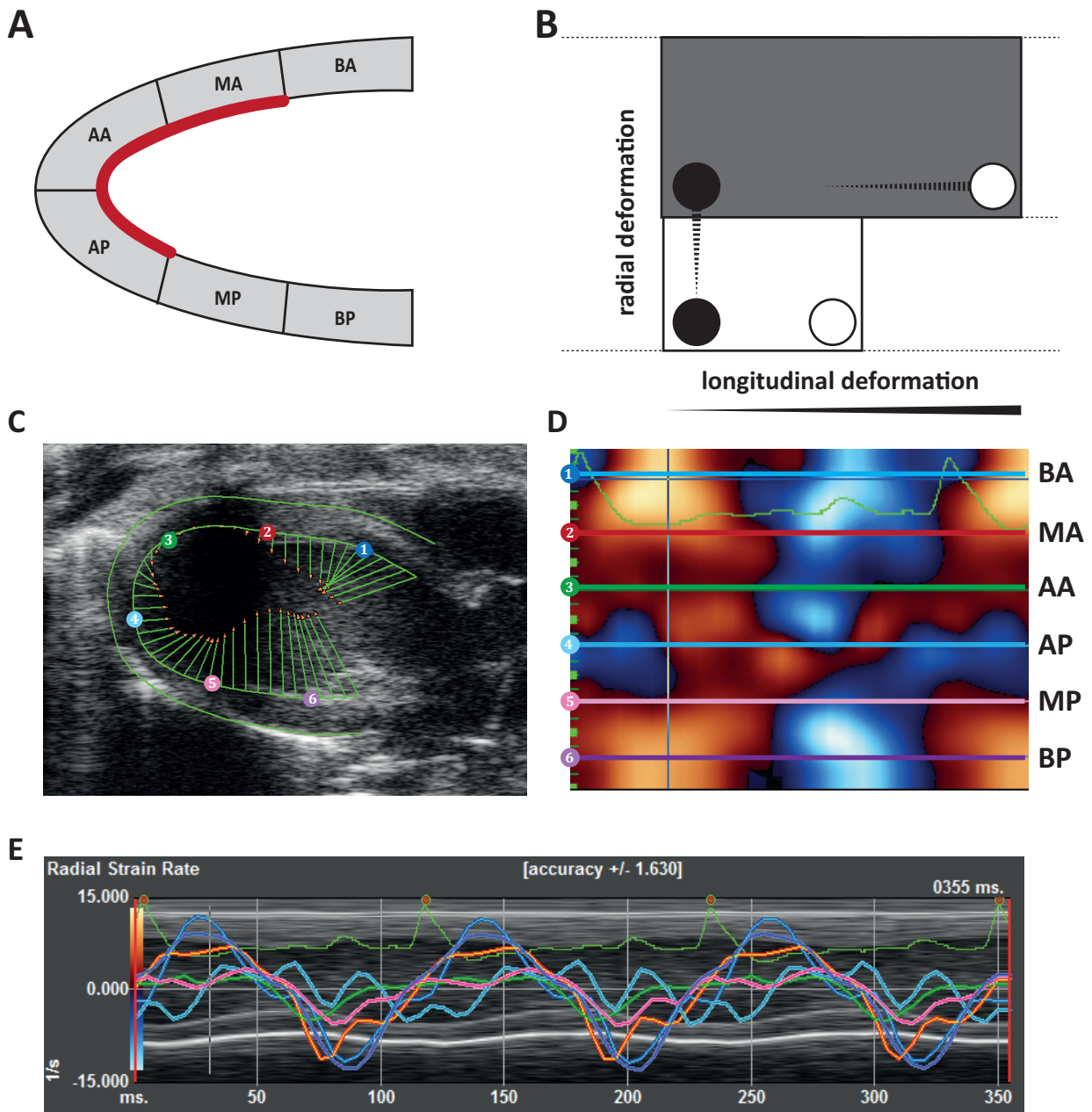


Figure 6. Myocardial deformation. (A) Schematic overview of 6 myocardial segments and deformation vectors; Basal-anterior (BA), mid-anterior (MA), apical-anterior (AA), apical-posterior (AP), mid-posterior (MP), basal-posterior (BP). Red line indicates infarct region. (B) Graphic representation of radial and longitudinal deformation. (C) Representative echocardiographic image of myocardial deformation (radial SR) after I/R injury, with concomitant vector lines, (D) for individual tracking points, and (E) combined with electrocardiogram and short axis view.

To gain insight in the effect of treatment, the difference of post- and pre-treatment was calculated for all individual mice (Table 1). None of the longitudinal measurements were different between the two groups. However, analysis of myocardial deformation on the radial axis did show significant differences over time in favor of the CPC group. Radial velocity was increased in CPC treated mice ($+0.2 \pm 0.1$ cm/s) while further decreased in vehicle treated mice (-0.1 ± 0.06 cm/s, $p=0.02$). Likewise, strain and SR significantly improved for CPC treatment compared to vehicle. SR improved from 6.1 ± 0.4 /s to 7.1 ± 0.6 /s compared to a decrease (8.0 ± 0.6 /s to 7.3 ± 0.6 /s) for vehicle treatment.

Regional deformation	baseline		pre-treatment			post-treatment (delta)			
	overall		overall (n=29)	CPC (n=13)	Vehicle (n=16)		CPC (n=13)	Vehicle (n= 16)	
Radial									
velocity (cm/s)	1.1±0.08	0.0002	0.8±0.04	0.7±0.06	0.9±0.06	0.0193	0.1±0.04	-0.1±0.06	0.0056
strain (%)	35.4±3.3	0.0007	21.6±2.0	18.8±2.3	23.9±3.2	0.218	4.7±2.1	-1.2±3.1	0.1548
SR (1/s)	9.8±0.4	0.0003	7.2±0.4	6.1±0.4	8.0±0.6	0.0131	1.0±0.5	-0.7±0.6	0.0409
Longitudinal									
velocity (cm/s)	0.9±0.07	0.0829	0.7±0.05	0.7±0.1	0.7±0.05	0.6916	0.06±0.1	0.04±0.1	0.8709
strain (%)	-17.9±1.9	0.0039	-12.8±0.7	-12.1±0.9	-13.4±1.1	0.3713	-0.8±1.0	-0.08±1.1	0.6614
SR (1/s)	-7.2±0.6	0.0046	-5.3±0.3	-5.0±0.5	-5.5±0.5	0.4912	0.2±0.3	0.1±0.5	0.5984

Table 1. Regional myocardial deformation. Segments denoted as infarct area (MA, AA, AP) were used for quantification of velocity, strain and SR. The average value of the infarct area is given for the deformation parameters (velocity, strain and SR). p-values in the baseline column denote differences between baseline and 28 days I/R. In addition, p-values in the pre-treatment and post-treatment column show differences between the CPC and vehicle group.

Discussion

Recently provided recommendations by the European Society of Cardiology, Working Group Cellular Biology of the Heart [20], aim to improve the therapeutic application of cell-based therapies for cardiac regeneration and repair by, among other recommendations, using more appropriate animal models that better resemble human chronic ischemic disease.

According to this, we tested CPC therapy in a clinically relevant mouse model of chronic cardiac remodeling. Minimally invasive intramyocardial injection of CPC was successfully applied 28 days after I/R injury and resulted in localized long-term engraftment. Although limited, transplantation of CPC resulted in attenuation of left ventricular dilatation and improved regional SR at 4 weeks follow-up with an effect size more closely resembling the results as obtained in large animal models and clinical studies. The challenge of clinical translation of cell therapy in small animal models is anticipated in this study by using an appropriate chronic I/R injury model with minimally invasive local therapy and clinically applicable functional outcome parameters.

We started off with a systematic assessment of the effect of CPC in sub-acute and chronic MI models compared to the acute setting. Our analyses show a large spread in effect size of CPC applied in the chronic setting and display a clear discrepancy in the number of small animal studies in chronic cardiac remodeling as compared to acute MI, which is worrisome due to the need for translation of this therapy to heart failure patients in particular. The observed translational failure in effect size might be attributed to animal size, but could also be caused by the models used, since 5 out of 11 placebo-controlled large animal CPC studies were done in chronic MI models, compared to only 2 out of 95 studies in small animal models [9].

Both Tang *et al.* and Tseliou *et al.* demonstrated an improvement of the LVEF upon treatment with CPC in a rat model of chronic cardiac injury with application of CPC 4 weeks after ischemic injury [14, 15]. Likewise, it was demonstrated that CPC treatment applied 7 days after permanent ligation of the LAD in mice resulted in improvement of LVEF and a lowering of the

ventricular scar burden [17]. In contrast to these results, we found that the application of CPC in a murine chronic I/R model did not result in significant restoration of cardiac function. However, it is noteworthy that our results demonstrated an early preservation of the diastolic diameter of the left ventricle upon CPC injection.

The apparent discrepancy in treatment effects between performed studies, including ours, is most likely attributed to the timing of therapy, the used injury model, delivery method, source of CPC and cell retention. Our study was designed to mimic the human clinical situation of chronic ischemic heart failure with timing of therapy as a key prerequisite. Accordingly, we used a model of I/R injury to provide insight in the effect of CPC in negative remodeling and used immune deficient (NOD-SCID) mice to accomplish this goal. Although a recent published report demonstrated that I/R injury in NOD-SCID mice does not result in sufficient cardiac damage [27], we show successful induction of cardiac remodeling upon I/R injury. Moreover, we administered local therapy 4 weeks after induction of MI to predominantly target chronic cardiac remodeling. In contrast, the previously described treatment at 7 days interferes with the extinguishing acute inflammatory response [28]. It is important to note that the therapeutic effect of cell therapy will be different in the distinct phases of cardiac injury and repair, e.g. tissue salvage in the acute phase and tissue remodeling in the chronic phase [12].

In line with the small beneficial results obtained in pre-clinical large animal research and clinical trials [29, 30], we demonstrated an attenuation of LVEDV increase upon treatment with CPC. In addition, there seems to be a difference in therapeutic benefit in mice with respect to pre-treatment extent of injury. These findings are in accordance with clinical meta-analysis demonstrating more effective treatment in patients with more severe cardiac dysfunction at the start of the therapy [31, 32].

With only two other placebo-controlled CPC studies in small animal models, the difference in beneficial effects remains difficult to explain and timing of therapy needs further exploration to better understand the role of the chosen injury model. In addition, it is known that CPC isolated with different isolation protocols display slightly dissimilar markers. However, this difference

most likely did not influence the treatment effect since a high degree of similarity is found in their individual transcriptomes, although Cardiospheres displayed a higher secretory pattern of molecules involved in the development of cardiac muscle, vasculogenesis and angiogenesis [33].

Since we observed an effect of CPC treatment on eccentric cardiac remodeling, we assessed histological parameters to provide insight in the structural and cellular changes of the myocardial matrix. Although infarct size and collagen density appeared slightly smaller in the treated group, a direct link between histological parameters and the observed changes in cardiac volumes were absent. Since histological assessment is subject to a need for sample selection and thereby creates additional experimental variation or bias, the findings do not rule out that CPC interferes with matrix remodeling. Recently, it was demonstrated that CPC reduced fibroblast proliferation and attenuated pro-fibrotic signaling in a rat model of chronic MI [34]. This notion is supported by the observed long term improved left ventricular remodeling upon CPC treatment [14, 15, 35]. Several reports suggest that early changes in matrix remodeling are detected with a higher sensitivity with measurements of regional wall motion parameters by speckle tracking analysis [36–39]. Therefore, we assessed velocity, strain and SR of the infarcted region and indeed we have identified beneficial regional deformation changes upon CPC treatment, consistent with another study showing improved strain and SR upon myocardial treatment with induced pluripotent stem cells [40].

Implementation of regional wall motion measurements in small animal research might be valuable to identify more sensitive markers of cardiac function and cardiac improvement upon novel therapies. In parallel, these novel techniques merit further investigation to identify key modulators of myocardial remodeling translatable to pre-clinical large animal models and clinical cell therapy studies.

The resemblance of effect size with (pre-)clinical studies in literature underlines the translatability of our small animal injury model and shows that the apparent discrepancy in

results can possibly be explained by the various approaches in the different models, of which timing of therapy and the type of injury model used are presumably the most important factors.

The model we present here can be exerted as a starting point to study the basic mechanisms behind cell therapy and to introduce more advanced methods in small animal research to examine therapies already tested in the acute post-MI phase. The tentative positive outcome of cell therapy in (pre-)clinical trials and the limited observed effects in our study force us to take the long view and to carefully address opportunities to optimize cell therapy to achieve clinical efficacy. Recently, tissue engineering approaches with the use of cell carriers improved initial cell retention and consequently resulted in a more beneficial treatment effect [41–43]. Furthermore, tailoring of cell differentiation protocols to direct cell fate is another promising approach to enhance therapeutic potential [44]. Therefore, exploration of different biomaterials and enhancing cell effectors would be of interest in future studies. To further maximize the success of preclinical research, co-morbidities and pharmacological agents should be incorporated in preclinical animal models [45–47]. The add-on effect of stem cell therapy will become clear when applied in combination with factors as hypercholesterolemia, diabetes, age, renal failure and gender [48].

Driven by the urge for clinical translation through proper animal models [49], the present study demonstrates a comprehensive small animal injury model to study chronic cardiac remodeling. We found that CPC transplantation can be adequately examined in this study set-up and by that provide a translatable small animal model facilitating advances in research for new local therapeutic approaches to treat chronic heart failure.

Acknowledgements

We would like to acknowledge H. Gremmels for the lamin A/C antibody.

Funding Sources

We acknowledge the support from Innovation and the Netherlands CardioVascular Research Initiative (CVON): The Dutch Heart Foundation, Dutch Federation of University Medical Centers, the Netherlands Organization for Health Research and Development and the Royal Netherlands Academy of Science and the Alexandre Suerman program for MD/PhD students of the University Medical Center Utrecht, the Netherlands. Additionally, the ZonMW Translational Adult Stem Cell grant 1161002016.

Ethical statements

This manuscript contains data based on the use of human fetal tissue, which was obtained by individual permission using standard informed consent procedures and prior approval of the ethics committee of the University Medical Center Utrecht, the Netherlands. This procedure is in accordance with the principles outlined in the Declaration of Helsinki for the use of human tissue or subjects. Furthermore, all animal experiments were carried out in accordance with the Guide for the Care and Use of Laboratory Animals, with prior approval by the Animal Ethical Experimentation Committee, Utrecht University, the Netherlands.

Disclosure

The authors declare that they have no conflict of interest.

References

1. Lecour S, Bøtker HE, Condorelli G, et al. ESC working group cellular biology of the heart: position paper: improving the preclinical assessment of novel cardioprotective therapies. *Cardiovasc Res* 2014;104:399–411.
2. Mozaffarian D, Benjamin EJ, Go AS, et al. Heart Disease and Stroke Statistics-2016 Update: A Report From the American Heart Association. *Circulation* 2015;133:e38–e360.
3. Menasché P, Hagège AA, Scorsin M, et al. Myoblast transplantation for heart failure. *Lancet (London, England)* 2001;357:279–80.
4. Strauer BE, Brehm M, Zeus T, et al. Repair of infarcted myocardium by autologous intracoronary mononuclear bone marrow cell transplantation in humans. *Circulation* 2002;106:1913–8.
5. Abdel-Latif A, Bolli R, Tleyjeh IM, et al. Adult bone marrow-derived cells for cardiac repair: a systematic review and meta-analysis. *Arch Intern Med* 2007;167:989–97.
6. Schächinger V, Erbs S, Elsässer A, et al. Intracoronary bone marrow-derived progenitor cells in acute myocardial infarction. *N Engl J Med* 2006;355:1210–21.
7. Makkar RR, Smith RR, Cheng K, et al. Intracoronary cardiosphere-derived cells for heart regeneration after myocardial infarction (CADUCEUS): a prospective, randomised phase 1 trial. *Lancet (London, England)* 2012;379:895–904.
8. Lara-Pezzi E, Menasché P, Trouvin J-H, et al. Guidelines for translational research in heart failure. *J Cardiovasc Transl Res* 2015;8:3–22.
9. Zwetsloot PP, Végh AM, Jansen Of Lorkeers SJ, et al. Cardiac Stem Cell Treatment in Myocardial Infarction: A Systematic Review and Meta-Analysis of Preclinical Studies. *Circ Res* 2016.
10. Jansen Of Lorkeers SJ, Eding JEC, Vesterinen HM, et al. Similar effect of autologous and allogeneic cell therapy for ischemic heart disease: systematic review and meta-analysis of large animal studies. *Circ Res* 2015;116:80–6.
11. Tongers J, Losordo DW, Landmesser U. Stem and progenitor cell-based therapy in ischaemic heart disease: promise, uncertainties, and challenges. *Eur Heart J* 2011;32:1197–206.
12. Goumans M-J, Maring JA, Smits AM. A straightforward guide to the basic science behind cardiovascular cell-based therapies. *Heart* 2014;100:1153–7.
13. Oskoueï BN, Lamirault G, Joseph C, et al. Increased potency of cardiac stem cells compared with bone marrow mesenchymal stem cells in cardiac repair. *Stem Cells Transl Med* 2012;1:116–24.
14. Tseliou E, Reich H, de Couto G, et al. Cardiospheres reverse adverse remodeling in chronic rat myocardial infarction: roles of soluble endoglin and Tgf- β signaling. *Basic Res Cardiol* 2014;109:443.
15. Tang X-L, Rokosh G, Sanganalmath SK, et al. Intracoronary administration of cardiac progenitor cells alleviates left ventricular dysfunction in rats with a 30-day-old infarction. *Circulation* 2010;121:293–305.
16. Rota M, Padin-Iruegas ME, Misao Y, et al. Local activation or implantation of cardiac progenitor cells rescues scarred infarcted myocardium improving cardiac function. *Circ Res* 2008;103:107–16.
17. Latham N, Ye B, Jackson R, et al. Human blood and cardiac stem cells synergize to enhance cardiac repair when cotransplanted into ischemic myocardium. *Circulation* 2013;128:S105–12.
18. Springer ML, Sievers RE, Viswanathan MN, et al. Closed-chest cell injections into mouse myocardium guided by high-resolution echocardiography. *Am J Physiol Heart Circ Physiol* 2005;289:H1307–14.
19. Prendiville TW, Ma Q, Lin Z, Zhou P, He A, Pu WT. Ultrasound-guided transthoracic intramyocardial injection in mice. *J Vis Exp* 2014:e51566.
20. Madonna R, Van Laake LW, Davidson SM, et al. Position Paper of the European Society of Cardiology Working Group Cellular Biology of the Heart: cell-based therapies for myocardial repair and regeneration in ischemic heart disease and heart failure. *Eur Heart J* 2016.

21. Smits AM, van Laake LW, den Ouden K, et al. Human cardiomyocyte progenitor cell transplantation preserves long-term function of the infarcted mouse myocardium. *Cardiovasc Res* 2009;83:527–35.
22. Smits AM, van Vliet P, Metz CH, et al. Human cardiomyocyte progenitor cells differentiate into functional mature cardiomyocytes: an in vitro model for studying human cardiac physiology and pathophysiology. *Nat Protoc* 2009;4:232–243.
23. Feyen D, Gaetani R, Liu J, et al. Increasing short-term cardiomyocyte progenitor cell (CMPC) survival by necrostatin-1 did not further preserve cardiac function. *Cardiovasc Res* 2013;99:83–91.
24. van Laake LW, Passier R, Monshouwer-Kloots J, et al. Monitoring of cell therapy and assessment of cardiac function using magnetic resonance imaging in a mouse model of myocardial infarction. *Nat Protoc* 2007;2:2551–67.
25. Xu Z, Alloush J, Beck E, Weisleder N. A murine model of myocardial ischemia-reperfusion injury through ligation of the left anterior descending artery. *J Vis Exp* 2014.
26. Motulsky HJ, Brown RE. Detecting outliers when fitting data with nonlinear regression - a new method based on robust nonlinear regression and the false discovery rate. *BMC Bioinformatics* 2006;7:123.
27. van Zuylen V-L, den Haan MC, Roelofs H, Fibbe WE, Schaliij MJ, Atsma DE. Myocardial infarction models in NOD/Scid mice for cell therapy research: permanent ischemia vs ischemia-reperfusion. *Springerplus* 2015;4:336.
28. van den Akker F, Deddens JC, Doevendans PA, Sluijter JPG. Cardiac stem cell therapy to modulate inflammation upon myocardial infarction. *Biochim Biophys Acta* 2013;1830:2449–58.
29. Johnston P V, Sasano T, Mills K, et al. Engraftment, differentiation, and functional benefits of autologous cardiosphere-derived cells in porcine ischemic cardiomyopathy. *Circulation* 2009;120:1075–83, 7 p following 1083.
30. Jansen Of Lorkeers SJ, Gho JMIH, Koudstaal S, et al. Xenotransplantation of Human Cardiomyocyte Progenitor Cells Does Not Improve Cardiac Function in a Porcine Model of Chronic Ischemic Heart Failure. Results from a Randomized, Blinded, Placebo Controlled Trial. *PLoS One* 2015;10:e0143953.
31. Delewi R, Hirsch A, Tijssen JG, et al. Impact of intracoronary bone marrow cell therapy on left ventricular function in the setting of ST-segment elevation myocardial infarction: a collaborative meta-analysis. *Eur Heart J* 2014;35:989–98.
32. Clifford DM, Fisher SA, Brunskill SJ, et al. Long-term effects of autologous bone marrow stem cell treatment in acute myocardial infarction: factors that may influence outcomes. *PLoS One* 2012;7:e37373.
33. Gaetani R, Feyen DAM, Doevendans PA, et al. Different types of cultured human adult cardiac progenitor cells have a high degree of transcriptome similarity. *J Cell Mol Med* 2014;18:2147–51.
34. Yee K, Malliaras K, Kanazawa H, et al. Allogeneic cardiospheres delivered via percutaneous transendocardial injection increase viable myocardium, decrease scar size, and attenuate cardiac dilatation in porcine ischemic cardiomyopathy. *PLoS One* 2014;9:e113805.
35. Tang X-L, Li Q, Rokosh G, et al. Long-Term Outcome of Administration of c-kit^{POS} Cardiac Progenitor Cells After Acute Myocardial Infarction: Transplanted Cells Do Not Become Cardiomyocytes, but Structural and Functional Improvement and Proliferation of Endogenous Cells Persist for At Lea. *Circ Res* 2016.
36. Thibault H, Gomez L, Donal E, et al. Acute myocardial infarction in mice: assessment of transmural strain by strain rate imaging. *Am J Physiol Heart Circ Physiol* 2007;293:H496-502.
37. Bauer M, Cheng S, Jain M, et al. Echocardiographic speckle-tracking based strain imaging for rapid cardiovascular phenotyping in mice. *Circ Res* 2011;108:908–16.
38. Peng Y, Popovic ZB, Sopko N, et al. Speckle tracking echocardiography in the assessment of mouse models of cardiac dysfunction. *Am J Physiol Heart Circ Physiol* 2009;297:H811-20.
39. Bhan A, Sirker A, Zhang J, et al. High-frequency speckle tracking echocardiography in the assessment of left ventricular function and remodeling after murine myocardial infarction.

- Am J Physiol Heart Circ Physiol 2014;306:H1371-83.
40. Yamada S, Nelson TJ, Kane GC, et al. Induced pluripotent stem cell intervention rescues ventricular wall motion disparity, achieving biological cardiac resynchronization post-infarction. *J Physiol* 2013;591:4335-49.
 41. Feyen DAM, Gaetani R, Deddens J, et al. Gelatin Microspheres as Vehicle for Cardiac Progenitor Cells Delivery to the Myocardium. *Adv Healthc Mater* 2016.
 42. van den Akker F, Feyen DAM, van den Hoogen P, et al. Intramyocardial stem cell injection: go(ne) with the flow. *Eur Heart J* 2016.
 43. Ye Z, Zhou Y, Cai H, Tan W. Myocardial regeneration: Roles of stem cells and hydrogels. *Adv Drug Deliv Rev* 2011;63:688-97.
 44. Aguirre A, Sancho-Martinez I, Izpisua Belmonte JC. Reprogramming toward heart regeneration: stem cells and beyond. *Cell Stem Cell* 2013;12:275-84.
 45. McMurray JJ V, Adamopoulos S, Anker SD, et al. ESC guidelines for the diagnosis and treatment of acute and chronic heart failure 2012: The Task Force for the Diagnosis and Treatment of Acute and Chronic Heart Failure 2012 of the European Society of Cardiology. Developed in collaboration with the Heart. *Eur J Heart Fail* 2012;14:803-69.
 46. Giricz Z, Lalu MM, Csonka C, Bencsik P, Schulz R, Ferdinandy P. Hyperlipidemia attenuates the infarct size-limiting effect of ischemic preconditioning: role of matrix metalloproteinase-2 inhibition. *J Pharmacol Exp Ther* 2006;316:154-61.
 47. Baranyai T, Nagy CT, Koncsos G, et al. Acute hyperglycemia abolishes cardioprotection by remote ischemic preconditioning. *Cardiovasc Diabetol* 2015;14:151.
 48. McCafferty K, Forbes S, Thiemermann C, Yaqoob MM. The challenge of translating ischemic preconditioning from animal models to humans: the role of comorbidities. *Dis Model Mech* 2014;7:1321-33.
 49. Bolli R, Ghafghazi S. Cell Therapy Needs Rigorous Translational Studies in Large Animal Models. *J Am Coll Cardiol* 2015;66:2000-4.

Supplementary

Supplementary Methods

Ischemia Reperfusion model

Male NOD-SCID mice (Harlan Laboratories), aged 10-12 weeks, underwent left coronary artery (LAD) ligation as previously described (21), followed by reperfusion. In short, mice were anesthetized with Fentanyl 0.05 mg/kg, Midazolam 5 mg/kg and Domitor 0.5 mg/kg through an intraperitoneal (ip) injection. Mice were intubated and ventilated with a mixture of oxygen and air (1:2) with a rate of 250 ventilations/min. The thorax was opened between the 3th and 4th rib and the LAD was ligated 2-3 mm below the left atrial appendage with a 8-0 Ethilon suture (Ethicon) around a soft tube (BD insyte-WA). After 60 minutes, reperfusion was initiated by releasing the ligature and removal of the tube. Reflow was confirmed by reversed discoloration of the heart. The chest was closed in layers and anesthesia was antagonized by a mixture of Antisedan 2.5 mg/kg and Anexate 0.5 mg/kg injected subcutaneously.

3D motor echocardiography

Echocardiography (echo) was performed on baseline, 28 days after I/R injury and at 7, 14 and 28 days after treatment using a high resolution ultrasound system (Vevo 2100, visual sonics) with a 18-38 MHz transducer (MS 400, visual sonics). Physiological parameters (heart rate, respiration and temperature) were monitored continuously and were maintained stable at physiological levels. In addition, an electrocardiogram (ECG) was used to identify left ventricular end-diastolic volume (LVEDV) and left ventricular end-systolic volume (LVESV) triggers. B-mode data were acquired in the parasternal long axis view (PSLAX). For reconstructed 3D-echo images, the transducer was positioned perpendicular to the long-axis view (short-axis view) and the left ventricle was scanned by consecutive images (0.064 mm intervals) of the short axis using a 3D-motor (visual sonics). 3D images were reconstructed based on the drawing of approximately 10-12 volumes of interest from apex to base (see Supplemental Figure 2). LVEDV and LVESV were used to calculate left ventricular ejection fraction (LVEF).

Post measurement speckle tracking based analysis were performed to determine myocardial deformation parameters (VevoStrain, VisualSonics). Echocardiographic images acquired from the PSLAX were used to measure peak velocity (cm/s), strain (%) and strain rate (1/s) in the longitudinal and radial axis.

Three consecutive cardiac cycles were selected for analysis and semi-automated tracing of the endocardial and epicardial border was performed resulting in 48 sampling points. The myocardium was automatically divided in 6 segments for regional speckle-tracking analysis; basal-anterior (BA), mid-anterior (MA), apical-anterior (AA), apical-posterior (AP), mid-posterior (MP) and basal-posterior (BP). Global measurements were defined as the average of all 6 segments, whereas the infarct and remote area were defined as the average of MA, AA, AP and MP, BP respectively.

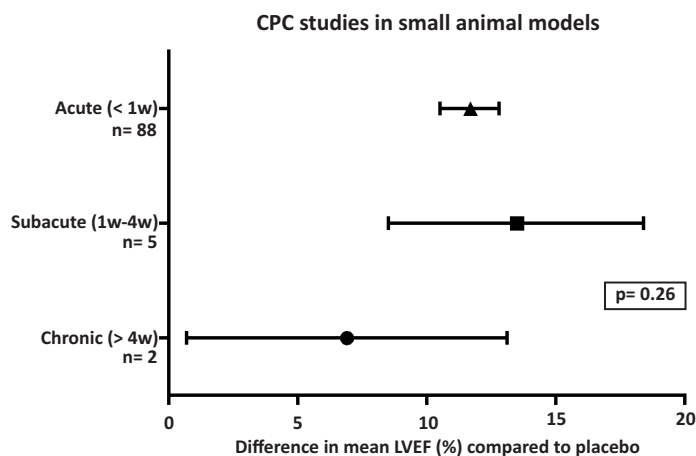
Histology

At day 28 after intramyocardial injection with either CPC or vehicle, mice were terminated by exsanguination under general anesthesia and their hearts were excised. The hearts were dehydrated and fixed in a 15% sucrose 0.4% PFA solution after which they were embedded in O.C.T. compound (Tissue Tek) and stored at -80 °C. Serial transverse cryosections of 7 µm were cut, base to apex, for histological and immunohistological stainings, which were performed by a blindend investigator.

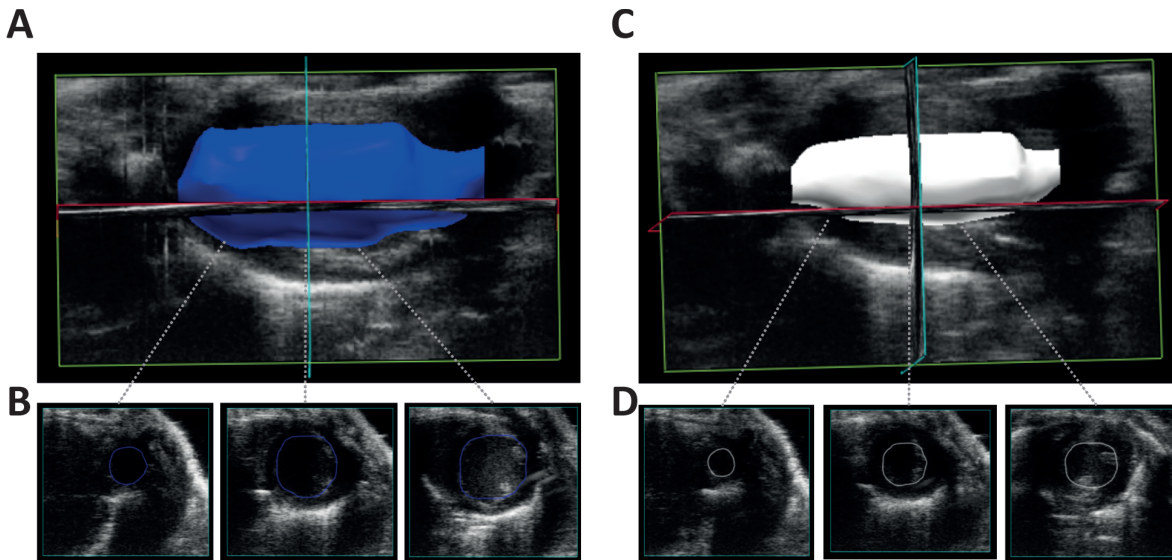
Sections were stained in haematoxylin solution (Boom) and eosin solution (BDH), followed by dehydration and embedding in entellan. Next, picrosirius red staining was performed to analyze the collagen composition and density in the infarcted area. Stained sections were imaged with light microscopy to define the infarct area and with polarized light microscopy to analyze collagen fibers. The infarct area was assessed visually as the area with disrupted myocardium. Collagen density is expressed as mean grey value per mm² infarct area. Analysis was performed with CellSense (Olympus).

Engraftment of human CPC and the effect on matrix composition was assessed by immunostaining and the visual aspect of the cardiomyocyte pattern as background layer. Cryosections were incubated for 1 hour at room temperature with primary antibodies against: human Lamin A/C antibody (1:100, VP-L550, Vector), Troponin-I (1:50, sc-15368, Santa Cruz), vimentin (1:100, sc-7557, santa cruz), α -SMA (1:100, F3777, Sigma), collagen type 1 (1:50, 600-4010103S, Rockland), collagen type 3 (1:50, ab-7778, Abcam), CD31 (1:50, 550274, eBioscience), CD45 (1:50, BD Pharmingen). Subsequently, sections were incubated o/n at 4°C using the appropriate Alexa 488 and Alexa 555 antibody (Invitrogen). Nuclei were stained with Hoechst (33342). For clear CD31 staining, an amplification step with biotin/streptavidin (DAKO) was included.

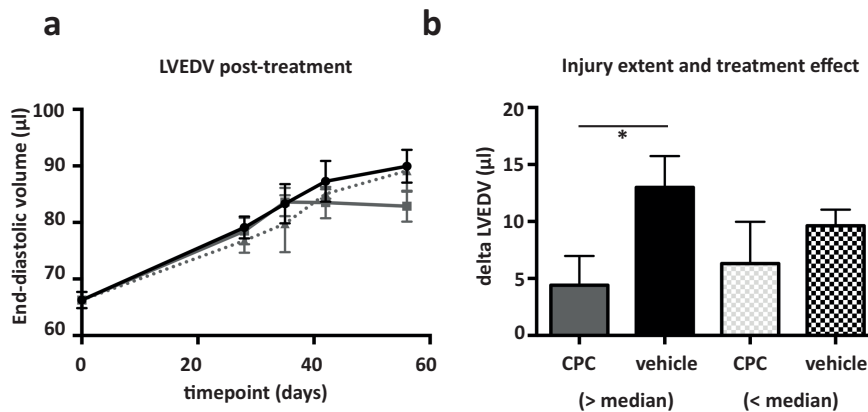
Supplementary Figures



Supplementary Figure 1. Meta-regression of timing of CPC therapy in small animal models. Analysis of CPC studies in small animal models showed a large spread in effect on EF for timing of therapy (p= 0.26) with only 2 studies performed in the chronic MI setting.



Supplementary Figure 2. Reconstructed 3D echocardiography. (A) Representative images of the contours of the LVEDV and (B) LVESV in a reconstructed 3D echocardiographic image. Bottom panels show examples of the contours drawn in the short axis images used to reconstruct the left ventricle.



Supplementary Figure 3. Subgroup analysis of functional outcome. (A) LVEDV is not preserved in mice with low retention at day 2 (unsuccessful injection). Black line indicates vehicle treated mice, grey line indicates mice with successful CPC injection and dotted grey line indicates mice with unsuccessful CPC injection. LVEDV= left ventricular end-diastolic volume. (B) The effect of treatment is higher in mice with a larger injury extent. Groups are divided by the median LVEDV as measured prior to treatment. * $p < 0.05$.

Regional deformation	baseline		pre-treatment			post-treatment (delta)			
	overall		overall (n=29)	CPC (n=13)	Vehicle (n=16)		CPC (n=13)	Vehicle (n=16)	
Radial									
velocity (cm/s)	1.4±0.08	0.0013	1.10±0.05	1.0±0.07	1.2±0.07	0.0471	0.1±0.04	-0.1±0.06	0.0042
strain (%)	35.3±3.3	0.0017	23.8±1.7	21.7±2.4	25.5±2.4	0.2813	4.4±2.2	0.02±2.4	0.2065
SR (1/s)	9.1±0.6	0.0001	6.0±0.4	5.2±0.5	6.6±0.6	0.0905	0.8±0.5	-0.7±0.5	0.0394
Longitudinal									
velocity (cm/s)	0.6±0.05	0.2444	0.5±0.03	0.6±0.03	0.6±0.05	0.7793	-0.1±0.06	-0.02±0.05	0.3123
strain (%)	-16.4±1.8	0.1017	-13.8±0.7	-13.6±0.6	-13.9±1.2	0.7999	1.2±0.9	1.6±1.6	0.8027
SR (1/s)	-5.7±0.4	0.0481	-4.6±0.3	-4.3±0.3	-4.9±0.5	0.2937	0.3±0.3	0.8±0.5	0.3949

Supplementary Table 1. Global myocardial deformation. All 6 myocardial segments were used for quantification of velocity, strain and SR. p-values in the baseline column denote differences between baseline and 28 days I/R. In addition, p-values in the pre-treatment and post-treatment column show differences between the CPC and vehicle group.

7

Rapid immune activation after human stem cell injection in Balb/C and NOD-SCID mice

*J.C. Deddens

*F. van den Akker

P. van den Hoogen

P.A. Doevendans

L.W. van Laake

J.P.G. Sluijter

*These authors contributed equally

In preparation

Abstract

Background: The immune system is increasingly recognized as an important determinant and tunable therapeutic target in CHF. Animal models currently used for human-based cardiac cell therapy, however, mainly use immune deficient animals or immunosuppressive drugs, as graft cells are non-autologous. Therefore the question was raised whether these models are appropriate and representative for human disease. Additionally, it remains controversial whether immune compromised animal models are necessary as progenitor cells are traditionally considered to be immune privileged.

Methods and results: In this short observational study, luciferase labeled mesenchymal stem cells and cardiac progenitor cells were injected into the myocardium of immunocompetent Balb/c mice and immunodeficient NOD-SCID (SCID) mice to determine whether transplantation of progenitor cells results in immune rejection. Cell retention was measured by using Bioluminescent imaging, which demonstrated that injection with either CPC or MSC resulted in a fast decline in cell retention after the initial engraftment. Interestingly, this decline was more pronounced in WT mice than in SCID mice for both injected stem cell populations. At the same time, activation of the immune system was observed as measured by flow cytometric analyses and via released plasma cytokines in both strains.

Conclusion: An immune rejection occurred in both immune competent and incompetent mice, for both MSC and CPC. In combination with the knowledge that even SCID-mice can induce a mild immune response after xenotransplantation, we believe that a shift towards humanized animals is necessary to obtain proper pre-clinical rodent models for cardiac human cell therapy.

Introduction

During a myocardial infarction, millions of cardiomyocytes die (1). Although the heart has a small reservoir of dividing progenitor cells, the sheer volume of lost tissue is too large for endogenous repair and the demand for novel therapies is high. In the past decades, different types of stem or progenitor cells have been investigated for their regenerative capacity (2). After successful isolation and characterization of progenitor cells, animal studies were conducted to investigate their reparative potential in animal models of myocardial infarction (3).

Interestingly, directly after the first promising results in animal studies, clinical trials were started (4).

As observed and reviewed many times, the functional outcome of these clinical trials was marginal at most (4). Moreover, as was observed for many drugs(5,6), a poor translation of laboratory work to clinical practice applies to cardiac cell therapy as well. The characterization of a progenitor cell population is time consuming and species differences in functional effects do exist. Additionally, even if the same progenitor cell can be found in multiple species, e.g. mesenchymal stem cells (MSC), the mechanisms of action can differ between species. For example, ample research has shown that MSC suppress T-cell proliferation using nitric oxide (7,8). However, this pathway of immunomodulation turned out to be specific for murine MSC only (7,9).

These observations led many researchers to focus on human stem and progenitor cells, as these are the cells ultimately to be used in clinical stem cell therapy. However, this creates other hurdles by using human cells in animal models. One of the most obvious problems is the immune system, which recognizes and eliminates everything that is recognized as being non-self. Initial reports claimed that many progenitor cells, including MSC, do not display HLA-antigens (10), and therefore had an immune privileged position. Yet, later publications showed the presence of HLA-antigens on the cell membranes of these progenitor cells (11-13). Interestingly, researchers either continued to use human cells in animal disease models (14-16) , or switched to the use of immunodeficient mice (17,18) or immunosuppressive drugs (19,20). However, in

cardiac diseases the immune system plays a strong role in determining short-term damage (reperfusion injury) and long-term outcome (8). Despite the known interactions between stem and progenitor cells and the immune system, it was hardly investigated if cross-species transplantation actually led to immune cell activation. In this short observational study, we injected mesenchymal stem cells (21) and cardiac progenitor cells (22) into the myocardium of immunocompetent Balb/c mice and immunodeficient NOD-SCID (SCID) mice. We investigated the survival of the cells and the immune activation to determine if the immune system was activated by the cells in this cardiac application of cell therapy.

Material and methods

Cell culture

Human fetal tissue was obtained by individual permission using standard informed consent procedures and prior approval of the ethics committee of the University Medical Center Utrecht, the Netherlands. This procedure is in accordance with the principles outlined in the Declaration of Helsinki for the use of human tissue or subjects. CPC and MSC were isolated and characterized as previously described (22,23). Cells were cultured in flasks coated with 0.1% gelatin (Sigma). CPC were cultured in SP++, containing 1 part EGM-2 (Lonza CC-3156) and 3 parts M199 (Lonza BE12-119F) supplemented with 10% fetal bovine serum (FBS; Gibco), 1% Penicillin/Streptomycin (P/S; Lonza 17-602E) and 1% Non-essential Amino Acids (Lonza 13-114). MSC were cultured in MEM-alpha (Gibco) supplemented with 10% FBS, 1% P/S and 0.2mM L-ascorbic acid-2-phosphate (Sigma A4034).

Cells were transduced with pLV-CMV-luc-GFP, a lentiviral construct, to facilitate their identification *in vivo* (24). After transduction, CPC and MSC were passaged and cultured until 80% confluency before injection at passage 14 and 13, respectively.

Animals

All experiments were carried out in accordance with the Guide for the Care and Use of Laboratory Animals, with prior approval by the Animal Ethical Experimentation Committee, Utrecht University, the Netherlands.

Intramyocardial cell injection

Male NOD.CB17-Prkdc^{scid} mice (Harlan Laboratories) and wildtype (WT) male Balb/cAnNcrI (Charles River), aged 10 weeks, were injected intramyocardially with either CPC (n= 3) or MSC (n= 3). Intramyocardial injections were performed via a percutaneous transthoracic approach with echo guidance (Vevo 2100, VisualSonics). Mice were anesthetized with 4% isoflurane and anesthesia was maintained with 1.5% isoflurane during echocardiography. Mice were

positioned in an adjusted parasternal long axis view and 0.5 million cells were injected with a 27 Gy needle in a volume of two times 5 μ l.

Bioluminescent imaging (BLI)

To determine the retention of the injected CPC-luc and MSC-luc *in vivo*, mice were imaged at 2 and 7 days after injection, as previously described (24). In short, mice were injected intraperitoneally with Luciferase (Promega E1605) and emitted photons by CPC-luc or MSC-luc were detected with a photon imager from Biospace Laboratory. Data was analyzed by PhotoVision software. Injections were considered successful based on location (mid-thorax) and a threshold of BLI signal at day 2 (> 20.000 ph/s/cm²/sr), as established with previously performed titrations (24). The absolute BLI values in the individual mice were used as primary outcome parameters and were denoted as BLI Signal Units (BSU; ph/s/cm²/sr).

Analyses of immunological response

Mice were terminated by exsanguination 7 days after intramyocardial injection of either CPC or MSC. Blood was collected in EDTA tubes. After flow cytometric samples were taken, the blood was centrifuged at 2,000 x g for 20 minutes and the serum was stored separately at -80 °C for cytokine analysis. After flushing with PBS, spleens were collected and strained through a 40 μ m nylon mesh (Greiner Bio-One 542040), creating a single cell suspension and washed twice with 5% FBS. Blood cells and splenocytes were incubated for 30 minutes at room temperature with a cocktail of fluorochrome-conjugated antibodies, allowing differentiation between the different types of immune cells. After incubation, cells were washed and subsequently Optilyse (Beckman Coulter A11895) was added to fix the cells and remove any erythrocytes.

Antibodies against the following markers were used: CD8a-APC-eFluor780 (Clone: 53-6.7; 47-0081-82), CD11b-AlexaFluor488 (Clone: M1/70; 53-0112-82), CD19-eFluor 450 (Clone: 1D3; 48-0193-82) and CD25-APC (Clone: PC61.5; 17-0251-82) purchased from eBioscience. From BD Bioscience CD4-PerCP (Clone RM4-5; 553052), CD62L-PE-CF594 (Clone MEL-14; 562404), and

Ly6C-PE-CF594 (Clone AL-21; 562728). Historical controls in Balb/cAnNcrI (Charles River) between 10-12 weeks of age were used for baseline. The Gallios Flow Cytometer (Beckman Coulter) was used to measure cell fluorescence and all analysis were performed with Kaluza Analysis Software (Beckman Coulter, version 1.3).

Serum measurements

A 36-multiplex panel (eBioscience, EPX360-26092-01) was used to measure the concentration of 36 cyto- and chemokines in the isolated serum using a Luminex-200 instrument (Bio-Plex 200). The luminex assay was performed according to manufacturer's instructions.

Statistical analysis

Statistical analyses were performed by GraphPad Prism 6.0 software (GraphPad Software). Data are presented as mean \pm SEM and were compared using the two-tailed Student's T-test. Flow cytometric data and cytokines were compared using one-way ANOVA with LSD post-hoc correction, after determining normal distribution. $p < 0.05$ was considered statically significant.

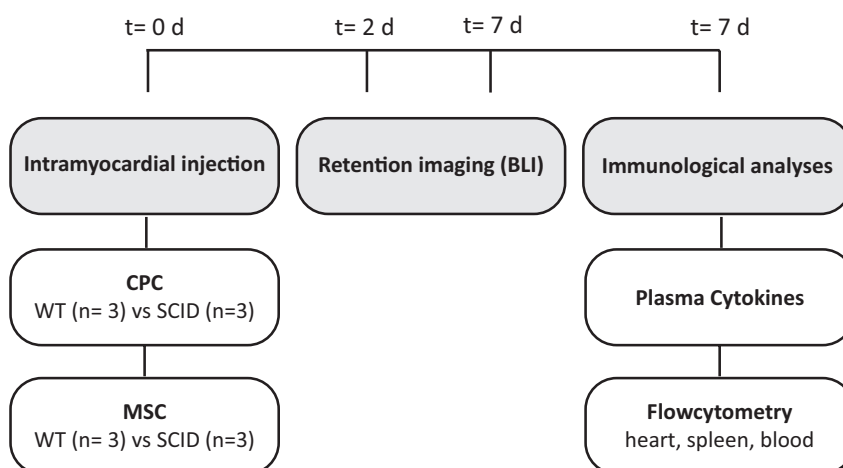


Figure 1. Study protocol

Results

Injection of CPC and MSC in WT mice resulted in an accelerated reduction of cell retention

To determine the course of human stem cell retention in immune competent and immune compromised mice, MSC-luc or CPC-luc were injected intramyocardially in WT and SCID mice, respectively (Figure 1).

In vitro analysis of the luciferase activity of CPC-luc and MSC-luc showed a linear dose dependency for cell count and BLI signal (Figure 2A-B). Consequently, higher BLI signals correspond to a higher cell retention. Two days after injection with CPC-luc, cell retention appeared higher in SCID mice than in WT mice (1.2 ± 0.5 vs. 0.5 ± 0.2 BSU $\times 10^5$, $p=0.18$). Likewise, injection with MSC-luc resulted in a higher signal in SCID mice compared to WT mice (5.4 ± 0.6 vs. 2.1 ± 1.0 BSU $\times 10^5$, $p=0.05$) (Fig 2C-E). Although cell retention was decreased dramatically in both SCID and WT mice after 7 days, the difference in cell retention between SCID and WT was even more pronounced than at day 2. In CPC-luc injected mice, cell retention decreased to 1.3 ± 0.3 BSU $\times 10^4$ in SCID mice and to background values of 0.3 ± 0.02 BSU $\times 10^4$ in WT mice, $p=0.08$. Also for MSC-luc injected mice, retention was significantly higher in SCID mice compared to WT mice (2.3 ± 0.5 vs. 0.4 ± 0.01 BSU $\times 10^4$, $p=0.05$) (Figure 2F-H). Notably, the overall BLI signal at day 2 was higher for MSC-luc injected mice than for CPC-luc injected mice (~4-fold) (Figure 2C, F).

Immune activation after cell injection

After the animals were terminated, we studied the blood and spleen for signs of systemic inflammation. The amount of T-helper cells in the blood, necessary for B-cell activation, remained constant in WT after injection with CPC, while the WT animals receiving MSC had a significantly decreased level of T-helper cells (figure 3A). On the other hand, cytotoxic T-cells, capable of directly killing their target after activation, appeared to increase mildly in the CPC treated WT, while levels in MSC-treated animals were comparable to historical baselines (figure 3B). The level of circulating B-cells showed a similar trend, with the CPC-treated animals

reaching slightly higher levels than MSC treated WT mice (figure 3C). As expected, the SCID mice had virtually no lymphocytes (figure 3A-C). However, this black and white difference was less obvious when examining the myeloid-derived immune cells. The neutrophils in WT mice were strongly increased, and again the CPC-injected mice reached slightly higher levels (figure 2D). Interestingly, this slight elevation was also visible in CPC-treated SCID mice although at a lower absolute number. With regard to monocytes, no significant differences were observed between WT and SCID in the circulating numbers (figure 3E).

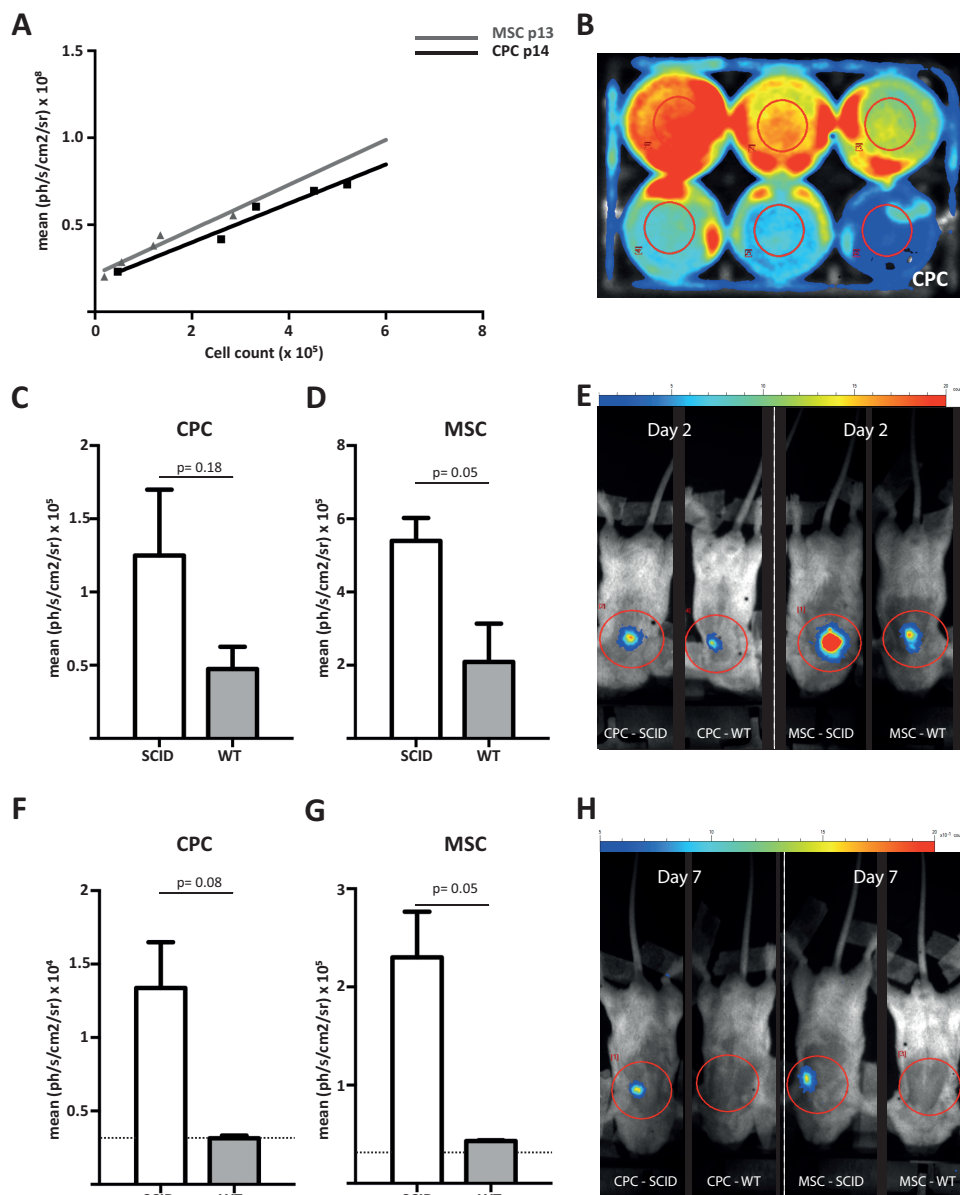


Figure 2. Stem cell retention is affected by the immunological status of mice. **A)** BLI signal of MSC-luc and CPC-luc is linear proportional to cell count *in vitro*. Grey line represent MSC-luc. Black line represent CPC-luc, as shown in **(B)**. At day 2 **(C-E)** and day 7 after injection **(F-H)**, BLI signals are lower in WT mice compared to SCID mice for both MSC-luc and CPC luc.

Interestingly, the spleen showed the opposite trend from the blood. After intramyocardial injection of MSC, the spleen contained slightly higher amounts of T_H-cells (figure 3F) and T_C-cells (figure 3G). CPC-treated animals showed hardly any variation in the level of T-cells compared to the historical baseline. The elevated CD4⁺ immune cells in the spleens of SCID mice was surprising. However, as macrophages can also display CD4, this might consist largely of non-lymphocytic CD4⁺ cells. In addition, the absolute number of B-cells in the spleen remained constant during the experiment.

Production of antibodies and inflammatory cytokines

In addition to measuring the leukocytes and splenocytes, we also collected serum to investigate the levels of antibodies and pro-inflammatory cytokines. IgM is the first antibody secreted after B-cell mature into plasma cells, and the levels observed here are comparable to our historical baseline (figure 4A). Meanwhile, the levels of the more mature IgG antibodies were strongly elevated, indicating a mature and ongoing immune response (25). This elevation was noticeable along the whole range of IgG subtypes (Figure 4A) in WT mice receiving either MSC or CPC. Obviously, no antibody production was observed in SCID mice. The panel of general inflammatory cytokines showed an increase in IFN-gamma in SCID mice, obtaining even higher levels than the WT mice (figure 4B). Although less pronounced, a similar trend was visible in TNF-alpha and IL-1beta. IL-6 showed a slight elevation in the CPC-treated WT mice. Cytokines associated with neutrophil chemotaxis (GRO-a) and activation (G-CSF) showed a marked increase in the WT group treated with CPC, corresponding to the high levels of circulating neutrophils found in that group (figure 4C). Lastly, the cytokines corresponding to macrophage activation (IL-18) and differentiation (M-CSF) showed a significant increase in the SCID mice, regardless of which progenitor cell had been injected (figure 4D; supplemental figure 1).

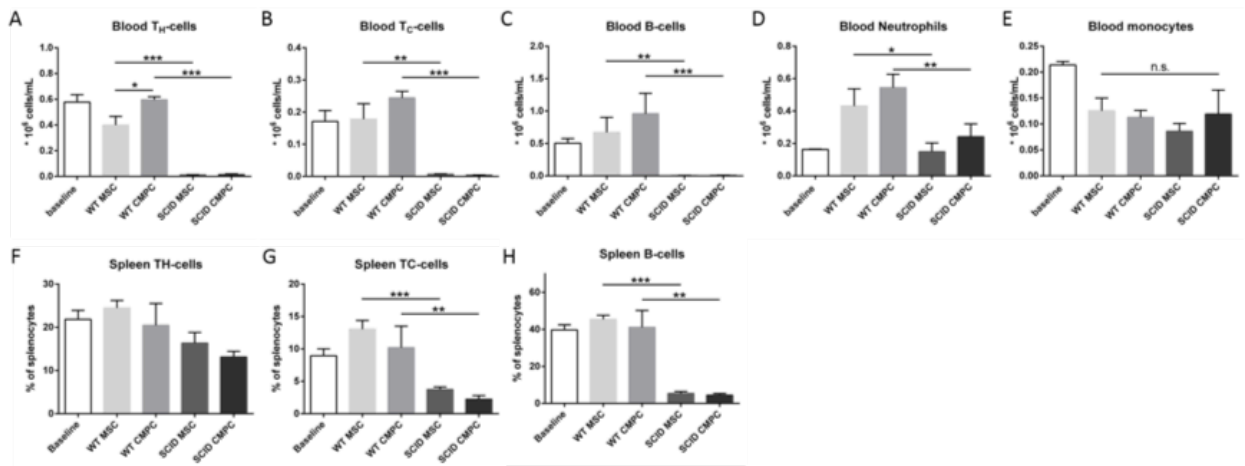


Figure 3. Activation of inflammatory cells in WT mice upon stem cell transplantation. Number of T_H-cells (A), T_C-cells (B), B-cells (C), neutrophils (D) and monocytes (E) in the blood after injection of MSC or CMPC in Wildtype (WT) and SCID mice. All circulating immune cells are elevated upon progenitor cell injection, and highest in the CMPC-injected animals. SCIDs only upregulate the myeloid-derived cells. Percentage of splenocytes formed by T_H-cells (F), T_C-cells (G) and B-cells (H). p<0.05, ** p<0.01, *** p<0.001.

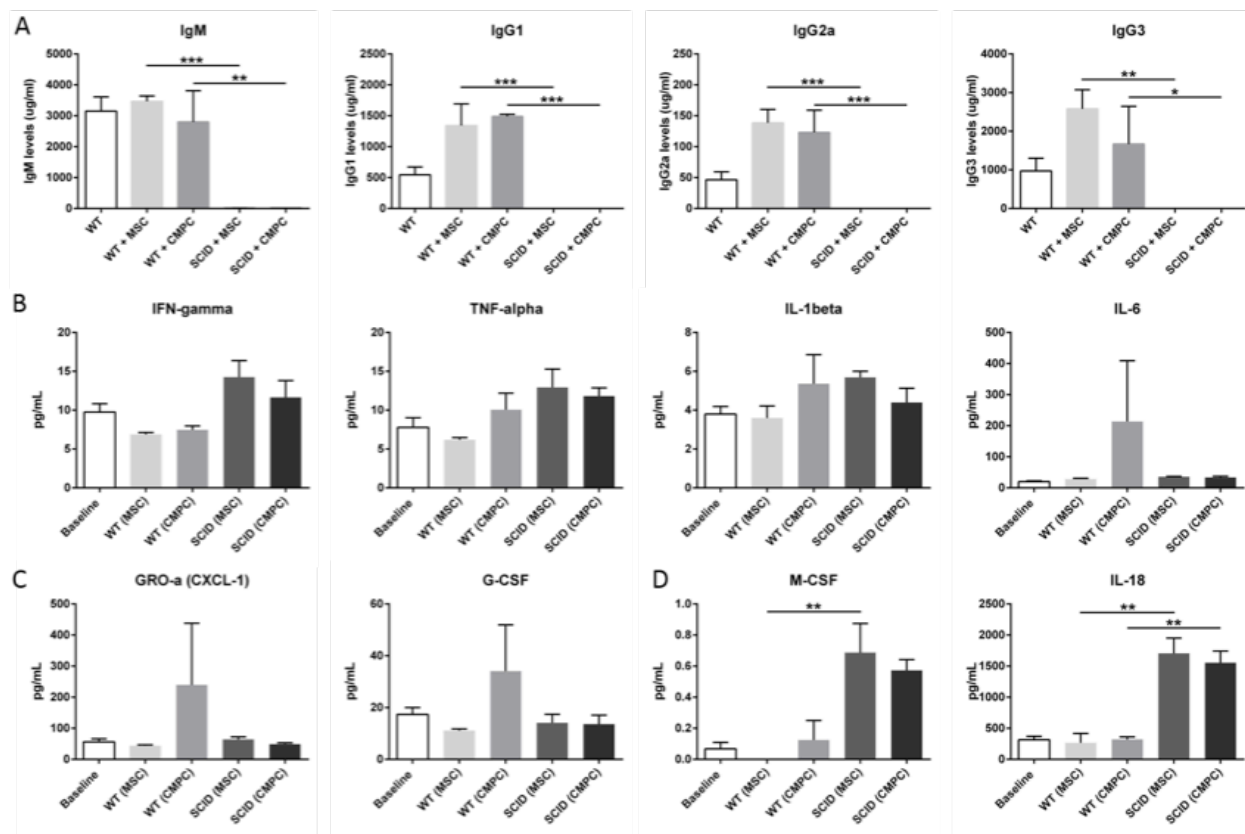


Figure 4. Stem cell injection result in elevated cytokine levels. (A) Production of IgGs is stimulated following the injection of progenitor cells in WT mice. (B) The general inflammatory cytokines are induced in both WT and SCID animals. (C) Neutrophil-associated cytokines peak especially in WT mice injected with CMPC. (D) Monocyte-related cytokines are strongly induced in SCID mice. * p<0.05, ** p<0.01, *** p<0.001.

Discussion

Small animal models are of great importance to study the mechanistic effects of human stem cell therapy to improve clinical efficacy. However, this necessitates clinically translatable animal models that resemble specific aspects of human disease (26). As presented here, intramyocardial injection with either CPC or MSC resulted in a fast decline in cell retention after the initial engraftment. Interestingly, this decline was more pronounced in WT mice than in SCID mice for both injected stem cell populations. At the same time, activation of the immune system was observed as measured by flow cytometry and plasma cytokines. Immune rejection occurred in both immune competent and incompetent mice, and for both MSC and CPC.

For a long time MSC were considered to be immune-privileged cells, allowing allogeneic transplantation and even xenotransplantation (27). This was initiated by publications claiming MSC to be MHC class I positive, protecting them from the innate immune system, while avoiding T-cell-mediated death by being class II negative (10). Others have found, however, an inducible or constitutive expression of both types of MHC molecules on MSC (11-13) with the implication that transplanted cells can be recognized by the host immune system leading to graft rejection. This notion is supported by our results, which showed a clearance of transplanted cells and activation of the immune system on all levels. The most likely explanation for this is an expression of MHC-antigens on both cell types. Although an immunomodulatory capacity has been described for MSC and CPC (8), this is most likely not strong enough to prevent the host-versus-graft-response triggered by xenogeneity.

As stated earlier, it is necessary to perform preclinical trials using the same cells that are used in the clinical setting, to avoid species-specific effects. In our study, a higher retention rate was observed in MSC injected mice than in CPC injected mice. Since several studies showed a higher cell retention with increasing cell or vehicle size (28,29), it is possible that the larger cell size of MSC contributed to this initial difference (30). Additionally, we did observe host responses, although several other studies suggest the immune privileged nature of stem cells

(10). Apparently, xenotransplantation from human to mouse is not optimal for either CPC or MSC in the currently used mouse models. Therefore, (partly) immune deficient mice (NOD-SCID) were developed, which are now widely used for xenotransplantation studies (17,18,31). Although we did observe a higher cell retention in SCID mice, even here an immune response was triggered by the transplanted human cells. Despite being immunodeficient on many levels, SCID mice do still have functional immune cells patrolling their tissues. Both phagocyte counts and cytokines indicate an innate immune response, although weak, that still forms against the foreign cells. To overcome this problem, another opportunity is provided by the generation of humanized mouse models, which are generated by engraftment of human hematopoietic cells or tissue in severe immune deficient mice (32). Reconstruction of the human immune system provides the opportunity to study human biological processes, including allograft rejection upon cell transplantation and the potential immune modulatory effects of CPC and MSC(33).

With the recognition of the role of the immune system in cardiac disease (34), it is obvious that animal models in immunodeficient mice are unrepresentative. In combination with the knowledge that even SCID-mice can induce a mild immune response after xenotransplantation, we believe a shift towards humanized animals is necessary to obtain proper pre-clinical rodent models for cardiac human cell therapy. Even when using fully humanized pre-clinical animal models, it could be worthwhile to perform HLA-matching before injecting stem cells. Ultimately any feasible approach to reduce cell rejection only a little, can increase the effectiveness of the cardiac cell therapy.

Funding Sources

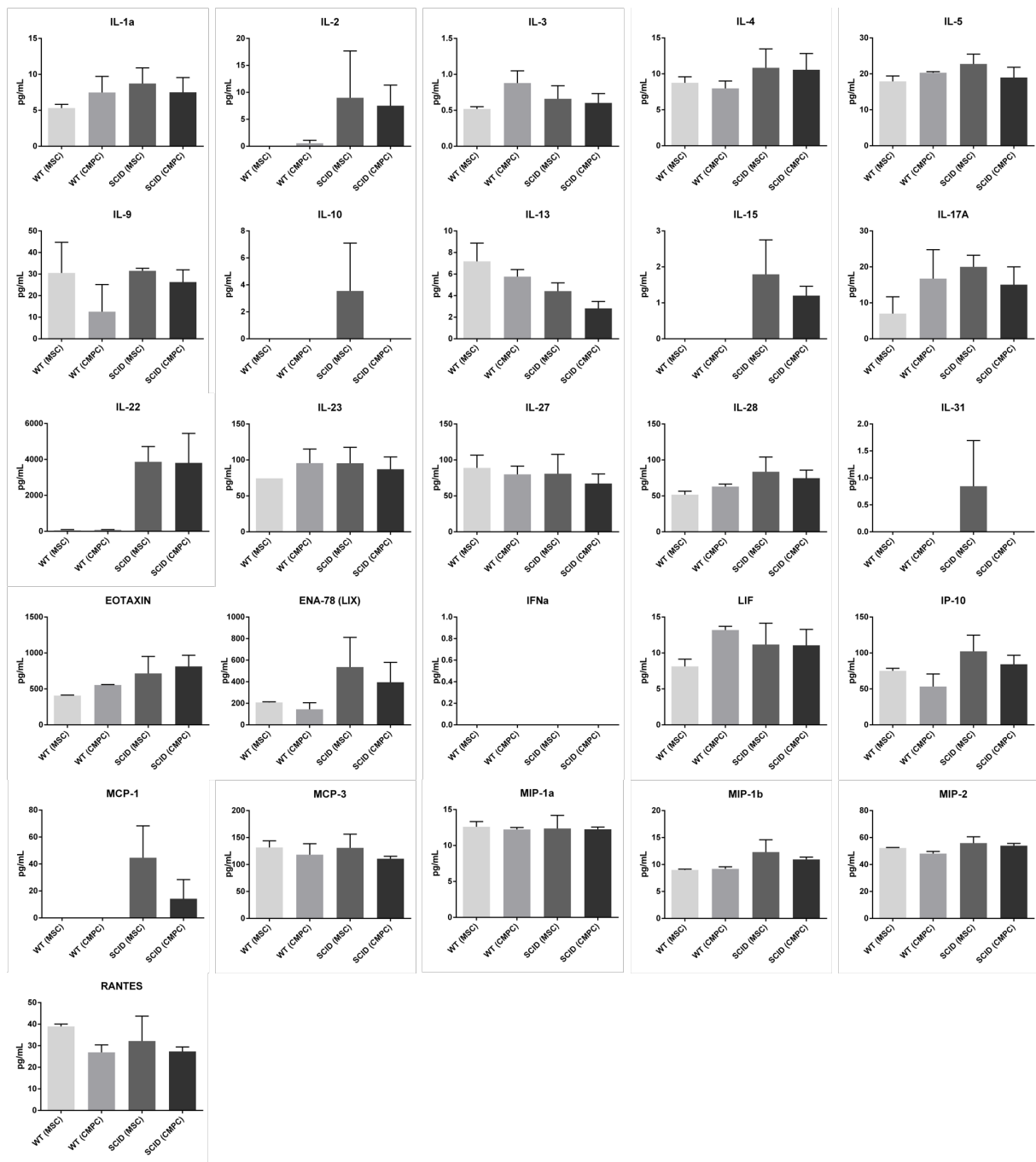
We acknowledge the support from Innovation and the Netherlands CardioVascular Research Initiative (CVON): The Dutch Heart Foundation, Dutch Federation of University Medical Centers, the Netherlands Organization for Health Research and Development and the Royal Netherlands Academy of Science and the Alexandre Suerman program for MD/PhD students of the University Medical Center Utrecht, the Netherlands.

References

1. Robey TE, Saiget MK, Reinecke H, Murry CE. Systems approaches to preventing transplanted cell death in cardiac repair. *J Mol Cell Cardiol* 2008;45:567-81.
2. Dimmeler S, Zeiher AM, Schneider MD. Unchain my heart: the scientific foundations of cardiac repair. *J Clin Invest* 2005;115:572-83.
3. van der Spoel TI, Jansen of Lorkeers SJ, Agostoni P et al. Human relevance of pre-clinical studies in stem cell therapy: systematic review and meta-analysis of large animal models of ischaemic heart disease. *Cardiovasc Res* 2011;91:649-58.
4. Abdel-Latif A, Bolli R, Tleyjeh IM et al. Adult bone marrow-derived cells for cardiac repair: a systematic review and meta-analysis. *Arch Intern Med* 2007;167:989-97.
5. Lecour S, Botker HE, Condorelli G et al. ESC working group cellular biology of the heart: position paper: improving the preclinical assessment of novel cardioprotective therapies. *Cardiovasc Res* 2014;104:399-411.
6. Hackam DG, Redelmeier DA. Translation of research evidence from animals to humans. *Jama* 2006;296:1731-2.
7. Ren G, Su J, Zhang L et al. Species variation in the mechanisms of mesenchymal stem cell-mediated immunosuppression. *Stem Cells* 2009;27:1954-62.
8. van den Akker F, Deddens JC, Doevendans PA, Sluijter JPG. Cardiac stem cell therapy to modulate inflammation upon myocardial infarction. *Biochim Biophys Acta* 2013;1830:2449-2458.
9. Su J, Chen X, Huang Y et al. Phylogenetic distinction of iNOS and IDO function in mesenchymal stem cell-mediated immunosuppression in mammalian species. *Cell Death Differ* 2014;21:388-96.
10. Pittenger MF, Mackay AM, Beck SC et al. Multilineage potential of adult human mesenchymal stem cells. *Science* 1999;284:143-7.
11. Zinocker S, Wang MY, Rolstad B, Vaage JT. Mesenchymal stromal cells fail to alleviate experimental graft-versus-host disease in rats transplanted with major histocompatibility complex-mismatched bone marrow. *Scand J Immunol* 2012;76:464-70.
12. Schnabel LV, Pezzanite LM, Antczak DF, Felipe MJ, Fortier LA. Equine bone marrow-derived mesenchymal stromal cells are heterogeneous in MHC class II expression and capable of inciting an immune response in vitro. *Stem Cell Res Ther* 2014;5:13.
13. Rossignol J, Boyer C, Thinard R et al. Mesenchymal stem cells induce a weak immune response in the rat striatum after allo or xenotransplantation. *J Cell Mol Med* 2009;13:2547-58.
14. Miteva K, Haag M, Peng J et al. Human cardiac-derived adherent proliferating cells reduce murine acute coxsackievirus B3-induced myocarditis. *PLoS ONE* 2011;6.
15. Van Linthout S, Savvatis K, Miteva K et al. Mesenchymal stem cells improve murine acute coxsackievirus B3-induced myocarditis. *Eur Heart J* 2011;32:2168-78.
16. Grauss RW, van Tuyn J, Steendijk P et al. Forced myocardin expression enhances the therapeutic effect of human mesenchymal stem cells after transplantation in ischemic mouse hearts. *Stem Cells* 2008;26:1083-93.
17. Wang J, Najjar A, Zhang S et al. Molecular imaging of mesenchymal stem cell: mechanistic insight into cardiac repair after experimental myocardial infarction. *Circulation Cardiovascular imaging* 2012;5:94-101.
18. Rosova I, Dao M, Capoccia B, Link D, Nolte JA. Hypoxic preconditioning results in increased motility and improved therapeutic potential of human mesenchymal stem cells. *Stem Cells* 2008;26:2173-82.
19. Jansen Of Lorkeers SJ, Hart E, Tang XL et al. Cyclosporin in cell therapy for cardiac regeneration. *Journal of cardiovascular translational research* 2014;7:475-82.
20. Jansen of Lorkeers SJ, Gho JM, Koudstaal S et al. Xenotransplantation of Human Cardiomyocyte Progenitor Cells Does Not Improve Cardiac Function in a Porcine Model of Chronic Ischemic Heart Failure. Results from a Randomized, Blinded, Placebo Controlled Trial. *PLoS One* 2015;10:e0143953.

21. Noort WA, Oerlemans MI, Rozemuller H et al. Human versus porcine mesenchymal stromal cells: phenotype, differentiation potential, immunomodulation and cardiac improvement after transplantation. *J Cell Mol Med* 2011.
22. Smits AM, van Vliet P, Metz CH et al. Human cardiomyocyte progenitor cells differentiate into functional mature cardiomyocytes: an in vitro model for studying human cardiac physiology and pathophysiology. *Nat Protoc* 2009;4:232-43.
23. Noort WA, Kruisselbrink AB, in't Anker PS et al. Mesenchymal stem cells promote engraftment of human umbilical cord blood-derived CD34(+) cells in NOD/SCID mice. *Exp Hematol* 2002;30:870-8.
24. Feyen D, Gaetani R, Liu J et al. Increasing short-term cardiomyocyte progenitor cell (CMPC) survival by necrostatin-1 did not further preserve cardiac function. *Cardiovasc Res* 2013;99:83-91.
25. Stavnezer J, Schrader CE. IgH chain class switch recombination: mechanism and regulation. *J Immunol* 2014;193:5370-8.
26. Madonna R, Van Laake LW, Davidson SM et al. Position Paper of the European Society of Cardiology Working Group Cellular Biology of the Heart: cell-based therapies for myocardial repair and regeneration in ischemic heart disease and heart failure. *Eur Heart J* 2016.
27. Atoui R, Shum-Tim D, Chiu RC. Myocardial regenerative therapy: immunologic basis for the potential "universal donor cells". *Ann Thorac Surg* 2008;86:327-34.
28. van den Akker F, Feyen DA, van den Hoogen P et al. Intramyocardial stem cell injection: go(ne) with the flow. *Eur Heart J* 2016.
29. Ishikawa K. Response to Letter Regarding Article, "Intracoronary Injection of Large Stem Cells: Size Matters". *Circulation Cardiovascular interventions* 2015;8:e002855.
30. Ge J, Guo L, Wang S et al. The size of mesenchymal stem cells is a significant cause of vascular obstructions and stroke. *Stem Cell Rev* 2014;10:295-303.
31. Smits AM, van Laake LW, den Ouden K et al. Human cardiomyocyte progenitor cell transplantation preserves long-term function of the infarcted mouse myocardium. *Cardiovasc Res* 2009;83:527-35.
32. Shultz LD, Ishikawa F, Greiner DL. Humanized mice in translational biomedical research. *Nat Rev Immunol* 2007;7:118-30.
33. Hogenes M, Huibers M, Kroone C, de Weger R. Humanized mouse models in transplantation research. *Transplantation reviews* 2014;28:103-10.
34. Frangogiannis NG. The inflammatory response in myocardial injury, repair, and remodelling. *Nature reviews Cardiology* 2014;11:255-65.

Supplementary



Supplementary Figure 1. Cytokine production by WT and SCID mice after progenitor cell injection.

8

Modeling the human scarred heart *in vitro*: toward new tissue engineered models

J.C. Deddens

H. Sadeghi

J. Hjortnaes

L.W. van Laake

M. Buijsrogge

P.A. Doevendans

A. Khademhosseini

J.P.G. Sluijter

Advanced Healthcare Materials. 2016 Dec 1

Abstract

Cardiac remodeling is critical for effective tissue healing, however, excessive production and deposition of extracellular matrix components contribute to scarring and failing of the heart. Despite the fact that novel therapies have emerged, there are still no lifelong solutions for this problem. An urgent need exists to improve the understanding of adverse cardiac remodeling in order to develop new therapeutic interventions that will prevent, reverse, or regenerate the fibrotic changes in the failing heart. With recent advances in both disease biology and cardiac tissue engineering, the translation of fundamental laboratory research toward the treatment of chronic heart failure patients becomes a more realistic option. Here, the current understanding of cardiac fibrosis and the great potential of tissue engineering are presented. Approaches using hydrogel-based tissue engineered heart constructs are discussed to contemplate key challenges for modeling tissue engineered cardiac fibrosis and to provide a future outlook for preclinical and clinical applications.

Keywords: Cardiac fibrosis, cardiac tissue engineering, cardiac remodeling, hydrogels, extracellular matrix, drug development

1. Introduction

Cardiovascular disease (CVD) is the most important cause of morbidity and mortality worldwide (1). CVD accounts for approximately 30% of all deaths in the United States (2). In patients with CVD, the most common cause of death is coronary heart disease, of which myocardial infarction (MI) is the most prominent (1). Upon cardiac stress (e.g. MI, hypertrophic cardiomyopathy, valvulopathy and hypertension) the heart initially adapts via several phases of cardiac remodeling (3-5), however, prolonged stress can lead to maladaptive and adverse cardiac remodeling. This in turn leads to additional loss of cardiomyocytes (CM), ventricular wall thinning, CM hypertrophy and interstitial fibrosis (5,6). Consequently, the risk of arrhythmias, sudden cardiac death, and heart failure (HF) is increased (3,7). In Europe, 1-2% of the population suffers from HF, which is characterized by clinical symptoms due to a reduced performance of the heart. Patients with HF have a 5-year survival rate of 50% and the overall prevalence of this disease is expected to rise (8-10).

When MI occurs, myocardial tissue is dying and the heart quickly undergoes remodeling to prevent myocardial rupture and compensate for the decrease in cardiac output. Remodeling facilitates dimensional changes and is mainly characterized by an increased turnover of the extracellular matrix (ECM) (3,11). Although scar formation is part of normal tissue repair, an excessive deposition of ECM can lead to cardiac fibrosis, which then results in systolic and/or diastolic dysfunction and HF. Diastolic HF, or HF with preserved ejection fraction, is characterized by an increase in ECM deposition, which leads to mechanical stiffening of the myocardial wall and poor relaxation and filling properties of the left ventricle. In turn this may lead to additional loss of CM, which like other causes of CM death (e.g. MI) may cause systolic dysfunction and HF with reduced ejection fraction (12).

Even though pharmacological and interventional revascularization procedures have improved the acute treatment of MI, the definitive loss of CM and the subsequent fibrotic

remodeling cannot be prevented completely by these therapies. Pharmacological agents, including ACE inhibitors and β -adrenergic receptor blockers, may slow down or even reverse the progression of cardiac pump dysfunction (13-15). Despite the fact that novel therapies, including LCZ696 (16) as examined in the PARADIGM-HF trial, and left ventricular assist devices have emerged, there are still no long term solutions for patients suffering from HF. Therefore, an urgent need exists to improve our understanding of adverse cardiac remodeling and to develop new therapeutic interventions that will prevent, reverse or regenerate the fibrotic changes in the failing heart (17-19).

Arguably, relying on standard tissue culture and animal models, which are unable to recapitulate the physiological environment of the human heart, is insufficient for a complete understanding of heart failure. Instead, well-defined advanced models are needed to improve understanding and generate novel insights, which most likely will originate from the field of tissue engineering.

Tissue engineered constructs can provide a tissue model able to simulate the human cellular 3-dimensional (3D) micro-environment as a result of their capacity to facilitate incorporation of native ECM proteins, different cell types and required signaling molecules (20-26). In cardiac physiology, ECM serves not only as a scaffold for structural support, but also plays a critical role in electrical, chemical and mechanical cellular interaction (27). Therefore, in order to mimic the natural ECM of cardiac tissue, micro-engineered scaffolds should provide an environment for both cellular attachment and cellular interactions.

Currently, engineered cardiac tissue constructs are being used with the goal of restoring and improving cardiac function in terms of tissue regeneration (28). However, tissue engineering strategies could also be used to develop 3D *in vitro* models able to mimic the native heart muscle (29). To this end, a range of innovative *in vitro* 3D-culture systems for cardiac disease modeling have been developed, including cardiomyopathy (30-33), and have been utilized for drug testing and pharmacology studies (34-36).

With recent advances in both disease biology and cardiac tissue engineering, the translation of fundamental laboratory research towards the treatment of chronic HF patients becomes a more realistic option. In this overview, we will describe our current understanding of cardiac fibrosis with important molecular and cellular constituents of normal and fibrotic human hearts. Approaches that use hydrogel-based tissue engineered heart constructs will be reviewed to contemplate key challenges for modeling tissue engineered cardiac fibrosis and to provide a future outlook for its (pre-)clinical applications.

2. Cardiac fibrosis

2.1 Myocardial tissue

Non-cardiomyocytes in the heart

The adult human heart consists of several cell types including ventricular and atrial CM, cardiac fibroblasts (CF), different immune cells, and vascular cells that include both endothelial cells (EC) and smooth muscle cells (SMC) (**Figure 1**). Although CM are crucial for the pump function of the heart muscle, other cells are equally important for cardiac homeostasis.

Among the non-CM, CF are the most abundant cell type in the adult human heart (~70% of total cells). CF are primarily responsible for the continuous production, deposition and maintenance of the myocardial ECM (37,38) and continuously communicate with CM through various mechanisms. CM-CF interactions are mediated by direct cell-cell contact, cell-ECM and paracrine signaling (39). Consequently, CF play an important role in direct electro-mechanical transduction in heart tissue and in paracrine hormone signaling to ensure cellular transitions such as CM hypertrophy and proliferation (40-43). Interestingly, CF also express receptors such as toll-like receptor 4 that play a role in the inflammatory response after myocardial injury. Stimulation of these receptors induces various signaling pathways, which activate the expression of pro-inflammatory cytokines (44).

As in most tissues, inflammatory cells are important for immune surveillance. Macrophages, dendritic cells, mast cells and small numbers of lymphocytes reside in native cardiac tissue (45).

They are activated upon myocardial injury and initiate an inflammatory cascade of events, which leads to the recruitment of predominantly neutrophils that play a critical role in cardiac repair processes (45).

EC play a key role in cardiac physiology and development (46). Apart from their role in the exchange of nutrients and oxygen between blood and myocardial cells, EC contribute to CM survival and organization (47-49). In addition, different types of communication (e.g. autocrine-paracrine coupling, growth factor signaling) between CM and EC have been identified to play a role in CM growth, repair and contraction (39,50,51). For example, nitric oxide is one of the paracrine factors produced by cardiac EC and causes vasodilatation of the myocardial blood vessels, but can also change CM contractile properties (52).

Cardiac extracellular matrix

In addition to the cellular components of myocardial tissue, the ECM plays a major role in normal cardiac functioning and homeostasis. The cardiac ECM is a complex network of structural and non-structural (matricellular) proteins, which is balanced by ECM degrading enzymes (matrix metalloproteinases (MMP)) and their inhibitors (tissue inhibitors of MMP (TIMP)). The ECM is tethered to CM and other myocardium residing cells in a functional and organized manner. The structural components of the ECM are important in maintaining cardiac architecture and LV function, whereas nonstructural proteins are important for the regulation of cell-ECM interaction and ECM turnover after cardiac injury (53,54). The main structural proteins include collagen (type I and III), fibronectin and elastin (53). Non-structural ECM is comprised of proteins such as osteopontin, thrombospondin, periostin and CCN family proteins (e.g. connective tissue growth factor (CTGF)). Interestingly, glycosaminoglycans and proteoglycans can serve as both structural and non-structural proteins (55). Commonly, non-structural proteins are inactive or are expressed at very low levels in healthy myocardium, but their expression is highly induced in response to injury (56). Simultaneously, MMPs are up-regulated to contribute to post-injury remodeling by degrading ECM, activating receptors and

releasing growth factors from the ECM (53,57). However, to maintain a well-balanced ECM metabolism and cardiac remodeling, the activity of MMPs are well controlled by TIMPs (57). The dynamic ECM also has biochemical and mechanobiological functions by serving as a depot for growth factors (e.g. fibroblast growth factor (FGF), transforming growth factor- β (TGF- β) and CTGF), and as a mediator for cell-cell, cell-ECM and ECM-ECM interaction (58,59).

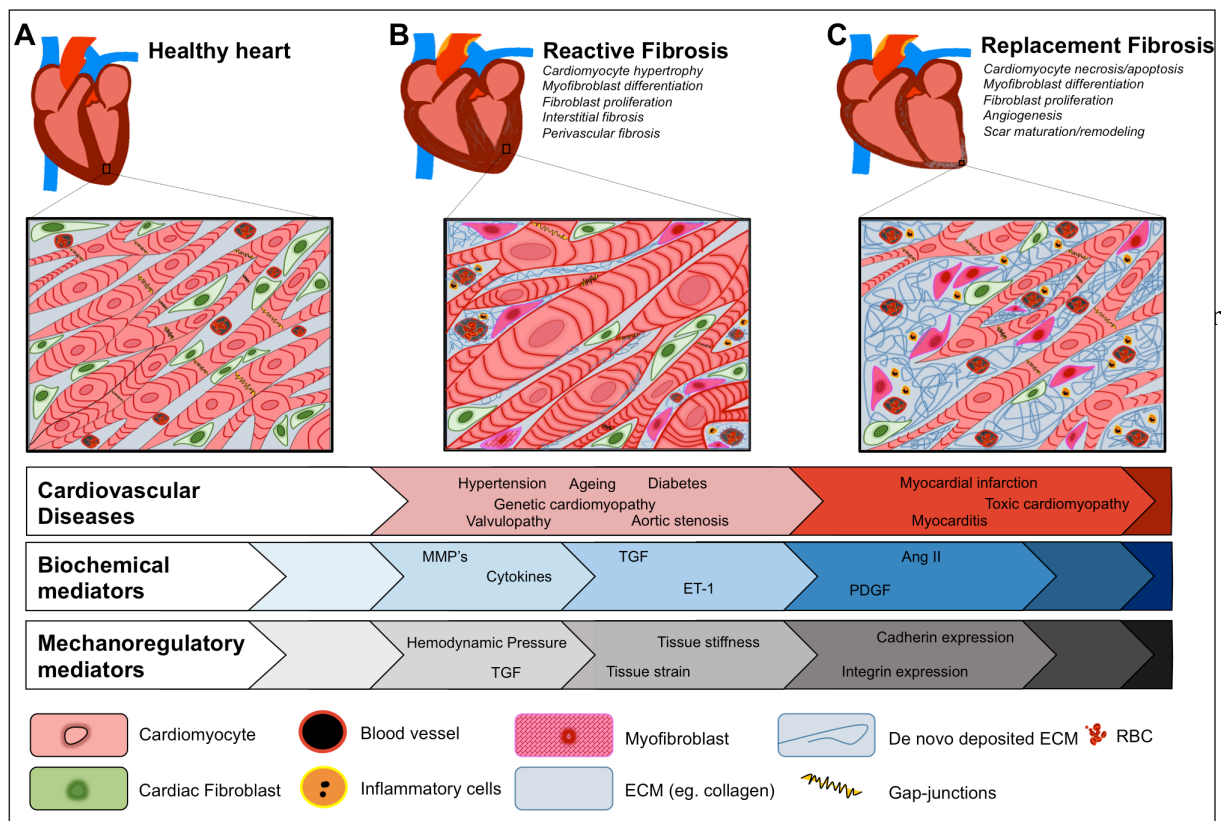


Figure 1. Schematic illustration representing myocardial tissue in healthy heart, reactive fibrosis and replacement fibrosis. (A) The healthy human heart is cone-shaped and pumps blood out efficiently in order to supply all the organs in the human body with oxygen and nutrients. Healthy myocardial tissue consists of different types of cells such as cardiac fibroblasts (CF), cardiomyocytes (CM) and endothelial cells (EC), which are embedded in a dynamic cardiac extracellular matrix (ECM). Cardiac cells are able to communicate through cell-cell and cell-ECM interactions in order to maintain physiological conditions. **(B)** In pressure overload, the heart goes through adverse remodeling, which is characterized by CM hypertrophy as well as reactive fibrosis, which is characterized by the differentiation of CF into myofibroblasts (MyoF). In addition, reactive fibrosis can take place as a consequence of volume overload (eg. aortic regurgitation), non-ischemic cardiomyopathies (eg. dilated, hypertrophic, diabetic) and ageing. Specific features of reactive fibrosis are perivascular and interstitial ECM deposition. With time, reactive fibrosis can progress into replacement fibrosis. **(C)** After myocardial infarction, dilation of the left ventricle (LV) is common, but may be self-limiting. However, dilatation may also progress and lead to deterioration in LV function and eventually to heart failure with reduced ejection fraction. In the infarcted areas of the myocardial tissue there is replacement fibrosis due to CM death, which is characterized by an increase in ECM stiffness and a large number of MyoF.

Cell-ECM and cell-cell interactions

Matrix proteins provide strength and elasticity to cardiac tissue and facilitate both electrical and mechanical signaling. Mechanical signaling between cells and their microenvironment, called mechano-sensing, is mainly facilitated by cadherins and integrins and allows cells to sense their mechanical environment and respond accordingly via mechano-transduction. Comparably, electrical transduction occurs through cell-cell adhesions termed connexins (gap junction proteins) (64,65). A disarrangement of these proteins consequently leads to changes in electrical conductance (66). Cadherins, a group of calcium-dependent transmembrane proteins, play a role in direct cell-cell mechano-coupling and mediate intracellular biochemical responses and consequently behavior between cells and their cytoskeletons (64). Integrins, a class of transmembrane ECM receptors, mediate cell-ECM mechano-coupling and can indirectly influence cell-cell interaction (67-69) and cellular response such as migration, proliferation, differentiation, tissue repair, and regeneration (67,70).

The ECM is highly dynamic and changes in the composition of the ECM are necessary for cardiac physiology and function. In addition, many cell types that reside within the heart are interacting to retain function within a physiological range (27). Consequently, it is important to take these physiological features into account in the engineering of a functional human myocardium (**Figure 1**). Moreover, it is essential to characterize important cellular (e.g. CF, CM) and non-cellular (e.g. collagen I/III, cadherins, intergrins) components in the engineered models to establish the re-creation of a native-like heart tissue

2.2 Post-MI inflammatory response

Cardiac tissue repair aims at repairing the injured myocardium and at returning the heart function to a physiological state. In general, wound healing is triggered by myocardial injury, which can be caused by an acute event (such as MI) or can be chronic as a consequence of chronic cardiac disease (such as hypertrophic cardiomyopathy, valvulopathy and hypertension). Both acute and chronic conditions lead to an inflammatory and pro-fibrotic state

of the myocardium (71), which is characterized by an increase in inflammatory cytokines (e.g. Interleukin (IL)-1 β , IL-6, and tumor necrosis factor (TNF)- α), chemokines and growth factors such as TGF- β 1 and FGF. Many resident cardiac cells (e.g. CF, CM, EC, and SMC) are responsible for the release of these pro-inflammatory mediators (72) upon stress and additionally express and release damage-associated proteins and lipids (71). As a result, the complement system is activated and inflammatory cells, predominantly macrophages and neutrophils, are attracted to the site of injury and contribute to wound healing by cleaning the site of injury (73,74). In addition, as an adaptive response after pathological stress, there is an inflammatory cell and CF mediated release of cytokines and chemokines that promote further ECM remodeling (75).

IL-1 β , IL-6 and TNF- α are mainly thought to contribute to the increase of MMP synthesis in CFs while inhibiting the expression of MMP inhibitors (TIMPs) (76). Consequently, during the early phase (inflammatory phase) of wound healing, inflammatory cells and CF release MMPs that lead to increased ECM degradation (77), which facilitate the migration of CF and allow for revascularization of the injured area. After the acute inflammatory phase, which is called the proliferative phase, a granulation tissue is formed by the clearance of dead cell debris, up-regulated MMPs, and an increase in activated CF (MyoF) and release of pro-angiogenic growth factors such as VEGF (75). Furthermore, MyoF synthesize ECM components and revascularization of the infarcted tissue is enhanced by VEGF (78). Scar formation occurs in the last phase of the wound healing process and is predominantly carried out by MyoF, which contribute to scar contraction and maturation (75).

2.3 Cardiac Fibroblasts

Cardiac fibrosis is defined by an increase in the collagen volume fraction of the myocardium (79) and is primarily mediated by activated CF. Although cardiac remodeling is critical for effective tissue healing, excessive production and deposition of ECM components contribute to adverse cardiac remodeling and cardiac fibrosis (80,81). Cardiac fibrosis can be subdivided in 2 types: reactive fibrosis and replacement fibrosis (**Figure 1A-C**). Reactive fibrosis reflects diffuse

fibrogenic changes due to interstitial and perivascular ECM deposition (82), whereas replacement fibrosis ensues when there is a local replacement of dead CM with ECM (mainly collagen). Reactive fibrosis commonly affects patients with hypertension, diabetic cardiomyopathy, chronic valve stenosis/regurgitation, and dilated/hypertrophic cardiomyopathy (83-89). It is progressive and can eventually lead to irreversible replacement fibrosis due to CM necrosis or apoptosis (90). Likewise, MI and toxic cardiomyopathy lead to CM loss and replacement fibrosis at the site of injury (91). Additional reactive fibrosis develops due to the deposition of collagen in the interstitial regions of the remote non-infarcted myocardium (92). Over time, both replacement and interstitial fibrosis contribute to ventricular wall stiffening and cardiac dysfunction.

Differentiation of CF

Physiologic wound healing necessitates a balanced ECM remodeling, since excessive MMP activation will lead to cardiac dilatation, while sustained or excessive ECM deposition can result in fibrosis. Fundamental for cardiac fibrosis and fibrotic remodeling is the excessive proliferation and differentiation of CF into MyoF (75,93,94). MyoF are characterized by the expression of contractile proteins such as α -smooth muscle actin (α -SMA) (93), by which they enforce scar remodeling due to mechanical linkage to the ECM-microenvironment through specialized intracellular structures (termed focal adhesions) (95). The source of MyoF not only include CF, since other cell sources have been indicated, including pericyte-like progenitor cells, bone marrow-derived circulating cells (fibrocytes), endothelial-to-mesenchymal transition (EndoMT), and epithelial mesenchymal transition (EMT) (42,53,96-98). The transformations of these cells into MyoF are thought to be mediated by pro-fibrotic cytokines, peptides and growth factors that are released by CF, CM, and inflammatory cells after myocardial injury (73-75,78,99-102). MyoF remodel the cardiac matrix and produce excessive amounts of ECM through multiple biochemical pathways of which TGF- β 1, Angiotensin II (Ang II), endothelin-1 (ET1) and platelet-derived growth factor (PDGF) are the most potent stimulators (80).

Interestingly, MyoF-secreted ECM proteins such as fibronectin, non-fibrillar collagen type VI, and thrombospondin-1 (TSP-1) also contribute to MyoF differentiation, thereby serving as a positive-feedback loop (76,103). In normal wound healing, MyoF disappear by apoptosis after the completion of scar maturation. However, in cardiac fibrosis, cardiac MyoF are promoted to persist by synergistic effects of Ang II, ET1, PDGF and TGF- β (104). Mechanical alterations in the tissue, including increased ECM stiffness and persistent hemodynamic stress, can lead to failure of MyoF apoptosis resulting in excessive ECM production and progression of fibrotic remodeling (94,105) (**Figure 2A-C**).

TGF- β 1 is one of the best-characterized pro-fibrotic growth factors and plays an important role in differentiation and proliferation of CF into MyoF (81,106). Under normal conditions, TGF- β 1 is released in an inactive form by various cells and can be proteolytically activated through integrin-mediated transduction of ECM contraction (107,108). In addition, a wide range of mediators including MMP-2, MMP-9, and TSP-1 can activate TGF- β 1. TGF- β 1 signals by binding to transmembrane receptor complexes of type I and type II serine/threonine kinases, of which several forms exist (109). TGF- β 1 predominantly signals via the activin linked kinase 5 (ALK5), a TGF- β 1 receptor type I receptor. Receptor activation results in the phosphorylation of Smad2/Smad3/Smad4, after which Smad4 translocate to the nucleus and activates fibrogenic gene expression, such as collagen, α -SMA and TIMPs (80). In addition, TGF- β 1 suppresses gene expression of MMPs (104,110,111).

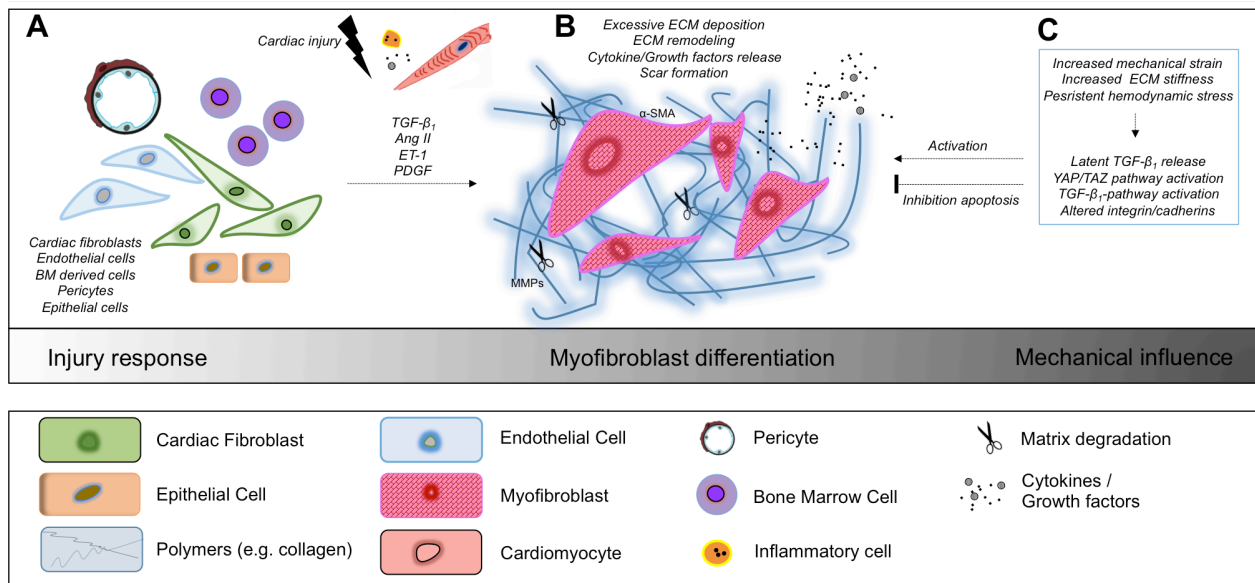


Figure 2. Myofibroblast differentiation and the influence of mechanical alterations on the fibrotic response.

(A) Upon cardiac injury, several cell sources, e.g. cardiac fibroblasts (CF) and pericytes, differentiate into MyoF. MyoF differentiation is primarily mediated by the pro-fibrotic growth factor $TGF-\beta_1$, Angiotension II (Ang II), Endothelin-1 (ET-1) and platelet derived growth factor (PDGF), which are released by CF, cardiomyocytes (CM) and inflammatory cells. (B) MyoF (α -SMA⁺) produce excessive amounts of extracellular matrix (ECM), increase their release of cytokines and growth factors and remodel the cardiac matrix to facilitate wound healing. In normal wound healing, MyoF disappear by apoptosis after the completion of scar formation. (C) However, the mechanical characteristics of the fibrotic tissue (increased mechanical strain, increased ECM stiffness and hemodynamic stress) result in perpetuation of pro-fibrotic signaling by activation of mechano-sensitive pathways and contribute to the persistence of MyoF activity, which mediate cardiac fibrosis.

Ang II is a mediator of the Renin-Angiotensin-System (RAAS) and RAAS activation results in vasoconstriction and an increased blood pressure. In addition, Ang II serves as a TGF- β 1 inducing factor and, by binding the angiotensin type 1 receptor, stimulates differentiation of CF into MyoF (112). Likewise, it has been demonstrated that ET-1 contributes to the development of cardiac fibrosis by inducing collagen type I synthesis through the interaction with endothelin-A receptors on CF. Similar to TGF- β 1, ET-1 can be produced by many different cells, including macrophages, CM and CF (113,114). Finally, PDGF causes elevation of TGF- β 1 synthesis and induces CF differentiation into MyoF (115-117). The biochemical actions of TGF- β 1, Ang II, endothelin-1 ET1 and PDGF facilitate CF differentiation and contribute to the progression of cardiac fibrosis.

Mechanosensing of CF

Myocardial cells reside in a highly dynamic environment and are exposed to continuous cyclic changes of mechanical stress, caused by rhythmic pressure/volume changes in the heart. On a micro-level, mechanical cues in myocardial tissue include mechanical strain and matrix stiffness, which play an important role in MyoF differentiation (70) During early fibrotic remodeling an increased mechanical strain inside myocardial tissue is observed, which is partly attributable to the increased synthesis and activity of MMPs after the inflammatory phase of remodeling (77). The breakdown of ECM results in a decreased density of ECM fibers and as a consequence, the local mechanical strain is elevated.

Another mechanical cue for increased mechanical stress during fibrotic remodeling is, on the contrary, the accumulation of ECM proteins. The resulting increased ECM stiffness contributes to MyoF differentiation of CF via direct and indirect mechanisms (118-120). Similar to CF, mechanical signaling between MyoF and between MyoF and the ECM is directly mediated through cadherins and integrins, respectively. Integrins sense increased ECM stiffness and ECM-induced strain and stimulate cellular growth, ECM synthesis and MyoF differentiation, and CF differentiation into MyoF. An altered expression of several integrin isoforms (eg. α 2 β 1, α 8 β 1,

and $\beta 1$) is observed in fibrotic cardiac tissue (70,121-123). Likewise, a shift in the expression of different types of cadherins has been observed after CF differentiation into MyoF (70,124,125). This demonstrates the importance of both cadherin and integrins in the pathophysiological and mechano-sensitive processes that play a role in cardiac fibrosis. In addition, an indirect mechano-sensitive pathway of MyoF differentiation can be induced by the liberation of ECM-stored TGF- $\beta 1$ as a result of MyoF contraction (increased cellular tension) and ECM stiffness in the tissue (108,126,127).

Altogether, mechanical signals need to be transmitted to the nucleus of effector cells to enable transcription of pro-fibrotic target genes. Several downstream signaling pathways including TGF- β , Focal Adhesion Kinase, and β -catenin have been associated with MyoF activation and fibrosis (128). In addition, recent studies on fibrotic tissue remodeling in other tissues have shown that a different signaling pathway called yes associated protein (YAP)/transcriptional co-activator with PDZ-binding motif (TAZ) is linked to the activation of MyoF by mechano-transduction (129-131). However, it not completely clear whether YAP/TAZ plays a role in the differentiation of cardiac MyoF.

It is evident that in response to injury, the heart undergoes a defective and excessive tissue repair process that plays a major role in the development of cardiac fibrosis. In addition, several biochemical and mechano-sensitive pathways play key roles in the activation of MyoF and the progression of fibrotic tissue remodeling. Consequently, these biological signaling molecules, in addition to the mechanical cues, should be integrated in engineered *in vitro* models that mimic native-like myocardium and myocardial fibrosis. Furthermore, it is important to confirm the effect of these cues and to characterize the behavior of CF and MyoF in these model systems. As a result, these models could have the potential of revealing mechanisms and signaling pathways that can be used as targets for novel therapies for cardiac remodeling. (see **Table 1** for a detailed overview).

Table 1. The expression of cardiac tissue components in healthy and fibrotic cardiac tissue.

Tissue Component	Main function	Healthy heart	Fibrotic heart	Effect	Ref.
<i>Extracellular Matrix</i>					
Collagen I (fibrillar)	Structure Tensile strength ECM organization Cell signaling Force transmission	Normal expression >70% of total ECM)	↑ Expression and deposition ↑ Collagen cross-linking ↑ CF proliferation Prolonged upregulation Main constituent of scar Deposition during intermediate/late remodeling	↑ Wound healing ↑ Stiffness and scarring ↑ Arrhythmogenicity ↑ MyoF differentiation ↑ Systolic and diastolic dysfunction ↑ Collagen I/III ratio ↓ Tissue compliance	54, 76, 184
Collagen III (fibrillar)	Elasticity Structure Strength ECM organization	Normal expression (10-15% of total ECM)	↑ Expression and deposition ↑ CF proliferation ↑ CF migration After collagen I, the main constituent of scar Deposition during early remodeling	↑ Wound healing ↑ Stiffness and scarring ↑ Arrhythmogenicity ↑ MyoF differentiation ↑ Systolic and diastolic dysfunction ↓ Tissue compliance	54, 76, 184
CollagenIV/VI (non-fibrillar)	Basement membrane ECM ECM organization	Normal expression	↑ Expression ↑ Deposition	↑ MyoF differentiation (type VI) ↓ CF Migration (IV+ VI)	54, 76, 152, 184
Fibronectin/Laminin	Basement membrane ECM Organization Structure	Normal expression	↑ Expression ↑ Deposition ↑ Expression of Fibronectin ED-A isoforms	↑ Stiffness ↑ MyoF differentiation ↑ CF proliferation ↑ CF migration ↑ Systolic and diastolic dysfunction ↓ Tissue compliance	54, 76, 184, 185
MMPs	ECM remodeling ECM degradation	Latent (pro-MMP) storage in ECM	<i>Early remodeling:</i> ↑ Activation ↑ Expression in cells <i>Late remodeling:</i> ↓ Activation	↑ CF migration ↑ Angiogenesis ↑ Inflammatory cell influx ↑ Granulation tissue ↑ ECM remodeling ↑ Release of growth factors (eg. TGF)	54, 76, 184, 185
TIMPs	MMP inhibition Cell specific activities	MMP regulation	Inhibition of MMPs	↑ CF proliferation ↑ MyoF differentiation ↑ Collagen deposition ↑ CM hypertrophy	54, 76, 184, 185
Stiffness	CM/CF phenotype and morphology CM/CF functioning Heart compliance Systolic and diastolic function	~10 kPa	~ >35 kPa	↑ Stiffness ↑ MyoF differentiation ↑ CF proliferation ↑ CF migration ↑ Systolic and diastolic dysfunction ↑ Arrhythmogenicity ↓ Tissue compliance ↓ CM beating ↓ CM striation	118, 119, 203, 205, 207, 208
<i>Cells</i>					
Cardiac Fibroblast	ECM synthesis ECM deposition ECM degradation CM phenotype regulation	ECM maintenance N-cadherin expression	↑ Proliferation, ↑ MyoF differentiation ↑ Migration ↑ ECM synthesis and deposition ↑ OB-cadherin expression ↑ Angiotensin II receptor (ATR1) expression	↑ Collagen I synthesis ↑ Stiffness and scarring ↑ Arrhythmogenicity ↑ Systolic and diastolic dysfunction ↑ Interstitial and/or replacement fibrosis	70, 83- 89, 118, 185
Myofibroblast	ECM synthesis ECM deposition ECM contraction Scar maturation	Rarely present	↑ Accumulation ↑ ECM synthesis and deposition ↑ α-SMA expression ↑ Ang I, ACE and ATR1 expression	↑ Collagen I synthesis ↑ Stiffness and scarring ↑ Arrhythmogenicity ↑ Systolic and diastolic dysfunction ↑ Interstitial and/or	70, 76, 83-89, 95, 103

			↑ TGF-β1 expression ↓ Apoptosis	replacement fibrosis ↑ Contraction of scar area	
Cardiomyocyte	- Cardiac contraction	Regular and synchronous beating	↑ Atrophy/hypertrophy ↑ Necrosis/apoptosis ↑ Pro-fibrotic mediators (secreted) ↑ Displacement/slippage of CM layers ↑ CM-MyoF interactions ↑ Mitochondrial dysfunction	↑ Oxidative stress ↑ Inflammatory cell influx ↑ MyoF differentiation ↑ Ventricular dilatation ↑ Arrhythmogenicity ↑ Adverse remodeling	30, 70, 76, 167
Biochemical mediators					
TGF-β	Multifunctional: eg. embryonic development, cell growth, and apoptosis	Expression of latent form stored in ECM Expressed by many cell types (eg. CF, CM)	↑ Expression by multiple cells (eg CF, macrophages) ↑ Activation of latent TGF-β ↑ TIMP expression ↑ CM hypertrophy ↑ CTGF expression ↓ MMP expression	↑ MyoF differentiation ↑ ECM deposition ↑ Ventricular Fibrosis ↑ Ventricular hypertrophy ↓ Inflammation	104, 108, 110
Angiotensin II	Vasoconstriction Blood pressure regulation Aldosterone synthesis Na ⁺ tubular reabsorption	Controlled by RAAS.	↑ Expression/enzymatic conversion ↑ TGF-β1 expression and excretion ↑ CM hypertrophy ↑ CF migration ↑ ATR1 expression ↑ ROS production ↑ TIMP expression ↑ CTGF expression ↑ PDGF-A expression	↑ Ventricular hypertrophy ↑ MyoF differentiation ↑ Systolic and diastolic dysfunction ↑ ECM synthesis and deposition ↑ Ventricular fibrosis ↓ Inflammation	94, 104, 184
Glucose	Energy metabolism	Normal blood levels Well regulated ATP production Normal ATPase functioning in cells (eg. CM)	↑ Blood levels ↑ Collagen I/III/IV expression ↑ Collagen crosslinking ↑ Advanced glycosylation endproducts ↑ CM hypertrophy ↑ ATR1 expression ↓ Collagen elasticity ↑ ROS production ↑ Mitochondrial dysfunction (↓ ATP) ↓ ATPase activity	↑ Ventricular hypertrophy ↑ Ventricular fibrosis ↑ Small vessel disease ↑ ECM synthesis and deposition ↑ Diastolic dysfunction (progressing to systolic dysfunction) ↑ Interstitial fibrosis	83
ET-1	Vasoconstriction	Controlled secretion by EC.	↑ EndoMT ↑ Expression ↑ MMP activation ↑ CF proliferation ↑ CTGF expression	↑ Ventricular fibrosis ↑ ECM synthesis and deposition ↑ Ventricular fibrosis ↑ MyoF differentiation	76, 83, 104, 184
CTGF/CCN2	Multifunctional; e.g. angiogenesis, cell adhesion, cell-ECM signaling	Controlled and low level expression by many cells (eg. CM, EC).	↑ Expression (by eg. CM, MyoF) ↑ CM hypertrophy ↑ Collagen I/III expression ↑ α-SMA expression ↑ Pro-fibrotic signaling through other pathways ↑ CF proliferation	↑ MyoF differentiation ↑ ECM synthesis and deposition ↑ Ventricular fibrosis ↑ Diastolic and systolic dysfunction ↑ Ventricular hypertrophy ↑ Arrhythmogenicity	36, 104
PDGF	Mitogenic functions for mesenchymal cells Important wound healing mediator	Normal expression by many cells (e.g. CF, SMC, platelets) and controlled by various external stimuli	↑ Expression during wound healing ↑ Granulation tissue formation ↑ CF proliferation ↑ CF migration ↑ Proliferation and migration of macrophages and SMC.	↑ MyoF differentiation ↑ MyoF contraction ↑ MyoF proliferation ↑ Ventricular fibrosis ↑ Ventricular hypertrophy ↑ Cardiac dilatation	104, 115, 184

3. Engineering cardiac tissue and cardiac fibrosis

3.1 Cardiac tissue engineering

Although conventional monolayer (2D) cell culture methods and animal models have provided valuable insights into cardiac tissue physiology, they do not adequately represent the human *in vivo* (3D) myocardial tissue. Conventional cell culture strategies are associated with major differences in structural and functional properties compared to native myocardium. These differences are mostly characterized by 1) the lack of native-like biochemical, electrophysiological, and mechanical cell-ECM and cell-cell interactions, 2) the differences in dynamic *in vivo* like conditions such as fluid flow and shear stress, and 3) variations in molecular expression profiles (lack of adult gene expression), cell morphology (low degree of bi-nucleation, flattened phenotype), and structural micro-architecture (lack of anisotropic sarcomere organization) (34,132-134). To date, animal models are the gold standard for pre-clinical pharmacological testing since they are more complex and arguably better at simulating multifactorial diseases. However, essential physiological differences between humans and animals exist and animal models often fail to adequately recapitulate human (cardiac) physiology (135,136). Therefore, more well-controlled *in vivo*-like cardiac tissue constructs could be of high value in the *in vitro* modeling of cardiac disease, safety pharmacology, drug discovery and patient specific clinical applications (30-32,34-36).

Currently, the development of bio-mimetic systems is evolving in order to understand normal cardiac processes and to develop regenerative medicine applications to restore, maintain or improve cardiac function (132). Furthermore, such *in vitro* models of cardiac tissue could be used to assess cardiovascular drug toxicity in the development of drugs for other diseases. This is of high relevance in the context of cardiac fibrosis, since several classes of drugs (e.g. cytostatics) have shown to induce toxic cardiomyopathy and subsequent cardiac fibrosis and HF (137).

Although tissue engineered human *in vitro* models of heart tissue are appealing to mimic human heart function, several challenges exist, including the identification of 1) a suitable

scaffold providing an environment for cell adhesion, maturation, and interaction, 2) a good mixture of CM and non-myocytes that resemble cellular components of myocardial tissue *in vitro*, and 3) appropriate culture and model conditions providing micro-environmental control and variability, including biochemical, mechanical, and electrophysiological cues.

3.2 Scaffolds for cardiac tissue engineering

Biomedical engineers have applied micro-fabrication techniques to make 3D heart tissue constructs by using biomaterial-based scaffolds that provide a 3D micro-environment for cells to attach and form a tissue. 3D constructs can either be made from synthetic or natural biomaterials, including decellularized cardiac ECM (138-140). Important criteria of these biomaterials include 1) cost efficiency, 2) high accessibility, and 3) ability to mimic natural cardiac ECM in terms of cell biocompatibility, mechanical properties, matrix porosity, and matrix degradability. Cellular biocompatibility is critical for cellular attachment, spreading, alignment, and proliferation, whereas the mechanical properties are important for structural support and transduction of mechanical signals (141). Mechanical stability is essential to withstand continuous pressure and stretch, which is exerted by the beating CM and modulatory CF. Furthermore, matrix porosity is necessary for the exchange of small molecules (eg. oxygen, metabolites) as well as the migration of cells inside the scaffold (141).

Engineered scaffolds should encourage electrical coupling and electrical conductance to allow for synchronized beating of CM. Additionally, the used biomaterial should be biodegradable, since degradation of the scaffold together with the renewal of ECM could contribute to a more biomimetic micro-environment.

In conclusion, the ideal scaffold is capable of interacting with cells through molecular, cellular, mechanical, and electrical mechanisms, is easy accessible and can be fabricated on a large scale with acceptable costs. Furthermore, for (pre-)clinical applications it is important that the fabrication processes can be automatized, ideally be suitable for higher throughput *in vitro* testing, and compatible with 'good manufacturing practice' (GMP).

Hydrogel-based tissue engineering has been employed as a promising technique in cardiac tissue engineering and are constructed from hydrophobic structures, constituted of either synthetic or natural polymers, that have the ability to swell after absorption of substantial amounts of water (26,142). This property together with some other essential characteristics make these biomaterials suitable as a scaffold, which allows them to serve as a 3D template for cell attachment and cell growth (143,144).

3.3 Hydrogel properties

As a scaffold serving biomaterial, hydrogels possess a high amount of essential scaffold requirements. They can provide for an adequate exchange of oxygen, nutrients and metabolites due to their porosity and water-like appearance (145). Interestingly, it is possible to incorporate growth factors and other molecules to mediate cross talk between cells (146,147). In order to induce the orientation and alignment of cells inside a tissue engineered construct, mechanical strain and structural stability are needed. Hydrogels can provide structural and mechanical stability for encapsulated cells and have shown to be capable of transducing mechanical strain to cells (141,148-150). Moreover, they possess intrinsic mechanical strain that can be sensed by cells through their integrins and triggers subsequent changes in cellular behavior (e.g. adhesion, contractility, motility, and spreading) (151). A large number of studies have demonstrated that electrical stimulation of engineered heart constructs results in better cell-cell connections (via connexins), better tissue alignment, and synchronized contractions (152-156). Therefore, a useful property of hydrogels is their ability to allow for electro-coupling of cells, probably mediated via their porosity. Interestingly, these biomaterials can also be modified to conduct electrical activity themselves after incorporation of nanostructures, such as gold and carbon nanotubes (156,157). In addition, the ability to tune mechano-physical features of hydrogels, including dynamic stiffening material, contributes to the modulation of mechanical properties to values that resemble native cardiac matrix (158) (159), which makes it easier to control cellular behavior in terms of proliferation and differentiation.

Naturally occurring proteins of the ECM, such as collagen and hyaluronic acid, are suitable materials to be used as a hydrogel-based scaffold in cardiac tissue engineering due to their bio-mimicking and bioactive properties (160-163). These properties enable the cells to communicate with the ECM through surface-receptor signaling, resulting in mechanical and chemical interactions as in native heart tissue. In contrast to synthetic polymers, natural hydrogels are hard to customize with respect to chemical and mechanophysical properties and are also less-well defined due to the variable nature of the product. However, synthetic polymers are limited in their functional interactions with cells, although successes have been made when polymers are patterned with structures that contain proteins (e.g. fibronectin) or RGD peptides. The latter is a tri-amino acid (arginine, glycine, L-aspartic acid) sequence that serves as an integrin-binding domain, and is present in various ECM proteins such as collagen and fibronectin (161,164). An alternative approach is to use hybrid hydrogels consisting of a mixture of natural or/and synthetic hydrogels. The mixture combines the advantages of both and therefore creates bio-mimicking hydrogels with tunable physical and chemical properties.

3.4 Hydrogel-based scaffolds in cardiac tissue engineering

Hydrogel-based scaffolds have been utilized for engineering cardiac tissue constructs due to their ability to mimic both the ECM and induce 3D tissue assembly (165). Some of the frequently used hydrogels from natural sources include collagen (148), Matrigel (155,165,166), fibrin (167), gelatin (134,157), hyaluronic acid (168,169), and alginate (170). An example of a widely used synthetic biomaterial for cardiac tissue engineering is poly-ethylene glycol (PEG) (171,172). In the next sections, we summarize the use of these biomaterials in the engineering of functional cardiac tissue constructs and discuss their applicability for the engineering of a fibrotic cardiac tissue construct. In addition, we review some of the already existing cardiac fibrosis models and discuss their advantages and shortcomings. An overview of these *in vitro* models can be seen in **Table 2**.

Table 2. Tissue engineered models of hydrogel-based cardiac tissue

<i>Study goal</i>	<i>Hydrogel</i>	<i>Cells</i>	<i>Characterized marker(s)</i>	<i>Functional characterization</i>	<i>Ref.</i>
Engineered cardiac tissue	Collagen-native heart ECM	hESC derived CMs	cTnT, cTnI, Cx-43,	Contractility	[165]
	Collagen I-Matrigel	Neonatal rat CM/CF	α -actinin, α -SMA, Propyl-4-hydroxylase	Contractility, β -Adrenergic response (isoproterenol), Ca^{2+} contractile response, sarcomeric structure.	[167]
	Collagen I-Matrigel	Neonatal rat CM/CF	α -actinin, vimentin, Myosin light chain protein, Tropomyosin, Desmin, M-type CK (creatine kinase), Col I/III, MMP-2, -14, TIMP-1, -2,	Sarcomeric maturation, CM phenotype, Sarcomeric structure, phenylephrine and Ang II response.	[30]
	GelMA-CNT	Neonatal rat CM	α -actinin, Cx-43, cTnI	Contractility, protection against drug-induced toxicity	[164]
	Decellularized heart ECM	hESC derived CM	cTnT	-	[176]
	Fibrin-decellularized heart ECM	Cardiac progenitor cells	α -SMA, cTnI, Nkx2.5, GATA4, Titin, c-kit+	-	[180]
	Fibrin	hESC derived CM	α -actinin, vimentin, Cx-43, α -MHC, β -MHC, cTnI, cTnT	CM action potential, Ca^{2+} contractile response, β -Adrenergic response (isoproterenol), pro-arrhythmic drug responses	[36]
	Fibrin	Neonatal rat CM/CF	α -actinin, α/β -MHC, α -actinin, SR^{2+} -ATPase 2 b, ANP, BNP. Fibrotic markers: Col1a1, Fn1, elastin, fibrillins, TGF- β 1, CTGF	Drugs and afterload induced hypertrophic changes, CM size,	[191]
Myofibroblast differentiation	RGD/ (HBP) - Alginate	Neonatal rat cardiac cells	α -actinin, N-cadherin, Cx-43; pAkt, F-actin, vinculin, PCNA, vimentin	CM and CF alignment, cell viability	[195, 196]
	RGD/ (HBP) - Alginate (micro-channel)	Neonatal rat CM/ CF and hEC	F-actin, CD31	Cellular organization, vascularization upon implantation in mice	[198]
	GelMA-HAMA	Pig VIC	α -SMA, vimentin, collagen1A1, MMP-9,	Proliferation	[171]
	PEG	Adult rat CF	α -SMA, fibronectin, DDR2, collagen,	Collagen contraction assay, CF migration,	[118]
	PEG	Porcine VIC	α -SMA, CTGF, collagen, fibronectin, vimentin,	Proliferation, apoptosis	[203]
	Collagen	Adult rat CF	α -SMA, TGF- β , procollagen, MMP-2, MMP-9	Collagen contraction assay, stiffness	[182]
	Collagen	Neonatal rat CF	α -SMA, TGF β 1, collagen I, collagen III,	Collagen contraction assay, elastic modulus (mechanical characterization)	[215]

Decellularized ECM hydrogels

Ideally, a hydrogel perfectly mimics native cardiac ECM and provides a physiological micro-environment for the cells. Recently, Freytes et al. described a method for making 3D hydrogel scaffolds from decellularized cardiac ECM with additional collagen type I (173). They found that native cardiac ECM has a positive effect on the differentiation and maturation of human embryonic stem cells (hESC) to CM. Hydrogels with a high cardiac ECM content showed an elevated expression of cardiac marker troponin T. Furthermore, there was an improvement in contractile function and maturation of the cardiac differentiated cells. Although this platform

was created by using only hESCs, it could potentially be used to create a 3D model with both CM and CF to study MyoF differentiation in the presence of differentiated and contractile CM. In addition, it was demonstrated that solubilized ECM from decellularized porcine myocardial tissue can be used to create a 3D hydrogel (174). Instead of a cell-laden hydrogel for *in vitro* modeling of the heart, these hydrogels were used as injectable biomaterial for the repair of MI (174,175). New 3D fabrication methods of native ECM-derived hydrogels could be utilized to study the effect of cardiac MyoF differentiation in the presence of naturally occurring structural and biochemical cues from native ECM components (176).

Challenges in creating natural ECM-based models are mainly characterized by the poor mechanical features (such as low stiffness) and limited cell encapsulation properties (172). However, hybrid cardiac ECM hydrogels, with PEG or fibrin, have shown to have tunable properties in terms of mechanical stiffness (172,177). In addition, these hybrid scaffolds were suitable for cardiovascular progenitor cell (CVPC) seeding, which was demonstrated by the ability of these cells to interact with, and remodel their ECM. Moreover, CVPC showed to have substantially higher cell viability in ECM-fibrin hydrogels in comparison to fibrin-only hydrogels (177). The use of these cardiac ECM-derived scaffolds have the potential to mimic properties of the heart very closely, however, most of these studies are based on rat heart ECM, which may have some important differences compared to the cardiac ECM of humans (138,140).

Collagen-based hydrogels

Fibrillar collagen type I is one of the most abundant proteins in cardiac ECM (178), and is therefore frequently used to form hydrogels. Collagen can provide cues for adhesion, growth, survival and proliferation of CM in engineered collagen-based heart constructs (162,163). Furthermore, collagen has biocompatible and biodegradable features and can mediate cell-ECM interactions through integrins (30,179).

The combination of collagen type I and Matrigel was used to make differentiated cardiac muscle constructs *in vitro* with neonatal rat CM (165). These constructs showed hallmarks of

differentiated myocardium including gap junctions, desmosomes and a well-developed T-tubular system. Also, a strong beta-adrenergic response and contractile activity was observed. To study cardiac tissue hypertrophy, neonatal rat CM were combined with CF and encapsulated in a similar collagen-I/Matrigel hydrogel (30). Remarkably, hydrogel components in these constructs were degraded during the first culture days and replaced by newly synthesized ECM. Apparently, incorporated cells are capable of remodeling the initial collagen-based matrix and gradually replace it with their own ECM. With regard to an *in vitro* model of cardiac fibrosis, biodegradability is an essential feature of a hydrogel, since turnover of ECM and the migration of CF play key roles in the pathophysiology of cardiac fibrosis. The hydrogel model of cardiac hypertrophy demonstrated the potential of cardiac disease modeling and could be further used to study CF phenotype during exposure to hypertrophic and pro-fibrotic stimuli such as TGF- β and Ang II.

As stated before, in cardiac fibrotic disease, collagen I synthesis and deposition is increased as a result of MyoF differentiation. Yet, newly deposited collagen could be hard to distinguish from the already existing fibers inside collagen-based scaffolds. Therefore, experimental characterization of fibrosis in collagen-based hydrogels should not solely rely on collagen production (119,180).

Gelatin methacryloyl (GelMA) hydrogels

Gelatin is another natural hydrogel that has been extensively used for cardiac tissue engineering (181). Although gelatin is collagen in its denaturated form, it still has the same biomimetic and biocompatible properties (182). By incorporation of methacryloyl to the amine-containing side group of gelatin a light polymerizable (or photocrosslinkable) hydrogel is fabricated (144,183). This gelatin methacryloyl (GelMA) hydrogel has been demonstrated to be a suitable scaffold for engineering micro-patterned 3D tissue constructs, which was shown by effective cell adhesion and cell proliferation (144). One of the main advantages of GelMA is that through variations in the gel concentration, the degree of methacryloyl modification, and the

time of UV polymerization, different GelMA gels can be generated with varying mechanical and swelling properties (181). Similar to collagen-based scaffolds, GelMA can be degraded by MMPs and by that allow cells to remodel their extracellular environment (181). GelMA is a tunable and biomimetic hydrogel, suitable for re-creating the native heart ECM.

In a recent study, neonatal rat CM were encapsulated in a hybrid GelMA hydrogel with incorporated carbon nanotubes (CNTs), hypothesizing that this combination would improve electrical and mechanical properties, while at the same time maintaining high porosity and biocompatibility (157). Results demonstrated that these gelatin-based scaffolds have functional mechanical integrity and electrical conductivity. The CNT-GelMA seeded constructs showed to be a proper environment for cell adhesion, cell spreading, and cell alignment. Additionally, the *in vitro* constructs were demonstrated to have a protective potential by preventing damage caused by cytotoxic compounds, making these cardiac scaffolds suitable for *in vitro* studies.

In a recent study from our group, a GelMA-based hybrid hydrogel was designed to study valvular interstitial cell (VIC) differentiation into MyoF-like cells (169). By combining naturally derived gelatin and hyaluronic acid (HA), it was demonstrated that a more physiologically mimicking scaffold can be made. VICs were found to remain quiescent when encapsulated in the GelMA-HAMA (hyaluronic acid methacryloyl) hybrid hydrogel and differentiated to MyoF-like cells upon addition of TGF- β 1. Therefore, incorporation of GelMA-HAMA into engineered tissue constructs could be useful in creating a 3D culture platform for controllably studying valvular fibrotic remodeling. However, it is unclear if VICs and CF behave in a comparable manner and whether or not it is acceptable to extrapolate these results to CF and CF differentiation.

Fibrin-based hydrogels

Fibrin, a major component of the coagulation cascade and the resulting product the enzymatic modulation of fibrinogen (184), has been used widely in cardiac tissue engineering (149,185). Despite its unstable degradation time and low mechanical stiffness, fibrin has attractive properties such as cell adhesiveness and a high cell seeding efficiency (186). In

addition, fibrin is a non-toxic and biocompatible material, which offers the opportunity to incorporate growth factors (e.g. FGF, TGF- β 1) and other possible mediators in the hydrogel (186,187). This might be useful in the engineering of *in vivo* like cardiac tissue, as it could mimic the native storage of, for instance, latent TGF- β 1 inside the ECM. The release of these growth factors could then be controlled by cell-mediated degradation of the fibrin matrix.

Fibrin-based hydrogels have been used to design functional cardiac tissue by using hESC derived CM (36). This fabrication method led to a properly orientated and interconnected CM organization, which showed uniform and strong contractions during the period of culture. Due to these characteristics, pharmacological testing of pro-arrhythmic compounds on these constructs was shown to be possible (36).

In addition to mimicking normal cardiac tissue, fibrin hydrogels have also been used to study disease conditions of heart tissue. To study the effect of afterload enhancement on CM and fibrotic remodeling, an experimental *in vitro* model for pathological cardiac hypertrophy was engineered by Hirt *et al* (188). To accomplish *in vitro* afterload enhancement, fibrin-based engineered heart tissue was cultured between two elastic posts and after 2 weeks the posts were reinforced with metal braces. The incorporated CM showed an increase in size as a result of afterload enhancement. In addition to hypertrophic changes, the results demonstrated that there was an elevated extracellular deposition of collagen I/II and fibronectin, indicating cardiac fibrotic remodeling. Therefore, this platform can especially be useful in mimicking pressure overload (e.g. hypertension, aortic stenosis) related cardiac fibrosis *in vitro*. Moreover, this could provide the opportunity to study cardiac fibrosis in the setting of a specific heart disease.

Alginate-based hydrogels

Alginate is, in terms of its origin, a natural biomaterial, consisting of hydrophilic polysaccharides derived from seaweed and bacteria (189). Alginate is easy to process, biocompatible, degradable and therefore has been widely used as ECM in biomedical applications (190). However, alginate polysaccharides do not naturally occur in mammalian

tissues and alginate hydrogels are, by the lack of appropriate receptors of mammalian cells for alginate, relatively inert in their original form. In addition, the internal architecture of alginate hydrogels is difficult to control due to their low mechanical strength, high degradability and large hydrophilicity (191). To overcome these problems in cardiac tissue constructs, alginates have been modified with natural peptides and synthetic polymers to change their biological and mechanical characteristics (192). To improve cellular adhesion in engineered cardiac tissue, Shachar *et al* covalently linked RGD peptides to alginate, which resulted in less cell apoptosis and an accelerated reorganization of CM (193). Moreover, also the CF benefited greatly from the added binding sites and surrounded the myofibers in a similar manner as observed in native myocardium. In addition, the combination of two alginate-attached peptides, G₄RGDY and heparin-binding peptide, even further induced isotropic myofiber arrangement and supported the formation of contractile muscle tissue in the scaffolds (194).

Novel methods to facilitate engineering of complex myocardial tissue not only include the processing of appropriate materials, but also the arrangement (e.g. vascularization) of the chosen material to allow for efficient reconstruction of the metabolic active myocardium. To that end, several attempts have been made to vascularize alginate-based cardiac tissue constructs using vascular EC. In a recent study, magnetic alginate scaffolds were used to physically stimulate the embedded aortic EC with an alternating magnetic field. After 14 days of stimulation, the magnetic properties and composition of the alginate scaffold has led to the formation of cellular vessel-like structures (195). In addition to induced vessel formation, alginate scaffolds are demonstrated to be suitable for fabrication of micro-channels using a CO₂ laser engraving system. The resulting channeled scaffolds were sequentially cultivated with EC and CM and showed organization of the EC in the micro-channels and maturation of CM within the matrix (196). These findings demonstrate the usability of alginate for cardiac tissue engineering by means of the numerous possibilities of material processing and biofabrication techniques.

PEG-based hydrogels

In contrast to many natural biomaterials, synthetic biomaterials have a higher reproducibility of mechanophysical properties due to tunable characteristics (197). PEG is a biocompatible polymer and is one of the few FDA approved biomaterials. PEG hydrogels have appropriate mechanical and structural features due to their elasticity and high water content, resembling native cardiac ECM (197). However, like other synthetic biomaterials, PEG hydrogels are not ideal for cell attachment because of their non-adhesive properties due to the lack of cell recognition motifs (198). In addition, low biodegradability of PEG hydrogels limits the breakdown of the matrix environment and prevents ECM renewal in these scaffolds. PEG-based hydrogels have been used to study CM-ECM interactions *in vitro*, by introducing RGD peptides to increase cell adhesion and viability (199). In addition, a hybrid hydrogel was engineered by combining PEG with decellularized myocardial ECM in order to expand the properties of the natural ECM with a tunable synthetic material such as PEG (172). These gels demonstrated similar nanofibrous structures as native myocardial ECM, showed increased material stiffness, and, above all, similar cell adhesion and migration. Synthesizing hybrids with PEG and natural ECM-based hydrogels can therefore be promising for *in vitro* applications. By using UV-polymerizing PEG-diacrylate with varying molecular weight, hydrogels with a tunable stiffness and degree of crosslinking can be fabricated (200). This technique has also been used to engineer *in vitro* models of VIC and CF differentiation into MyoF (118,201). As expected, CF and VICs cultured on stiffer substrates (mimicking fibrotic tissue), showed an increased MyoF differentiation as determined by α -SMA expression. Interestingly, by reducing the stiffness of the PEG-substrate *in situ* by a photosensitive degradation, MyoF were deactivated (201). However, even though these studies have provided valuable insights in the mechano-biological and biochemical factors that play a role in MyoF differentiation, they lack the existence of a third-dimension and therefore do not adequately mimic *in vivo* conditions. Consequently, new engineering methods to encapsulate cardiac cells in mechanically tunable PEG-hydrogels could contribute to the development of better physiologic-like culture models.

The use of natural and synthetic hydrogels can provide cues for a cardiac ECM-like environment that can encourage cellular and molecular interactions. It is important, however, to consider many different factors in the use of hydrogels toward the engineering of a 3D cardiac fibrosis model. In this context, a suitable hydrogel should have biocompatible properties, provide a native-like 3D micro-environment, and a high tunability in terms of mechanical stiffness and strain. With regard to mechanical properties, the hydrogel should also be able to withstand repetitive mechanical forces that can be exerted by the beating construct and contractile MyoF. Moreover, the material should not interfere with the experimental characterization and readouts of fibrotic remodeling.

3.5 Cellular components, micro-environmental control and culture conditions

To study fibrosis in engineered heart constructs, it is important to take into account that beside cells and matrix components, also other micro-environmental factors (e.g. bio-mechanical cues, growth factors, oxygen tension) can affect disease physiology. Bioreactors exist that are able to control these environmental conditions. Hence, it is relevant to design tissue constructs that consist of multiple (non-)cardiac cells within the appropriate micro-environmental condition.

The use of cell types to model fibrosis

It is suggested that the inclusion of non-myocytes in tissue engineered constructs promotes the stability, growth and the functional properties of the engineered myocardium. Recently, a 3D cardiac tissue construct was engineered by co-culturing CM with CF, as they form the most important cellular components of native myocardium (134). Results demonstrated a higher expression of integrin- β 1 and cardiac markers (such as sarcomeric α -actinin, connexin-43, and troponin-I) in co-culture as compared to the mono-culture condition, which suggest that the cell-ECM and cell-cell interactions of co-cultured CM have been improved. Additionally, mono-

culture constructs showed individual cellular contraction, whereas co-culture constructs exhibited tissue-like synchronous contraction. Although CF were part of the tissue construct, no results on activation state or role of CF in matrix modulation was described. Furthermore, Caspi *et al.* engineered vascularized 3D cultures by including (hESC-derived) CM, ECs and embryonic fibroblasts in a synthetic poly-L-lactic acid/polylactic-glycolic acid (PLGA) based scaffold (202). CM in these tri-culture scaffolds showed a relative high degree of proliferation in comparison with the mono-culture of CM. In addition, these constructs were demonstrated to have typical features of cardiac tissue by the presence of sarcomeres, T-tubules and sarcoplasmic reticulum. Furthermore, functional gap-junction formation and synchronous contractions of the engineered cardiac tissue were observed. With the use of co-culture hydrogels, MyoF differentiation could be studied in the presence of myocardial-like synchronous contraction. In addition, the dynamic changes in the expression of different types of integrins and cadherins that play a role in fibrotic remodeling can be assessed.

By seeding CM on pre-formed networks of fibroblasts and ECs, Iyer *et al.* demonstrated that pre-cultured mixtures of EC/CF result in the formation of contractile 3D cardiac organoids (171). In contrast to pre-cultured constructs, the simultaneous tri-culture lacked typical properties of cardiac tissue, such as connexin-43 expression. These findings suggest that not only the composition of the cells are important, but also the sequence by which the cells are introduced in the scaffolds. Vascularization inside tissue engineered constructs could especially be relevant in studying cardiac disease, since it allows the integration of hemodynamic factors inside a myocardial-like tissue. In addition, vascularized tissue allows perfusion with medium containing bio-active substances, and thus can be used for *in vitro* drug testing.

Micro-environmental factors and culture conditions

Native-like myocardial tissue has a mechanical stiffness of 10-30 kPa, whereas a post-MI fibrotic tissue has a mechanical stiffness of 35-70 kPa (203,204). Consequently, properties of the extracellular environment, including matrix stiffness, are relevant for the engineering of a

native-like cardiac (fibrosis) model. Engineered cardiac-like tissue with high ECM stiffness can contribute to persistence of fibrotic remodeling, through the promotion of MyoF differentiation (118,119,201). Moreover, ECM stiffness is not only important for MyoF differentiation, but it also plays a role in the CM functioning and contractility. It has been shown that CM that are seeded on substrates with a stiffness comparable to fibrotic scar tissue (>35 kPa), have a lower contraction rate, a lower percentage of beating CM, a higher electrical excitability, and less striation (205,206). Furthermore, CF showed an increased proliferation when they were co-cultured with CM on substrates with an elastic modulus above 50 kPa (206), suggesting the stimulation of proliferation by mechano-regulatory pathways. Together, these data emphasize the importance of matrix stiffness for cardiac tissue modeling. In addition, matrix stiffness could potentially be used to characterize fibrotic changes in engineered fibrotic micro-tissues (180).

Similar to the fact that mechanical stiffness can influence the functional properties of CM and CF, mechanical strain could contribute to the development of better *in vivo* like micro-tissues. By exposing engineered cardiac micro-tissues to cyclic mechanical strain, improved changes in the tissue structure and functionality were shown by Fink *et al* (207) These changes were characterized by increased expression of cardiac markers (such as α -sarcomeric actin), better cellular organization (alignment and rod shaped cells), and better contractility (207). Moreover, cyclic strain aids in bio-mimicking hemodynamic changes of hydrostatic pressure in the beating

The most essential feature of the heart is its regular, synchronous and forceful contraction. In order to create a functional cardiac construct, there is a need for proper excitation-contraction coupling. The presence and distribution of gap-junctions is an essential property of native myocardium and is important for the development of the heart (208). Although engineered cardiac constructs have the ability to beat spontaneously, external electrical stimulation of CM in 3D culture will lead to improved functional properties and a more regular and synchronous beating (155,209). Furthermore, the electrophysiological properties can be used to monitor excitation-contraction coupling and conduction of engineered fibrotic tissue for an improved understanding of fibrotic cardiac disease. (210).

ECM conditions and hydrogels have also proven their importance with respect to electrophysiological functions of cardiac tissue constructs. For example, a 3D hydrogel culture system as a model for cardiac dysrhythmia was developed using neonatal mouse CM (211). It was demonstrated that a disordered scaffold organization can mimic the disordered ECM conditions related to cardiac fibrosis and thereby can exert arrhythmogenic effects on the CM. This indicates that it is possible to engineer a disease model, which does not only resemble cardiac fibrosis, but also mimics pathophysiology.

3.6 Modeling MyoF differentiation and fibrosis

As stated before, the differentiation of MyoF is a hallmark of fibrotic cardiac disease and is therefore an important parameter for the evaluation of fibrotic remodeling. Many factors that contribute to the phenotypical changes from CF to MyoF have been identified. However, most of these studies have been performed in static conventional cell culture or engineered 2D systems. In addition, co-cultures of cardiac cells (CM, ECs, CF) have been created to engineer normal cardiac tissue, but to date no such models have been used to study cardiac MyoF differentiation. Some groups have however used 2D and 3D engineered mono-cultures of CF to study MyoF differentiation. Deng *et al.* aimed to measure the effect of a thrombin receptor inhibitor (protease-activated receptor 1 (PAR1)) on cardiac fibrosis (180). PAR1 is a receptor that is associated with fibrotic changes in lung fibrosis (212), and was hypothesized to play a role in cardiac fibrosis. A 3D CF tissue was engineered by encapsulating isolated rat adult CF in a collagen-based hydrogel and tissue contractility and tissue stiffness after culture were measured (180). By adding thrombin, it was shown that the tissue stiffness increased significantly, which then was reduced after incubation with a PAR1 inhibitor. Although the expression of TGF- β , α -SMA, and pro-collagen I was only measured in the conventionally (2D) cultured CF, the study of Deng *et al.* indicates the importance of a cardiac fibrosis model in the identification of drug targets as well as the identification of pathophysiological processes that play a key role in cardiac fibrosis and ventricular remodeling.

Furthermore, a 2D PEG hydrogel-based model of cardiac fibrosis was designed *in vitro* in order to study cardiac MyoF differentiation (118). By varying polymer concentrations, a substrate with areas that varied in mechanical stiffness was constructed, ranging from soft (10 kPa) to stiffer (40 kPa) environments. Hereby, the mechanical heterogeneity of fibrotic heart after MI was mimicked. CF migrated across the hydrogel and differentiated into MyoF in areas with a higher stiffness, implicating the crucial role of mechanical stiffness in maintaining CF in a quiescent state. In addition, Zhao *et al.* examined the effect of a Rho-associated protein kinase inhibitor and showed the feasibility of engineered micro-tissues for *in vitro* drug testing. To have better bio-mimetic features, this platform would need the incorporation of other cardiac cell populations. In addition, the encapsulation of these cells inside a 3D hydrogel-based scaffold would improve native-like cell-ECM interactions. Finally, by the incorporation of other biological cues, such as fluid flow and cyclic mechanical strain, cellular behavior could also be affected and this would potentially contribute to a better cardiac fibrosis model. To incorporate both fluid flow and cyclic mechanical strain, Galie *et al.* have designed a bioreactor, which is able to apply both these cues to 3D CF-encapsulated hydrogels (213). Varying circumstances in a collagen-based hydrogels, such as serum concentration and matrix stiffness, stimulated CF differentiation into MyoF, indicating the relevance of both culture conditions and matrix properties (119).

4. Future outlook and conclusions

Human-derived cells and cardiac fibrosis models

In the past few years, many tissue engineered constructs have been developed using cell mixtures from animal sources. These tissue constructs have proven their added value in clarifying myocardial biology and disease modeling for drug testing purposes (30,36,165,167,188,214). Additionally, these animal-based engineered constructs have contributed to the development of better bioengineering methods and more advanced *in vitro* systems. However, in order to introduce cardiac tissue engineering to (pre-)clinical pharmacological testing and disease modeling, it is essential to bioengineer human myocardial tissue *in vitro* (215). By doing this, better bio-mimicking and physiological *in vitro* systems would become available for biological-mechanistic studies and medium- and high-throughput drug screening. In addition, although far from realistic at this stage, bioengineering functional human myocardium could help in repairing the heart.

Substantial progress has been made in the use of human stem cells, such as human pluripotent stem cells (hPSC), including ESC and induced pluripotent stem cells (iPSC), and cardiac progenitor cells (CPC) as a source for human differentiated cardiac cells (216,217). The use of human iPSC may introduce a new perspective into the field of cardiac tissue engineering and would allow engineers and clinicians to use patient cells to create 3D patient-specific cardiac fibrosis model systems. Consequently, these patient-specific models could be used in different research and pre-clinical settings, such as studying pathophysiology, drug targeting and drug toxicology. In addition, these models could be used to identify the best drug for a patient and lead to personalized drug therapy for clinical use. Studies on the use of these stem cell sources in tissue engineered cardiac disease models are still scarce. However, a recent study by Guyette *et al.* demonstrated the possibility to engineer functional human myocardium by using decellularized myocardial tissue as a native ECM, and human iPSC as a cellular source (140). In addition, human iPSC-derived cardiac cells have been used extensively in conventional monolayer disease modeling of several inherited cardiomyopathies (reviewed by Martins *et al.*

(218)), but thus far, only one pluripotent stem cell derived model has been engineered serving as a platform for drug testing (36).

Unfortunately, hPSC-derived CM still lack some essential phenotypic properties of terminally differentiated adult human CM (reviewed by Mummery *et. al* and Martins *et. al* (217,218)). To construct an *in vitro* model of human fibrotic myocardial tissue, engineered cardiac tissue needs to recapitulate human cardiac cells in terms of cell morphology, cell functioning and cell maturation. The integration of other cardiac cell populations should also be considered in these model systems. Furthermore, the addition of fibrogenic factors that could initiate fibrotic remodeling should be selected carefully to reproduce a pathophysiological environment. Designing human engineered cardiac constructs for (pre-)clinical applications remains a challenge and further studies are needed to understand the processes underlying the incomplete differentiation and maturation of hPSC to CM, and to find suitable co-culture conditions.

Challenges and conclusion

Cardiac fibrosis is a hallmark of adverse cardiac remodeling and is a substantial problem in multiple forms of heart disease that lead to HF. Currently, there are no surgical or pharmacological therapies available for fibrosis related heart failure and therefore mechanical support or heart transplantation remains the best option. Cardiac tissue constituents including CM, CF, EC and ECM components are very important for normal cell-cell and cell-ECM interactions and are crucial for normal cardiac structure and functioning. Abundant data suggests that multiple and complex interactions between these constituents and other molecular, chemical and mechanical pathways contribute to cardiac fibrogenesis. A better understanding of these mechanisms offers opportunities for the identification of possible targets for efficacious therapy in cardiac fibrosis. For example, mechano-regulated (integrins and cadherins) and molecular pathways (TGF- β) that are involved in the differentiation of CF into MyoF could be interesting targets for novel treatments against cardiac fibrosis.

The field of cardiac tissue engineering is rapidly advancing. Although most studies to date are focused on tissue engineered applications in cardiac regeneration, tissue engineered 3D models have the potential to become an important research tool in physiology and disease. In addition, these 3D cell cultures could also provide an alternative to animal models and can therefore serve as a drug discovery and toxicity instrument. More interestingly, these 3D *in vitro* models could eventually result in advanced clinical tools for personalized therapies. This could be achieved by designing patient-specific engineered heart constructs with the use of patient-specific cells. Subsequently, several pharmacological treatments can be tested *in vitro* and drugs with the highest potential can be selected for further clinical treatment.

Most of the relevant *in vitro* research that has been conducted until now focused on either engineering healthy myocardial tissue or engineering mono-culture constructs to study MyoF differentiation. Combining the techniques and methods of these two strategies could result in the creation of functional myocardial tissue to study MyoF differentiation and changes in the ECM quality and quantity in the setting of different fibrotic etiologies. Despite significant developments in the field of cardiac tissue engineering, certain challenges in designing 3D cardiac fibrosis models still remain. We think that in order to be able to engineer fully functional 3D cardiac fibrosis *in vitro* models, the following factors need to be taken into account (**Figure 3A-D**).

1. **Cells:** The use of multiple cell sources (EC, CM, CF, etc.) in co-culture to study the behavior and differentiation of CF in the presence of other cardiac residing cells. In addition, we think that the use of human-derived cells (e.g. iPSC) could contribute to the development of better human-like *in vitro* systems.
2. **Scaffolds:** The use of biocompatible hydrogels that can be controlled and tuned easily to influence micro-environmental factors. This is important since high mechanical stiffness can stimulate MyoF differentiation, and thus will prevent accurate control of this process. On the other hand, the stiffness should be strong enough to resist the cyclic beating of CM inside the micro-tissues. Although all scaffolds have pro's and con's,

combining the controllability of (natural) synthetic materials (e.g. PEG, GelMA) with biocompatible native ECM components (e.g. hyaluronic acid, laminin) appear promising for *in vitro* application.

3. **Micro-environmental control:** The possibility to incorporate biochemical, electrical and bio-mechanical cues to stimulate the maturation, structural organization, and functionality of the engineered micro-tissues. Furthermore, it could be valuable to integrate hemodynamic cues (by vasculature) within engineered cardiac disease models. This could help to recapitulate organ-level physiology by, for example, enabling the circulation of immune cells that also play a key role in the fibrosis pathogenesis.
4. **Translational criteria:** To create valuable cardiac fibrosis *in vitro* models for drug testing and disease modeling, the engineered micro-tissues should preferably be suitable for automatized high throughput screening and multifunctional analysis of several fibrotic makers. In addition, these platforms should have a high reproducibility and get regulatory approval, including high standard GMP conditions, for the use in pre-clinical and clinical settings.

All together these challenges are related to the current limitation to investigate fibrogenic changes under dynamic and physiologic-like conditions. However, with the recent advancements in the development of microfluidic systems of myocardial tissue (hearts-on-a-chip), it may be expected that these challenges can be addressed more easily in the future (219,220). These microfluidic organ-on-a-chip systems are capable of recapitulating organ-level structures and allow accurate control of bio-chemical, mechanical, and cellular components (221). Therefore, we think that microfluidic systems hold great promise on the engineering of cardiac fibrosis models with controllable environmental properties. In addition, we think that in the future these systems could be used to not only mimic hallmarks of cardiac fibrosis, but also to enable personalized medicine strategies. However, creating standardized methods for the engineering of these platforms are evenly important, since it characterizes scalability and reliability, and eventual regulatory approval.

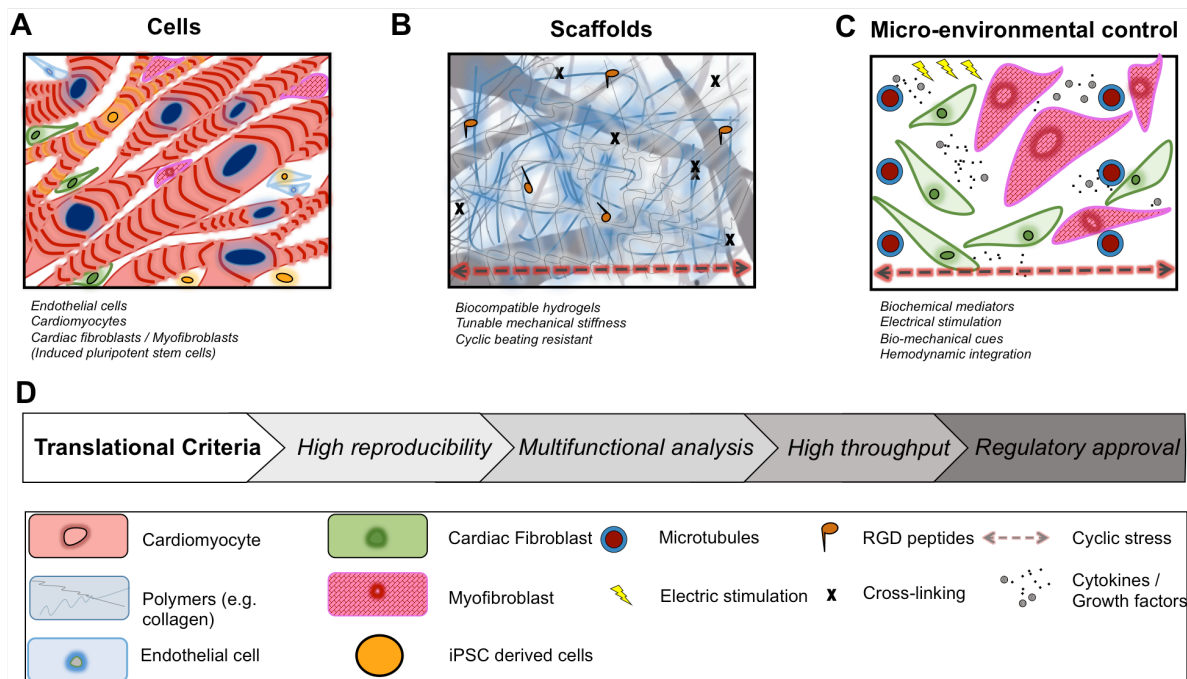


Figure 3. Factors that influence the engineering of cardiac fibrosis. To engineer a comprehensive 3D model of cardiac fibrosis, the following aspects are essential for the success of the model: **(A)** the use of multiple cell sources, **(B)** the use of a tunable and biocompatible scaffold, and **(C)** the possibility to incorporate micro-environmental factors. **(D)** To ensure implementation of cardiac fibrosis models in drug testing platforms and disease modeling, translational criteria are essential and include all aspects of A-C.

In conclusion, to mimic the natural microenvironment of CM and CF in studying cardiac fibrosis, the properties of the scaffold, the cell-mixture and the appropriate environmental factors need to be taken into account. In addition, integration of the information obtained from adult cardiac disease biology and cardiac tissue engineering should provide us with the opportunity to design biomimetic models of cardiac fibrosis. With the recent developments in hydrogel fabrication, stem cell biology, tissue engineering methods, and microfluidic technologies, it is likely that the first human biomimetic heart fibrosis model (on-a-chip) will become available in the near future and provide a platform for disease modeling, pre-clinical high throughput screening, and clinical personalized medicine.

Acknowledgements

J.C.D and A.H.S. contributed equally to this work. The authors acknowledge the support from Innovation and the Netherlands CardioVascular Research Initiative (CVON): The Dutch Heart Foundation, Dutch Federation of University Medical Centers, the Netherlands Organization for Health Research and Development and the Royal Netherlands Academy of Science.

References

1. Mozaffarian D, Benjamin EJ, Go AS et al. Heart disease and stroke statistics--2015 update: a report from the American Heart Association. *Circulation* 2015;131:e29-322.
2. Danaei G, Ding EL, Mozaffarian D et al. The preventable causes of death in the United States: comparative risk assessment of dietary, lifestyle, and metabolic risk factors. *PLoS Med* 2009;6:e1000058.
3. Hill JA, Olson EN. Cardiac plasticity. *N Engl J Med* 2008;358:1370-80.
4. Heusch G, Libby P, Gersh B et al. Cardiovascular remodelling in coronary artery disease and heart failure. *Lancet* 2014;383:1933-43.
5. Sutton MG, Sharpe N. Left ventricular remodeling after myocardial infarction: pathophysiology and therapy. *Circulation* 2000;101:2981-8.
6. Eichhorn EJ, Bristow MR. Medical therapy can improve the biological properties of the chronically failing heart. A new era in the treatment of heart failure. *Circulation* 1996;94:2285-96.
7. Wu KC, Weiss RG, Thiemann DR et al. Late gadolinium enhancement by cardiovascular magnetic resonance heralds an adverse prognosis in nonischemic cardiomyopathy. *J Am Coll Cardiol* 2008;51:2414-21.
8. Laribi S, Aouba A, Nikolaou M et al. Trends in death attributed to heart failure over the past two decades in Europe. *Eur J Heart Fail* 2012;14:234-9.
9. Roger VL, Weston SA, Redfield MM et al. Trends in heart failure incidence and survival in a community-based population. *JAMA* 2004;292:344-50.
10. Mortality multiple cause micro-data files. National center for health statistics. Mortality multiple cause micro-data files 2011, http://www.cdc.gov/nchs/data_access/Vitalstatsonline.htm-Mortality_Multiple (accessed: June, 2015).
11. Kurrelmeyer K, Kalra D, Bozkurt B et al. Cardiac remodeling as a consequence and cause of progressive heart failure. *Clin Cardiol* 1998;21:114-9.
12. Spinale FG. Myocardial matrix remodeling and the matrix metalloproteinases: influence on cardiac form and function. *Physiol Rev* 2007;87:1285-342.
13. Diez J, Querejeta R, Lopez B, Gonzalez A, Larman M, Martinez Ubago JL. Losartan-dependent regression of myocardial fibrosis is associated with reduction of left ventricular chamber stiffness in hypertensive patients. *Circulation* 2002;105:2512-7.
14. Greenberg B, Quinones MA, Koilpillai C et al. Effects of long-term enalapril therapy on cardiac structure and function in patients with left ventricular dysfunction. Results of the SOLVD echocardiography substudy. *Circulation* 1995;91:2573-81.
15. Hall SA, Cigarroa CG, Marcoux L, Risser RC, Grayburn PA, Eichhorn EJ. Time course of improvement in left ventricular function, mass and geometry in patients with congestive heart failure treated with beta-adrenergic blockade. *J Am Coll Cardiol* 1995;25:1154-61.
16. Jhund PS, Fu M, Bayram E et al. Efficacy and safety of LCZ696 (sacubitril-valsartan) according to age: insights from PARADIGM-HF. *Eur Heart J* 2015;36:2576-84.
17. Mann DL, Bristow MR. Mechanisms and models in heart failure: the biomechanical model and beyond. *Circulation* 2005;111:2837-49.
18. McMurray JJ, Packer M, Desai AS et al. Angiotensin-neprilysin inhibition versus enalapril in heart failure. *N Engl J Med* 2014;371:993-1004.
19. Mancini D, Colombo PC. Left Ventricular Assist Devices: A Rapidly Evolving Alternative to Transplant. *J Am Coll Cardiol* 2015;65:2542-55.

20. Chau Y, Luo Y, Cheung AC et al. Incorporation of a matrix metalloproteinase-sensitive substrate into self-assembling peptides - a model for biofunctional scaffolds. *Biomaterials* 2008;29:1713-9.
21. Webber MJ, Khan OF, Sydlik SA, Tang BC, Langer R. A perspective on the clinical translation of scaffolds for tissue engineering. *Ann Biomed Eng* 2015;43:641-56.
22. Kharaziha M, Nikkhah M, Shin SR et al. PGS:Gelatin nanofibrous scaffolds with tunable mechanical and structural properties for engineering cardiac tissues. *Biomaterials* 2013;34:6355-66.
23. Shin SR, Aghaei-Ghareh-Bolagh B, Dang TT et al. Cell-laden microengineered and mechanically tunable hybrid hydrogels of gelatin and graphene oxide. *Adv Mater* 2013;25:6385-91.
24. Schukur L, Zorlutuna P, Cha JM, Bae H, Khademhosseini A. Directed differentiation of size-controlled embryoid bodies towards endothelial and cardiac lineages in RGD-modified poly(ethylene glycol) hydrogels. *Adv Healthc Mater* 2013;2:195-205.
25. Chen YC, Lin RZ, Qi H et al. Functional Human Vascular Network Generated in Photocrosslinkable Gelatin Methacrylate Hydrogels. *Adv Funct Mater* 2012;22:2027-2039.
26. Camci-Unal G, Cuttica D, Annabi N, Demarchi D, Khademhosseini A. Synthesis and characterization of hybrid hyaluronic acid-gelatin hydrogels. *Biomacromolecules* 2013;14:1085-92.
27. Bowers SL, Banerjee I, Baudino TA. The extracellular matrix: at the center of it all. *J Mol Cell Cardiol* 2010;48:474-82.
28. Alrefai MT, Murali D, Paul A, Ridwan KM, Connell JM, Shum-Tim D. Cardiac tissue engineering and regeneration using cell-based therapy. *Stem Cells Cloning* 2015;8:81-101.
29. Annabi N, Tsang K, Mithieux SM et al. Highly Elastic Micropatterned Hydrogel for Engineering Functional Cardiac Tissue. *Adv Funct Mater* 2013;23(29).
30. Tiburcy M, Didie M, Boy O et al. Terminal differentiation, advanced organotypic maturation, and modeling of hypertrophic growth in engineered heart tissue. *Circ Res* 2011;109:1105-14.
31. Kana K, Song H, Laschinger C, Zandstra PW, Radisic M. PI3K Phosphorylation Is Linked to Improved Electrical Excitability in an In Vitro Engineered Heart Tissue Disease Model System. *Tissue Eng Part A* 2015;21:2379-89.
32. de Lange WJ, Hegge LF, Grimes AC et al. Neonatal mouse-derived engineered cardiac tissue: a novel model system for studying genetic heart disease. *Circ Res* 2011;109:8-19.
33. Benam KH, Dauth S, Hassell B et al. Engineered in vitro disease models. *Annu Rev Pathol* 2015;10:195-262.
34. Ralphe JC, de Lange WJ. 3D engineered cardiac tissue models of human heart disease: learning more from our mice. *Trends Cardiovasc Med* 2013;23:27-32.
35. Turnbull IC, Karakikes I, Serrao GW et al. Advancing functional engineered cardiac tissues toward a preclinical model of human myocardium. *FASEB J* 2014;28:644-54.
36. Schaaf S, Shibamiya A, Mewe M et al. Human engineered heart tissue as a versatile tool in basic research and preclinical toxicology. *PLoS One* 2011;6:e26397.
37. Eghbali M, Blumenfeld OO, Seiffter S et al. Localization of types I, III and IV collagen mRNAs in rat heart cells by in situ hybridization. *J Mol Cell Cardiol* 1989;21:103-13.
38. Sullivan KE, Black LD. The role of cardiac fibroblasts in extracellular matrix-mediated signaling during normal and pathological cardiac development. *J Biomech Eng* 2013;135:71001.

39. Sluijter JP, Verhage V, Deddens JC, van den Akker F, Doevendans PA. Microvesicles and exosomes for intracardiac communication. *Cardiovasc Res* 2014;102:302-11.
40. Kakkar R, Lee RT. Intramyocardial fibroblast myocyte communication. *Circ Res* 2010;106:47-57.
41. Zeisberg EM, Kalluri R. Origins of cardiac fibroblasts. *Circ Res* 2010;107:1304-12.
42. Krenning G, Zeisberg EM, Kalluri R. The origin of fibroblasts and mechanism of cardiac fibrosis. *J Cell Physiol* 2010;225:631-7.
43. Ieda M, Tsuchihashi T, Ivey KN et al. Cardiac fibroblasts regulate myocardial proliferation through beta1 integrin signaling. *Dev Cell* 2009;16:233-44.
44. van Hout GP, Arslan F, Pasterkamp G, Hoefler IE. Targeting danger-associated molecular patterns after myocardial infarction. *Expert Opin Ther Targets* 2015;20:223-39.
45. Epelman S, Liu PP, Mann DL. Role of innate and adaptive immune mechanisms in cardiac injury and repair. *Nat Rev Immunol* 2015;15:117-29.
46. Brutsaert DL. Cardiac endothelial-myocardial signaling: its role in cardiac growth, contractile performance, and rhythmicity. *Physiol Rev* 2003;83:59-115.
47. Hsieh PC, Davis ME, Lisowski LK, Lee RT. Endothelial-cardiomyocyte interactions in cardiac development and repair. *Annu Rev Physiol* 2006;68:51-66.
48. Haigh JJ, Gerber HP, Ferrara N, Wagner EF. Conditional inactivation of VEGF-A in areas of collagen2a1 expression results in embryonic lethality in the heterozygous state. *Development* 2000;127:1445-53.
49. Giordano FJ, Gerber HP, Williams SP et al. A cardiac myocyte vascular endothelial growth factor paracrine pathway is required to maintain cardiac function. *Proc Natl Acad Sci U S A* 2001;98:5780-5.
50. Zhao YY, Sawyer DR, Baliga RR et al. Neuregulins promote survival and growth of cardiac myocytes. Persistence of ErbB2 and ErbB4 expression in neonatal and adult ventricular myocytes. *J Biol Chem* 1998;273:10261-9.
51. Bersell K, Arab S, Haring B, Kuhn B. Neuregulin1/ErbB4 signaling induces cardiomyocyte proliferation and repair of heart injury. *Cell* 2009;138:257-70.
52. Godecke A, Heinicke T, Kamkin A et al. Inotropic response to beta-adrenergic receptor stimulation and anti-adrenergic effect of ACh in endothelial NO synthase-deficient mouse hearts. *J Physiol* 2001;532:195-204.
53. Ma Y, Halade GV, Lindsey ML. Extracellular matrix and fibroblast communication following myocardial infarction. *J Cardiovasc Transl Res* 2012;5:848-57.
54. Bornstein P. Thrombospondins function as regulators of angiogenesis. *J Cell Commun Signal* 2009;3:189-200.
55. Rienks M, Papageorgiou AP, Frangogiannis NG, Heymans S. Myocardial extracellular matrix: an ever-changing and diverse entity. *Circ Res* 2014;114:872-88.
56. Frangogiannis NG. Matricellular proteins in cardiac adaptation and disease. *Physiol Rev* 2012;92:635-88.
57. Vanhoutte D, Heymans S. TIMPs and cardiac remodeling: 'Embracing the MMP-independent-side of the family'. *J Mol Cell Cardiol* 2010;48:445-53.
58. Freedman BR, Bade ND, Riggin CN et al. The (dys)functional extracellular matrix. *Biochim Biophys Acta* 2015;1853:3153-64.
59. Takawale A, Sakamuri SS, Kassiri Z. Extracellular matrix communication and turnover in cardiac physiology and pathology. *Compr Physiol* 2015;5:687-719.
60. Hansen NU, Genovese F, Leeming DJ, Karsdal MA. The importance of extracellular matrix for cell function and in vivo likeness. *Exp Mol Pathol* 2015;98:286-94.
61. Leask A. Focal Adhesion Kinase: A Key Mediator of Transforming Growth Factor Beta Signaling in Fibroblasts. *Adv Wound Care (New Rochelle)* 2013;2:247-249.

62. Gershlak JR, Black LD, 3rd. Beta 1 integrin binding plays a role in the constant traction force generation in response to varying stiffness for cells grown on mature cardiac extracellular matrix. *Exp Cell Res* 2015;330:311-24.
63. Corda S, Samuel JL, Rappaport L. Extracellular matrix and growth factors during heart growth. *Heart Fail Rev* 2000;5:119-30.
64. Leckband DE, le Duc Q, Wang N, de Rooij J. Mechanotransduction at cadherin-mediated adhesions. *Curr Opin Cell Biol* 2011;23:523-30.
65. Kohl P, Camelliti P, Burton FL, Smith GL. Electrical coupling of fibroblasts and myocytes: relevance for cardiac propagation. *J Electrocardiol* 2005;38:45-50.
66. Camelliti P, Borg TK, Kohl P. Structural and functional characterisation of cardiac fibroblasts. *Cardiovasc Res* 2005;65:40-51.
67. Bokel C, Brown NH. Integrins in development: moving on, responding to, and sticking to the extracellular matrix. *Dev Cell* 2002;3:311-21.
68. Israeli-Rosenberg S, Manso AM, Okada H, Ross RS. Integrins and integrin-associated proteins in the cardiac myocyte. *Circ Res* 2014;114:572-86.
69. Aplin AE, Howe A, Alahari SK, Juliano RL. Signal transduction and signal modulation by cell adhesion receptors: the role of integrins, cadherins, immunoglobulin-cell adhesion molecules, and selectins. *Pharmacol Rev* 1998;50:197-263.
70. Schroer AK, Merryman WD. Mechanobiology of myofibroblast adhesion in fibrotic cardiac disease. *J Cell Sci* 2015;128:1865-75.
71. Akker van den F, Deddens JC, Doevendans PA, Sluijter JP. Cardiac stem cell therapy to modulate inflammation upon myocardial infarction. *Biochim Biophys Acta* 2013;1839:2449-58.
72. Nicoletti A, Michel JB. Cardiac fibrosis and inflammation: interaction with hemodynamic and hormonal factors. *Cardiovasc Res* 1999;41:532-43.
73. Frangogiannis NG. Regulation of the inflammatory response in cardiac repair. *Circ Res* 2012;110:159-73.
74. Yang F, Liu YH, Yang XP, Xu J, Kapke A, Carretero OA. Myocardial infarction and cardiac remodelling in mice. *Exp Physiol* 2002;87:547-55.
75. van Nieuwenhoven FA, Turner NA. The role of cardiac fibroblasts in the transition from inflammation to fibrosis following myocardial infarction. *Vascul Pharmacol* 2013;58:182-8.
76. Kong P, Christia P, Frangogiannis NG. The pathogenesis of cardiac fibrosis. *Cell Mol Life Sci* 2014;71:549-74.
77. Ma Y, Yabluchanskiy A, Lindsey ML. Neutrophil roles in left ventricular remodeling following myocardial infarction. *Fibrogenesis Tissue Repair* 2013;6:11.
78. Czubryt MP. Common threads in cardiac fibrosis, infarct scar formation, and wound healing. *Fibrogenesis Tissue Repair* 2012;5:19.
79. Schaper J, Speiser B. The extracellular matrix in the failing human heart. *Basic Res Cardiol* 1992;87 Suppl 1:303-9.
80. Leask A. Getting to the heart of the matter: new insights into cardiac fibrosis. *Circ Res* 2015;116:1269-76.
81. Dobaczewski M, Gonzalez-Quesada C, Frangogiannis NG. The extracellular matrix as a modulator of the inflammatory and reparative response following myocardial infarction. *J Mol Cell Cardiol* 2010;48:504-11.
82. Weber KT, Janicki JS, Shroff SG, Pick R, Chen RM, Bashey RI. Collagen remodeling of the pressure-overloaded, hypertrophied nonhuman primate myocardium. *Circ Res* 1988;62:757-65.
83. Boudina S, Abel ED. Diabetic cardiomyopathy revisited. *Circulation* 2007;115:3213-23.

84. Factor SM, Bhan R, Minase T, Wolinsky H, Sonnenblick EH. Hypertensive-diabetic cardiomyopathy in the rat: an experimental model of human disease. *Am J Pathol* 1981;102:219-28.
85. Jellis C, Wright J, Kennedy D et al. Association of imaging markers of myocardial fibrosis with metabolic and functional disturbances in early diabetic cardiomyopathy. *Circ Cardiovasc Imaging* 2011;4:693-702.
86. Konduracka E, Gackowski A, Rostoff P, Galicka-Latala D, Frasik W, Piwowarska W. Diabetes-specific cardiomyopathy in type 1 diabetes mellitus: no evidence for its occurrence in the era of intensive insulin therapy. *Eur Heart J* 2007;28:2465-71.
87. Marijianowski MM, Teeling P, Mann J, Becker AE. Dilated cardiomyopathy is associated with an increase in the type I/type III collagen ratio: a quantitative assessment. *J Am Coll Cardiol* 1995;25:1263-72.
88. Brooks A, Schinde V, Bateman AC, Gallagher PJ. Interstitial fibrosis in the dilated non-ischaemic myocardium. *Heart* 2003;89:1255-6.
89. Schwarz F, Flameng W, Schaper J, Hehrlein F. Correlation between myocardial structure and diastolic properties of the heart in chronic aortic valve disease: effects of corrective surgery. *Am J Cardiol* 1978;42:895-903.
90. Weber KT, Brilla CG. Pathological hypertrophy and cardiac interstitium. Fibrosis and renin-angiotensin-aldosterone system. *Circulation* 1991;83:1849-65.
91. de Haas HJ, Arbustini E, Fuster V, Kramer CM, Narula J. Molecular imaging of the cardiac extracellular matrix. *Circ Res* 2014;114:903-15.
92. van den Borne SW, Diez J, Blankesteyn WM, Verjans J, Hofstra L, Narula J. Myocardial remodeling after infarction: the role of myofibroblasts. *Nat Rev Cardiol* 2010;7:30-7.
93. Deb A, Ubil E. Cardiac fibroblast in development and wound healing. *J Mol Cell Cardiol* 2014;70:47-55.
94. Weber KT, Sun Y, Bhattacharya SK, Ahokas RA, Gerling IC. Myofibroblast-mediated mechanisms of pathological remodeling of the heart. *Nat Rev Cardiol* 2013;10:15-26.
95. Gabbiani G. The myofibroblast in wound healing and fibrocontractive diseases. *J Pathol* 2003;200:500-3.
96. Hinz B, Phan SH, Thannickal VJ et al. Recent developments in myofibroblast biology: paradigms for connective tissue remodeling. *Am J Pathol* 2012;180:1340-55.
97. Manner J. Does the subepicardial mesenchyme contribute myocardioblasts to the myocardium of the chick embryo heart? A quail-chick chimera study tracing the fate of the epicardial primordium. *Anat Rec* 1999;255:212-26.
98. Visconti RP, Markwald RR. Recruitment of new cells into the postnatal heart: potential modification of phenotype by periostin. *Ann N Y Acad Sci* 2006;1080:19-33.
99. Kis K, Liu X, Hagood JS. Myofibroblast differentiation and survival in fibrotic disease. *Expert Rev Mol Med* 2011;13:e27.
100. Lajiness JD, Conway SJ. Origin, development, and differentiation of cardiac fibroblasts. *J Mol Cell Cardiol* 2014;70:2-8.
101. Wynn TA, Barron L. Macrophages: master regulators of inflammation and fibrosis. *Semin Liver Dis* 2010;30:245-57.
102. Christia P, Bujak M, Gonzalez-Quesada C et al. Systematic characterization of myocardial inflammation, repair, and remodeling in a mouse model of reperfused myocardial infarction. *J Histochem Cytochem* 2013;61:555-70.
103. Yong KW, Li Y, Huang G et al. Mechanoregulation of cardiac myofibroblast differentiation: implications for cardiac fibrosis and therapy. *Am J Physiol Heart Circ Physiol* 2015;309:H532-42.

104. Leask A. Potential therapeutic targets for cardiac fibrosis: TGFbeta, angiotensin, endothelin, CCN2, and PDGF, partners in fibroblast activation. *Circ Res* 2010;106:1675-80.
105. Lal H, Ahmad F, Zhou J et al. Cardiac fibroblast glycogen synthase kinase-3beta regulates ventricular remodeling and dysfunction in ischemic heart. *Circulation* 2014;130:419-30.
106. Thannickal VJ, Lee DY, White ES et al. Myofibroblast differentiation by transforming growth factor-beta1 is dependent on cell adhesion and integrin signaling via focal adhesion kinase. *J Biol Chem* 2003;278:12384-9.
107. Sarrazy V, Koehler A, Chow ML et al. Integrins alphavbeta5 and alphavbeta3 promote latent TGF-beta1 activation by human cardiac fibroblast contraction. *Cardiovasc Res* 2014;102:407-17.
108. Wipff PJ, Rifkin DB, Meister JJ, Hinz B. Myofibroblast contraction activates latent TGF-beta1 from the extracellular matrix. *J Cell Biol* 2007;179:1311-23.
109. Goumans MJ, Liu Z, ten Dijke P. TGF-beta signaling in vascular biology and dysfunction. *Cell Res* 2009;19:116-27.
110. Leask A, Abraham DJ. TGF-beta signaling and the fibrotic response. *FASEB J* 2004;18:816-27.
111. Trojanowska M. Noncanonical transforming growth factor beta signaling in scleroderma fibrosis. *Curr Opin Rheumatol* 2009;21:623-9.
112. Rosenkranz S. TGF-beta1 and angiotensin networking in cardiac remodeling. *Cardiovasc Res* 2004;63:423-32.
113. Dashwood MR, Abraham D. Endothelin: from bench to bedside and back. *Pharmacol Res* 2011;63:445-7.
114. Chen S, Evans T, Mukherjee K, Karmazyn M, Chakrabarti S. Diabetes-induced myocardial structural changes: role of endothelin-1 and its receptors. *J Mol Cell Cardiol* 2000;32:1621-9.
115. Rhee S, Grinnell F. P21-activated kinase 1: convergence point in PDGF- and LPA-stimulated collagen matrix contraction by human fibroblasts. *J Cell Biol* 2006;172:423-32.
116. Jinnin M, Ihn H, Mimura Y, Asano Y, Yamane K, Tamaki K. Regulation of fibrogenic/fibrolytic genes by platelet-derived growth factor C, a novel growth factor, in human dermal fibroblasts. *J Cell Physiol* 2005;202:510-7.
117. Tuuminen R, Nykanen AI, Krebs R et al. PDGF-A, -C, and -D but not PDGF-B increase TGF-beta1 and chronic rejection in rat cardiac allografts. *Arterioscler Thromb Vasc Biol* 2009;29:691-8.
118. Zhao H, Li X, Zhao S et al. Microengineered in vitro model of cardiac fibrosis through modulating myofibroblast mechanotransduction. *Biofabrication* 2014;6:045009.
119. Galie PA, Westfall MV, Stegemann JP. Reduced serum content and increased matrix stiffness promote the cardiac myofibroblast transition in 3D collagen matrices. *Cardiovasc Pathol* 2011;20:325-33.
120. Engler AJ, Sen S, Sweeney HL, Discher DE. Matrix elasticity directs stem cell lineage specification. *Cell* 2006;126:677-89.
121. Burgess ML, Terracio L, Hirozane T, Borg TK. Differential integrin expression by cardiac fibroblasts from hypertensive and exercise-trained rat hearts. *Cardiovasc Pathol* 2002;11:78-87.
122. Okada H, Lai NC, Kawaraguchi Y et al. Integrins protect cardiomyocytes from ischemia/reperfusion injury. *J Clin Invest* 2013;123:4294-308.

123. Bouzeghrane F, Mercure C, Reudelhuber TL, Thibault G. Alpha8beta1 integrin is upregulated in myofibroblasts of fibrotic and scarring myocardium. *J Mol Cell Cardiol* 2004;36:343-53.
124. Thompson SA, Blazeski A, Copeland CR et al. Acute slowing of cardiac conduction in response to myofibroblast coupling to cardiomyocytes through N-cadherin. *J Mol Cell Cardiol* 2014;68:29-37.
125. Aisagbonhi O, Rai M, Ryzhov S, Atria N, Feoktistov I, Hatzopoulos AK. Experimental myocardial infarction triggers canonical Wnt signaling and endothelial-to-mesenchymal transition. *Dis Model Mech* 2011;4:469-83.
126. Majkut S, Dingal PC, Discher DE. Stress sensitivity and mechanotransduction during heart development. *Curr Biol* 2014;24:R495-501.
127. Hinz B. The extracellular matrix and transforming growth factor-beta1: Tale of a strained relationship. *Matrix Biol* 2015;47:54-65.
128. Piersma B, Bank RA, Boersema M. Signaling in Fibrosis: TGF-beta, WNT, and YAP/TAZ Converge. *Front Med (Lausanne)* 2015;2:59.
129. Liu F, Lagares D, Choi KM et al. Mechanosignaling through YAP and TAZ drives fibroblast activation and fibrosis. *Am J Physiol Lung Cell Mol Physiol* 2015;308:L344-57.
130. Mannaerts I, Leite SB, Verhulst S et al. The Hippo pathway effector YAP controls mouse hepatic stellate cell activation. *J Hepatol* 2015;63:679-88.
131. Calvo F, Ege N, Grande-Garcia A et al. Mechanotransduction and YAP-dependent matrix remodelling is required for the generation and maintenance of cancer-associated fibroblasts. *Nat Cell Biol* 2013;15:637-46.
132. Hirt MN, Hansen A, Eschenhagen T. Cardiac tissue engineering: state of the art. *Circ Res* 2014;114:354-67.
133. Akins RE, Jr., Rockwood D, Robinson KG, Sandusky D, Rabolt J, Pizarro C. Three-dimensional culture alters primary cardiac cell phenotype. *Tissue Eng Part A* 2010;16:629-41.
134. Saini H, Navaei A, Van Putten A, Nikkhah M. 3D cardiac microtissues encapsulated with the co-culture of cardiomyocytes and cardiac fibroblasts. *Adv Healthc Mater* 2015;4:1961-71.
135. Kaese S, Verheule S. Cardiac electrophysiology in mice: a matter of size. *Front Physiol* 2012;3:345.
136. Chu X, Bleasby K, Evers R. Species differences in drug transporters and implications for translating preclinical findings to humans. *Expert Opin Drug Metab Toxicol* 2013;9:237-52.
137. Albin A, Pennesi G, Donatelli F, Cammarota R, De Flora S, Noonan DM. Cardiotoxicity of anticancer drugs: the need for cardio-oncology and cardio-oncological prevention. *J Natl Cancer Inst* 2010;102:14-25.
138. Ott HC, Matthiesen TS, Goh SK et al. Perfusion-decellularized matrix: using nature's platform to engineer a bioartificial heart. *Nat Med* 2008;14:213-21.
139. Wang RM, Christman KL. Decellularized myocardial matrix hydrogels: In basic research and preclinical studies. *Adv Drug Deliv Rev* 2016;96:77-82.
140. Guyette JP, Charest JM, Mills RW et al. Bioengineering Human Myocardium on Native Extracellular Matrix. *Circ Res* 2016;118:56-72.
141. Vunjak Novakovic G, Eschenhagen T, Mummery C. Myocardial tissue engineering: in vitro models. *Cold Spring Harb Perspect Med* 2014;4:a014076.
142. Jeong B, Kim SW, Bae YH. Thermosensitive sol-gel reversible hydrogels. *Adv Drug Deliv Rev* 2002;54:37-51.

143. Aubin H, Nichol JW, Hutson CB et al. Directed 3D cell alignment and elongation in microengineered hydrogels. *Biomaterials* 2010;31:6941-6951.
144. Nichol JW, Koshy ST, Bae H, Hwang CM, Yamanlar S, Khademhosseini A. Cell-laden microengineered gelatin methacrylate hydrogels. *Biomaterials* 2010;31:5536-44.
145. Wang C, Varshney RR, Wang DA. Therapeutic cell delivery and fate control in hydrogels and hydrogel hybrids. *Adv Drug Deliv Rev* 2010;62:699-710.
146. Davis ME, Hsieh PC, Takahashi T et al. Local myocardial insulin-like growth factor 1 (IGF-1) delivery with biotinylated peptide nanofibers improves cell therapy for myocardial infarction. *Proc Natl Acad Sci U S A* 2006;103:8155-60.
147. Chen FM, Zhang M, Wu ZF. Toward delivery of multiple growth factors in tissue engineering. *Biomaterials* 2010;31:6279-308.
148. Eschenhagen T, Fink C, Remmers U et al. Three-dimensional reconstitution of embryonic cardiomyocytes in a collagen matrix: a new heart muscle model system. *FASEB J* 1997;11:683-94.
149. Black LD, 3rd, Meyers JD, Weinbaum JS, Shvelidze YA, Tranquillo RT. Cell-induced alignment augments twitch force in fibrin gel-based engineered myocardium via gap junction modification. *Tissue Eng Part A* 2009;15:3099-108.
150. Baar K, Birla R, Boluyt MO, Borschel GH, Arruda EM, Dennis RG. Self-organization of rat cardiac cells into contractile 3-D cardiac tissue. *FASEB J* 2005;19:275-7.
151. Discher DE, Janmey P, Wang YL. Tissue cells feel and respond to the stiffness of their substrate. *Science* 2005;310:1139-43.
152. Nunes SS, Miklas JW, Liu J et al. Biowire: a platform for maturation of human pluripotent stem cell-derived cardiomyocytes. *Nat Methods* 2013;10:781-7.
153. Tandon N, Marsano A, Cannizzaro C, Voldman J, Vunjak-Novakovic G. Design of electrical stimulation bioreactors for cardiac tissue engineering. *Conf Proc IEEE Eng Med Biol Soc* 2008;2008:3594-7.
154. Tandon N, Cannizzaro C, Chao PH et al. Electrical stimulation systems for cardiac tissue engineering. *Nat Protoc* 2009;4:155-73.
155. Radisic M, Park H, Shing H et al. Functional assembly of engineered myocardium by electrical stimulation of cardiac myocytes cultured on scaffolds. *Proc Natl Acad Sci U S A* 2004;101:18129-34.
156. You JO, Rafat M, Ye GJ, Auguste DT. Nanoengineering the heart: conductive scaffolds enhance connexin 43 expression. *Nano Lett* 2011;11:3643-8.
157. Shin SR, Jung SM, Zalabany M et al. Carbon-nanotube-embedded hydrogel sheets for engineering cardiac constructs and bioactuators. *ACS Nano* 2013;7:2369-80.
158. Marsano A, Maidhof R, Wan LQ et al. Scaffold stiffness affects the contractile function of three-dimensional engineered cardiac constructs. *Biotechnol Prog* 2010;26:1382-90.
159. Young JL, Engler AJ. Hydrogels with time-dependent material properties enhance cardiomyocyte differentiation in vitro. *Biomaterials* 2011;32:1002-9.
160. Dawson E, Mapili G, Erickson K, Taqvi S, Roy K. Biomaterials for stem cell differentiation. *Adv Drug Deliv Rev* 2008;60:215-28.
161. Bellis SL. Advantages of RGD peptides for directing cell association with biomaterials. *Biomaterials* 2011;32:4205-10.
162. Gonnerman EA, Kelkhoff DO, McGregor LM, Harley BA. The promotion of HL-1 cardiomyocyte beating using anisotropic collagen-GAG scaffolds. *Biomaterials* 2012;33:8812-21.
163. Duan Y, Liu Z, O'Neill J, Wan LQ, Freytes DO, Vunjak-Novakovic G. Hybrid gel composed of native heart matrix and collagen induces cardiac differentiation of human

- embryonic stem cells without supplemental growth factors. *J Cardiovasc Transl Res* 2011;4:605-15.
164. Hersel U, Dahmen C, Kessler H. RGD modified polymers: biomaterials for stimulated cell adhesion and beyond. *Biomaterials* 2003;24:4385-415.
 165. Zimmermann WH, Schneiderbanger K, Schubert P et al. Tissue engineering of a differentiated cardiac muscle construct. *Circ Res* 2002;90:223-30.
 166. Kleinman HK, McGarvey ML, Liotta LA, Robey PG, Tryggvason K, Martin GR. Isolation and characterization of type IV procollagen, laminin, and heparan sulfate proteoglycan from the EHS sarcoma. *Biochemistry* 1982;21:6188-93.
 167. Hansen A, Eder A, Bonstrup M et al. Development of a drug screening platform based on engineered heart tissue. *Circ Res* 2010;107:35-44.
 168. Khademhosseini A, Eng G, Yeh J et al. Microfluidic patterning for fabrication of contractile cardiac organoids. *Biomed Microdevices* 2007;9:149-57.
 169. Hjortnaes J, Camci-Unal G, Hutcheson JD et al. Directing valvular interstitial cell myofibroblast-like differentiation in a hybrid hydrogel platform. *Adv Healthc Mater* 2015;4:121-30.
 170. Khalil S, Sun W. Bioprinting endothelial cells with alginate for 3D tissue constructs. *J Biomech Eng* 2009;131:111002.
 171. Iyer RK, Chiu LL, Radisic M. Microfabricated poly(ethylene glycol) templates enable rapid screening of triculture conditions for cardiac tissue engineering. *J Biomed Mater Res A* 2009;89:616-31.
 172. Grover GN, Rao N, Christman KL. Myocardial matrix-polyethylene glycol hybrid hydrogels for tissue engineering. *Nanotechnology* 2014;25:014011.
 173. Freytes DO, O'Neill JD, Duan-Arnold Y, Wrona EA, Vunjak-Novakovic G. Natural cardiac extracellular matrix hydrogels for cultivation of human stem cell-derived cardiomyocytes. *Methods Mol Biol* 2014;1181:69-81.
 174. Singelyn JM, DeQuach JA, Seif-Naraghi SB, Littlefield RB, Schup-Magoffin PJ, Christman KL. Naturally derived myocardial matrix as an injectable scaffold for cardiac tissue engineering. *Biomaterials* 2009;30:5409-16.
 175. Seif-Naraghi SB, Singelyn JM, Salvatore MA et al. Safety and efficacy of an injectable extracellular matrix hydrogel for treating myocardial infarction. *Sci Transl Med* 2013;5:173ra25.
 176. Gaetani R, Yin C, Srikumar N et al. Cardiac derived extracellular matrix enhances cardiogenic properties of human cardiac progenitor cells. *Cell Transplant* 2015;25(9):1653-1663.
 177. Williams C, Budina E, Stoppel WL et al. Cardiac extracellular matrix-fibrin hybrid scaffolds with tunable properties for cardiovascular tissue engineering. *Acta Biomater* 2015;14:84-95.
 178. Fan D, Takawale A, Lee J, Kassiri Z. Cardiac fibroblasts, fibrosis and extracellular matrix remodeling in heart disease. *Fibrogenesis Tissue Repair* 2012;5:15.
 179. Ross RS, Borg TK. Integrins and the myocardium. *Circ Res* 2001;88:1112-9.
 180. Sonin DL, Wakatsuki T, Routhu KV et al. Protease-activated receptor 1 inhibition by SCH79797 attenuates left ventricular remodeling and profibrotic activities of cardiac fibroblasts. *J Cardiovasc Pharmacol Ther* 2013;18:460-75.
 181. Yue K, Trujillo-de Santiago G, Alvarez MM, Tamayol A, Annabi N, Khademhosseini A. Synthesis, properties, and biomedical applications of gelatin methacryloyl (GelMA) hydrogels. *Biomaterials* 2015;73:254-71.
 182. Zorlutuna P, Annabi N, Camci-Unal G et al. Microfabricated biomaterials for engineering 3D tissues. *Adv Mater* 2012;24:1782-804.

183. Van Den Bulcke AI, Bogdanov B, De Rooze N, Schacht EH, Cornelissen M, Berghmans H. Structural and rheological properties of methacrylamide modified gelatin hydrogels. *Biomacromolecules* 2000;1:31-8.
184. Weisel JW, Litvinov RI. Mechanisms of fibrin polymerization and clinical implications. *Blood* 2013;121:1712-9.
185. Syedain ZH, Weinberg JS, Tranquillo RT. Cyclic distension of fibrin-based tissue constructs: evidence of adaptation during growth of engineered connective tissue. *Proc Natl Acad Sci U S A* 2008;105:6537-42.
186. Ahmed TA, Dare EV, Hincke M. Fibrin: a versatile scaffold for tissue engineering applications. *Tissue Eng Part B Rev* 2008;14:199-215.
187. Rajangam T, An SS. Improved fibronectin-immobilized fibrinogen microthreads for the attachment and proliferation of fibroblasts. *Int J Nanomedicine* 2013;8:1037-49.
188. Hirt MN, Sorensen NA, Bartholdt LM et al. Increased afterload induces pathological cardiac hypertrophy: a new in vitro model. *Basic Res Cardiol* 2012;107:307.
189. Sun J, Tan H. Alginate-Based Biomaterials for Regenerative Medicine Applications. *Materials* 2013;6:1285-1309.
190. Kuo CK, Ma PX. Ionically crosslinked alginate hydrogels as scaffolds for tissue engineering: part 1. Structure, gelation rate and mechanical properties. *Biomaterials* 2001;22:511-21.
191. Augst AD, Kong HJ, Mooney DJ. Alginate hydrogels as biomaterials. *Macromol Biosci* 2006;6:623-33.
192. Rowley JA, Madlambayan G, Mooney DJ. Alginate hydrogels as synthetic extracellular matrix materials. *Biomaterials* 1999;20:45-53.
193. Shachar M, Tsur-Gang O, Dvir T, Leor J, Cohen S. The effect of immobilized RGD peptide in alginate scaffolds on cardiac tissue engineering. *Acta Biomater* 2011;7:152-62.
194. Sapir Y, Kryukov O, Cohen S. Integration of multiple cell-matrix interactions into alginate scaffolds for promoting cardiac tissue regeneration. *Biomaterials* 2011;32:1838-47.
195. Sapir Y, Cohen S, Friedman G, Polyak B. The promotion of in vitro vessel-like organization of endothelial cells in magnetically responsive alginate scaffolds. *Biomaterials* 2012;33:4100-9.
196. Zieber L, Or S, Ruvinov E, Cohen S. Microfabrication of channel arrays promotes vessel-like network formation in cardiac cell construct and vascularization in vivo. *Biofabrication* 2014;6:024102.
197. Li J, Guan J. Hydrogels for Cardiac Tissue Engineering. *Polymers* 2011;3:740-761.
198. Bearinger JP, Terrettaz S, Michel R et al. Chemisorbed poly(propylene sulphide)-based copolymers resist biomolecular interactions. *Nat Mater* 2003;2:259-64.
199. Jongpaiboonkit L, King WJ, Lyons GE et al. An adaptable hydrogel array format for 3-dimensional cell culture and analysis. *Biomaterials* 2008;29:3346-56.
200. Nguyen QT, Hwang Y, Chen AC, Varghese S, Sah RL. Cartilage-like mechanical properties of poly (ethylene glycol)-diacrylate hydrogels. *Biomaterials* 2012;33:6682-90.
201. Wang H, Haeger SM, Kloxin AM, Leinwand LA, Anseth KS. Redirecting valvular myofibroblasts into dormant fibroblasts through light-mediated reduction in substrate modulus. *PLoS One* 2012;7:e39969.
202. Caspi O, Lesman A, Basevitch Y et al. Tissue engineering of vascularized cardiac muscle from human embryonic stem cells. *Circ Res* 2007;100:263-72.
203. Janmey PA, Miller RT. Mechanisms of mechanical signaling in development and disease. *J Cell Sci* 2011;124:9-18.

204. Berry MF, Engler AJ, Woo YJ et al. Mesenchymal stem cell injection after myocardial infarction improves myocardial compliance. *Am J Physiol Heart Circ Physiol* 2006;290:H2196-203.
205. Engler AJ, Carag-Krieger C, Johnson CP et al. Embryonic cardiomyocytes beat best on a matrix with heart-like elasticity: scar-like rigidity inhibits beating. *J Cell Sci* 2008;121:3794-802.
206. Bhana B, Iyer RK, Chen WL et al. Influence of substrate stiffness on the phenotype of heart cells. *Biotechnol Bioeng* 2010;105:1148-60.
207. Fink C, Ergun S, Kralisch D, Remmers U, Weil J, Eschenhagen T. Chronic stretch of engineered heart tissue induces hypertrophy and functional improvement. *FASEB J* 2000;14:669-79.
208. Severs NJ. The cardiac muscle cell. *Bioessays* 2000;22:188-99.
209. Tandon N, Marsano A, Maidhof R, Wan L, Park H, Vunjak-Novakovic G. Optimization of electrical stimulation parameters for cardiac tissue engineering. *J Tissue Eng Regen Med* 2011;5:e115-25.
210. Thompson SA, Copeland CR, Reich DH, Tung L. Mechanical coupling between myofibroblasts and cardiomyocytes slows electric conduction in fibrotic cell monolayers. *Circulation* 2011;123:2083-93.
211. Chiu YW, Chen WP, Su CC, Lee YC, Hsieh PH, Ho YL. The arrhythmogenic effect of self-assembling nanopeptide hydrogel scaffolds on neonatal mouse cardiomyocytes. *Nanomedicine* 2014;10:1065-73.
212. Deng X, Mercer PF, Scotton CJ, Gilchrist A, Chambers RC. Thrombin induces fibroblast CCL2/JE production and release via coupling of PAR1 to Galphaq and cooperation between ERK1/2 and Rho kinase signaling pathways. *Mol Biol Cell* 2008;19:2520-33.
213. Galie PA, Russell MW, Westfall MV, Stegemann JP. Interstitial fluid flow and cyclic strain differentially regulate cardiac fibroblast activation via AT1R and TGF-beta1. *Exp Cell Res* 2012;318:75-84.
214. Takahashi K, Tanabe K, Ohnuki M et al. Induction of pluripotent stem cells from adult human fibroblasts by defined factors. *Cell* 2007;131:861-72.
215. Doevendans PA. Humanise basic research in cardiology from here! *Neth Heart J* 2009;17:271.
216. Goumans MJ, de Boer TP, Smits AM et al. TGF-beta1 induces efficient differentiation of human cardiomyocyte progenitor cells into functional cardiomyocytes in vitro. *Stem Cell Res* 2007;1:138-49.
217. Mummery CL, Zhang J, Ng ES, Elliott DA, Elefanty AG, Kamp TJ. Differentiation of human embryonic stem cells and induced pluripotent stem cells to cardiomyocytes: a methods overview. *Circ Res* 2012;111:344-58.
218. Martins AM, Vunjak-Novakovic G, Reis RL. The current status of iPS cells in cardiac research and their potential for tissue engineering and regenerative medicine. *Stem Cell Rev* 2014;10:177-90.
219. Zhang YS, Aleman J, Arneri A et al. From cardiac tissue engineering to heart-on-a-chip: beating challenges. *Biomed Mater* 2015;10:034006.
220. Bhatia SN, Ingber DE. Microfluidic organs-on-chips. *Nat Biotechnol* 2014;32:760-72.
221. Ribas J, Sadeghi H, Manbachi A et al. Cardiovascular Organ-on-a-Chip Platforms for Drug Discovery and Development. *Applied In Vitro Toxicology* Jun 2016;2:82-96.

9

Anti-fibrotic effects of cardiac progenitor cells in a 3D-model of human cardiac fibrosis

J.C. Deddens

E.A. Mol

M.M. Ferrer

L.W. van Laake

V. Verhage

C.C. Bouten

P.A. Doevendans

J. Hjortnaes

J.P.G. Sluijter

In preparation

Abstract

Purpose: Excessive matrix deposition upon cardiac injury results in perpetuation of pro-fibrotic signaling and contributes to progressive adverse cardiac remodeling during heart failure. It has recently been recognized that cardiac cell therapy for chronic ischemic heart failure might target fibroblast behavior. However, the underlying processes are poorly defined. Therefore, we developed a three dimensional (3D), tunable model of cardiac fibrosis to allow for physiologically relevant *in vitro* testing of fibroblast-behavior upon cell therapy.

Methods: A photo-cross linkable hydrogel, composed of methacrylated gelatin (GelMA) combined with human fetal cardiac fibroblasts (hfCF), was used to study fibroblast characteristics. hfCF-laden gels were cultured for 7 days in normal or pro-fibrotic medium (2 ng/ml TGF- β_1). To determine possible paracrine effects of cardiac progenitor cells (CPC), hfCF were co-cultured with 1) CPC, 2) CPC conditioned medium (CM) or 3) CPC derived extracellular vesicles (EV). As a measure of hfCF activation, α -SMA and Col1a1 levels were analyzed by qPCR and immunohistochemistry.

Results: 3D culture of hfCF resulted in a quiescent cell behavior as demonstrated by a low α -SMA expression. However, TGF- β_1 -mediated simulation of a pro-fibrotic environment resulted in fibroblast activation and accumulation of extracellular matrix. This fibrogenic response was strongly attenuated upon co-culture with CPC. The anti-fibrotic effect was transferable via co-cultured CPC-CM and reproduced by isolated CPC-EV.

Conclusions: We showed the suitability of hfCF-laden GelMA as a 3D culture model to study aspects of cardiac fibrosis and the possibility to modulate responses. Moreover, our approach demonstrated inhibitory effects of CPC and CPC-EV on matrix remodeling *in vitro*.

Introduction

Chronic heart failure (CHF) is a major public health issue and with a 5-year mortality rate of 50% still the leading cause of cardiovascular death [1]. Treatment of CHF with existing pharmacological agents, including β -adrenergic blockers and ACE inhibitors, may slow down the progression of the disease [2]. Moreover, promising results of the novel angiotensin receptor-neprilysin inhibitor LCZ696 (PARADIGM-HF trial) [3, 4] and the observed reverse remodeling in heart failure patients receiving mechanical support [5] contribute to the notion that improvement can be achieved by targeting cardiac fibrosis [6, 7]. The involved progressive adverse cardiac remodeling is primarily mediated by cardiac fibroblasts (CF) [8–10], which are activated upon myocardial injury and fail to undergo apoptosis. They remain constitutively active and the subsequent ongoing deposition of extracellular matrix (ECM) results in perpetuation of pro-fibrotic signaling and cardiac fibrosis [11, 12].

It has recently been suggested that cardiac cell therapy for chronic ischemic heart failure might target fibroblast behavior [13]. Several studies showed tentatively positive results of cardiac progenitor cells (CPC) on cardiac function, which is reflected in a lower scar mass [14, 15]. It was demonstrated that CPC reduced fibroblast proliferation and attenuated pro-fibrotic signaling in a rat model of chronic MI [16]. However, the mechanism of action is largely unknown and hampered by a lack of mechanistic *in vivo* insights in matrix remodeling and the role of associated CF.

Cellular behavior is strongly influenced by the biochemical and mechanical characteristics of their ECM environment [17] and three-dimensional (3D) models have been proposed to study in more detail the biological, chemical and mechanical properties of living target tissues [18]. The ability to tune the mechanical properties of hydrogels, as previously described for gelatin methacrylate (GelMA), [19] makes the hydrogels attractive platforms to elucidate mechanisms involved in CF activation in a more physiologically relevant environment. In the current study, we investigated the potential of hfCF-laden GelMA as a platform to explore mechanisms involved

in ECM remodeling and regression of fibrosis by using CPC as a potential anti-fibrotic therapeutic.

Methods

Hydrogel fabrication and preparation

The synthesis of methacrylamide modified gelatin (GelMA) has been described before [19]. Briefly, type A gelatin from porcine skin (Sigma Aldrich) was dissolved in phosphate buffered saline (PBS; Gibco) at 60°C to obtain a 10% w/v gelatin solution. Gelatin was methacrylated (80%) by addition of 8 ml methacrylic anhydride (MA) to 100ml gelatin solution at a rate of 0.5ml/min under stirred conditions at 50°C. After that, GelMA was diluted and dialyzed against distilled water to remove salts and methacrylic acid. Finally, the solution was lyophilized and stored at -80°C until further use.

Hydrogels were prepared by radical cross-linking of solubilized (GelMA) in PBS (Gibco) in the presence of a photo-initiator (PI; Igracure 2595, CIBA chemicals). In short, 1mg of PI was dissolved in 1ml of PBS at 80°C. Lyophilized GelMA macromere (5% w/v or 10% w/v) was mixed with 0.1% PBS-PI and incubated for 15 minutes at 80°C to dissolve completely. The pre-polymer solution was allowed to cool down to 37°C before either direct use or resuspension with pelleted hfCF in a final concentration of 10 million cells/ml. 30 µl of pre-polymer solution was pipetted on a petri dish between two spacers with a height of 0.45 mm and was covered with a sterile glass slide. The pre-polymer solution was cross-linked by exposure to UV light (wavelength 365nm) of 2.5W/cm² at 10 cm distance for 50 seconds as calibrated with a R2000 UV Radiometer (Omnicure R2000 Series 2000, Excelitas Technologies®). The hydrogel was removed from the glass plate and immersed in PBS at room temperature (RT). Empty gels were incubated in PBS at 37°C for 24h before mechanical testing and hydrogel swelling analysis. Cell-laden hydrogels were directly transferred to a wells-plate containing warm culture medium.

Hydrogel characterization

The compressive modulus of (empty) GelMA hydrogels was assessed through a micro-indentation test, applying unconfined compression at a constant rate (0.1 mm/s) up to a strain

of 70% at room temperature (RT). Compressive modulus was then calculated from the linear region of the stress-strain curve.

Hydrogel swelling analysis was performed directly after incubation at 37°C in PBS. Swollen GelMA hydrogels were weighted (ww) and subsequently dried by lyophilization in order to determine its mass-swelling ratio. After that, dried weight (wd) of GelMA gels was obtained and swelling ratio (q) was calculated as $q = ww / wd$.

Cell culture

For primary cell isolation, human fetal tissue was obtained by individual permission using standard informed consent procedures and prior approval of the ethics committees of the University Medical Center Utrecht and Leiden University Medical Center, the Netherlands. This in accordance with the principles outlined in the Declaration of Helsinki for the use of human tissue or subjects. Isolation of CPC was performed as described previously [20]. In short, fetal cardiac tissue was enzymatically digested and cells were isolated using Sca-1 conjugated magnetic beads. CPCs were cultured in SP++ (66% M199 (Gibco, 31150), 22% EGM-2 (Lonza, CC-4176), 10% fetal bovine serum (FBS) (Life-Tech, 102700), 1% Penicillin/Streptomycin (Invitrogen, 15140122), and 1% minimal essential medium nonessential amino acids (Gibco, 11140)) until 70-80% confluency and used for co-culture experiments at passage 14-18.

Human fetal cardiac fibroblasts (hfCF) were isolated by a simultaneously performed procedure. After subtraction of sca-1 positive cells, dissolved heart tissue was plated overnight (o/n) on tissue culture treated plastic to allow fibroblast to adhere. HfCF were cultured in fibroblast medium (FM) containing DMEM (4,5 g/L glucose; Gibco), 10% FBS and 1% P/S. Cells were cultured until 90% confluency and passaged in a 1:3 ratio before experimental use at passage 4-7. Cells were maintained at 5% CO₂, 20% O₂, 37°C. To obtain conditioned medium (CM), cell cultures were maintained for 2-3 days in a humidified atmosphere. The CM was directly used in experiments, or used for isolation of extracellular vesicles (EV).

Human microvascular endothelial cells (HMEC-1) were cultured as before in HMEC culture medium (MCDB131, 10% FBS, hydrocortisone (50 nM, Sigma, H6909-10), human endothelial growth factor (10 ng/ml, Peprotech, 016100-15-A), freshly added L-glutamine (200 nM, Gibco, 25030-024) and 1% P/S) [21].

HfCF-laden hydrogels were prepared as described above (day 0= D0) and maintained in a 1:1 mixture of SP++ and FM. Starting at day 1 (D1), gels were stimulated with TGF- β_1 (2 ng/ml; Peprotech, 100-21C) for the time of the experiment (up to 4, 7 or 14 days). At D0, CPCs were plated at a density of 10.000 cells/cm² in mixed medium. A transwell (0.4 μ m; Greiner bio-one) was used for co-culture experiments with CPCs and hfCF-laden hydrogels, where hydrogels were placed in the transwells at D1 and were maintained until D7. Medium, including CM and TGF- β_1 , was changed every other day. Control experiments were performed on tissue culture plastic in two dimensions (2D), with a cell density of 10.000 cells/cm².

Isolation of extracellular vesicles

To isolate extracellular vesicles (EV), including exosomes, CPC-CM was collected after 3 days of culture and EV were isolated by differential centrifugation (Beckmann Coulter LE-80K Optima), as described before [22]. In short, CM was centrifuged by subsequently 2,000 x g, 10,000 x g and 100,000 x g steps. The resulting 100,000 x g pellet was resuspended in PBS and centrifuged again at 100,000 x g. The washed EV pellet was resuspended in a small volume of PBS and the EV protein concentration was determined with the BCA protein assay kit (ThermoScientific). EV were stored at 4 °C and added to hfCF-laden GelMA in a concentration of 3 μ g/ml.

Characteristics of hfCF encapsulated in GelMA

Viability of hfCF cells within 5 or 10% (w/v) GelMA was assessed with the Live/Dead Viability kit for mammalian cells (Life Technologies), following manufacturer instructions. In brief, hfCF-laden hydrogels (day 1, 7, 14) were quickly rinsed in PBS and then incubated with 4 μ M Calcein AM and 2 μ M Ethidium Homodimer-1 for 20 minutes at 37°C. After incubation, the gels were washed with PBS and directly imaged using a confocal microscope (Zeiss LSM 700). At three different locations of each gel, z-stacks (3.3 μ m) were made and the resulting 2D projection stacks were used for quantification by manual counting live (green) versus red (dead) cells in Image J.

RNA isolation and quantitative real-time polymerase chain reaction

RNA was isolated from hfCF-laden GelMA hydrogels using the Nucleospin® RNA kit from Macherey-Nagel. After mechanical disruption in 1ml TriPure (Roche), (extracellular) debris was removed by centrifugation at 12.000 x g for 10 minutes. 200 μ l of chloroform was added to the supernatant and the aqueous phase was separated by centrifugation at 12.000 x g for 15 minutes. The liquid phase (~350 μ l) was mixed 1:1 with 70% ethanol and transferred to the isolation column after which the manufacturers indications were followed. Total RNA was treated with DNase (Qiagen) and reverse transcribed with the iScript Advanced cDNA synthesis kit (Bio-RAD). Quantitative polymerase chain reaction (qPCR) was performed in iCycler qPCR (Bio-Rad) using SYBR Green (BioRad) and specific primers for: GAPDH: F: 5'-ACAGTCAGCCGCATCTTC-3' and R: 5'-GCCCAATACGACCAAATC -3'; α -SMA: F: 5'-AGCCAGCCAAGCACTG-3' and R: 5'-CAAAGCCGGCCTTACAGAG-3'; collagen type 1 alpha chain 1 (COL1a1): F: 5'-TGCCATCAAAGTCTTCTGC-3' and R: 5'-CATACTCGAACYGGAATCCATC-3'; collagen type 3 (COL3): F: 5'-AGGGGAGCTGGCTACTTCTC-3' and R: 5'-GGACTGACCAAGATGGGAA-3'; metalloprotease 2 (MMP2): F: 5'-CCCACTGCGTTTTCTCGAAT-3'

and R: 5'-CAAAGGGGTATCCATCGCCAT-3'. Threshold cycle values (Ct) were analyzed and expression was quantified using the $2^{-\Delta\Delta C_t}$ method [23].

Histological analysis and immunofluorescent staining of human fibroblast laden hydrogels

HfCF-laden hydrogels were washed in PBS and fixed in 4% paraformaldehyde for 20 minutes. Before embedding in OCT (Tissue Tek), hydrogels were partly dehydrated in a 30% (w/v) sucrose solution overnight at 4°C. Cryosections of 7 μm were obtained and all images were taken with a fluorescent microscope system BX53 (Olympus).

Immunofluorescent staining for α -SMA and COL1a1 was performed using Alexa fluor 488 labeled anti-human α -SMA (A2547, 1:400, Sigma-Aldrich) and anti pro-collagen type 1 (SP1.D8, 1:50, DSHB), followed by incubation with an Alexa fluor 555 (Invitrogen, 1:1000) labeled secondary antibody. Sections were counterstained with Hoechst (33342).

Seeded and empty GelMA hydrogels with different macromere concentrations were stained with picosirius red (sigma Aldrich) to analyze the collagen composition of the matrix as measured by polarized light. Analysis of the images was performed manually using ImageJ Software. Collagen density is expressed as mean grey value, adjusted for area fraction [24].

Statistical analysis

Statistical analysis was performed by using GraphPad Prism 6.0 (Graphpad Software, La Jolla). Differences between two groups were analyzed using unpaired two-tailed Student's T-test. The one-way ANOVA with a Dunnett's post-hoc test was used to evaluate differences in multiple groups. $P < 0.05$ was considered statically significant. Data is presented as mean \pm SEM, unless indicated otherwise.

Results

Cardiac fibroblast characterization and construction of a cardiac ECM model with GelMA hydrogel

In this study, we aimed to construct a human model of cardiac fibrosis using hfCFs and a gelatin-based hydrogel (GelMA) (Figure 1a). Therefore, hfCF were isolated by enzymatic digestion of human fetal cardiac tissue. Immunofluorescent staining confirmed the fibroblast-like phenotype of hfCF as shown by protein expression of vimentin and fibroblast specific protein (FSP). In addition, hfCF expressed Col1a1, Col3a1 and α -SMA (Supplemental Figure 1a-b), demonstrating their secretory nature.

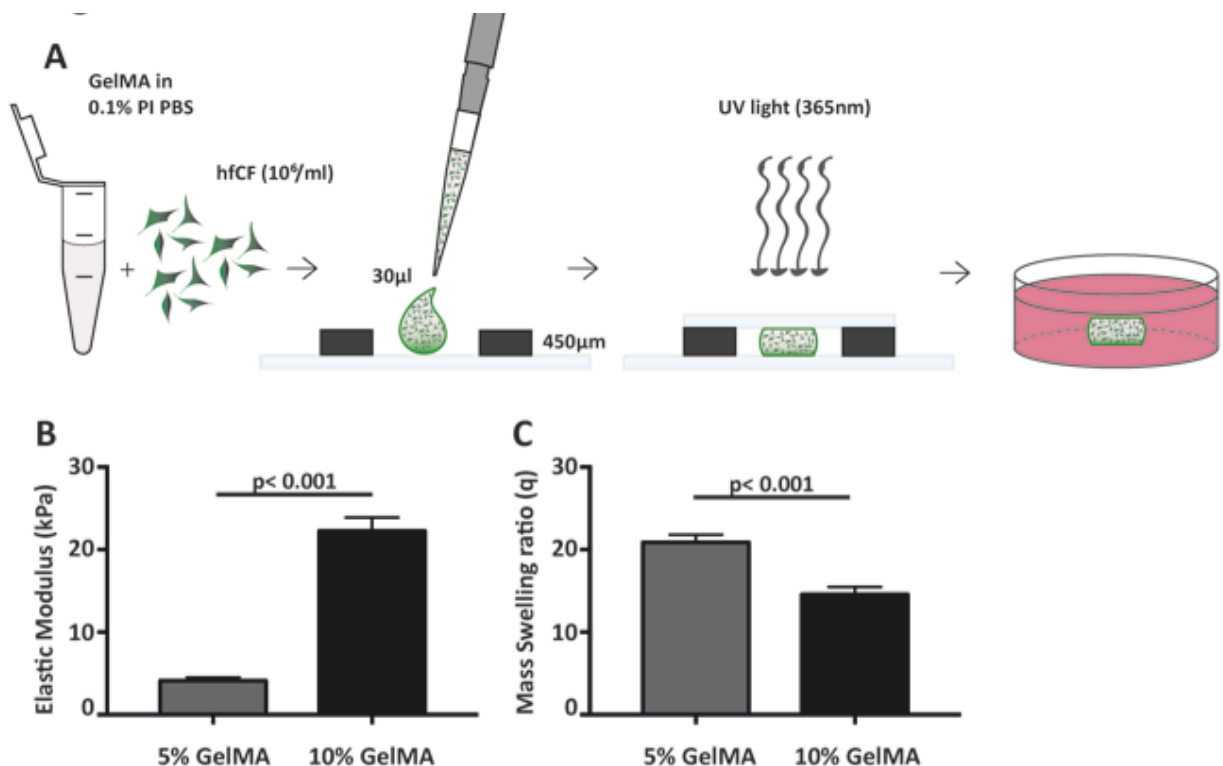


Figure 1. Fabrication and mechanical characterization of GelMA hydrogels. A) Schematic overview of hydrogel preparation. B) Compressive properties of GelMA hydrogels upon varying gel percentage (w/v), 5% GelMA (n= 3) and 10% GelMA (n=4), p < 0.001. C) Mass Swelling ratio (q) differed with GelMA concentration, 5% GelMA (n= 5) and 10% GelMA (n=6), p < 0.001. q= wet weight/ dry weight.

Since 5% and 10% GelMA (w/v) hydrogels have previously been demonstrated to be compatible with cells of mesenchymal origin [25], we have determined the mechanical properties of both preparations (Figure 1b). Mechanical analysis demonstrated an elastic modulus of 4.1 ± 0.4 kPa for 5% GelMA and 22.3 ± 1.6 kPa for 10% GelMA ($p < 0.001$). In addition, the mass swelling ratio (q), inversely proportional to pore size, was determined and showed a higher q for 5% than for 10% GelMA (20.9 ± 0.9 vs. 14.6 ± 0.9 , $p < 0.001$; Figure 1c). Subsequently, hfCF were encapsulated in GelMA and their compatibility, as measured by cell spreading and viability, was examined. After encapsulation, hfCF were homogeneously distributed throughout the GelMA (Figure 2a) and showed an average viability of 89% in 5% GelMA (Supplemental Figure 2a-b) and 85% in 10% GelMA (Figure 2b-c). After 7 days of culture, hfCF encapsulated in 5% GelMA had an elongated phenotype as visualized by life/death staining. In contrast, a more rounded phenotype was observed for hfCF encapsulated in 10% GelMA. However, cells in 10% GelMA did appear attached to the matrix after 7 days of culture and remained alive until day 14.

Cardiac fibroblasts remain quiescent in 3D culture constructs and respond to pro-fibrotic stimulation with TFG- β_1

To determine the influence of a 3D culture environment, the expression of α -SMA and Col1a1 of encapsulated hfCF was analyzed and compared to 2D cultured hfCF. Conventional 2D culture resulted in a higher α -SMA expression (7.4 ± 6.8) than 3D culture in 5% (2.5 ± 2.1 , $p = 0.06$) or 10% GelMA (2.5 ± 1.8), Figure 3a. In contrast, no difference was observed for Col1a1 in 2D culture (1.7 ± 2) versus 3D culture in 5% GelMA (1.5 ± 10.1) and 10% GelMA (1.5 ± 1.8), Figure 3b.

Considering the observations that hfCF behavior is more constant in 10% GelMA hydrogels and that 10% GelMA hydrogels mimic the mechanical characteristics of the myocardial tissue better [26], we used 10% GelMA for follow-up.

To examine the potential of hfCF-laden 10% GelMA as a model for cardiac fibrosis, hfCF-laden hydrogels were cultured for 7 days in medium containing 2 ng/ml TGF- β_1 . Upon stimulation with TGF- β_1 , the expression of α -SMA increased 2.1 fold ($p < 0.001$, Figure 3c). In addition, the expression of Col1a1 increased 10.3 times ($p < 0.01$, Figure 3d), which was reflected in a higher number of Col1a1+ cells ($21 \pm 7\%$ vs. $35 \pm 9\%$, $p = 0.01$, Figure 3e-f) and an accumulation of deposited collagen fibers as measured by picrosirius red staining (0.02 ± 0.003 vs. 0.04 ± 0.016 , mean grey value, $p = 0.1$, Figure 3g-h).

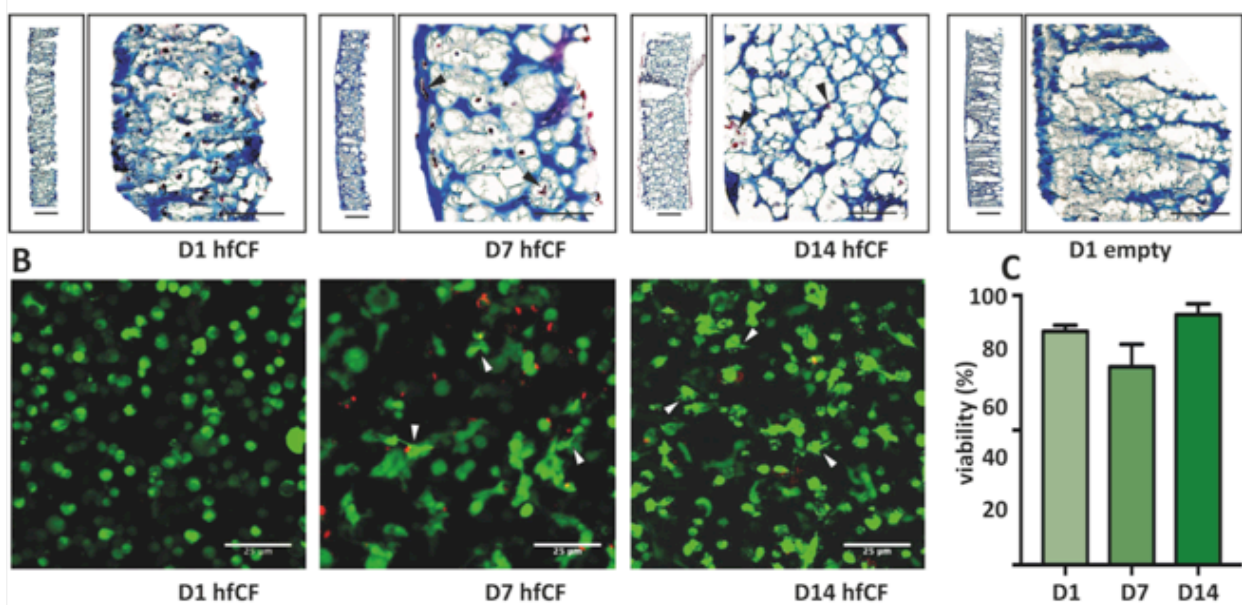
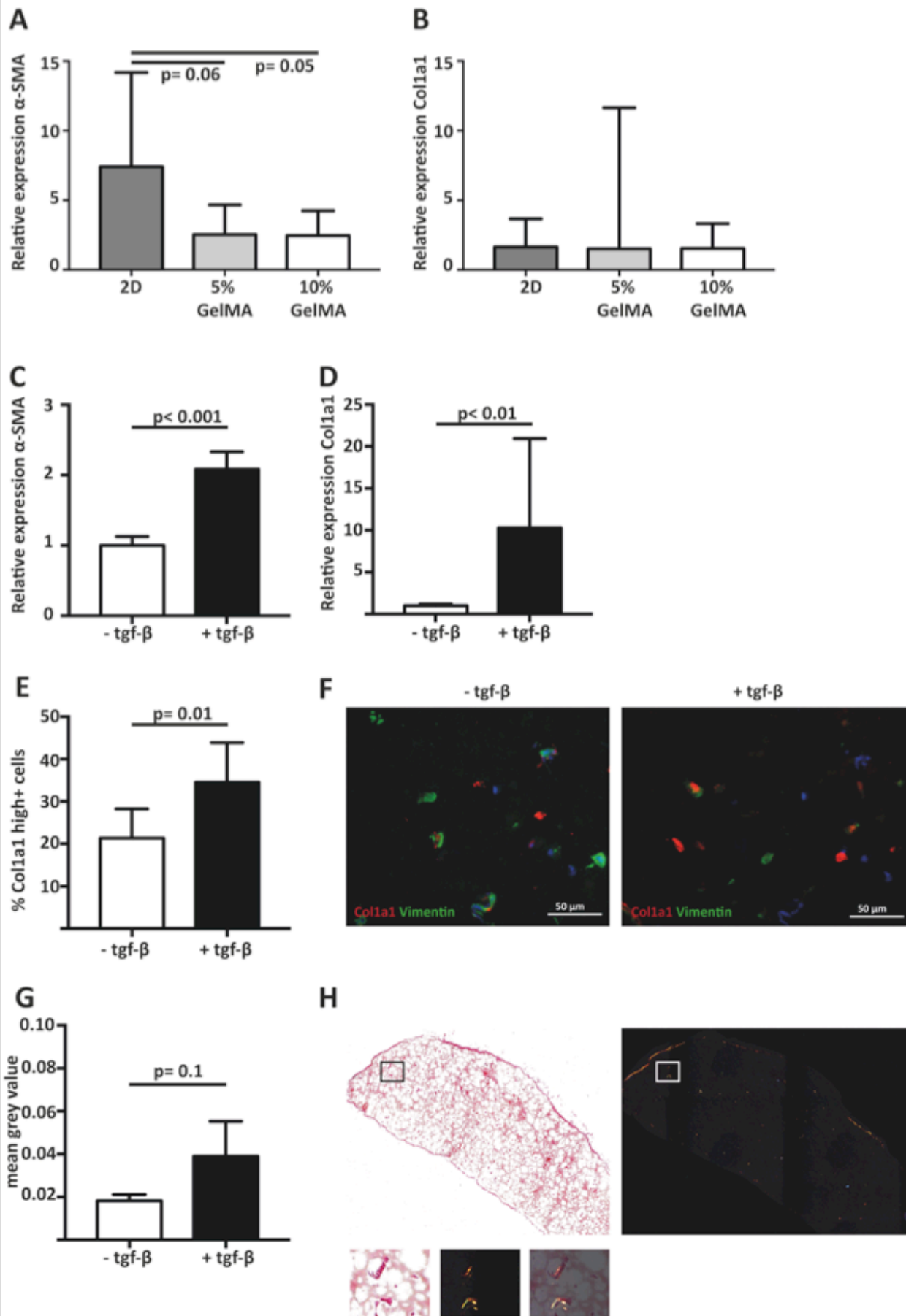


Figure 2. Encapsulation of human fetal cardiac fibroblasts in GelMA hydrogel. A) Trichrome blue staining demonstrating homogenous encapsulation of hfCF. **B)** Life/Death staining showed that cells remained viable (>80%) in the GelMA hydrogels, up till 14 days. Directly after encapsulation, cells displayed a rounded morphology, whereas after 7 days cells appeared more spread and attached to the matrix (arrowheads). Life cells= Green. Death cells= Red. Bars= 25 μ m.

Figure 3. Stimulating cardiac fibroblast mediated fibrosis with the pro-fibrotic mediator TGF- β_1 . **(A)** Gene expression analysis showed that hfCF had a lower α -SMA expression after 7 days of culture when encapsulated in 5% (w/v) or 10% (w/v) GelMA. **(B)** Col1a1 expression remained equal. Values are relative to the corresponding 2D cultured hfCF at day 1, $n = 8$. **(C)** Stimulation with TGF- β_1 (for 7 days) resulted in a 2.1-fold increase in α -SMA expression and **(D)** a 10.3-fold increase in Col1a1 expression, $n = 8$. **(E-F)** Immunohistochemistry showed an increased number of Col1a1+ cells upon stimulation with TGF- β_1 (Col1a1= red, vimentin= green, nuclei= blue) and **(G)** an accumulation of collagen fibers in the extracellular matrix, as demonstrated by **(H)** picrosirius red staining and quantification. $n = 4$. Left panel= bright field image. Right panel= polarized light image. Lower panel shows a higher magnification of the box.



Co-culture of hfCF-laden hydrogels with CPC attenuate fibrotic response

To analyze if CPC are able to inhibit the observed fibrotic response via paracrine signaling, hfCF-laden GelMA were co-cultured with CPC using a transwell system (Figure 4a). After 7 days of co-culture with CPC, α -SMA expression of hfCF was attenuated. Stimulation with TGF- β_1 resulted in an increased α -SMA expression, whereas in co-culture with CPC this increase was not observed (Figure 4b). Co-culture with CPC resulted in a 2.7-fold lower α -SMA expression ($p=0.04$) and a 3.3 fold lower Col1a1 expression ($p=ns$, Figure 4c). This inhibitory effect was not observed in a similar set-up with HMEC, as non-cardiac control cells (Supplemental Figure 4). Interestingly, an even more pronounced effect was observed in conditions without TGF- β_1 stimulation; α -SMA expression decreased 8.5-fold ($p=0.02$). In addition, this apparent decrease in activity of hfCF in the presence of CPC was also demonstrated by the amount of Col1a1 positive hfCF in the hydrogels (Figure 4d), which showed a non-significant 2-fold decrease in co-culture conditions.

Paracrine effects are (in part) transferable

As the co-culture experiments were performed using transwell systems of 0.4 μm , the observed inhibitory effect of CPC on hfCF is consequently paracrine. To confirm this paracrine nature and to test its stability, co-culture conditioned media (co-CM) experiments were performed to determine if the inhibitory effect of CPC-hfCF co-culture is transferable to 'native' hfCF-laden GelMA (Figure 5a). To this intent, expression of α -SMA was measured, which showed that co-CM caused a similar inhibition of the fibrotic response (Figure 5b).

Since an inhibitory effect occurred in the non-stimulated conditions as well, we hypothesized that CM of CPC only would result in a consubstantial outcome. Therefore, CPC-CM was collected and was added freshly to hfCF gels. However, CPC-CM did not result in an inhibitory effect, but caused a 1.9-fold increase in α -SMA expression upon stimulation with TGF- β_1 ($p=0.01$; Figure 5c). To further examine the contribution of known paracrine mediators, EV were isolated from CPC-CM and applied to hfCF-laden GelMA in regular culture medium. Interestingly,

supplementation with CPC-EV resulted in a decrease in hfCF activation in both native (1.7-fold, $p = 0.01$; Figure 5d) and TFG- β_1 -stimulated (1.4-fold, $p = \text{ns}$; Figure 5e) conditions.

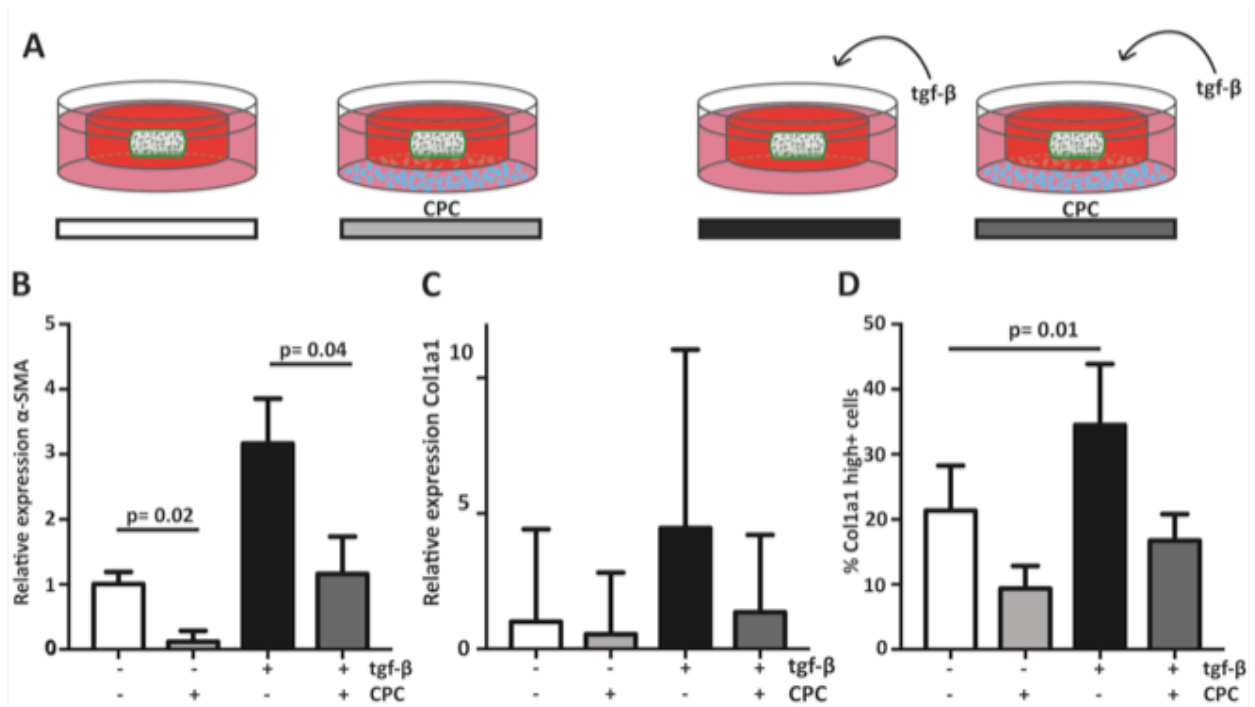


Figure 4. Cardiac progenitor cells attenuate cardiac fibroblast mediated fibrotic response. (A) Schematic overview of experimental set-up. **(B)** CPC significantly attenuated α -SMA expression in hfCF-laden GelMA in culture conditions with or without 2 ng/ml TGF- β_1 stimulation. **(C)** Col1a1 expression appeared lower in co-culture conditions ($n = 11$) and **(D)** likewise, the amount of Col1a1+ cells was 2-fold lower in CPC treated gels.

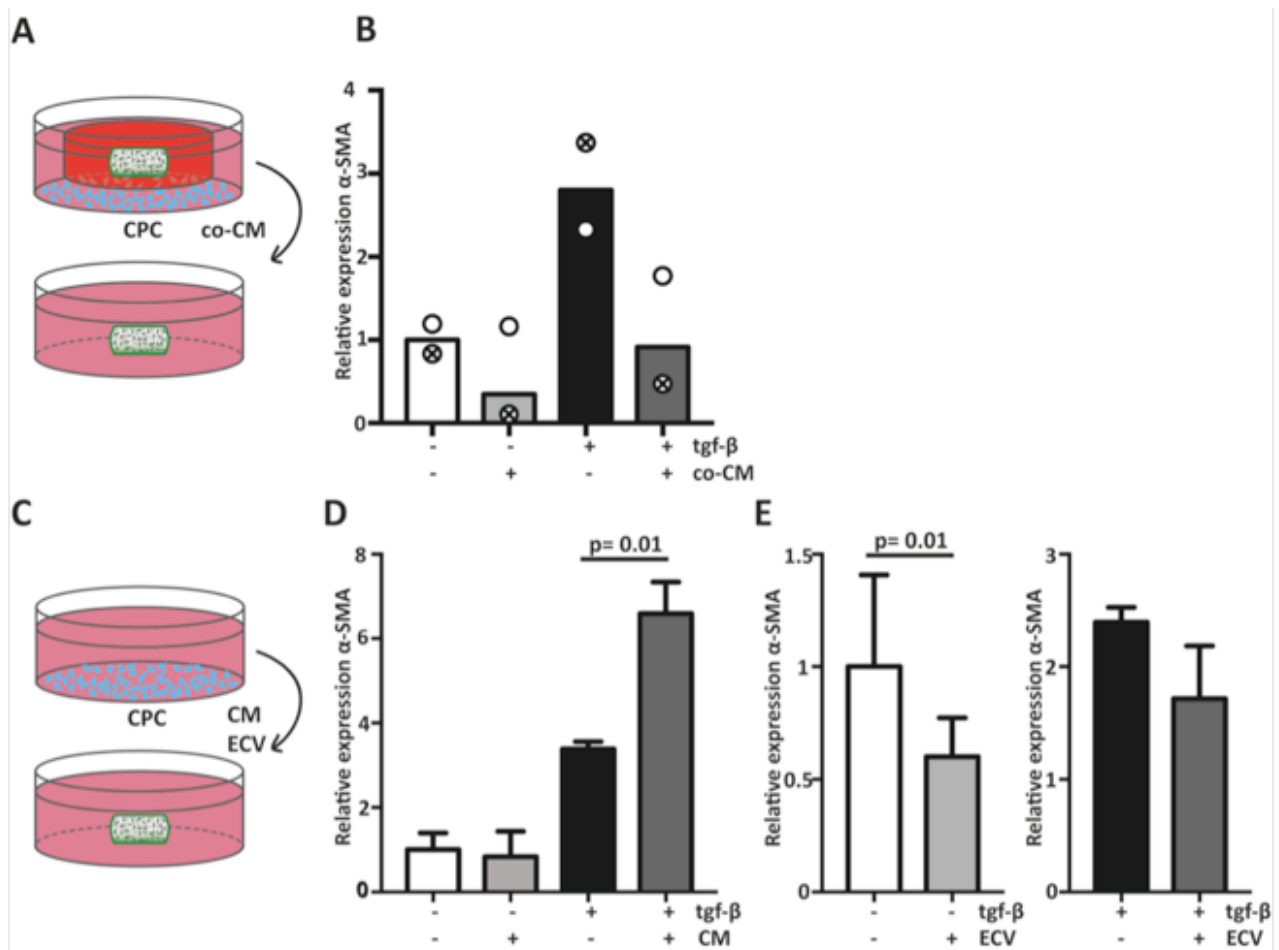


Figure 5. Cardiac progenitor cells act via paracrine mediators. (A) Schematic overview of experimental set-up of transfer of co-culture CM (co-CM) to a naïve hfCF-laden GelMA. **(B)** co-CM attenuated α -SMA expression in hfCF-laden GelMA in culture conditions with or without 2 ng/ml TGF- β_1 , (n= 2). **(C)** Schematic overview of experimental set-up of treatment with CPC-CM or CPC-EV. **(D)** CPC-CM did not influence hfCF activation in an un-stimulated condition, however, in pro-fibrotic medium the expression of α -SMA was significantly increased, (n= 5). **(E)** Isolated CPC-EV showed similar effects as compared to co-cultured CM in normal (left graph) and pro-fibrotic medium (right graph).

Discussion

To examine the potential of 3D culture platforms for testing of possible anti-fibrotic therapeutics, we investigated the paracrine effects of CPC on hfCF-laden GelMA. Firstly, our data showed that 3D culture of hfCF resulted in a quiescent cell behavior as demonstrated by a relatively low α -SMA expression. This allowed us to reproducibly stimulate hfCF-laden GelMA with TGF- β_1 , which resulted in cell activation and accumulation of ECM. By using this novel tunable fibrotic model, we were able to investigate the potential therapeutic effect of CPC *in vitro* and found that these cells were potent inhibitors of the induced fibrotic response. Interestingly, despite the fact that pure CPC-CM caused the opposite effect, this inhibition could be reproduced by isolated EV.

Since fibrosis is an extracellular phenomenon, there is a high need for *in vitro* culture models that capture specific aspects, e.g. mechanical stiffness and composition of the complex ECM, to study the influence of CF in matrix remodeling [17, 18]. It is well known that during 2D cell culture, CF are activated by mechanical stress and consequently differentiate into a myofibroblast-like phenotype [7, 11]. Mechanical stiffness has long been thought to be directly related to the degree of differentiation of CF, as demonstrated by studies using substrates with a tunable stiffness [27–29]. However, it was demonstrated recently that valvular interstitial cells encapsulated in soft 5% GelMA spontaneously differentiated towards a myofibroblast-phenotype [30]. Our results showed that hfCF were indeed less activated when cultured in a 3D environment, which in general has a lower matrix stiffness than 2D tissue culture plates, and remained sensitive for TGF- β_1 stimulation. Yet, we did not find an increased differentiation in our hfCF-laden 5% GelMA. This discrepancy can possibly be explained by the origin of fibroblasts, the duration of the experiment or slight differences in the degree of crosslinking [31]. In addition, the mRNA expression of Col1a1 in our experiments showed variable changes upon encapsulation. Since we did find stable results at the protein level, the indecisive results at

the transcriptional level might be indicative for proteins with a high turnover. Our results accentuate the importance of choosing the appropriate model and demonstrated the potential of this model by its controllable cellular and extracellular fibrotic response.

With the emerging demand for appropriate culture systems for disease modeling and drug testing, tissue engineered models of cardiac fibrosis are indispensable for advancements in the field of anti-fibrotic therapeutics. As illustrated by Sonin *et al* [32], 3D models are valuable tools to study fibrotic remodeling with comparable results between *in vivo* and the 3D model. In addition, Galie *et al* [33] used a 3D fibrosis model to illuminate the role of mesenchymal stem cells (MSC) on myofibroblast transition and showed the inhibitory effect of MSC on the fibrotic response. Likewise, it has been observed that cardiospheres downregulate the TGF- β pathway in fibroblasts in a paracrine fashion [34, 35]. This is in line with the paracrine hypothesis [36] postulating that stem cells exert their actions via paracrine mediators.

It can be hypothesized that CPC interfere with the TGF- β cascade, however, broad targeting of TGF- β activities appears not to be beneficial [6] and is challenged by the miscellaneous functions of the TGF- β pathway and its dual role in both activation and inhibition of the fibrogenic response, via ALK5 and ALK1, respectively [37]. Although we observed a strong attenuation of the fibrogenic response upon CPC treatment, we also noticed that stimulation with TGF- β_1 did result in a relative increase in hfCF activation. This result bolsters the idea that CPC probably modulate, instead of completely attenuate, the TGF- β pathway.

The applicability of CPC as anti-fibrotic treatment was further investigated by examining CPC-CM and CPC-EV and resulted in an ambiguous outcome. Apparently, the composition of CPC-CM is divergent and changes upon co-culture; addition of CPC-CM to CF displayed a stimulatory effect, whereas co-culture of CF with CPC resulted in an overall inhibition of the fibrogenic response. Accordingly, Tesliou *et al* [34] demonstrated a strong inhibitory effect of CPC and CPC-CM on fibroblast activation, which was mediated by secreted endoglin. In contrast to CPC,

CPC-CM did not act via inhibition of the ALK5 pathway and thereby supports the notion that the CPC-CF co-culture itself directly influences CPC secretion. Interestingly, this divergent effect was not observed for CPC-EV, which showed a co-culture independent inhibitory effect. Therefore, it appears reasonable to speculate that hfCF in a 3D environment have an active cellular communication [38] and mediate a fine balance between the stimulatory ALK5 and inhibitory ALK1 pathway, via paracrine factors.

Of note, the beneficial effects of CPC co-culture in this study were evident and as recently supported by others [39], presumably mediated by CPC-EV. Focusing on the inhibitory effects of CPC-EV opens new doors to stem cell treatment by means of their non-living nature and therefore better manageability as off-the-shelf therapeutic [38]. Identification of the responsible EV-related inhibitors of fibrosis would even take the therapeutic potential to a higher level. In order to find further evidence for EV-mediated modulation of the TGF- β pathway, we performed a miRNA array and did a subsequent pathway analysis on the CPC-EV, with the TGF- β pathway as central nominator. Analysis of the miRNA content of CPC-EV revealed that 32 miRNAs target 69 mRNAs, including the TGF- β receptor and Smad7. Potential therapeutic miRNAs, e.g. miRNA-21 [40] and miRNA-29 [41], were found in the complex network (Supplemental Figure 4). Since we did not yet test the anti-fibrotic potential of EV-related miRNAs, they can serve as starting points for future experiments to provide insight in the mechanism of action of EV and endoglin mediated anti-fibrotic effects

The strengths of the current study include the use of a tunable 3D platform to study the fibrotic response of fibroblasts. As demonstrated by the smaller variation in outcome parameters and the lower expression of cell-activation markers, a more naïve phenotype was obtained for hfCF cultured in 3D, which resulted in reproducible results in response to TGF- β_1 . In addition, the additive value of focusing on the fibroblasts in this single culture model provides

valuable mechanical information and is constructive for future tissue engineered models. This model does not, however, bring a complete representation of the human situation. To capture the full process of cardiac fibrosis, it is important to incorporate e.g. cardiomyocytes and endothelial cells, since it has been demonstrated that the interactions between these cell types are crucial for cardiac homeostasis [42]. Since fibroblasts in the heart are subjected to beating, it would be of interest to subject static fibrosis models to cyclic strain to elucidate the role of mechanical stress on the behavior of fibroblasts and the development of fibrosis.

Taken together, our data suggest that hfCF-laden GelMA are suitable as model for cardiac fibrosis, thereby providing a platform for pathophysiological studies and drug testing. Moreover, our data shows that CPC have a strong paracrine anti-fibrotic effect and emphasize the concept of cardiac fibrosis as a powerful tunable therapeutic target.

Acknowledgements

We thank Rob Driessen for his excellent technical assistance. We acknowledge the support from Innovation and the Netherlands CardioVascular Research Initiative (CVON): The Dutch Heart Foundation, Dutch Federation of University Medical Centers, the Netherlands Organization for Health Research and Development and the Royal Netherlands Academy of Science. Additionally, the ZonMW Translational Adult Stem Cell grant 1161002016

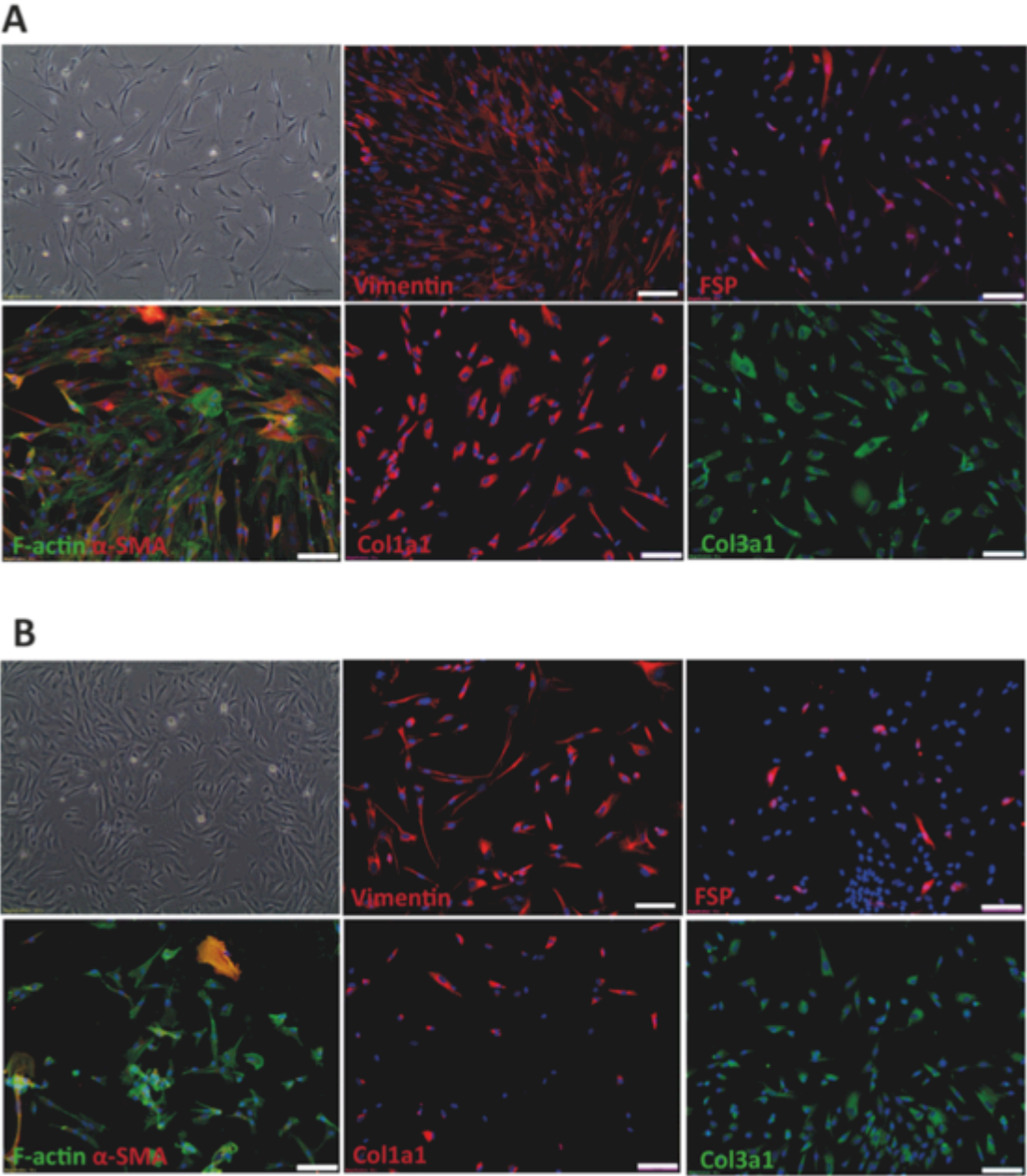
References

1. Mozaffarian D, Benjamin EJ, Go AS, et al. Heart Disease and Stroke Statistics-2016 Update: A Report From the American Heart Association. *Circulation* 2015;133:e38–e360.
2. McMurray JJ V, Adamopoulos S, Anker SD, et al. ESC guidelines for the diagnosis and treatment of acute and chronic heart failure 2012: The Task Force for the Diagnosis and Treatment of Acute and Chronic Heart Failure 2012 of the European Society of Cardiology. Developed in collaboration with the Heart. *Eur J Heart Fail* 2012;14:803–69.
3. McMurray JJV, Packer M, Desai AS, et al. Angiotensin–Neprilysin Inhibition versus Enalapril in Heart Failure. *N Engl J Med* 2014;371:140830040023009.
4. von Lueder TG, Wang BH, Kompa AR, et al. Angiotensin receptor neprilysin inhibitor LCZ696 attenuates cardiac remodeling and dysfunction after myocardial infarction by reducing cardiac fibrosis and hypertrophy. *Circ Heart Fail* 2015;8:71–8.
5. Birks EJ, George RS. Molecular changes occurring during reverse remodelling following left ventricular assist device support. *J Cardiovasc Transl Res* 2010;3:635–42.
6. Leask A. Potential therapeutic targets for cardiac fibrosis: TGFbeta, angiotensin, endothelin, CCN2, and PDGF, partners in fibroblast activation. *Circ Res* 2010;106:1675–80.
7. Weber KT, Sun Y, Bhattacharya SK, Ahokas RA, Gerling IC. Myofibroblast-mediated mechanisms of pathological remodelling of the heart. *Nat Rev Cardiol* 2013;10:15–26.
8. Hill JA, Olson EN. Cardiac plasticity. *N Engl J Med* 2008;358:1370–1380.
9. Li A-H, Liu PP, Villarreal FJ, Garcia RA. Dynamic changes in myocardial matrix and relevance to disease: translational perspectives. *Circ Res* 2014;114:916–27.
10. Dobaczewski M, Chen W, Frangogiannis NG. Transforming growth factor (TGF)- β signaling in cardiac remodeling. *J Mol Cell Cardiol* 2011;51:600–6.
11. Tomasek JJ, Gabbiani G, Hinz B, Chaponnier C, Brown RA. Myofibroblasts and mechano-regulation of connective tissue remodelling. *Nat Rev Mol Cell Biol* 2002;3:349–63.
12. Hinz B, Phan SH, Thannickal VJ, et al. Recent developments in myofibroblast biology: paradigms for connective tissue remodeling. *Am J Pathol* 2012;180:1340–55.
13. Patel AN, Silva F, Winters AA. Stem cell therapy for heart failure. *Heart Fail Clin* 2015;11:275–86.
14. Zwetsloot PP, Végh AM, Jansen Of Lorkeers SJ, et al. Cardiac Stem Cell Treatment in Myocardial Infarction: A Systematic Review and Meta-Analysis of Preclinical Studies. *Circ Res* 2016.
15. Tang X-L, Li Q, Rokosh G, et al. Long-Term Outcome of Administration of c-kit^{POS} Cardiac Progenitor Cells After Acute Myocardial Infarction: Transplanted Cells Do Not Become Cardiomyocytes, but Structural and Functional Improvement and Proliferation of Endogenous Cells Persist for At Lea. *Circ Res* 2016.
16. Yee K, Malliaras K, Kanazawa H, et al. Allogeneic cardiospheres delivered via percutaneous transendocardial injection increase viable myocardium, decrease scar size, and attenuate cardiac dilatation in porcine ischemic cardiomyopathy. *PLoS One* 2014;9:e113805.
17. Griffith LG, Swartz MA. Capturing complex 3D tissue physiology in vitro. *Nat Rev Mol Cell Biol* 2006;7:211–24.
18. Pampaloni F, Reynaud EG, Stelzer EHK. The third dimension bridges the gap between cell culture and live tissue. *Nat Rev Mol Cell Biol* 2007;8:839–45.
19. Nichol JW, Koshy ST, Bae H, Hwang CM, Yamanlar S, Khademhosseini A. Cell-laden microengineered gelatin methacrylate hydrogels. *Biomaterials* 2010;31:5536–5544.
20. Smits AM, van Vliet P, Metz CH, et al. Human cardiomyocyte progenitor cells differentiate into functional mature cardiomyocytes: an in vitro model for studying human cardiac physiology and pathophysiology. *Nat Protoc* 2009;4:232–243.
21. Vrijisen KR, Sluijter JPG, Schuchardt MWL, et al. Cardiomyocyte progenitor cell-derived exosomes stimulate migration of endothelial cells. *J Cell Mol Med* 2010;14:1064–70.
22. Théry C, Amigorena S, Raposo G, Clayton A. Isolation and characterization of exosomes from

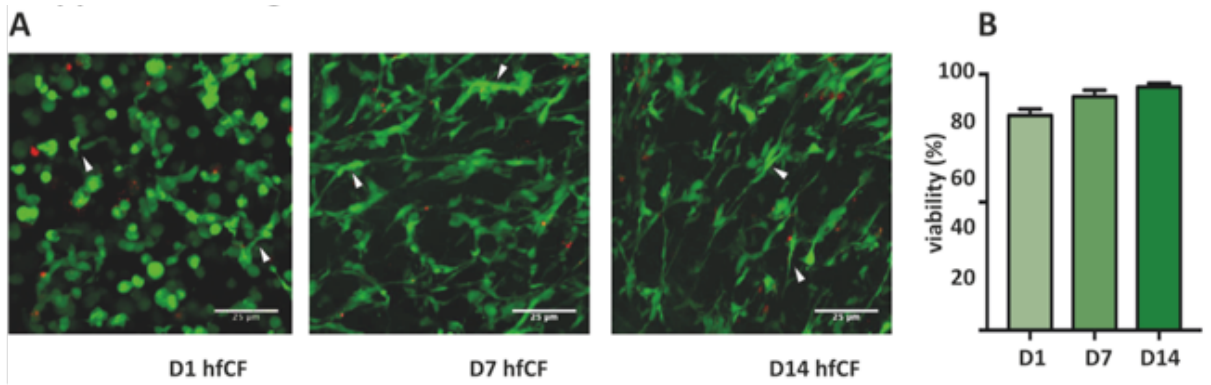
- cell culture supernatants and biological fluids. *Curr Protoc Cell Biol* 2006;Chapter 3:Unit 3.22.
23. Sluijter JPG, Smeets MB, Velema E, Pasterkamp G, de Kleijn DP V. Increased collagen turnover is only partly associated with collagen fiber deposition in the arterial response to injury. *Cardiovasc Res* 2004;61:186–95.
 24. Sluijter JPG, Verloop RE, Pulskens WPC, et al. Involvement of furin-like proprotein convertases in the arterial response to injury. *Cardiovasc Res* 2005;68:136–43.
 25. Hjortnaes J, Camci-Unal G, Hutcheson JD, et al. Directing valvular interstitial cell myofibroblast-like differentiation in a hybrid hydrogel platform. *Adv Healthc Mater* 2015;4:121–130.
 26. Berry MF, Engler AJ, Woo YJ, et al. Mesenchymal stem cell injection after myocardial infarction improves myocardial compliance. *Am J Physiol Heart Circ Physiol* 2006;290:H2196-203.
 27. Discher DE, Janmey P, Wang Y-L. Tissue cells feel and respond to the stiffness of their substrate. *Science* 2005;310:1139–1143.
 28. Wang H, Haeger SM, Kloxin AM, Leinwand LA, Anseth KS. Redirecting valvular myofibroblasts into dormant fibroblasts through light-mediated reduction in substrate modulus. *PLoS One* 2012;7:e39969.
 29. Zhao H, Li X, Zhao S, et al. Microengineered in vitro model of cardiac fibrosis through modulating myofibroblast mechanotransduction. *Biofabrication* 2014;6:45009.
 30. Hjortnaes J, Camci-Unal G, Hutcheson JD, et al. Directing valvular interstitial cell myofibroblast-like differentiation in a hybrid hydrogel platform. *Adv Healthc Mater* 2015;4:121–30.
 31. Cha C, Liechty WB, Khademhosseini A, Peppas NA. Designing biomaterials to direct stem cell fate. *ACS Nano* 2012;6:9353–8.
 32. Sonin DL, Wakatsuki T, Routhu K V, et al. Protease-activated receptor 1 inhibition by SCH79797 attenuates left ventricular remodeling and profibrotic activities of cardiac fibroblasts. *J Cardiovasc Pharmacol Ther* 2013;18:460–475.
 33. Galie PA, Stegemann JP. Injection of mesenchymal stromal cells into a mechanically stimulated in vitro model of cardiac fibrosis has paracrine effects on resident fibroblasts. *Cytotherapy* 2014;16:906–14.
 34. Tseliou E, Reich H, de Couto G, et al. Cardiospheres reverse adverse remodeling in chronic rat myocardial infarction: roles of soluble endoglin and Tgf- β signaling. *Basic Res Cardiol* 2014;109:443.
 35. Tseliou E, de Couto G, Terrovitis J, et al. Angiogenesis, cardiomyocyte proliferation and anti-fibrotic effects underlie structural preservation post-infarction by intramyocardially-injected cardiospheres. *PLoS One* 2014;9:e88590.
 36. Gneocchi M, Zhang Z, Ni A, Dzau VJ. Paracrine mechanisms in adult stem cell signaling and therapy. *Circ Res* 2008;103:1204–19.
 37. Goumans M-J, Liu Z, ten Dijke P. TGF-beta signaling in vascular biology and dysfunction. *Cell Res* 2009;19:116–27.
 38. Sluijter JPG, Verhage V, Deddens JC, van den Akker F, Doevendans PA. Microvesicles and exosomes for intracardiac communication. *Cardiovasc Res* 2014;102:302–11.
 39. Tseliou E, Fouad J, Reich H, et al. Fibroblasts Rendered Antifibrotic, Antiapoptotic, and Angiogenic by Priming With Cardiosphere-Derived Extracellular Membrane Vesicles. *J Am Coll Cardiol* 2015;66:599–611.
 40. Thum T, Gross C, Fiedler J, et al. MicroRNA-21 contributes to myocardial disease by stimulating MAP kinase signalling in fibroblasts. *Nature* 2008;456:980–4.
 41. van Rooij E, Olson EN. Searching for miR-acles in cardiac fibrosis. *Circ Res* 2009;104:138–40.
 42. Leask A. Getting to the Heart of the Matter: New Insights Into Cardiac Fibrosis. *Circ Res* 2015;116:1269–1276.

Supplementary

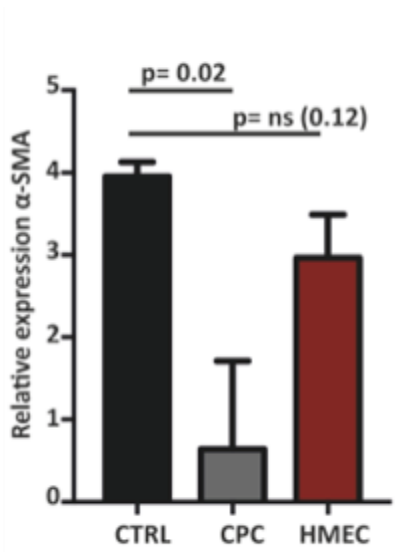
Supplementary Figures



Supplementary Figure 1. Immunofluorescent stainings of human fetal cardiac fibroblasts (hfCF). hfCF were isolated from different donor hearts (A and B) and stained positive for the mesenchymal marker vimentin and partly positive for fibroblast specific protein (FSP). They also expressed collagen type 1a1 (Col1a1), collagen type 3a1 (Col3a1) and alpha smooth muscle actin (α -SMA). Nuclei were stained with Hoechst (blue). Bar= 100 μ m.

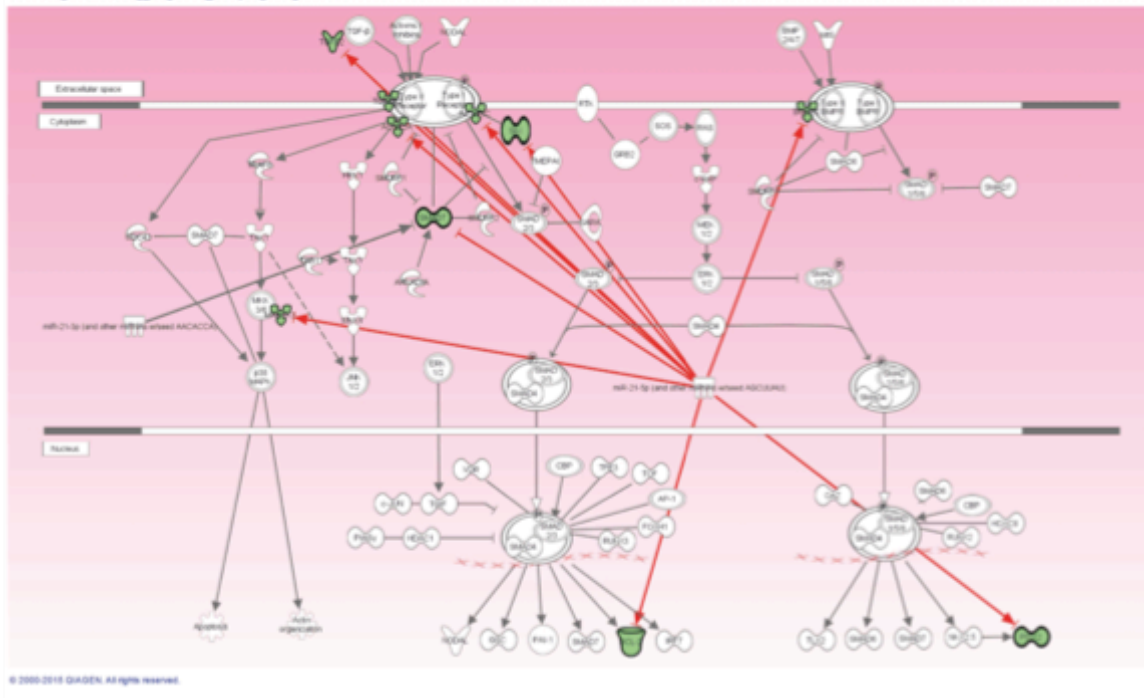


Supplementary Figure 2. Viability of hfCF in 5% GelMA. Life/Death staining showed that cells had a high viability (>85%) in the GelMA hydrogels. Cell appeared attached to the matrix at day 1 and displayed an elongated phenotype at D7 and D14 (white arrowheads). Life cells= Green. Death cells= Red. Bars= 25 µm.



Supplementary Figure 3. Inhibitory effect of CPC is cell-specific.

α-SMA expression, as measure of hfCF activation, was inhibited upon co-culture with CPC, but not when co-cultured with HMEC. Gels were stimulated with TGF-β₁ and co-cultured for 7 days with either CPC or HMEC.



Supplementary Figure 4. Ingenuity pathway analysis of CPC-EV. Predicted network of miRNA-21 within the TGF- β pathway.

10

General discussion

General Discussion – A guide to improve clinical translational research

This thesis describes the use of novel preclinical and clinical study set-ups to facilitate advancements in diagnosis and treatment of ischemic heart disease. We reported on the early identification of patients with stable coronary artery disease (CAD) and evaluated the additive diagnostic value of circulating miRNAs for patients suspected of acute coronary syndrome (ACS) (Chapters 2, 3, 4). The results underline the importance of hypothesis driven discovery studies and the necessity for validation studies. Furthermore, we developed a novel murine model of chronic ischemic cardiac remodeling (Chapters 5, 6, 7) and a 3D *in vitro* model of cardiac fibrosis (Chapters 8, 9) to provide a platform to gain insight in the disease biology of the chronic manifestations of CAD and to identify new therapeutic targets. In particular, this thesis highlights the shortcomings of the currently used models and provides clinical translatable solutions to maximize potential therapeutic efficacy of cardiac cell therapy. Based on our findings, it can be concluded that to bridge the gap between basic science and clinical application a comprehensive approach is needed respecting the individual patient within the targeted disease population.

1. Thoughtful biomarker handling

Essential biomarker characteristics

A biomarker is defined as “a biological characteristic that can be objectively measured and evaluated as an indicator of normal biological processes, pathogenic processes, or pharmacologic responses to a therapeutic intervention” [1]. In general, the ideal biomarkers has several crucial properties, which we, in this thesis (chapters 2-4), evaluated for circulating miRNAs and extracellular vesicles (EV), including 1) high sensitivity and specificity for the disease of interest, 2) high reproducibility, 3) high stability, 4) measurable in linear proportion to injury or disease progression 5) directly measurable after disease onset, 6) a long biological half-life, and 7) advantages above the existing biomarkers [2, 3]. The intended use of biomarkers guide the importance of these characteristics [4]. To direct the use of biomarkers

towards application in cardiovascular diseases, it is important to realize that several pathophysiological pathways play a role in both stable and acute CAD, e.g. inflammation, endothelial dysfunction, hypoxic stress and cardiomyocyte injury [5, 6]. The recognition of a clear disease target will facilitate improvements in biomarker discovery, development and implementation.

Pathophysiology guided markers for CAD: 'fenestrae' biomarkers

As demonstrated in this thesis, high sensitivity is crucial for evaluation of stable angina pectoris at the level of the general practitioner, whereas high specificity is necessary for the diagnosis of ACS in the emergency department [2]. In addition, for the diagnosis of an acute event, it is pivotal to detect a biomarker as soon as possible. It is well known that the main release of cardiac Troponin I (cTnI), the 'gold standard' for cardiac injury, is a result of cardiomyocyte necrosis and the successive passive leakage of cellular constituents [7–9]. However, necrosis is not the first mechanism activated upon cardiac stress and as shown in [chapter 3](#), the detection of miRNAs and EV precede cTnI. Given the reported release of EV upon cellular stress (e.g. hypoxia, neurohormonal stimulation) and the post-transcriptional role of miRNAs, it seems very likely that the release of miRNAs and EV are the result of an active process regulated by intracellular communication [10–13]. As we showed that the detection of circulating miRNAs strongly correlates with cTnI, an alternative explanation can be that, similar to the increasingly recognized release of cTnI as a result of early membrane permeabilization (e.g. inflammation [14]), it reflects a more passive process.

Despite the development of high sensitive and ultra-sensitive cTnI detection assays, the detected levels in patients with cardiac injury are not consistent enough to solve the diagnostic uncertainty in 25% of patients with suspected ACS [7, 15–18]. Therefore, the hypothesis that the release of miRNAs and EV are actively regulated might indicate a new class of 'fenestrae' biomarkers, which can add pathophysiology-based diagnostic information and strengthen the powerful cTnI ([chapter 2-3](#)). However, for gradual processes such as CAD the use of these

'fenestrae' biomarkers appear more complex ([chapter 4](#)). As described in this thesis, no additive value of circulating miRNAs for the diagnosis of myocardial ischemia could be observed.

Although promising in a discovery cohort, the potential markers could not be confirmed in the successive replication study, which clearly showed the lack of differential diagnostic power of circulating miRNAs for myocardial ischemia. We speculated that miRNAs, as effector and modulators of disease [19], are deregulated at an earlier time-point, resulting in a discordance with the onset of disease or clinical parameters. The gradual process of CAD might already be reflected in the reference group, cancelling out intergroup differences in miRNA expression.

Ideally, the expression pattern of potential biomarkers for myocardial ischemia should be assessed during the course of the disease in a prospective study to gain insight in its onset [20]. Furthermore, as demonstrated in [chapter 3](#) of this thesis, the use of specific EV subgroups can be exploited to narrow the numerous opportunities and provide for more specific markers [21, 22].

Validation of novel biomarkers

The main goal of novel biomarkers is to aid in clinical decision-making by means of reproducible results and clear-cut points. One of the challenges in biomarker development and clinical translation lies in the use of small specific cohorts for discovery with an application for larger heterogeneous patient populations. Therefore, hypothesis-driven biomarker discovery is indisputable for clinical translation [23], which especially applies to 'big data' requiring network approach analysis [24]. In this thesis, we aimed to contribute to the discovery and validation of novel biomarkers for CAD, with special attention for a comprehensive study design facilitating translational research. One of the hurdles we took into account is that the discovery and validation of biomarkers must be performed in a study cohort reflecting the target population [25–28]. Since a biomarker should have sufficient power to discriminate high and low risk patients in a diseased population, the inclusion of patients with complaints suspected for myocardial ischemia ([chapter 4](#)) strengthen our study. Furthermore, the failure to validate the proposed miRNAs for the diagnosis of myocardial ischemia stresses the notion that large

validation cohorts (internal and external) are urgently needed to circumvent unnecessary and costly studies and to accelerate implementation of the most potential candidates [29].

2. Choose appropriate small animal models

To date, translational failure of novel therapies for cardiovascular disease (CVD), including chronic heart failure (CHF), is a major research hurdle and involves both high research costs and an ongoing lack of novel treatment modalities reaching the bedside [30]. A poor translation of laboratory work to clinical practice applies to cardiac cell therapy as well. Despite highly promising initial results in animal studies, the quick transition to clinical trials resulted in disappointing measures of therapeutic efficacy with a marginal outcome at most [31–33]. Evaluating the last decade of stem cell therapy within the rapidly advancing field of regenerative medicine, it becomes clear that crucial steps needed for proper clinical translation were neglected, presumably mediated by the high unmet need for novel therapeutics for patients with CHF. In short, cardiac cell therapy is still in its infancy [34]. To avoid rejecting the essential along with the inessential, it is imperative to take a step backwards and agree upon the future directions of stem cell therapy [35].

One of the major shortcomings along the translational axis of CPC discovery to men is the lack of comprehensive small animal models. Small animal models are of great importance to study the mechanistic effects of human stem cell therapy to improve clinical efficacy. As emphasized in this thesis ([chapter 5, 6, 7](#)), this necessitates clinically translatable animal models that resemble specific aspects of human disease [35]. To fully understand the true therapeutic potential of novel therapeutics, including cardiac cell therapy, several aspects need to be addressed. Challenges to improve translational research using small animal models can be summarized in four points: 1) definition of the disease target and 2) enhancing the therapeutic potential while respecting 3) the intrinsic and extrinsic factors involved in disease development and 4) clinical outcome parameters.

Define disease target

The first challenge in translatable research is to define the pathology of interest and to adjust the timing of therapy accordingly. As stated in this thesis, the currently used small animal models for stem- and progenitor cell studies are merely inadequate. The choice of which murine model fits the study purpose best is often, regrettably, determined by practical issues. The advantages of small animal models, including their low costs and genetically selection options, are negated by their small size and lack of accessibility to the heart. Consequently, cell therapy in small animal models is predominantly investigated in an acute myocardial injury setting [36–40], whereas the results are translated to preclinical and clinical studies for CHF. One way to overcome this accessibility issue is to use advanced techniques, such as intracoronary delivery [41] or minimally invasive echo-guided intramyocardial injections, as we have carried out in this thesis (chapter 5, 6). By using minimally invasive techniques, the pathology of interest can be targeted more easily, which is essential for future translation of novel therapeutics.

It is well known that cardiomyocyte death and inflammation play a major role in the acute phase upon cardiac injury and that adverse cardiac remodeling is dominant in the chronic phase. It is therefore recognized that every phase upon cardiac injury might benefit differently from cardiac cell therapy as different molecular pathways are active [42–44]. Initial studies showed cardioprotective effects of CPC in the acute phase upon cardiac injury, including a prevention of cell death, attenuation of inflammation and enhanced angiogenesis, which resulted in a lower scar mass and LV function preservation [45–47]. Although a regenerative approach becomes more important for the chronically injured heart, the fact that adverse cardiac remodeling is a dynamic process creates a therapeutic window for preservative therapy as indicated by Tang *et al.* and chapter 6 of this thesis. In spite of the fact that we investigated the feasibility of stem cell injection at several time-points upon cardiac injury (chapter 5), the optimal timing of therapy still needs further elucidation.

As the therapeutic effect of cell therapy presumably depends on the disease target, 3D *in vitro*

models should be considered as valued components to investigate the cellular interaction of the extracellular matrix and CPC ([chapter 9](#)) and to specify molecular pathways. Therefore, clinical relevant 3D models [48, 49] and small animal models are essential to contribute to better clinical translation and therapeutic efficacy.

Enhance therapeutic potential of cardiac cell therapy

The tentative positive outcome of cell therapy in (pre-)clinical trials and the limited observed effects in our CPC study ([chapter 6](#)) forced us to carefully address opportunities to optimize cell therapy to further maximize clinical efficacy. One of the major limitations of cardiac cell therapy is their extreme low retention rate. At the moment of cell injection, the majority of cells (>80%) are washed out immediately [50]. After this initial hurdle, an additional decrease in cell retention is observed ([chapter 5](#)), presumably caused by apoptosis and immunological elimination ([chapter 7](#)). Despite the fact that not the cells themselves but their paracrine mediators are responsible for the therapeutic effect [51, 52], it has been demonstrated that a higher cell retention is more beneficial [53, 54]. Therefore, identification and implementation of novel approaches is needed to prevent quick cell wash out and to improve retention. Solutions can be expected from the field of 'tissue engineering' and 'cell engineering'. Recently, tissue engineering approaches with the use of cell carriers improved initial cell retention and consequently resulted in a more beneficial treatment effect [50, 55, 56]. Furthermore, tailoring of cell differentiation and cell enhancer protocols to decrease the susceptibility for cell death and to direct cell fate are other promising approaches to improve therapeutic potential [57, 58]. Next, enhancing the therapeutic potential of cardiac cell therapy by immunological matching (e.g. HLA) of graft and host cells can be of additive value. Originally, the use of immune deficient mice (e.g. NOD-SCID) was established to overcome cross-species reactivity. However, immune rejection is still observed upon stem- and progenitor cell transplantation. In combination with the recently recognized role of the immune system in cardiac disease [59], it can be stated that NOD-SCID mice lack essential features of the human immunological system and are therefore

merely unrepresentative for human disease and clinical translatable research. A shift towards humanized animals is necessary to obtain proper pre-clinical rodent models for cardiac human cell therapy. Using 3D engineered heart constructs, with incorporated inflammatory components, would accelerate the development of small animal models to study the human immune system. In addition, reconstruction of the human immune system provides the opportunity to study human biological processes, including allograft rejection upon cell transplantation and the potential immune modulatory effects of CPC and MSC [60].

Clinical approach

To maximize the success of preclinical research, systemic factors need to be taken into account in future studies. Many patients potentially benefit from experimental therapies, such as cardiac cell therapy, have co-morbidities and use numerous pharmacological agents [61]. These factors are confounders for the potential therapeutic effect of cell therapy [62, 63]. To achieve clinical translatability, however, these intrinsic and extrinsic factors need to be incorporated in preclinical animal models. The add-on effect of stem cell therapy will become clear when applied in combination with factors as hypercholesterolemia, diabetes, age, renal failure and gender [64]. Interestingly, *in vitro* 3D models can be used to elucidate molecular targets and potential synergistic effects.

Besides, to improve the appreciation of findings in small animal research, we believe that the use of clinical outcome parameters is imperative. As shown in [chapter 5, 6 and 7](#), the use of small animals does not exclude incorporation of advanced methods. Methods as 3D echocardiography, myocardial deformation imaging and local delivery techniques will contribute to clinical translation, as it will provide for standardized assessments, transferability, and more local effectiveness. Using clinical outcome parameters will provide for more insight in the therapeutic effect and can directly guide clinical relevant adjustments to the experimental set-up.

3. Focus on personalized approaches

Finally, clinical translation can be improved by focusing on the uniqueness of individual patients while categorizing their disease. Precision medicine can be defined as ‘treatments targeted to the needs of individual patients on the basis of genetic, biomarker, phenotypic, or psychosocial characteristics that distinguish a given patient from other patients with similar clinical presentations’ [65]. This accounts for identifying patients at high risk for acute cardiac injury, diagnosing those in need for revascularization and providing appropriate treatment to prevent or improve adverse cardiac remodeling [66–68].

For the identification of patients with ACS, cTnI is still the preferred biomarker reflecting cause and consequence [8]. Novel biomarkers, including miRNAs and EV, can add value by their presumed active release mechanism and involvement in disease development. However, the use of a single biomarker only reflects a single pathophysiological pathway, which assumes 100% similarity between patients with the same disease. Therefore, a multi-marker approach appears more promising by means of collecting information of several ongoing processes ([chapter 2 and 3](#)) [2, 69]. This multi-marker approach could be a step toward individualized diagnosis and prognosis based on individualized ‘fingerprint’ information obtained from different markers. Besides diagnostic use of biomarkers, an improved understanding of their pathophysiological origin might contribute to a better prognosis and personalized treatment of patients with CAD. Next, identifying patients at risk for developing heart failure upon cardiac injury would help target preventive therapies. Currently, patients with chronic heart failure receive similar pharmacological treatment, despite differences in etiology or co-morbidity [61]. However, variable responses to treatment with beta-blockers or ACE-inhibitors have been described for patients with different heart failure etiologies [68]. This variation in response underscores the need to better understand heart failure pathophysiology for individual patient profiles [68] and the necessity to create a patient-specific platform for novel therapeutics to improve and, conceptually, predict patient outcome. Moreover, there is an urgent need to improve and

personalize the effect of existing and new anti-fibrotic therapeutics ([chapter 8 and 9](#)).

3D *in vitro* models could eventually result in advanced clinical tools for personalized therapies. In this thesis ([chapter 9](#)), we demonstrated the feasibility and potential of a cardiac fibrosis model using cardiac fibroblasts. As cardiac fibrosis is a multicellular process, the addition of cardiomyocytes and endothelial cells is essential to study the fibrosis interplay. The goal of developing a multi-cellular fibrosis platform can be achieved by designing patient-specific engineered heart constructs with the use of patient-specific cells, e.g induced pluripotent stem cells (iPSC). Consequently, these patient-specific models could be used in different research and pre-clinical settings, such as studying pathophysiology, drug targeting and drug toxicology [70]. Moreover, these models could be used to identify the best drug for a patient and lead to personalized drug therapy for clinical use [71].

The key of translational cardiology

Taken together, this work illustrates the importance of preclinical and clinical translational research to facilitate advancements in the diagnosis and treatment of ischemic heart disease. Successful clinical translation of novel biomarkers for early detection of CAD and successive targeted treatment of chronic manifestations of CAD can only be achieved by using appropriate study models. Therefore, a clear recognition of the pathophysiological processes, biological targets and a clinical approach are mandatory. By presenting data on the use of miRNAs and EV for the early detection of stable CAD and ACS, this thesis contributes to the quest for sensitive and specific novel early biomarkers for the different expressions of CAD and emphasizes the importance of hypothesis driven discovery and validation studies. Furthermore, the presented small animal models and 3D *in vitro* model add to the current understanding of chronic cardiac remodeling and the therapeutic effect of cardiac cell therapy. In particular, this thesis highlights the shortcomings of the currently used models and provides clinical translatable solutions to maximize potential therapeutic efficacy (see Figure 1). Future work should continue to put effort in bridging the gap between basic science and clinical application. By using the valuable

information regarding biomarker release and miRNA and EV detection, new studies can be designed aiming at improved diagnosis of the different manifestations of CAD. Furthermore, using the developed mouse model of chronic cardiac remodeling and the proposed tissue engineered heart construct, research of chronic heart failure can be accelerated and the place of cardiac cell therapy within the current treatment modalities can be determined. Ultimately, translational research will be a comprehensive approach respecting the individual patient within the targeted disease population.

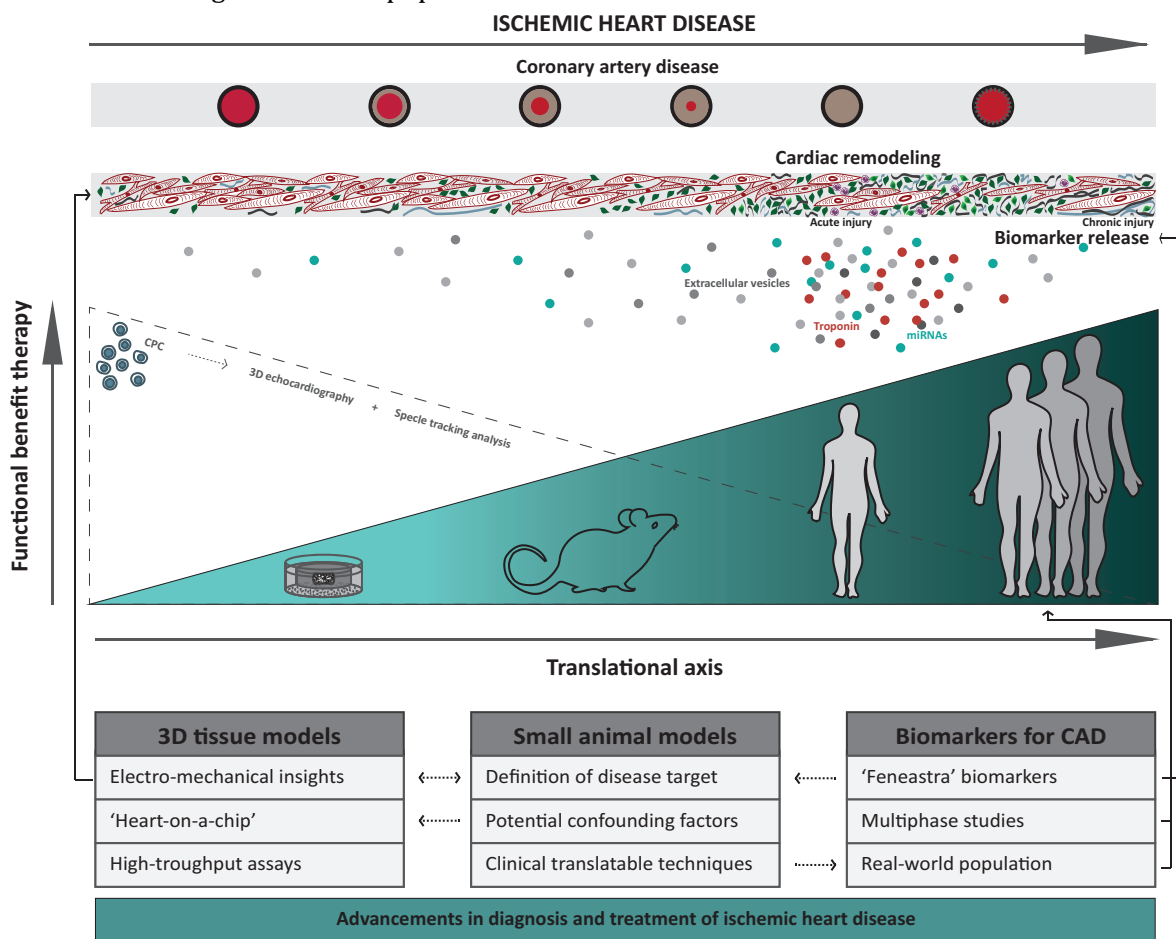


Figure 1. Overview of ischemic heart disease and translational strategies for preclinical and clinical research.

In the upper bars the gradual process of atherosclerosis in coronary artery disease and the related structural changes of the myocardium are visualized. Upon a (sub)total occlusion of the coronaries, the myocardium is damaged and cardiac repair is initiated (acute injury). Troponin, miRNAs and extracellular vesicles are released and can serve as biomarkers. In time, excessive production and deposition of extracellular matrix components contribute to scarring and failing of the heart (chronic injury). As demonstrated in the graph, the clinical translation of novel therapeutics (including cardiac cell therapy) along the translational axis from mice to man is poor. The lower panels show strategies to improve (pre)clinical research to maximize potential therapeutic efficacy. For this, a clear recognition of the pathophysiological processes, biological targets and a clinical approach is essential. New studies can be designed aiming at improved diagnosis of the different manifestations of CAD. Additionally, the developed mouse model of chronic cardiac remodeling and the proposed tissue engineered heart construct can be used to accelerate research of chronic heart failure.

References

1. Biomarkers Definition Working Group, Bethesda. Biomarkers and surrogate endpoints: preferred definitions and conceptual framework. *Clin Pharmacol Ther* 2001;69:89–95.
2. Vasan RS. Biomarkers of cardiovascular disease: molecular basis and practical considerations. *Circulation* 2006;113:2335–62.
3. Deddens JC, Colijn JM, Oerlemans MIFJ, et al. Circulating MicroRNAs as Novel Biomarkers for the Early Diagnosis of Acute Coronary Syndrome. *J Cardiovasc Transl Res* 2013;6:884–898.
4. LaBaer J. So, you want to look for biomarkers (introduction to the special biomarkers issue). *J Proteome Res* 4:1053–9.
5. Libby P, Theroux P. Pathophysiology of coronary artery disease. *Circulation* 2005;111:3481–8.
6. Grech ED. Pathophysiology and investigation of coronary artery disease. *BMJ* 2003;326:1027–30.
7. Roffi M, Patrono C, Collet J-P, et al. 2015 ESC Guidelines for the management of acute coronary syndromes in patients presenting without persistent ST-segment elevation. *Eur Heart J* 2015;37:ehv320.
8. Steg PG, James SK, Atar D, et al. ESC Guidelines for the management of acute myocardial infarction in patients presenting with ST-segment elevation. *Eur Heart J* 2012;33:2569–619.
9. Thygesen K, Alpert JS, Jaffe AS, et al. Third universal definition of myocardial infarction. *Eur Heart J* 2012;33:2551–67.
10. Sluijter JPG, Verhage V, Deddens JC, van den Akker F, Doevendans PA. Microvesicles and exosomes for intracardiac communication. *Cardiovasc Res* 2014;102:302–11.
11. Colombo M, Raposo G, Théry C. Biogenesis, Secretion, and Intercellular Interactions of Exosomes and Other Extracellular Vesicles. *Annu Rev Cell Dev Biol* 2014;30:255–289.
12. Sluijter JPG, van Mil A, van Vliet P, et al. MicroRNA-1 and -499 regulate differentiation and proliferation in human-derived cardiomyocyte progenitor cells. *Arterioscler Thromb Vasc Biol* 2010;30:859–68.
13. Lin CJ-F, Gong H-Y, Tseng H-C, Wang W-L, Wu J-L. miR-122 targets an anti-apoptotic gene, Bcl-w, in human hepatocellular carcinoma cell lines. *Biochem Biophys Res Commun* 2008;375:315–20.
14. Higgins JP, Higgins JA. Elevation of cardiac troponin I indicates more than myocardial ischemia. *Clin Investig Med Médecine Clin Exp* 2003;26:133–47.
15. Shah AS V, Anand A, Sandoval Y, et al. High-sensitivity cardiac troponin I at presentation in patients with suspected acute coronary syndrome: a cohort study. *Lancet (London, England)* 2015;386:2481–8.
16. Wilson SR, Sabatine MS, Braunwald E, Sloan S, Murphy SA, Morrow DA. Detection of myocardial injury in patients with unstable angina using a novel nanoparticle cardiac troponin I assay: observations from the PROTECT-TIMI 30 Trial. *Am Heart J* 2009;158:386–91.
17. Reichlin T, Hochholzer W, Bassetti S, et al. Early diagnosis of myocardial infarction with sensitive cardiac troponin assays. *N Engl J Med* 2009;361:858–67.
18. Nestelberger T, Wildi K, Boeddinghaus J, et al. Characterization of the observe zone of the ESC 2015 high-sensitivity cardiac troponin 0h/1h-algorithm for the early diagnosis of acute myocardial infarction. *Int J Cardiol* 2016;207:238–45.
19. Condorelli G, Latronico MVG, Cavarretta E. microRNAs in cardiovascular diseases: current knowledge and the road ahead. *J Am Coll Cardiol* 2014;63:2177–87.
20. Zampetaki A, Willeit P, Tilling L, et al. Prospective study on circulating MicroRNAs and risk of myocardial infarction. *J Am Coll Cardiol* 2012;60:290–9.
21. Witwer KW. Circulating microRNA biomarker studies: pitfalls and potential solutions. *Clin Chem* 2015;61:56–63.
22. Bank IE, Timmers L, Gijsberts CM, et al. The diagnostic and prognostic potential of plasma extracellular vesicles for cardiovascular disease. *Expert Rev Mol Diagn* 2015;15:1577–88.

23. Azuaje FJ, Dewey FE, Brutsaert DL, Devaux Y, Ashley EA, Wagner DR. Systems-based approaches to cardiovascular biomarker discovery. *Circ Cardiovasc Genet* 2012;5:360–7.
24. Rumsfeld JS, Joynt KE, Maddox TM. Big data analytics to improve cardiovascular care: promise and challenges. *Nat Rev Cardiol* 2016;13:350–9.
25. Wang G-K, Zhu J-Q, Zhang J-T, et al. Circulating microRNA: a novel potential biomarker for early diagnosis of acute myocardial infarction in humans. *Eur Heart J* 2010;31:659–66.
26. Corsten MF, Dennert R, Jochems S, et al. Circulating MicroRNA-208b and MicroRNA-499 reflect myocardial damage in cardiovascular disease. *Circ Cardiovasc Genet* 2010;3:499–506.
27. D'Alessandra Y, Carena MC, Spazzafumo L, et al. Diagnostic potential of plasmatic MicroRNA signatures in stable and unstable angina. *PLoS One* 2013;8:e80345.
28. Gao H, Guddeti RR, Matsuzawa Y, et al. Plasma Levels of microRNA-145 Are Associated with Severity of Coronary Artery Disease. *PLoS One* 2015;10:e0123477.
29. Hunter DJ, Losina E, Guermazi A, Burstein D, Lasserre MN, Kraus V. A pathway and approach to biomarker validation and qualification for osteoarthritis clinical trials. *Curr Drug Targets* 2010;11:536–45.
30. Lecour S, Bøtker HE, Condorelli G, et al. ESC working group cellular biology of the heart: position paper: improving the preclinical assessment of novel cardioprotective therapies. *Cardiovasc Res* 2014;104:399–411.
31. Hirsch A, Nijveldt R, van der Vleuten PA, et al. Intracoronary infusion of mononuclear cells from bone marrow or peripheral blood compared with standard therapy in patients after acute myocardial infarction treated by primary percutaneous coronary intervention: results of the randomized controlled HEBE . *Eur Heart J* 2011;32:1736–47.
32. Abdel-Latif A, Bolli R, Tleyjeh IM, et al. Adult bone marrow-derived cells for cardiac repair: a systematic review and meta-analysis. *Arch Intern Med* 2007;167:989–97.
33. Martin-Rendon E, Brunskill SJ, Hyde CJ, Stanworth SJ, Mathur A, Watt SM. Autologous bone marrow stem cells to treat acute myocardial infarction: a systematic review. *Eur Heart J* 2008;29:1807–18.
34. Hong KU, Bolli R. Cardiac stem cell therapy for cardiac repair. *Curr Treat Options Cardiovasc Med* 2014;16:324.
35. Madonna R, Van Laake LW, Davidson SM, et al. Position Paper of the European Society of Cardiology Working Group Cellular Biology of the Heart: cell-based therapies for myocardial repair and regeneration in ischemic heart disease and heart failure. *Eur Heart J* 2016.
36. Tseliou E, Reich H, de Couto G, et al. Cardiospheres reverse adverse remodeling in chronic rat myocardial infarction: roles of soluble endoglin and Tgf- β signaling. *Basic Res Cardiol* 2014;109:443.
37. Tang X-L, Rokosh G, Sanganalmath SK, et al. Intracoronary administration of cardiac progenitor cells alleviates left ventricular dysfunction in rats with a 30-day-old infarction. *Circulation* 2010;121:293–305.
38. Rota M, Padin-Iruegas ME, Misao Y, et al. Local activation or implantation of cardiac progenitor cells rescues scarred infarcted myocardium improving cardiac function. *Circ Res* 2008;103:107–16.
39. Latham N, Ye B, Jackson R, et al. Human blood and cardiac stem cells synergize to enhance cardiac repair when cotransplanted into ischemic myocardium. *Circulation* 2013;128:S105-12.
40. Zwetsloot PP, Végh AM, Jansen Of Lorkeers SJ, et al. Cardiac Stem Cell Treatment in Myocardial Infarction: A Systematic Review and Meta-Analysis of Preclinical Studies. *Circ Res* 2016.
41. Ladage D, Ishikawa K, Tilemann L, Müller-Ehmsen J, Kawase Y. Percutaneous methods of vector delivery in preclinical models. *Gene Ther* 2012;19:637–41.
42. Li A-H, Liu PP, Villarreal FJ, Garcia RA. Dynamic changes in myocardial matrix and relevance to disease: translational perspectives. *Circ Res* 2014;114:916–27.

43. Goumans M-J, Maring JA, Smits AM. A straightforward guide to the basic science behind cardiovascular cell-based therapies. *Heart* 2014;100:1153–7.
44. Tongers J, Losordo DW, Landmesser U. Stem and progenitor cell-based therapy in ischaemic heart disease: promise, uncertainties, and challenges. *Eur Heart J* 2011;32:1197–206.
45. Smits AM, van Laake LW, den Ouden K, et al. Human cardiomyocyte progenitor cell transplantation preserves long-term function of the infarcted mouse myocardium. *Cardiovasc Res* 2009;83:527–35.
46. Chimenti I, Smith RR, Li T-S, et al. Relative roles of direct regeneration versus paracrine effects of human cardiosphere-derived cells transplanted into infarcted mice. *Circ Res* 2010;106:971–80.
47. Dawn B, Stein AB, Urbanek K, et al. Cardiac stem cells delivered intravascularly traverse the vessel barrier, regenerate infarcted myocardium, and improve cardiac function. *Proc Natl Acad Sci U S A* 2005;102:3766–71.
48. Galie PA, Stegemann JP. Injection of mesenchymal stromal cells into a mechanically stimulated in vitro model of cardiac fibrosis has paracrine effects on resident fibroblasts. *Cytotherapy* 2014;16:906–14.
49. Sonin DL, Wakatsuki T, Routhu K V, et al. Protease-activated receptor 1 inhibition by SCH79797 attenuates left ventricular remodeling and profibrotic activities of cardiac fibroblasts. *J Cardiovasc Pharmacol Ther* 2013;18:460–475.
50. van den Akker F, Feyen DAM, van den Hoogen P, et al. Intramyocardial stem cell injection: go(ne) with the flow. *Eur Heart J* 2016.
51. Gneocchi M, Zhang Z, Ni A, Dzau VJ. Paracrine mechanisms in adult stem cell signaling and therapy. *Circ Res* 2008;103:1204–19.
52. Tang X-L, Li Q, Rokosh G, et al. Long-Term Outcome of Administration of c-kit^{POS} Cardiac Progenitor Cells After Acute Myocardial Infarction: Transplanted Cells Do Not Become Cardiomyocytes, but Structural and Functional Improvement and Proliferation of Endogenous Cells Persist for At Lea. *Circ Res* 2016.
53. Golpanian S, Schulman IH, Ebert RF, et al. Concise Review: Review and Perspective of Cell Dosage and Routes of Administration From Preclinical and Clinical Studies of Stem Cell Therapy for Heart Disease. *Stem Cells Transl Med* 2016;5:186–91.
54. Liu J, Narsinh KH, Lan F, et al. Early stem cell engraftment predicts late cardiac functional recovery: preclinical insights from molecular imaging. *Circ Cardiovasc Imaging* 2012;5:481–90.
55. Feyen DAM, Gaetani R, Deddens J, et al. Gelatin Microspheres as Vehicle for Cardiac Progenitor Cells Delivery to the Myocardium. *Adv Healthc Mater* 2016.
56. Ye Z, Zhou Y, Cai H, Tan W. Myocardial regeneration: Roles of stem cells and hydrogels. *Adv Drug Deliv Rev* 2011;63:688–97.
57. Aguirre A, Sancho-Martinez I, Izpisua Belmonte JC. Reprogramming toward heart regeneration: stem cells and beyond. *Cell Stem Cell* 2013;12:275–84.
58. Feyen DAM, Gaetani R, Doevendans PA, Sluijter JPG. Stem cell-based therapy: Improving myocardial cell delivery. *Adv Drug Deliv Rev* 2016.
59. Frangogiannis NG. The inflammatory response in myocardial injury, repair, and remodelling. *Nat Rev Cardiol* 2014;11:255–265.
60. Hogenes M, Huibers M, Kroone C, de Weger R. Humanized mouse models in transplantation research. *Transplant Rev (Orlando)* 2014;28:103–10.
61. McMurray JJ V, Adamopoulos S, Anker SD, et al. ESC guidelines for the diagnosis and treatment of acute and chronic heart failure 2012: The Task Force for the Diagnosis and Treatment of Acute and Chronic Heart Failure 2012 of the European Society of Cardiology. Developed in collaboration with the Heart. *Eur J Heart Fail* 2012;14:803–69.
62. Giricz Z, Lalu MM, Csonka C, Bencsik P, Schulz R, Ferdinandy P. Hyperlipidemia attenuates the infarct size-limiting effect of ischemic preconditioning: role of matrix metalloproteinase-2 inhibition. *J Pharmacol Exp Ther* 2006;316:154–61.

63. Baranyai T, Nagy CT, Koncsos G, et al. Acute hyperglycemia abolishes cardioprotection by remote ischemic preconditioning. *Cardiovasc Diabetol* 2015;14:151.
64. McCafferty K, Forbes S, Thiemermann C, Yaqoob MM. The challenge of translating ischemic conditioning from animal models to humans: the role of comorbidities. *Dis Model Mech* 2014;7:1321–33.
65. Jameson JL, Longo DL. Precision Medicine — Personalized, Problematic, and Promising. *N Engl J Med* 2015;372:2229–2234.
66. Zhang Y, Barocas VH, Berceli SA, et al. Multi-scale Modeling of the Cardiovascular System: Disease Development, Progression, and Clinical Intervention. *Ann Biomed Eng* 2016.
67. Dweck MR, Doris MK, Motwani M, et al. Imaging of coronary atherosclerosis - evolution towards new treatment strategies. *Nat Rev Cardiol* 2016.
68. Liu LCY, Voors AA, Valente MAE, van der Meer P. A novel approach to drug development in heart failure: towards personalized medicine. *Can J Cardiol* 2014;30:288–95.
69. Ky B, French B, Levy WC, et al. Multiple biomarkers for risk prediction in chronic heart failure. *Circ Heart Fail* 2012;5:183–90.
70. Schaaf S, Shibamiya A, Mewe M, et al. Human engineered heart tissue as a versatile tool in basic research and preclinical toxicology. *PLoS One* 2011;6:e26397.
71. Martins AM, Vunjak-Novakovic G, Reis RL. The current status of iPS cells in cardiac research and their potential for tissue engineering and regenerative medicine. *Stem Cell Rev* 2014;10:177–90.

Appendix

Summary

Samenvatting

Dankwoord

Curriculum Vitae

Summary

Coronary artery disease (CAD) is the most influential disease in the western world and is accountable for the death of 7.4 million people each year. To guide early identification of patients with a low risk for acute coronary syndrome (ACS), to accelerate immediate treatment in the emergency department for patients with a high risk of cardiac death, and to minimize healthcare costs, there is an ongoing need for novel early biomarkers for CAD. Attention for novel treatment modalities for chronic heart failure (CHF) is evenly important, as numerous patients with a myocardial infarction (MI) develop CHF. Although advancements have been made in therapeutic options for patients with CHF, the 5-year mortality rate is still 60%. To gain insight in the pathophysiological processes involved in CHF and to identify therapeutic targets, novel *in vivo* and *in vitro* models are necessary. To facilitate clinical translation of potential therapeutics, including cardiac cell therapy, it is mandatory to define the biological targets in an early stage of preclinical research.

Considering the heterogeneity of CAD and the quest for translational research, efforts should be made to design and employ appropriate preclinical and clinical studies. Therefore, the first aim of this thesis was to demonstrate the importance of hypothesis driven discovery studies and the necessity for validation studies ([chapter 2-4](#)). Secondly, this thesis aimed at improving the currently used small animal models and cell models by acknowledging both disease targets and potential shortcomings of the models and therapeutic approaches ([chapter 5-9](#)).

In [chapter 2](#), we highlighted the nature and cellular release mechanisms of circulating miRNAs and explored their potential role in the diagnosis of MI. We found that > 20 studies showed an early up-regulation of muscle-specific miRNAs during MI, which are related to the extent of myocardial damage. However, the clinical translation of these markers is delayed by some major limitations, e.g. the currently used study population sizes and the time needed for RNA detection. Therefore, we concluded that miRNAs as early biomarker for MI should be validated in larger patient cohorts and that the additional value of new biomarker candidates from micro-

array discoveries need to be elucidated.

Circulating miRNAs are transported by protein complexes, lipids and extracellular vesicles (EV). Interestingly, it has been demonstrated that the release of EV correlates with the severity of cardiac disease. Consequently, it is likely that the combination of both the amount and content of EV upon cardiac injury has diagnostic potential. Therefore, we evaluated the role of EV in miRNA transportation in [chapter 3](#). We showed that EV are released from the ischemic myocardium upon I/R injury. In addition, we provided evidence that cardiac and muscle specific miRNAs are selectively transported by EV and are rapidly detectable in plasma. Interestingly, EV-linked miRNAs are detectable in plasma at an earlier time-point than cardiac troponin I, which suggests that EV release is stress-induced. We concluded that the enrichment of EV with miRNAs hold great potential as novel early biomarkers for cardiac injury. Moreover, these results accentuated the importance of preclinical research for a better understanding of temporo-spatial characteristics of potential biomarkers.

In [chapter 4](#) we performed a two-phase study to assess whether circulating miRNAs could be used as diagnostic blood-based biomarkers for myocardial ischemia, a late manifestation of CAD. In the discovery phase, profiling of circulating miRNAs was performed in 12 patients with myocardial ischemia and 8 matched controls. Overall, the number of differentially expressed miRNAs was low ($n= 15$, fold difference >1.5 and p value <0.15). Seven out of the 15 differentially expressed miRNAs (fold difference >1.5 and p value <0.15) had an AUC ≥ 0.70 and were selected for the large replication phase of this study. In addition to the miRNA panel derived from the discovery study, four miRNAs were added on the basis of their described role in literature as biomarkers for stable angina or CAD. Their diagnostic accuracy was assessed in a case-cohort study, consisting of patients with complaints of stable angina ($n=346$, of which 51.6% cases). Unfortunately, we did not observe a differential expression of any of the evaluated miRNAs. Based on this study, we concluded that miRNAs are unsuitable as biomarkers for myocardial ischemia, which can possibly be explained by the gradual process of CAD and the involvement of miRNAs in the disease process.

For preclinical research, small animal models are indispensable to gain insight in the basic mechanism of disease. Whereas the opportunities within small animal research are numerous, the success of preclinical research is often limited by the use of inadequate injury models or clinically incompatible delivery methods and timing of therapy. In order to achieve appropriate murine models for clinical translation of cardiac cell therapy, it is important to develop models of chronic cardiac remodeling and to apply novel techniques to measure therapeutic effects.

In pre-clinical and clinical research, cardiac stem cell therapy is applied by either systemic or local delivery strategies. In murine models, the most commonly used local delivery strategy is intramyocardial injection after sternotomy or thoracotomy. However, the invasive nature of these procedures is arguably only convenient for acute MI studies and underlies the lack of stem cell studies in chronic cardiac remodeling. To bypass these hurdles, echocardiography (echo)-guided intramyocardial injections (echo-IMI) can remedy the situation. Consequently, in [chapter 5](#) we assessed the feasibility of a murine chronic I/R injury model combined with a minimally invasive echo-based local delivery strategy for cardiac progenitor cell (CPC) delivery. We observed that upon I/R injury, adverse cardiac remodeling was initiated with a time-dependent decrease in left ventricular function. Moreover, in the distinct phases of cardiac remodeling, echo-IMI resulted in comparable cell retentions *in vivo*. Subsequent immuno-histochemical CPC tracing revealed the intramyocardial presence of CPC and indicated the anterior and septal position of the cells upon injection. Therefore, we concluded that echo-IMI is reproducible, safe and provides a platform for numerous options regarding timing and location of therapy to improve preclinical small animal research.

In [chapter 6](#), we assessed the therapeutic effect of CPC therapy in the proposed comprehensive murine model of chronic I/R injury and evaluated cardiac function by 3D echocardiography and speckle tracking analysis. Minimally invasive intramyocardial injection of CPC was successfully applied 28 days after I/R injury and resulted in localized long-term engraftment. We did not find a significant restoration of cardiac function upon injection of CPCs

in the chronic remodeling heart. However, a relative preservation of the left ventricular end-diastolic volume was observed at 4 weeks follow-up compared to vehicle control. This difference was reflected in an increased strain rate in CPC treated mice. Our results seems to resemble the effect sizes of previous preclinical and clinical studies in chronic cardiac conditions and by that provide a translatable murine model to ultimately improve clinical efficacy for novel local therapeutics in chronic heart failure.

The immune system is increasingly recognized as an important determinant and tunable therapeutic target in CHF. Animal models currently used for human-based cardiac cell therapy, however, mainly use immune deficient animals or immunosuppressive drugs, as graft cells are non-autologous. Therefore the question was raised whether these models are appropriate and representative for human disease. Additionally, it remains controversial whether immune compromised animal models are necessary as progenitor cells are traditionally considered to be immune privileged. In [chapter 7](#), we used echo-IMI to deliver human mesenchymal stem cells (MSC) and CPC to the myocardium of immunocompetent Balb/c mice and immunodeficient NOD-SCID (SCID) mice and evaluated whether the immune system was activated upon transplantation of progenitor cells. Echo-IMI with either CPC or MSC resulted in a fast decline in cell retention after the initial engraftment. Interestingly, this decline was more pronounced in WT mice than in SCID mice for both injected stem cell populations. At the same time, activation of the immune system was observed as measured by flow cytometric analyses and via released plasma cytokines in both strains. Obviously, an immune rejection occurred in both immune competent and incompetent mice, for both MSC and CPC. In combination with the knowledge that even SCID-mice can induce a mild immune response after xenotransplantation, we believe that a shift towards humanized animals is necessary to obtain proper pre-clinical rodent models for cardiac human cell therapy.

Cardiac remodeling is critical for effective tissue healing, however, excessive production and deposition of extracellular matrix components contribute to scarring and failing of the heart.

The urgent need exists to improve our understanding of adverse cardiac remodeling in order to develop new therapeutic interventions that will prevent or reverse the fibrotic changes in the failing human heart. Therefore, we described the current understanding of cardiac fibrosis and explored the possibilities of tissue engineering to model tissue engineered cardiac fibrosis in chapter 8. We concluded that with the recent developments in hydrogel fabrication, stem cell biology, tissue engineering methods, and microfluidic technologies, it is likely that the first human biomimetic heart fibrosis model (on-a-chip) will become available in the near future and provide a platform for disease modeling, pre-clinical high throughput screening, and clinical personalized medicine.

Chapter 9 reports on a novel *in vitro* 3D-model of cardiac fibrosis composed of methacrylated gelatin (GelMA) and human fetal cardiac fibroblasts (hfCF), which we used to gain insight in the pathophysiology of adverse cardiac remodeling and to investigate whether CPC have anti-fibrotic effects. We observed reproducible cell activation and accumulation of extracellular matrix in a pro-fibrotic environment and showed that the fibrogenic response was strongly attenuated upon co-culture with CPC, mediated via paracrine factors including CPC-EV. We demonstrated the suitability of hfCF-laden GelMA as 3D culture model to study cardiac fibrosis and showed the possibility to modulate the fibrotic response.

We conclude this thesis with a discussion on key elements for successful clinical translational research, which involve the emphasis on a multi-phase study set-up for validation of novel clinical findings, a clear definition of disease targets respecting the potential of cell therapy and possible confounding factors and the use of more personalized therapeutic approaches.

Samenvatting
Dankwoord
Curriculum Vitae

volgt